DISSERTATION

CATALYTIC BIOMASS CONVERSION AND UPGRADING INTO PLATFORM CHEMICALS AND LIQUID FUELS

Submitted by

Dajiang Liu

Department of Mechanical Engineering

In partial fulfillment of the requirements

For the Degree of Doctor of Philosophy

Colorado State University

Fort Collins, Colorado

Spring 2014

Doctoral Committee:

Advisor: Susan James
Co-Advisor: Eugene Chen

John Williams
Anthony Marchese
Nick Fisk

ABSTRACT

CATALYTIC BIOMASS CONVERSION AND UPGRADING INTO PLATFORM CHEMICALS AND LIQUID FUELS

The development of novel, efficient catalytic processes for plant biomass conversion and upgrading into versatile platform chemicals as well as oxygenated biodiesel and premium hydrocarbon kerosene/jet fuels is described in this dissertation. The chief motivation of using annually renewable biomass as the source of chemical building blocks and transportation fuels is to reduce societal dependence on depleting fossil fuels. Towards this goal, 5-hydroxymethylfurfural (HMF), the dehydration product from C_6 (poly)sugars, has been intensively investigated as it has been identified as a versatile C_6 intermediate or platform for value-added chemicals and biofuels. This work has developed several highly efficient and cost-effective catalyst systems for C_6 (poly)sugars conversion to HMF under mild conditions, including ubiquitous and inexpensive aluminum alkyl or alkoxy compounds, recyclable polymeric ionic liquid (PIL)-supported metal (Cr, Al) catalysts, and thiazolium chloride, a recyclable Vitamine B1 analog. An integrated, semi-continuous process for the HMF production from fructose has also been developed, affording the high-purity HMF as needle crystals.

Towards HMF upgrading into higher-energy-density fuel intermediates, developing new strategies of C–C bond formation or chain extension is of particular interest. In this context, this

study has discovered that *N*-heterocyclic carbenes (NHCs) are highly effective organic catalysts for HMF self-condensation to 5,5'-dihydroxymethylfuroin (DHMF), a new C_{12} biorefining building block. This new upgrading process has 100% atom economy, can be carried out under solvent-free conditions, and produces the C_{12} DHMF with quantitative selectivity and yield, the hallmarks of a "green" process. More significantly, the C_{12} DHMF has been transformed catalytically into oxygenated biodiesels, high-quality alkane jet fuels, and sustainable polymers, thereby establishing DHMF as a new C_{12} biomass platform chemical.

ACKNOWLEDGEMENTS

This work was supported by US Department of Energy-Office of Basic Energy Sciences, grant DE-FG02-10ER16193. I would like to acknowledge Prof. Eugene Chen and Susan James as my advisors, who have been generously providing hands-on guidance through my Ph.D. reasearch. I also would like to extend my thanks to my parents and friends for their continuous support and encouragement, which is, in a sense, an invaluable emotional stimulus for me. Specifically, I appreciate the help from Dr. Yuetao Zhang with X-ray diffraction analysis and GPC measurements of PIL samples, Nicole Escúde with DSC analysis, and Prof. Anthony Marchese with the measurement of heating values of the liquid fuels.

TABLE OF CONTENTS

Chapter 1

Introduction

This dissertation is written in a "journals-format" style that is accepted by the Graduate School at Colorado State University and is based on six peer-reviewed, first-author publications that have appeared in *Green Chemistry*, *ChemSusChem*, *ACS Catalysis*, *Biomass & Bioenergy*, *Applied Catalysis A: General*. The central goal of this dissertation is to develop highly efficient and cost-effective catalyst systems for biomass conversion and upgrading into renewable chemicals and liquid fuels, consisting of three major areas: catalytic production of 5-hydroxymethylfurfural (HMF) from biomass, upgrading of the C_6 HMF to the C_{12} 5,5'-dihydroxymethylfuroin (DHMF), and establishment of a new C_{12} biomass chemical platform based on DHMF. The author has studied six topics, which are discussed in detail in the proceeding chapters:

2.) Ubiquitous Aluminum Alkyls and Alkoxides as Effective Catalysts for Glucose to HMF Conversion in Ionic Liquids

3.) Polymeric Ionic Liquid (PIL)-Supported Recyclable Catalysts for Biomass Conversion into HMF

4.) Organocatalytic Upgrading of the Key Biorefinding Building Block by a Catalytic Ionic Liquid and *N*-Heterocyclic Carbenes

5.) Diesel and Alkane Fuels from Biomass by Organocatalysis and Metal-Acid Tandem

Catalysis

6.) An Integrated Catalytic Process for Biomass Conversion and Upgrading to C_{12} Furoin and Alkane Fuel

7.) Organocatalysis in Biorefining for Biomass Conversion and Upgrading

Chapter 2 describes glucose-to-HMF conversion in ILs catalyzed by aluminum alkyl or alkoxy compounds as Lewis acid catalysts. Specifically, under the optimized conditions (1-ethyl-3-methylimidazolium chloride [EMIM]Cl, 120 ℃, 6 h), simple trialkyl and trialkoxy aluminum species such as $AlEt_3$ and $Al(O^iPr)_3$, which are much cheaper than the benchmark catalyst $CrCl_2$ (by a factor of 5 for $AlEt_3$ or 180 for $Al(O^iPr)_3$), are at least as effective as $CrCl_2$ to catalyze this conversion process. A gradual substitution of the chloride ligand on aluminum by the alkyl ligand brings about a drastic enhancement on the HMF yield, from 1.6 % by $AlCl_3$ to 7.6 % by $MeAlCl_2$ to 17 % by Et_2AlCl and to 51% by $AlEt_3$. The catalyst structure was also characterized by single-crystal X-ray diffraction analysis.

Chapter 3 reports the first study of recyclable PIL-supported metal (Cr, Al) catalysts for effective biomass (glucose and cellulose) conversion into HMF. Of the five different PILs investigated, poly(3-butyl-1-vinylimidazolium chloride), P[BVIM]Cl, was revealed to be the most effective; when combined with $CrCl_2$ *in situ* or used the as the preformed PIL-metalate $P[BVIM]^+[CrCl_3]^-$ in DMF, this PIL-supported catalyst converts glucose to HMF in 66 % yield at 120 ℃ for 3 h. The analogous PIL-Al catalyst, P[BVIM]Cl-Et_2AlCl, is less effective than the PIL-$CrCl_2$ system, but the PIL-Al system is more recyclable thus achieving a nearly constant HMF yield upon 6 cycles.

Chapter 4 reveals a novel, highly efficient method of upgrading HMF into DHMF, a promising C_{12} kerosene/jet fuel intermediate. This upgrading reaction is carried out under industrially favorable conditions (i.e., ambient atmosphere and 60-80 ℃), catalyzed by organic *N*-heterocyclic carbenes (NHCs), and complete within 1 h. Two types of NHCs, 1-ethyl-3-methylimidazolium acetate ([EMIM]OAc, as a masked NHC) and 1,3,4-triphenyl-4,5-dihdydro-1*H*-1,2,4-triazol-5-ylidene (TPT, as a discrete NHC), were identified to be highly efficient, producing DHMF with yields up to 98% (by HPLC or NMR) or 87% (unoptimized, isolated yield). Mechanistic studies have yielded four lines of evidence that support the proposed carbene catalytic cycle for this upgrading transformation.

Chapters 5 and 6 detail the highly efficient production of DHMF from biomass resources and subsequent conversion of DHMF to liquid fuels. Chapter 5 is a Communication that reports organocatalytic self-condensation (Umpolung) of biomass furaldehydes into $C_{10\text{-}12}$ furoin intermediates, followed by hydrogenation, etherification, or esterification into oxygenated biodiesel, or hydrodeoxygenation (HDO) by metal-acid tandem catalysis into premium alkane jet fuels (*n*-$C_{10}H_{22}$, *n*-$C_{11}H_{24}$ and *n*-$C_{12}H_{26}$). Chapter 6 develops an integrated catalytic process for conversion and upgrading of biomass feedstocks into C_{12} alkane fuels through three steps. The first step of the process involves semi-continuous organocatalytic conversion of biomass (fructose, in particular) to the high-purity HMF; the second step is the NHC-catalyzed coupling of C_6 HMF produced by the semi-continuous process to C_{12} DHMF; the third step of the process converts C_{12} DHMF selectively to *n*-$C_{12}H_{26}$ via HDO with a bifunctional catalyst system consisting of Pd/C + acetic acid + $La(OTf)_3$.

Chapter 7 is a critical review article on applications of organocatalysis in biorefining for catalytic biomass conversion and upgrading into sustainable chemicals, materials, and biofuels. This review captures highlights of this emerging area by specifically focusing on utilization of organocatalytic means for catalytic conversions of mono- and polysugars, upgrading of furaldehydes, and organocatalytic polymerization of biomass feedstocks.

Chapter 8 is a summary of the work presented herein. The majority of the research conducted by the author during the graduate stage has been included in this dissertation. However, to maintain consistency and conscientiousness, the research appeared in publications where the dissertation author is not the first author or the topics are not closely pertaining to the central theme of this dissertation, and the research that is still in progress have been excluded. For reference, lists of all the work that has resulted in publications and patents during the course of this dissertation can be found in Appendix I and II.

Chapter 2

Ubiquitous Aluminum Alkyls and Alkoxides as Effective Catalysts for Glucose to HMF Conversion in Ionic Liquids

2.1 Summary

Metal halides (chlorides in particular) are employed almost exclusively as Lewis acid catalysts for the homogeneous conversion of glucose (or cellulose) to HMF (5-hydroxymethylfurfural) in ionic liquids (ILs), with $CrCl_2$ being arguably the most effective benchmark catalyst. Reported herein is a discovery that ubiquitous aluminum alkyl or alkoxy compounds are very effective Lewis acid catalysts for the glucose-to-HMF conversion in ILs. Under the current reaction conditions (1-ethyl-3-methylimidazolium chloride [EMIM]Cl, 120 ℃, 6 h), simple trialkyl and trialkoxy aluminum species such as $AlEt_3$ and $Al(O^iPr)_3$, which are much cheaper than $CrCl_2$ (by a factor of 5 for $AlEt_3$ or 180 for $Al(O^iPr)_3$), are at least as effective as $CrCl_2$ to catalyze this conversion process. The molecular structure of $[EMIM]^+[ClAlMe(BHT)_2]^-$, formed upon mixing the alkylaryloxy aluminum $MeAl(BHT)_2$ and the IL [EMIM]Cl, has been determined by X-ray diffraction; the structure is similar to that of the metallate $[EMIM]^+[CrCl_3]^-$, the proposed active species responsible for the effective glucose to HMF conversion by $CrCl_2$ in [EMIM]Cl. Another significant finding is that a gradual substitution of the chloride ligand on aluminum by the alkyl ligand brings about a drastic enhancement on the HMF yield, from 1.6% by $AlCl_3$ to 7.6% by $MeAlCl_2$ to 17% by Et_2AlCl

and to 51% by $AlEt_3$, thus showing approximately an overall 32-fold HMF yield enhancement going from $AlCl_3$ to $AlEt_3$.

2.2 Introduction

Research directed at developing effective conversion of nonfood plant biomass into fuels and/or chemicals has intensified in recent years,[1] as this process, once becoming technologically and economically competitive as compared to oil refinery, can provide humanity with a sustainable source of fuels and chemicals. The majority (60–90 wt%) of plant biomass is the biopolymer carbohydrates (sugars) stored in the form of cellulose and hemicelluloses. The biomass-derived sugars can be converted into fuels and value-added chemicals by liquid-phase catalytic processing.[2] Alternatively, cellulosic materials can be directly converted into the biomass platform chemical 5-hydroxymethylfurfural (HMF),[3] a versatile intermediate for top-value-added chemicals and fuels (e.g., 2,5-dimethylfuran, a biofuel with a 40% higher energy density than ethanol[4]). As environmentally benign alternatives to volatile organic solvents, recyclable ionic liquids (ILs) have attracted rapidly growing interest,[5] particularly in the pursuit of renewable energy and chemicals from lignocellulosic biomass.[6] These advances were made possible by the discovery of Rogers and co-workers[7] that showed a class of water-stable and -miscible ILs, 1-alkyl (R)-3-methylimidazolium chloride salts,[8] [RMIM]Cl, can solubilize cellulose in appreciable wt% by disrupting the extensive H-bonding network present in cellulose through H-bonding of the anion of ILs with the hydroxyl groups of cellulose.[9] Excitingly, IL solvents enabled homogenous hydrolysis of cellulose to water-soluble reducing sugars in high to

quantitative conversion, either catalyzed by mineral or organic acids,[10] or even in the absence of any additional catalyst (i.e., with IL-H_2O mixtures).[11]

Through acid-catalyzed dehydration, fructose can be readily converted to HMF typically in high yields.[12] However, glucose, a more desirable feedstock derived from non-food, cellulosic biomass, has been showed to be resistant to its conversion into HMF, thus achieving typically low yields (~10%) by a variety of catalyst systems, such as lanthanide halides $LnCl_3$ (Ln = La^{3+}–Lu^{3+}) in water or organic solvents;[13] the use of $AlCl_3$ in water or organic solvents assisted by microwave radiation improves the HMF yield.[14] Seminal work of Zhang et al. revealed that glucose can also be converted into HMF in good yields when using $CrCl_2$ as catalyst in ILs such as [EMIM]Cl.[15] Thus, the $CrCl_2$-catalyzed process in [EMIM]Cl at 100 ℃ for 3 h achieved a HMF yield of 68–70%; the process was proposed to proceed via *in situ* glucose-to-fructose isomerization catalyzed by the anion $CrCl_3^-$ in the resulting metallate $[EMIM]^+CrCl_3^-$ formed upon mixing $CrCl_2$ and [EMIM]Cl, followed by dehydration of fructose to HMF.[15] A subsequent study reported a lower HMF yield of 62% under the same conditions ([EMIM]Cl, 6 mol% $CrCl_2$, 100 ℃, 3 h). This study provided both experimental and theoretical evidence to support the proposed reaction sequence which involves initial isomerization of glucose to fructose followed by subsequent dehydration of fructose to HMF.[16] Interestingly, the HMF yields for catalyst systems that did not contain $CrCl_x$, including a large number of metal (main-group, transition-metal, and rare-earth) halides, were only 10% or less.[15] Additionally, replacing the $CrCl_x$ catalyst with a BrØnsted acid, either H_2SO_4 [17] or acidic IL [EMIM][HSO_4] ,[18] failed to convert glucose to HMF, although such a system is still very effective in converting fructose to

HMF, the results of which seemed to point out that aldohexoses such as glucose do not have a direct dehydration pathway to HMF and thus require an isomerization catalyst such as $CrCl_2$. On the other hand, Chidambaram and Bell recently showed that a combination of a heteropolyacid, $H_3PMo_{12}O_{40}$, with [EMIM]Cl and co-solvent acetonitrile converted glucose to HMF in high to quantitative conversion.[19]

Since the important discovery of the effective $CrCl_2$/IL system,[15] many other metal halides were reported to catalyze the glucose-to-HMF conversion in the IL media. Ying and co-workers reported that addition of the in situ generated *N*-heterocyclic carbene (NHC) ligand to the $CrCl_2$/IL system enhanced the conversion with a HMF yield up to 81% ([BMIM]Cl, 9 mol% NHC/$CrCl_3$, 100 ℃, 6 h) and concluded that the NHC/$CrCl_x$ complex is the catalyst responsible for the conversion.[20] Han and co-workers found that $SnCl_4$ to be also effective for the conversion of glucose into HMF in [EMIM]BF_4, achieving up to 62% yield,[21] while Zhao et al. revealed that $GeCl_4$ in ILs converted glucose to HMF in 38% or 48% (with addition of molecular sieves) yield.[22] Lanthanide salts $YbCl_3$ and $Yb(OTf)_3$ afforded 12% and 24% HMF yields from glucose conversion in [BMIM]Cl, which were double of those yields achieved in [EMIM]Cl.[23] Binder and Raines reported that cellulose, in a solvent mixture containing *N*,*N*-dimethylacetamide, LiCl and [EMIM]Cl, can also be directly converted into HMF in 54% yield at 140 ℃ for 2 h, using $CrCl_2$ (25 mol%) and HCl (6 mol%) as catalysts.[24] We showed that the reducing sugar mixture resulted from the cellulose hydrolysis with the IL-H_2O mixture can be effectively converted into HMF in the presence of $CrCl_2$; this conversion to HMF can also be carried out in a one-pot fashion starting directly from cellulose.[11] Even without adding additional

catalysts or reagents besides IL [EMIM]Cl and water, Wu and co-workers showed that, under optimized conditions, cellulose can be converted to HMF in up to 21% yield.[25] Zhang et al. utilized the $CrCl_2/CuCl_2$ pair for direct conversion of cellulose to HMF in [EMIM]Cl achieving ~55% yield,[26] while a somewhat higher HMF yield (~60%) was reported later by Cho et al. using the $CrCl_2/RuCl_3$ pair.[27] Zhao et al. reported high HMF yields of 91% and 61% by $CrCl_3$ in [BMIM]Cl under microwave irradiation from glucose and cellulose, respectively,[28] but a subsequent study by Qi et al. reported a HMF yield of 67% from glucose by $CrCl_3$ in [BMIM]Cl also under microwave irradiation.[29] A two-step process involving gradual addition of water in the acid-catalyzed hydrolysis of cellulose step in [EMIM]Cl, which was shown to achieve a high glucose yield of nearly 90% by Binder and Raines,[30] followed by addition of the $CrCl_3$ catalyst in the subsequent step afforded a higher HMF yield of 73% based on cellulose.[31] A lower cellulose-to-HMF yield of 34% was observed using $FeCl_2$ as catalyst for the cellulose conversion in a protic IL.[32] Other metal halides or a combination of them, such as $CrCl_3/LaCl_3$[33] and $MnCl_2$,[34] have also been employed for the cellulose-to-HMF conversion in ILs.

It can be readily seen from the above overview, metal halides (chloride salts in particular) are employed nearly exclusively as *Lewis acid catalysts* for the glucose (or cellulose)-to-HMF conversion in ILs, with $CrCl_2$ being one of the most effective catalysts. We report herein that ubiquitous aluminum alkyl or alkoxy compounds, which are widely used in the olefin polymerization industry and also in general catalysis,[35] are effective catalysts for the glucose-to-HMF conversion in ILs. Significantly, aluminum alkyls (e.g., $AlEt_3$) and alkoxides (e.g., $Al(O^iPr)_3$) are far more effective catalysts than aluminum halides (by 32-fold than $AlCl_3$),

and exhibit comparable or higher HMF yields with the benchmark catalyst $CrCl_2$ under the same conditions, but $AlEt_3$ and $Al(O^iPr)_3$ are ~5 and ~180 times cheaper than $CrCl_2$, respectively.

2.3 Experimental

Materials, reagents, and methods. All syntheses and manipulations of air- and moisture-sensitive materials were carried out in flamed Schlenk-type glassware on a dual-manifold Schlenk line or in an argon or nitrogen-filled glovebox. HPLC-grade organic solvents were sparged extensively with nitrogen during filling of the solvent reservoir and then dried by passage through activated alumina (for Et_2O, THF, and CH_2Cl_2) followed by passage through Q-5-supported copper catalyst (for toluene and hexanes) stainless steel columns. HPLC-grade DMF was degassed, dried over CaH_2 overnight, followed by vacuum transfer (not by distillation). NMR solvents $CDCl_3$ and CD_2Cl_2 were dried over activated Davison 4-Å molecular sieves, and NMR spectra were recorded on a Varian Inova 300 (FT 300 MHz, ^1H; 75 MHz, ^{13}C) or a Varian Inova 400 MHz spectrometer. Chemical shifts for ^1H spectra were referenced to internal solvent resonances and are reported as parts per million relative to tetramethylsilane. The HMF-containing products were analyzed by Agilent 1260 Infinity HPLC system equipped with an Agilent Eclipse Plus C18 Column (100×4.6 mm; 80/20 water/methanol, 0.6 ml/min, 30 ℃) and a UV detector (284 nm). Sugar contents of the products were measured by Agilent 1260 Infinity HPLC system equipped with a Biorad Aminex HPX-87H Column (300×7.8 mm; water, 0.6 ml/min, 45 ℃) and an ELSD (65 ℃, 3.5 bar, gain 6); under such conditions possible sugars (e.g., glucose and fructose) in the reaction mixture can be well

separated and quantified (Figure 2.1a).

D-Glucose (Granular powder, Fisher Chemical), $CrCl_2$ (Alfa Aesar), and aluminum species ($AlCl_3$, $MeAlCl_2$, Et_2AlCl, $Al(O^tBu)_3$, $Al(O^iPr)_3$, $AlMe_3$, $AlEt_3$, and Al^iBu_3, Strem Chemicals) were used as received. Ionic liquids (Fluka) were further purified as follows: 1-ethyl-3-methylimidazolium acetate [EMIM]OAc, dried under vacuum at 100 ℃ for 24 h; 1-ethyl-3-methylimidazolium chloride [EMIM]Cl and 1-butyl-3-methylimidazolium chloride [BMIM]Cl), dried under vacuum at 100 ℃ for 24 h, followed by repeated recrystallization from CH_2Cl_2 and hexanes at room temperature; and 1-H-3-methylimidazolium chloride [HMIM]Cl, purified by sublimation at 120 ℃/500 mTorr for 12 h. The purified ionic liquids were stored in an argon-filled glovebox.

Solution alkyl aluminoxanes (MAO in toluene, Sigma-Aldrich; MMAO in heptanes, Akzo Nobel) were used as received, while the corresponding solid alkyl aluminoxanes were prepared by removing all volatiles of the solutions under vacuum. Butylated hydroxytoluene (BHT-H, 2,6-di-*tert*-butyl-4-methylphenol, Sigma-Aldrich) was recrystallized from hexanes prior to use, and $MeAl(BHT)_2$ was prepared by the reaction of $AlMe_3$ with BHT-H according literature procedures.[36] Tris(pentafluorophenyl)borane, $B(C_6F_5)_3$ was obtained as research gifts from Boulder Scientific Co and further purified by recrystallization from hexanes at –30 ℃; tris(pentafluorophenyl)alane, $Al(C_6F_5)_3$, as a 0.5 toluene adduct $Al(C_6F_5)_3 \cdot (C_7H_8)_{0.5}$ (for vacuum-dried samples), was prepared by the reaction of $B(C_6F_5)_3$ and $AlMe_3$ in a 1:3 toluene/hexanes solvent mixture in quantitative yield (extra caution should be exercised when handling this material, especially the unsolvated form, because of its thermal and shock

sensitivity).[37]

Conversion of glucose to HMF. In a typical experiment, glucose (40.0 mg, 0.220 mmol) was premixed with [EMIM]Cl (200 mg, 1.36 mmol) in a 5 mL vial in the argon-filled glove box, followed by further loading of an aluminum catalyst (0.022 mmol, 10 mol% relative to glucose). Co-solvent (1 mL), when applicable, was added into the mixture. The sealed vial was placed in a temperature-controlled orbit shaker (120 ℃, 300 RPM) and heated at this temperature for 6 h. The reaction was quenched with ice-water and then diluted with a known amount of deionized water. HMF was quantified with calibration curves generated from the commercially available standard in water. A typical HPLC chromatogram of the reaction product for HMF analysis is shown in Figure 2.1b.

Experiments were also performed to analyze possible residue sugars such as glucose and fructose. [EMIM]Cl (1.0 g) and glucose (0.2 g) were charged into a 5 mL vial in a glovebox, followed by further loading of $AlEt_3$ or $MeAl(BHT)_2$ (10 mol% relative to glucose). The mixture was heated at 120 ℃ for 6 h, under which condition the highest HMF yield was achieved. The resulting mixture was diluted to 25 mL after quenching by ice-water, and 0.5 mL of the supernatant was passed through the cation and anion exchange columns to discharge the ionic liquid. A total of 5 mL eluent was collected for HPLC (ELSD detector) analysis (*vide supra*). Glucose recovery after passing through the ions-exchange column was also performed, which showed 96.2 % of recovery. For both $AlEt_3$ and $MeAl(BHT)_2$ catalyzed conversion systems analyzed, no sugars (glucose and fructose) were detected, thus showing glucose was quantitatively converted into HMF (major product) and other side products. Analysis of other

minor products by HPLC [Agilent 1260 Infinity HPLC system equipped with a Biorad Aminex HPX-87H Column (300×7.8 mm; 0.005 M H_2SO_4, 0.6 ml/min, 45 ℃) and a UV detector (268 nm)] showed no levulinic acid but contained other common HMF degradation products such as formic and acetic acids.

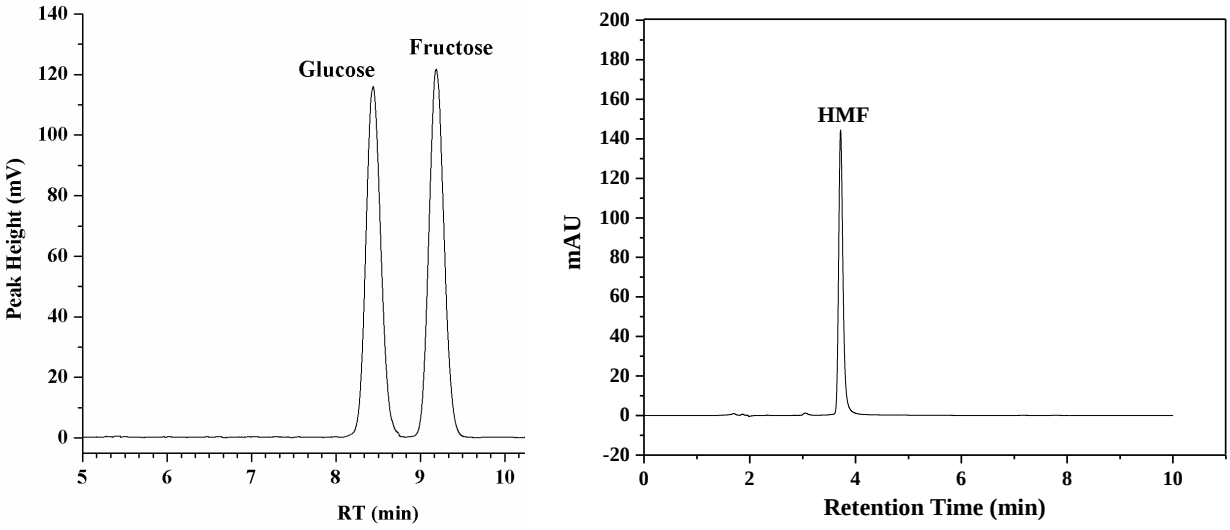

(a) (b)

Figure 2.1 (a) Example of sugar analysis of a mixture containing glucose and fructose by HPLC with an ELSD detector and (b) example of HMF analysis of the product, derived from Et_3Al-catalyzed glucose conversion to HMF at 120 ℃ for 6 h, by HPLC with a UV detector (284 nm).

Formation and X-ray crystallographic analysis of $[EMIM]^+[ClAlMe(BHT)_2]^-$. [EMIM]Cl (15.0 mg, 0.102 mmol) and $MeAl(BHT)_2$ (50.0 mg, 0.104 mmol) were mixed in the argon-filled glovebox and heated at 120 ℃ for 6 h. After being cooled to room temperature, the solid product was dissolved in warm chloroform (40 ℃). The resulting clear solution was stored in a freezer inside the glovebox at –30°C for 3 d, affording colorless single crystals suitable for X-ray diffraction analysis. ^{1}H NMR of the product is consistent with the structure of the title imidazolium aluminate compound. ^{1}H NMR (CD_2Cl_2, 23 ℃) for $[EMIM]^+[ClAlMe(BHT)_2]^-$: δ

8.30 (s,1H, NC*H*N), 7.15, 7.11 (d, 2H, N(C*H*)$_2$N), 6.94 (s, 4H, Ar), 4.08 (q, 2H, C*H*$_2$CH$_3$), 3.75 (s, 3H, N-*Me*), 2.20 (s, 6H, Ar-*Me*), 1.49 (t, 3H, CH$_2$C*H*$_3$), 1.44 (s, 36H, Ar-C*Me*$_3$), –0.55 (s, 3H, Al-*Me*). The molecular structure of this compound was confirmed by X-ray diffraction analysis. Single crystals of this complex were quickly covered with a layer of Paratone-N oil (Exxon, dried and degassed at 120 °C/10^{-6} Torr for 24 h) after decanting the mother liquor. A crystal was then mounted on a thin glass fiber and transferred into the cold nitrogen stream of a Bruker SMART CCD diffractometer. The structure was solved by direct methods and refined using the Bruker SHELXTL program library.[38] The structure was refined by full-matrix least-squares on F^2 for all reflections. All atoms were located by difference Fourier synthesis and refined anisotropically, whereas hydrogen atoms were included in the structure factor calculations at idealized positions, except for the C(2)–H on the imidazolium ring which was located by the difference Fourier synthesis and refined. There is a distorted $CHCl_3$ molecule (crystallization solvent) in the lattice. CCDC-845942 contains the supplementary crystallographic data for this paper. These data can be obtained free of charge from The Cambridge Crystallographic Data Centre via www.ccdc.cam.ac.uk/ data_request/cif.

X-ray crystal structural data for $[EMIM]^+[ClAlMe(BHT)_2]^- \cdot CHCl_3$: $C_{38}H_{61}AlCl_4N_2O_2$, M_r = 746.67, T = 120(2) K, λ = 0.71073 Å, crystal dimensions 0.26 × 0.19 × 0.086 mm^3, monoclinic, *C*2/*c*, a = 38.6843 (10) Å, b = 10.8212(3) Å, c = 20.4111(5) Å, β = 102.708(3)°, V = 8335.0(4) Å^3, Z = 8, ρ_{calcd} = 1.190 Mg/m^3, θ range for data collection = 2.05–24.72°, 64684 reflections collected, 7097 unique (R_{int} = 0.0494), zero restraints, 99.9% completeness to θ = 24.72°, goodness-of-fit on F^2 = 1.013, final R_1 = 0.0617 and wR_2 = 0.1591 with $I > 2\sigma(I)$, and

residual electron density extremes = 0.711 and –0.685 $eÅ^{-3}$.

2.4 Results and Discussion

Comparative studies of aluminum-based catalysts. A total of 12 different aluminum species were investigated for their effectiveness as catalyst for the glucose-to-HMF conversion under identical reaction conditions: [EMIM]Cl (*purified*, see Experimental), 10 mol% Al relative to glucose, 120 ℃, and 6 h, which are optimal conditions for these aluminum-based catalysts (*vide infra*). These aluminum species can be grouped into 5 different classes: (a) aluminum halides or alkyl halides ($AlCl_3$, $MeAlCl_2$, Et_2AlCl); (b) alkyl aluminoxanes (MAO and MMAO, both in solution and solid state); (c) triaryl aluminum ($Al(C_6F_5)_3$), (d) trialkoxy or alkylaryloxy aluminum ($Al(O^iPr)_3$, $Al(O^tBu)_3$, $MeAl(BHT)_2$), and (e) trialkyl aluminum ($AlMe_3$, $AlEt_3$, and Al^iBu_3). It is clear from the results summarized in Figure 2.2 that $AlCl_3$ is least effective, with a low HMF yield of only 1.6%, while $AlEt_3$ is most effective, achieving a much higher HMF yield of 51%. Analysis of sugars in the reaction products produced by the two representative catalysts, $MeAl(BHT)_2$ and $AlEt_3$, showed absence of glucose and fructose, indicating quantitative conversion of glucose to HMF (the major product) and other side products resulted from degradation of HMF (formic and acetic acids, see Experimental). In our hand, the benchmark catalyst $CrCl_2$ under conditions identical to those employed for the current aluminum catalysts (i.e., [EMIM]Cl, 10 mol% catalyst, 120 ℃) gave a HMF yield in the range of 45–50%, depending on reaction time.

Noteworthy are several interesting trends. *First*, a gradual substitution of the chloride

ligand on Al by the alkyl ligand brought about a drastic enhancement on the HMF yield: $AlCl_3$, 1.6%; $MeAlCl_2$, 7.6%; Et_2AlCl, 17%; and $AlEt_3$, 51%. *Second*, alkyl aluminoxanes, having a typical structural formula of $[–(R)Al–O–]_n$,[35] are good catalysts for the glucose-to-HMF conversion, with MMAO derived from mixed trialkyl aluminum ($AlMe_3$ and Al^iBu_3)[35] being considerably more effective than the $AlMe_3$-derived MAO. For both MAO and MMAO, the catalyst state (solution vs solid) gave only modest variations in the HMF yield: 30% (solution) and 27% (solid) for MAO; 45% (solution) and 46% (solid) for MMAO. Consistent with this finding, Al^iBu_3 was noticeably more effective (48%) than $AlMe_3$ (39%). *Third*, Lewis acidity of these aluminum catalysts is *not* an important factor for achieving highly HMF yield. For example, highly Lewis acidic $Al(C_6F_5)_3$ and $AlCl_3$ achieved only modest 31% and low 1.6% yields, respectively, whereas aluminum catalysts with lower Lewis acidity, such as $Al(O^iPr)_3$, $Al(O^tBu)_3$, $MeAl(BHT)_2$, and $AlEt_3$, afforded much higher HMF yields of 49%, 49%, 50%, and 51%, respectively. It is worth noting that the freshly vacuum-distilled $Al(O^iPr)_3$ performed identically to that as received.

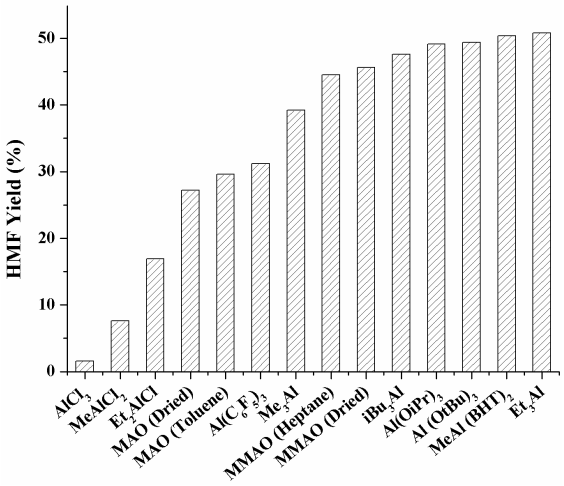

Figure 2.2 Plot of the HMF yield vs. aluminum species under identical conditions: [EMIM]Cl, 10 mol% Al (relative to glucose), 120 ℃, 300 RPM (shaker), and 6 h.

Effects of temperature, time, catalyst loading, IL structure, and co-Solvent. We selectively describe herein our investigations into the three representative, more effective systems, including MMAO (solution), $MeAl(BHT)_2$, and $AlEt_3$, in more detail through variations in reaction temperature and time, catalyst loading, and IL structure. These studies were attempted in order to optimize the catalyst performances.

In the case of MMAO (10 mol%), the glucose-to-HMF conversion was first carried out in [EMIM]Cl for 6 h at four different temperatures of 80 ℃, 100 ℃, 120 ℃, and 130 ℃, achieving HMF yields of 2.0%, 13%, 45%, and 44%, respectively (Figure 2.3). Next, the temperature was fixed at 120 ℃, but the reaction time was varied from 1 h to 24 h (Figure 2.4a). This time profile clearly showed the HMF yield increased initially as time increased, from 24% (1 h) to 36% (3 h) to 45% (6 h), but a further increase in time caused the HMF yield to drop to 34% (12 h) and only 9.8% (24 h), as a result of side reactions associated with the gradual HMF degradation at high temperature with time.[23] Using the conditions with the optimized temperature (120 ℃) and time (6 h), we varied the MMAO catalyst loading from 0 mol% to 30 mol% (Figure 2.4b). Under these conditions, the control run (no catalyst) produced HMF in 5.5% yield; with a catalyst loading of 1, 2, 5, 10, and 20 mol%, the HMF yield steadily increased to 14, 28, 39, 45, and 48%, respectively. A further increase in catalyst loading to 30 mol% actually decreased the HMF yield to 37%, presumably due to the Lewis acid-assisted degradation of the product. Lastly, four different types of ILs were investigated for their relative performances in the glucose-to-HMF conversion catalyzed by MMAO under fixed conditions: 10 mol% catalyst, 120 ℃, and 6 h. The results of this study, summarized in Figure 2.5, clearly showed the best performing IL is

[EMIM]Cl (46%), while the worst performing IL is the basic IL with the acetate anion, [EMIM]OAc (0%), which is known to rapidly degrade HMF even at 100 ℃.[23] Amongst the ILs with the same chloride anion, the one with the smallest *N*-substituents (H, Me), [HMIM]Cl, which is also a protic IL, gave the lowest HMF yield (26%); between the two 1-alkyl-3-methylimidazolium chloride ILs, the ^{n}Bu substituted IL, [BMIM]Cl, gave a lower HMF yield (38%) than the Et substituted IL, [EMIM]Cl (45%). Overall, the optimized conditions for the glucose-to-HMF conversion catalyzed by MMAO are in [EMIM]Cl at 120 ℃ for 6 h, with a 10 mol% catalyst loading. Although the reaction with 20 mol% catalyst gave somewhat higher yield (by 3%), this condition is not desirable, considering the cost associated with a doubling of the catalyst loading.

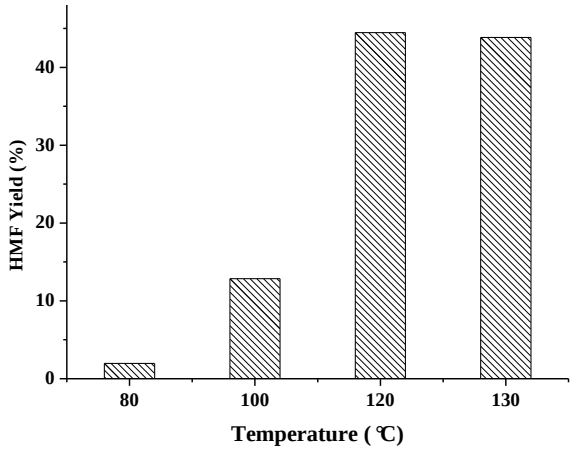

Figure 2.3 Plot of HMF yield as a function of temperature for the glucose-to-HMF conversion by MMAO (10 mol%) in [EMIM]Cl for 6 h.

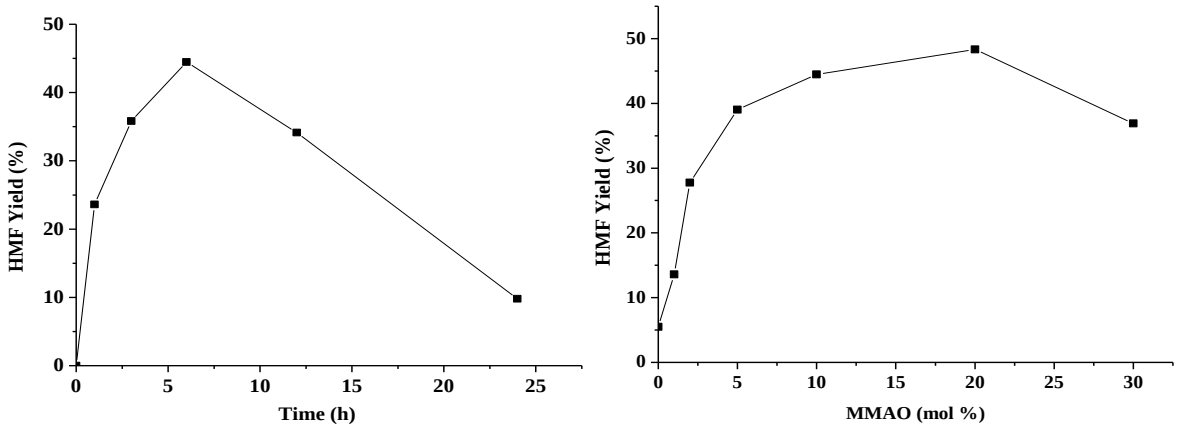

Figure 2.4 Plot of HMF yield as a function of reaction time (a) and catalyst loading (b, 6 h) for the glucose-to-HMF conversion by MMAO (10 mol%) in [EMIM]Cl at 120 ℃.

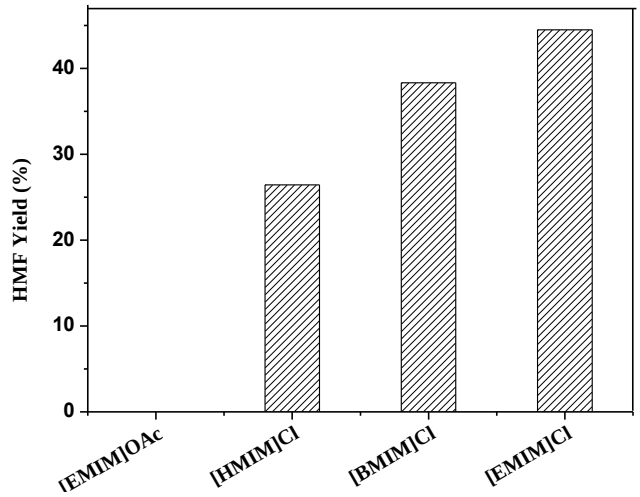

Figure 2.5 Plot of HMF yield as a function of ionic liquid structure for the glucose-to-HMF conversion by MMAO (10 mol%) at 120 ℃ for 6 h.

The alkylaryloxy aluminum catalyst, $MeAl(BHT)_2$, was also investigated for its performance in the glucose-to-HMF conversion, carried out in [EMIM]Cl at 120 ℃ for 6 h, as a function of time and catalyst loading (Figure 2.6a). It is clear from Figure 2.6 that the reaction reached a peak yield of 50% between 3 h and 6 h, but a longer reaction time of 12 h lowered the yield to 46%. On catalyst loading, the reactions with 5 and 10 mol% catalyst loadings gave a same HMF yield of 50%, while the yield was reduced to 42% or 21% when catalyst loading was

either increased to 20 mol% or lowered to 2.5 mol% (Figure 2.6b).

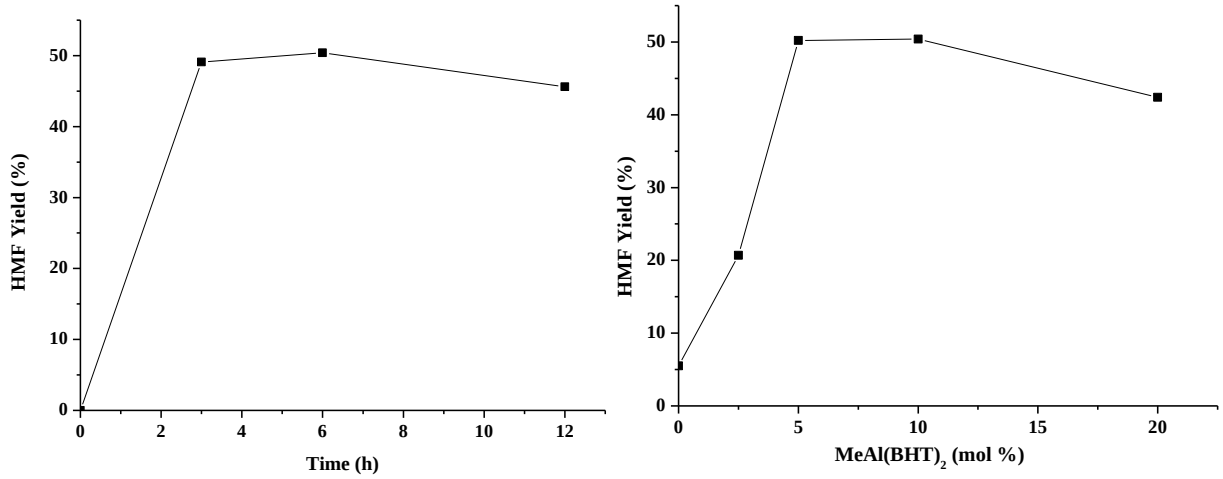

Figure 2.6 Plot of HMF yield as a function of reaction time (a) and catalyst loading (b, 6 h) for the glucose-to-HMF conversion by $MeAl(BHT)_2$ (10 mol%) in [EMIM]Cl at 120 ℃.

Lastly, the most effective catalyst of this series, $AlEt_3$, was further investigated for its performance in the glucose-to-HMF conversion at 120 ℃ with different reaction time, catalyst loading, and IL structure. The reaction time profile, summarized in Figure 2.7a, showed that the peak yield of 51% was achieved at 6 h and that shorter time (3 h) or longer time (12 h) gave lower yields of 45% and 46%, respectively. Similarly to $MeAl(BHT)_2$, the reactions with 5 and 10 mol% $AlEt_3$ gave a same HMF yield of 51%, while the yield was reduced to 30% or 37% when catalyst loading was either increased to 20 mol% or lowered to 2.5 mol% (Figure 2.7b). Investigations into IL structure effects revealed that [BMIM]Cl was less effective (47%) than [EMIM]Cl (51%), under otherwise identical conditions (10 mol% catalyst, 120 ℃, 6 h). Potential organic co-solvent effects were also examined; addition of 1 mL toluene to the reaction carried out in [EMIM]Cl (10 mol% catalyst, 120 ℃, 6 h) did not significantly alter the HMF yield (47%), while the polar donor solvent DMF substantially reduced the HMF yield to 36%. A

similar co-solvent effect was also observed for other trialkyl aluminum catalysts such as Al^{i}Bu$_3$.

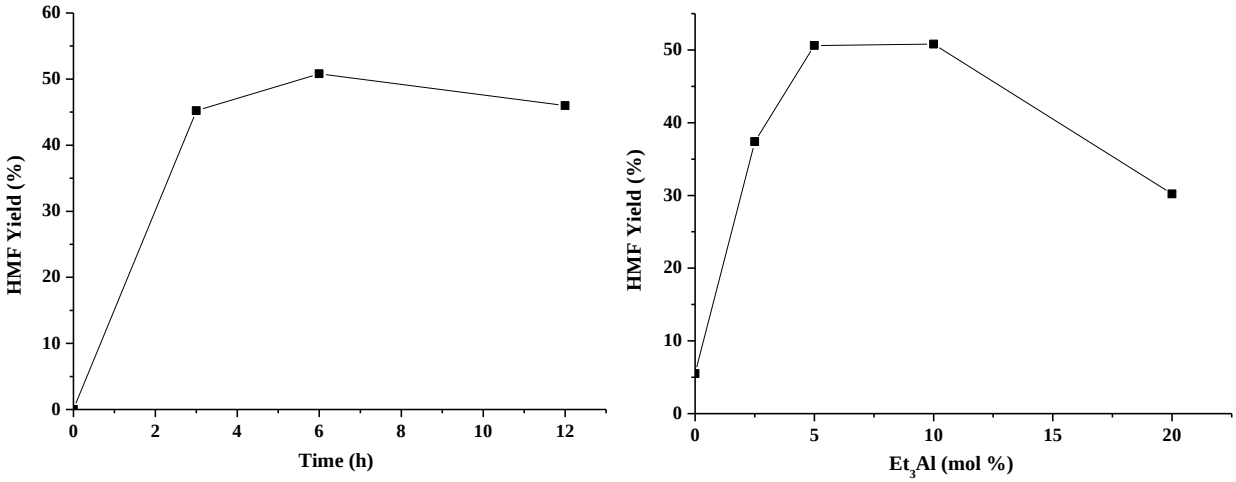

Figure 2.7 Plot of HMF yield as a function of reaction time (a) and catalyst loading (b, 6 h) for the glucose-to-HMF conversion by $AlEt_3$ (10 mol%) in [EMIM]Cl at 120 ℃.

Structure of aluminum catalyst in IL. The active species responsible for the effective conversion of glucose to HMF by $CrCl_2$ in [EMIM]Cl has been proposed to be the metallate $[EMIM]^+CrCl_3^-$, formed upon mixing the $CrCl_2$ catalyst with the IL.[15] To examine if an analogous metallate salt is formed upon mixing the aluminum catalyst with the IL or not, we carried out the reaction of the aluminum alkyl catalyst $MeAl(BHT)_2$ with [EMIM]Cl under the glucose conversion conditions (120 ℃, 6 h, see Experimental). The ^{1}H NMR spectrum (Figure 2.8) of the resulting product is indicative of imidazolium aluminate ion pair $[EMIM]^+[ClAlMe(BHT)_2]^-$, where the chloride is now attached to the aluminum center forming the aluminate anion. The overlay plot (Figure 2.8) of ^{1}H NMR spectra of $[EMIM]^+[ClAlMe(BHT)_2]^-$ and the starting reagents, aluminum Lewis acid $MeAl(BHT)_2$ and IL [EMIM]Cl, clearly shows that, upon the aluminate formation, the Al-*Me* signal is high-field shifted by 0.22 ppm from –0.33 ppm for the neutral aluminum Lewis acid to –0.55 ppm for the

anionic aluminate product, and the C(2)–*H* signal in the imidazolium cation is also shifted to a higher field by 2.6 ppm (from 10.9 ppm to 8.30 ppm). All other signals are also high-field shifted upon the imidazolium aluminate formation, although to a lesser extent.

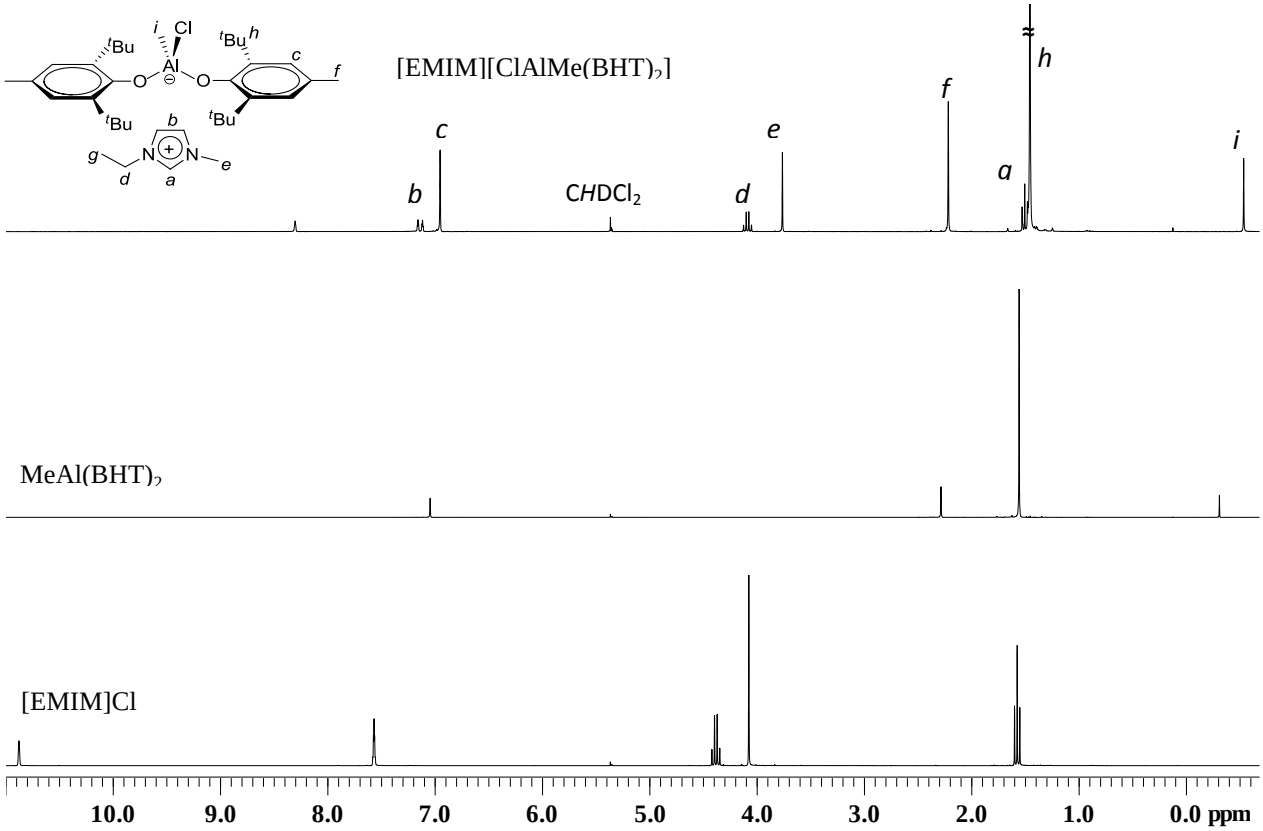

Figure 2.8 Overlay plot of ^{1}H NMR (CD_2Cl_2, 23 ℃) spectra of $[EMIM]^{+}[ClAlMe(BHT)_2]^{-}$ (top), $MeAl(BHT)_2$ (middle), and [EMIM]Cl (bottom).

The molecular structure of this compound was confirmed by X-ray diffraction analysis, featuring the ion pair consisting of the unassociated imidazolium cation $[EMIM]^{+}$ and the aluminate anion $[ClAlMe(BHT)_2]^{-}$ (Figure 2.9). However, the crystal packing diagram depicted in Figure 2.10 clearly shows close intermolecular contacts between the cation $[EMIM]^{+}$ of one molecular with the anion $[ClAlMe(BHT)_2]^{-}$ of another molecule, via intermolecular H–bonding between the C(2)–*H* on the imidazolium ring and the Al–*Cl* on the aluminate anion. Metric

parameters involved in this intermolecular H–bonding motif consist of C(2A)–H(2A) = 0.93(4) Å, H(2A)–Cl(1B) = 2.742 Å, C(2A)–Cl(1B) = 3.416 Å, and C(2A)–H(2A)–Cl(1B) = 130.08°, pointing to weak (electrostatic) H–bonding.[39] Hence, this structure is significantly different from $[EMIM]_{2n}^{+}[Cr_2Cl_6]_n^{-}$, derived from the reaction of [EMIM]Cl + $CrCl_2$, in which the resulting anion forms one-dimensional chains of chloride-bridged distorted octahedral Cr(II) centers.[40] The geometry around the four-coordinate aluminum center is that of a distorted tetrahedron with a sum of the O–Al–O(Cl) angles of 321.8º, as in the case of another rare example of the $MeAl(BHT)_2$-derived anion, $Li^{+}[Me_2C{=}C(O^{i}Pr)OAlMe(BHT)_2]^{-}$.[41] The Al–C bond [2.019(3) Å] is somewhat longer than that found in the neutral $MeAl(BHT)_2$ [1.927(3) Å],[36] as predicted on changing from a planar to tetrahedral geometry in terms of the increased p character in the Al–C bond. The Al–O (BHT) bonds [1.752(2), 1.757(2) Å] are also longer than those found in the neutral $MeAl(BHT)_2$ [1.687(2), 1.685(2) Å].[36]

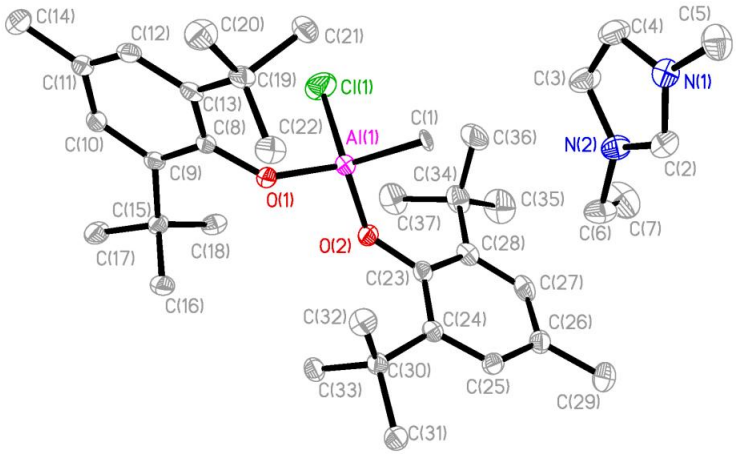

Figure 2.9 X-ray single crystal structure of $[EMIM]^{+}[ClAlMe(BHT)_2]^{-}$, with thermal ellipsoids drawn at the 50% probability. Selected bond lengths [Å] and angles [°]: Al(1)–O(1) = 1.752(2), Al(1)–O(2) = 1.757(2), Al(1)–C(1) = 2.019(3), Al(1)–Cl(1) = 2.203(1), C(2)–H(2) = 0.93(4); C(1)–Al(1)–Cl(1) = 111.81(10), C(1)–Al(1)–O(1) = 116.97(11), C(1)–Al(1)–O(2) = 106.24(11), Cl(1)–Al(1)–O(1) = 100.78(8), Cl(1)–Al(1)–O(2) = 110.57(8), O(1)–Al(1)–O(2) = 110.46(10).

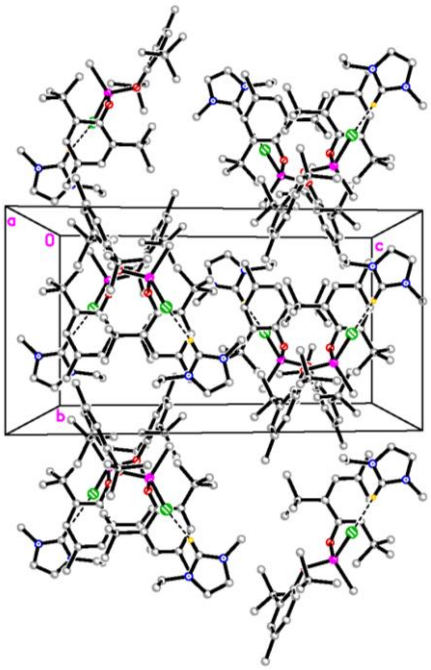

Figure 2.10 Molecular packing diagram of $[EMIM]^+[ClAlMe(BHT)_2]^-$, highlighting weak intermolecular (electrostatic) H–bonding between the C(2)–H on the imidazolium ring and the Al–Cl on the aluminate anion: C(2A)–H(2A) = 0.93(4) Å, H(2A)–Cl(1B) = 2.742 Å, C(2A)–Cl(1B) = 3.416 Å; C(2A)–H(2A)–Cl(1B) = 130.08°.

Overall, the structure $[EMIM]^+[ClAlMe(BHT)_2]^-$ simulates $[EMIM]^+[CrCl_3]^-$, the proposed active metallate species responsible for the effective glucose-to-HMF conversion by $CrCl_2$ in [EMIM]Cl,[15] thereby reasoning why the [EMIM]Cl + $AlMe(BHT)_2$ system is also very effective for this conversion. In comparison, the [EMIM]Cl + $AlCl_3$ or [EMIM]Cl + $MeAlCl_2$ system is much inferior. Although room-temperature chloroaluminate molten salts can be readily formed by mixing [EMIM]Cl with $AlCl_3$, the structure depends on the mole fraction (N) of $AlCl_3$ used in preparing the melt.[42] Specifically, when N is less than 0.5 (i.e., the current scenario), it contains Cl^-, which acts as a Lewis base, and is basic; when $N > 0.50$, the melt is considered acidic because it contains $Al_2Cl_7^-$. Hence, the structure and feature of the chloroaluminate from $AlCl_3$ is different from that of $[ClAlMe(BHT)_2]^-$ or $[CrCl_3]^-$, which is considered bifunctional in

catalyzing glucose-to-fructose isomerization and subsequent dehydration to HMF,[15] with the chloride ligand serving as the basic site and the metal as the acidic site. Another key difference between the metallate salts derived from aluminum chloride and aluminum alkyl or alkoxy compounds is their relative hydrolytic stability; as the conversion process eliminates water, the less hydrolytically stable chloroaluminate salts from $AlCl_3$ are expected to undergo rapid catalyst deactivation as soon as the dehydration reaction takes place.

2.5 Conclusions

Five classes of aluminum species have been investigated as Lewis acid catalysts for the glucose-to-HMF conversion in IL solvents. Amongst several interesting trends observed for these aluminum-based catalysts, the most significant is the drastic enhancement of the HMF yield upon a gradual substitution of the chloride ligand on Al by the alkyl ligand. Hence, $AlEt_3$, which achieved 51% HMF yield from the reaction carried out in [EMIM]Cl at 120 ℃ for 6 h, is a much better catalyst than $AlCl_3$, which gave only 1.6% HMF yield, under otherwise identical conditions.

Investigations into effects of temperature, time, catalyst loading and IL structure on the HMF yield revealed that: (a) [EMIM]Cl is the most effective IL amongst the four ILs investigated herein; (b) reactions carried out at 120 ℃ for 6 h afford higher yields than the reactions under other conditions; and (c) 5 or 10 mol% aluminum alkyl catalyst loadings typically give similar yields, which are higher than those with lower or higher catalyst loadings. Under the current reaction conditions, $AlEt_3$ and $Al(O^iPr)_3$ are at least as effective as

$CrCl_2$—the most effective benchmark metal halide catalyst reported in literature, and yet $AlEt_3$ and $Al(O^iPr)_3$ are about 5 and 180 times cheaper than $CrCl_2$, respectively, thereby showing cost-saving features of the present alkyl aluminum catalyst system.

The molecular structure of $[EMIM]^+[ClAlMe(BHT)_2]^-$, formed upon mixing the aluminum Lewis acid $MeAl(BHT)_2$ and the IL [EMIM]Cl under the glucose conversion conditions, shows no intramolecular but weak intermolecular H–bonding between the C(2)–*H* and the Al–*Cl*. This structure simulates that of the metallate $[EMIM]^+[CrCl_3]^-$, the proposed active species responsible for the effective glucose to HMF conversion by $CrCl_2$ in [EMIM]Cl, thereby reasoning why the [EMIM]Cl + $AlMe(BHT)_2$ system is also very effective for this conversion. Significantly, the unexpected finding that the aluminum alkyl (alkoxy) catalysts are ~32-fold more effective than the aluminum halide catalyst should impact future developments of new and more effective catalysts based on other metals.

2.6 Referenes

(1) For selected reviews, see: (a) Alonso, D. M.; Bond J. Q.; Dumesic, J. A. *Green Chem.* **2010**, *12*, 1493−1513. (b) Stöcker M. *Angew. Chem. Int. Ed.* **2008**, *47*, 9200−9211. (c) "NSF 2008. Breaking the Chemical and Engineering Barriers to Lignocellulosic Biofuels: Next Generation Hydrocarbon Biorefineries", Huber, G. W. Ed. report from the NSF Workshop. (d) Corma, A.; Iborra S.; Velty, A. *Chem. Rev.* **2007**, *107*, 2411−2502. (e) Chheda, J. N.;

Huber, G. W.; Dumesic, J. A. *Angew. Chem. Int. Ed.* **2007**, *46*, 7164−7183. (f) Huber G. W.; Iborra S.; Corma A. *Chem. Rev.* **2006**, *106*, 4044−4098.

(2) (a) Chheda, J. N.; Huber, G. W.; Dumesic J. A. *Angew. Chem. Int. Ed.* **2007**, *46*, 7164−7183. (b) Huber, G. W.; Chheda, J. N.; Barrett C. J.; Dumesic, J. A. *Science* **2005**, *308*, 1446−1450.

(3) "Top Value Added Chemicals from Biomass", Werpy, T.; Petersen, G. Eds. U.S. Department of Energy (DOE) report: DOE/GO-102004-1992, 2004.

(4) Román-Leshkov, Y.; Barrett, C. J.; Liu Z. Y.; Dumesic, J. A. *Nature* **2007**, *447*, 982−986.

(5) (a) Ionic Liquids in Synthesis, 2nd ed., Wasserscheid, P.; Welton, T. Eds. Wiley-VCH: Weinheim, 2008. (b) Pârvulescu, V. I.; Hardacre, C. *Chem. Rev.* **2007**, *107*, 2615−2665. (c) Stark, A.; Seddon, K. Ionic Liquids in Kirk-Othmer Encyclopedia of Chemical Technology; John Wiley and Sons: New York, **2007**; Vol. *26*; pp 836–920.

(6) (a) Sun, N.; Rodriguez, H.; Rahman, M.; Rogers, R. D. *Chem. Commun.* **2011**, *47*, 1405−1421. (b) Pinkert, A.; Marsh, K. N.; Pang, S.; Staiger, M. P. *Chem. Rev.* **2009**, *109*, 6712−6728.

(7) Swatloski, R. P.; Spear, S. K.; Holbrey, J. D.; Rogers, R. D. *J. Am. Chem. Soc.* **2002**, *124*, 4974−4975.

(8) Wilkes, J. S.; Zaworotko, M. J. *Chem. Commun.* **1992**, 965−967.

(9) Remsing, R. C.; Swatloski, R. P.; Rogers, R. D.; Moyna, G. *Chem. Commun.* **2006**, 1271−1273.

(10) (a) Sean, J. D.; Bell, A. T. *ChemSusChem* **2011**, *4*, 1166−1173. (b) Vanoye L.; Fanselow, M.; Holbrey, J.; Atkins, M. P.; Seddon, K. R. *Green Chem.* **2009**, *11*, 390−396. (c) Li, C.; Wang, Q.; Zhao, Z. K. *Green Chem.* **2008**, *10*, 177−182. (d) Li, C.; Zhao, Z. K. *Adv. Synth. Catal.* **2007**, *349*, 1847−1850.

(11) Zhang, Y.; Du, H.; Qian, X.; Chen, E. Y.-X. *Energy & Fuels* **2010**, *24*, 2410–2417.

(12) For selected examples, see: (a) Lai, L.; Zhang, Y. *ChemSusChem* **2010**, *3*, 1257−1259. (b) Chan, J. Y. G.; Zhang, Y. *ChemSusChem* **2009**, *2*, 731−734. (c) Qi, X.; Watanabe, M.; Aida, T. M.; Smith, R. L. Jr. *ChemSusChem* **2009**, *2*, 944−946. (d) Román-Leshkov, Y.; Chheda, J. N.; Dumesic, J. A. *Science* **2006**, *312*, 1933−1937. (e) Moreau, C.; Finiels, A.; Vanoye, L. *J. Mol. Catal. A: Chem.* **2006**, *253*, 165−169. (f) Lansalot-Matras, C.; Moreau, C. *Catal. Commun.* **2003**, *4*, 517−520.

(13) (a) Seri, K.-I.; Inoue, Y.; Ishida, H. *Bull. Chem. Soc. Japn.* **2001**, *74*, 1145–1150. (b) Seri, K.-I.; Inoue, Y.; Ishida, H. *Chem. Lett.* **2000**, 22–23. (c) Ishida, H.; Seri, K.-I. *J. Mol. Catal. A. Chem.* **1996**, *112*, L163–L165.

(14) De, S.; Dutta, S.; Saha, B. *Green Chem.* **2011**, *13*, 2859–2868.

(15) Zhao, H.; Holladay, J. E.; Brown, H.; Zhang, Z. C. *Science* **2007**, *316*, 1597−1600.

(16) Pidko, E.; Degirmenci, V.; van Santen, R. A.; Hensen, E. J. M. *Angew. Chem. Int. Ed.* **2010**, *49*, 2530−2534.

(17) Sievers, C.; Musin, I.; Marzialetti, T.; Olarte, M. B. V.; Agrawal, P. K.; Jones, C. W. *ChemSusChem* **2009**, *2*, 665−671.

(18) Lima, S.; Neves, P.; Antunes, M. M.; Pillinger, M.; Ignatyev, N.; Velente, A. A. *Appl. Catal. A.* **2009**, *363*, 93−99.

(19) Chidambaram, M.; Bell, A. T. *Green Chem.* **2010**, *12*, 1253−1262.

(20) Yong, G.; Zhang, Y.; Ying, J. Y. *Angew. Chem. Int. Ed.* **2008**, *47*, 9345−9348.

(21) Hu, S.; Zhang, Z.; Song, J.; Zhou, Y.; Han, B. *Green Chem.* **2009**, *11*, 1746−1749.

(22) Zhang, Z.; Wang, Q.; Xie, H.; Liu, W.; Zhao, Z. K. *ChemSusChem* **2011**, *4*, 131−138.

(23) Ståhlberg, T.; Sørensen, M. G.; Riisager, A. *Green Chem.* **2010**, *12*, 321−325.

(24) Binder, J. B.; Raines, R. T. *J. Am. Chem. Soc.* **2009**, *131*, 1979−1985.

(25) Hsu, W.-H.; Lee, Y.-Y.; Peng, W.-H.; Wu, K. C.-W. *Catal. Today* **2011**, *174*, 65−69.

(26) Su, Y.; Brown, H. M.; Huang, X.; Zhou, X.-D.; Amonette, J. E.; Zhang, Z. C. *Appl. Catal. A.* **2009**, *361*, 117−122.

(27) Kim, B.; Jeong, J.; Lee, D.; Kim, S.; Yoon, H.-J.; Lee, Y.-S.; Cho, J. K. *Green Chem.* **2011**, *13*, 1593−1506.

(28) Li, C.; Zhang, Z.; Zhao, Z. K. *Tetrahedron Lett.* **2009**, *50*, 5403−5405.

(29) Qi, X.; Watanabe, M.; Aida, T. M.; Smith, R. L. Jr. *ChemSusChem* **2010**, *3*, 1071−1077.

(30) Binder, J. B.; Raines, R. T. *Proc. Natl. Acad. Sci.* **2010**, *107*, 4516−4521.

(31) Qi, X.; Watanabe, M.; Aida, T. M.; Smith, R. L. Jr. *Cellulose* **2011**, *18*, 1327−1333.

(32) Tao, F.; Song, H.; Chou, L. *ChemSusChem* **2010**, *3*, 1298−1303.

(33) Wang, P.; Yu, H.; Zhan, S.; Wang, S. *Biores. Tech.* **2011**, *102*, 4179−4183.

(34) Tao, F.; Song, H.; Yang, J.; Chou, L. *Carbohydrate Polym.* **2011**, *85*, 363−368.

(35) Chen, E. Y.-X.; Marks, T. J. *Chem. Rev.* **2000**, *100*, 1391−1434.

(36) Shreve, A. P.; Mulhaupt, R.; Fultz, W.; Calabrese, J.; Robbins, W.; Ittel, S. *Organometallics* **1988**, *7*, 409–416.

(37) Feng, S.; Roof, G. R.; Chen, E. Y.-X. *Organometallics* **2002**, *21*, 832–839.

(38) SHELXTL, Version 6.12; Bruker Analytical X-ray Solutions: Madison, WI, **2001**.

(39) Jeffrey, G. A. An Introduction to Hydrogen Bonding, Oxford University Press, **1997**.

(40) Danford, J. J.; Arif, A. M.; Berreau, L. M. *Acta Cryst.* **2009**, *E65*, m227.

(41) Rodriguez-Delgado, A.; Chen, E. Y.-X. *J. Am. Chem. Soc.* **2005**, *127*, 961−974.

(42) Dieter, K. M.; Dymek, C. J. Jr.; Heimer, N. E.; Rovang, J. W.; Wilkes, J. S. *J. Am. Chem. Soc.* **1988**, *110*, 2722−2726.

Chapter 3

Polymeric Ionic Liquid (PIL)-Supported Recyclable Catalysts for Biomass Conversion into HMF

3.1 Summary

This contribution reports the first study of recyclable PIL-supported metal (Cr, Al) catalysts for effective biomass (glucose and cellulose) conversion into 5-hydroxymethylfurfural (HMF), a key biorefining building block and biomass platform chemical. Of the five different PILs investigated, poly(3-butyl-1-vinylimidazolium chloride), P[BVIM]Cl, has been found to be most effective; when combined with $CrCl_2$ *in situ* or used as the preformed PIL-metallate $P[BVIM]^+[CrCl_3]^-$ in DMF, this PIL-supported catalyst converts glucose to HMF in 65.8% yield at 120 ℃ for 3 h. This yield is higher than those achieved by the catalysts based on the PIL monomer, [BVIM]Cl-$CrCl_2$, as well as by the most commonly used molecular IL based catalyst, 1-ethyl-3-methylimidazolium chloride ([EMIM]Cl)-$CrCl_2$, under otherwise identical conditions. The P[BVIM]Cl-$CrCl_2$ catalyst system also works well for the cellulose-to-HMF conversion via a two-step process. The analogous PIL-Al catalyst, P[BVIM]Cl-Et_2AlCl, is less effective than the PIL-$CrCl_2$ system, but recyclability tests indicate the PIL-Al system is more recyclable thus achieving a nearly constant HMF yield upon 6 cycles.

3.2 Introduction

Sustainability is an emerging global issue of importance to all humanity. To address this issue, major efforts have been directed at developing effective pathways to convert nonfood plant biomass into biofuels and/or feedstock chemicals, as this biomass conversion process holds promise to provide humanity with a sustainable source of fuels, materials and chemicals, once it becomes technologically and economically competitive compared to traditional oil refinery.[1] In this context, 5-hydroxymethylfurfural (HMF),[2] a dehydration product from fructose or glucose, has been identified as a biomass platform chemical and key biorefining building block from plant biomass to bio-based sustainable polymers and promising biofuels such as 2,5-dimethylfuran.[1,3-5] With its immiscible property with water and close energy content (31.5 MJ/L) with gasoline (35 MJ/L),[4,6] 2,5-dimethylfuran is considered as a potential replacement of traditional fossil fuels. We recently showed that HMF can also be quantitatively upgraded into 5,5'-di(hydroxymethyl)furoin, a promising C_{12} kerosene/jet fuel intermediate by organic catalysts.[7]

Quantitative conversion of fructose to HMF has been reported with acid catalysts[8-10] and even without such catalysts[11] or at room temperature.[12] Seminal work by Zhang et al. revealed that glucose, a more desirable feedstock derived from nonfood cellulosic biomass, can be effectively converted to HMF by $CrCl_2$ in ionic liquid (IL) solvents[13, 14] such as 1-ethyl-3-methylimidazolium chloride ([EMIM]Cl) at 100 ℃ for 3 h, achieving 70% HMF yield, accompanied by a negligible amount of levulinic acid.[3] The metallate complex $[EMIM]^+CrCl_3^-$, formed upon mixing $CrCl_2$ with [EMIM]Cl[3,15] has been proposed to be the active species that

catalyzes the glucose-to-fructose isomerization, followed by dehydration of fructose to HMF. A subsequent study by Hensen et al. reported a lower HMF yield of 62% under the same conditions ([EMIM]Cl, 6 mol% $CrCl_2$, 100 ℃, 3 h), but this study provided both experimental and theoretical evidence to support the proposed reaction sequence involving initial isomerization of glucose to fructose, likely catalyzed by a Cr^{2+} dimer ($Cr_2Cl_5^-$, derived from $CrCl_2$ + $CrCl_3^-$), followed by subsequent dehydration of fructose to HMF.[16] On the other hand, Ying et al. concluded that the *N*-heterocyclic carbene (NHC)/$CrCl_x$ complex is the catalyst responsible for the glucose-to-HMF conversion, largely based on the observation that addition of the *in situ* generated NHC ligand to the $CrCl_2$/IL system noticeably enhanced the HMF yield.[17] Many other catalyst systems have also been reported to be effective for the glucose-to-HMF conversion in ILs.[18-24] We recently disclosed that ubiquitous and inexpensive aluminum alkyl or alkoxy compounds, are as effective as the benchmark catalyst $CrCl_2$ under identical conditions, for catalyzing the glucose-to-HMF conversion in [EMIM]Cl.[25]

From an economical point of view, it is more desirable to convert cellulose directly into HMF. Binder and Raines reported that cellulose, in a solvent mixture containing DMA, LiCl and [EMIM]Cl as well as using $CrCl_2$ (25 mol%) and HCl (6 mol%) as catalyst, can be converted directly into HMF in 54% yield at 140 ℃ for 2 h.[4] Zhang et al. developed the paired metal catalyst $CuCl_2$/$CrCl_2$ in [EMIM]Cl for cellulose-to-HMF conversion, achieving up to 55% HMF yield in a one-pot conversion at 120 ℃ for 8 h,[26] while a higher HMF yield (~60%) was reported later by Cho et al. using the $CrCl_2$/$RuCl_3$ pair.[27] We showed that reducing sugars, produced near quantitatively from the cellulose hydrolysis with the IL-H_2O mixture, can be

effectively converted into HMF in the presence of $CrCl_2$; this conversion can also be carried out in a one-pot fashion starting from cellulose.[28] A stepwise water addition procedure in the cellulose hydrolysis by HCl at 105 ℃ over a 12 h period achieved a high yield of glucose (~90%).[29] Adopting the stepwise water addition procedure in the presence of the strong acid cation exchange resin, Qi et al. achieved a considerably higher HMF yield of 73% at 120 ℃ with the [EMIM]Cl-$CrCl_3$ system.[30] Moreover, microwave irradiation was utilized, achieving good HMF yields from cellulose.[31,32] Other metal halides or a combination, such as $CrCl_3$/$LaCl_3$[33] and $MnCl_2$[34] have also been employed for the cellulose-to-HMF conversion in ILs.

Considering the costs associated with the ILs and catalysts employed in the above biomass conversion processes, it is even more desirable to render the IL solvent and the metal catalyst recyclable. Accordingly, several studies have been carried out to investigate the recyclability of the above catalyst systems.[18,19,26,35] For example, Han et al. recycled the [EMIM]Cl-$SnCl_4$ catalyst by performing ethyl acetate extraction of HMF produced at each cycle and achieved a consistent HMF yield of 60% from glucose during 4 cycles.[18] By recycling the [EMIM]Cl-$CuCl_2$/$CrCl_2$ catalyst system, Zhang et al. achieved a near consistent HMF yield of ~55% from cellulose during 12 recycles.[26] While achieving a considerable recovery and yield of HMF by performing extraction with organic solvents such as diethyl ether, ethyl acetate, and methyl isobutyl ketone, the IL phase after exaction exists as viscous liquid, even after extensive vacuum drying, thus making the transport and storage undesirable. Hence, the central objective of this work was to develop a new strategy to render catalysts recyclable: use of a polymeric ionic liquid (PIL) as a catalyst support for efficient biomass conversion and convenient catalyst

recovery. As polymers are commonly used as suitable supports for anchoring molecular catalysts in catalysis,[36] we were intrigued by the potential of the PIL-supported metal catalyst for biomass conversion. Accordingly, we investigated five different imidazolium halide-based PILs, depicted in Scheme 3.1, in replacement of the prototype molecular IL [EMIM]Cl, to formulate PIL-supported catalysts by either in situ mixing with metal (Cr, Al) species or performing PIL-metallate complexes (Scheme 3.1) and subsequently utilize them for biomass conversion in the presence of an organic co-solvent. Significantly, PIL-supported catalysts have been found to catalyze effectively the conversion of glucose or cellulose into HMF and be readily recyclable. The best-performing PIL-supported catalyst, P[BVIM]Cl-$CrCl_2$ or P[BVIM]$^+$[$CrCl_3$]$^-$, converts glucose to HMF in 65.8% yield at 120 ℃ for 3 h, the yield of which is considerably higher than the 49.0% yield achieved by the catalyst system based on its monomeric form, [BVIM]Cl-$CrCl_2$, and is also higher than the 54.9% yield afforded by the most commonly used molecular IL based catalyst, [EMIM]Cl-$CrCl_2$, under otherwise identical conditions.

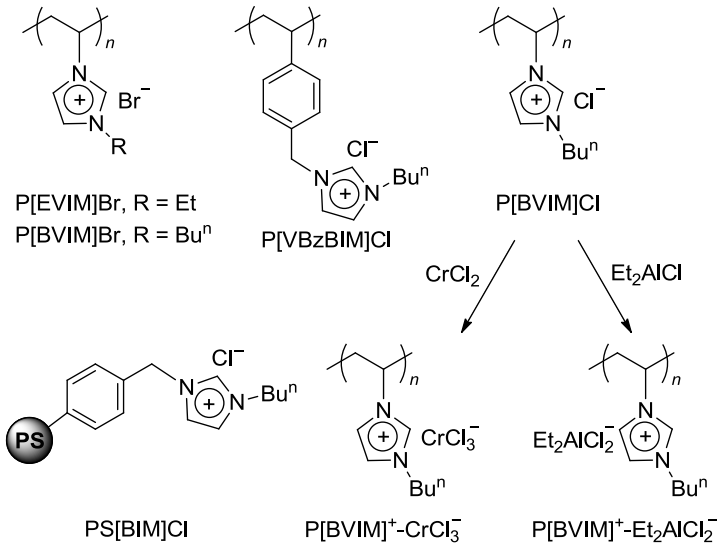

Scheme 3.1 Structure of the five PILs and selected two PIL-metallates investigated in this study.

3.3 Experimental

Materials, reagents, and methods. All syntheses and manipulations of air- and moisture-sensitive materials were carried out in flamed Schlenk-type glassware on a dual-manifold Schlenk line or in an inert gas (Ar or N_2) filled glovebox. HPLC-grade organic solvents were sparged extensively with nitrogen during filling of the solvent reservoir and then dried by passage through activated alumina (for Et_2O, THF, and CH_2Cl_2) followed by passage through Q-5-supported copper catalyst (for toluene and hexanes) stainless steel columns. Acetic acid, pyridine, hexamethylphosphoramide (HMPA), acetonitrile (ACN), dimethyl sulfoxide (DMSO), and dimethylacetamide (DMA) were degassed and dried over activated Davison 4-Å molecular sieves overnight. HPLC-grade *N*,*N*-dimethylformamide (DMF) was degassed, dried over CaH_2, filtered, and vacuum-distilled; the dried DMF was stored over activated molecular sieves overnight.

NMR spectra were recorded on a Varian Inova 300 (FT 300 MHz) or a Varian Inova 400 MHz spectrometer. Chemical shifts for ^1H spectra were referenced to internal solvent resonances and were reported as parts per million relative to tetramethylsilane. The HMF-containing products were analyzed by Agilent 1260 Infinity HPLC system equipped with an Agilent Eclipse Plus C18 Column (100×4.6 mm; 80/20 water/methanol, 0.6 ml/min, 30 ℃) and a UV detector (284 nm). Sugar contents of the products were measured by Agilent 1260 Infinity HPLC system equipped with a Biorad Aminex HPX-87H Column (300×7.8 mm; water, 0.6 ml/min, 45 ℃) and an ELSD (65 ℃, 3.5 bar, gain 6); under such conditions possible sugars (e.g., glucose and fructose) in the reaction mixture can be well separated and quantified. Glass transition

temperatures (T_g) of polymers were measured by differential scanning calorimetry (DSC) on a TA DSC 2920 instrument. Polymer samples were first heated to 220 ℃ at 20 ℃/min, equilibrated isothermally for 4 min, then cooled to 30 ℃ at 20 ℃/min, held at this temperature for 4 min, and reheated to 250 ℃ at 10 ℃/min. All T_g values were obtained from the second scan after the removal of thermal history by the first scan. Gel Permeation chromatography (GPC) analyses of PILs were carried out at 40 ℃ and a flow rate of 1.0 mL/min, with 0.025 M LiBr DMF solution as the eluent, on a Waters University 1500 GPC instrument equipped with two 5μm PL gel columns (Polymer Laboratories) and calibrated using 10 poly(methyl methacrylate) (PMMA) standards. Chromatograms were processed with Waters Empower software (2002); number-average molecular weight (M_n) and polydispersity index (PDI = M_w/M_n) of polymers were given relative to PMMA standards. Metal analysis of the isolated PIL-supported catalysts was carried out by inductively coupled plasma optical emission spectrometry (ICP-OES) with the modified version of EPA methods (2007).

1-Bromoethane, 1-bromobutane, N-butylimidazole, 1-chlorobutane, 1-vinylimidazole, 4-vinylbenzyl chloride, microcrystalline cellulose (Aldrich, 230 DPv, 66 % crystallinity), D-glucose (Granular powder, Fisher Chemical), $CrCl_2$ (Alfa Aesar), merrifield resin (Alfa Aesar, 1% crosslinked, 200-400 mesh, 1.0-1.3 mmol/g), lithium bis(Trifluoromethanesulphonyl)imide $(CF_3SO_2)_2NLi$ (Acros Organics), t-BuOK (Acros Organics) and aluminum compounds ($AlCl_3$, $MeAlCl_2$, Et_2AlCl, $Al(O^iPr)_3$, Et_3Al, Strem Chemicals) were used as received. NaH was prewashed with hexane and dried in vacuum. Butylated hydroxytoluene (BHT-H, 2,6-di-*tert*-butyl-4-methylphenol, Sigma-Aldrich) was recrystallized from hexanes prior to use,

and $MeAl(BHT)_2$ was prepared by the reaction of $AlMe_3$ with BHT-H according literature procedures. [37] Azobisisobutyronitrile (AIBN) was recrystallized in methanol. 1-ethyl-3-methylimidazolium chloride ([EMIM]Cl, Fluka) and 1-butyl-3-methylimidazolium chloride ([BMIM]Cl, Fluka) were dried under vacuum at 100 ℃ for 24 h, followed by repeated recrystallization from CH_2Cl_2 and hexanes at room temperature. The purified ionic liquids were stored in an argon-filled glovebox.

Water-soluble PILs. Literature procedures[38,39] were modified to prepare water-soluble PILs, poly(3-alkyl-1-vinylimidazolium halide)s. Described below was a typical procedure, using the preparation of poly(3-butyl-1-vinylimidazolium chloride), P[BVIM]Cl (M_n = 70,400 g/mol, PDI = 1.20, T_g = 213 ℃), as an example. Poly(3-butyl-1-vinylimidazolium bromide), P[BVIM]Br (M_n = 4,620 g/mol, PDI = 1.15), and poly(3-ethylvinylimidazolium bromide), P[EVIM]Br (M_n = 5,120 g/mol, PDI = 1.11), were prepared in the similar fashion, whereas poly[1-(4-vinylbenzyl)-3-butylimidazolium chloride], P[VBzBIM]Cl, was prepared following a quite different literature procedures.[40]

Poly(3-butyl-1-vinylimidazolium chloride), P[BVIM]Cl. 1-Chlorobutane (46 g, 0.50 mol) was fully mixed with 1-vinylimidazole (25 g, 0.26 mol) at room temperature. The solution was heated under reflux at 70 ℃ for 50 h. Phase separation occurred and the product (viscous liquid) was washed with ethyl acetate for several times, affording 17 g (34% yield) of the corresponding monomer 3-butylvinylimidazolium chloride, [BVIM]Cl, as light-yellow solid after filtration and vacuum drying overnight. ^{1}H NMR ($CDCl_3$) for [BVIM]Cl (Figure 3.1): 11.50 (s, 1H, N-C*H*-N), 7.76 (s, 1H, N-C*H*-CH-N), 7.54 (dd, 1H, CH_2=C*H*-N), 7.45 (s, 1H,

N-CH-C*H*-N), 5.97 (dd, 1H, CH_2=), 5.39 (dd, 1H, CH_2=), 4.40 (t, 2H, N-CH_2), 1.94 (m, 2H, N-CH_2-CH_2), 1.41 (m, 2H, N-CH_2-CH_2-CH_2), 0.98 (t, 3H, CH_3).

[BVIM]Cl (10.0 g, 0.054 mol) was dissolved in 100 mL of chloroform in a round bottom flask with AIBN (0.20 g, 1.2 mmol) fully mixed. The solution was degassed through the freeze-pump-thaw cycle for three times and then heated at 70 ℃ for 24 h under N_2 atmosphere. The resulting dark yellow solution was washed with diethyl ether several times and dried under vacuum at room temperature to afford 9.8 g (98% yield) of P[BVIM]Cl as off-white solid with M_n = 70,400 g/mol and PDI = 1.20. The NMR spectrum of this PIL was depicted in Figure 3.1.

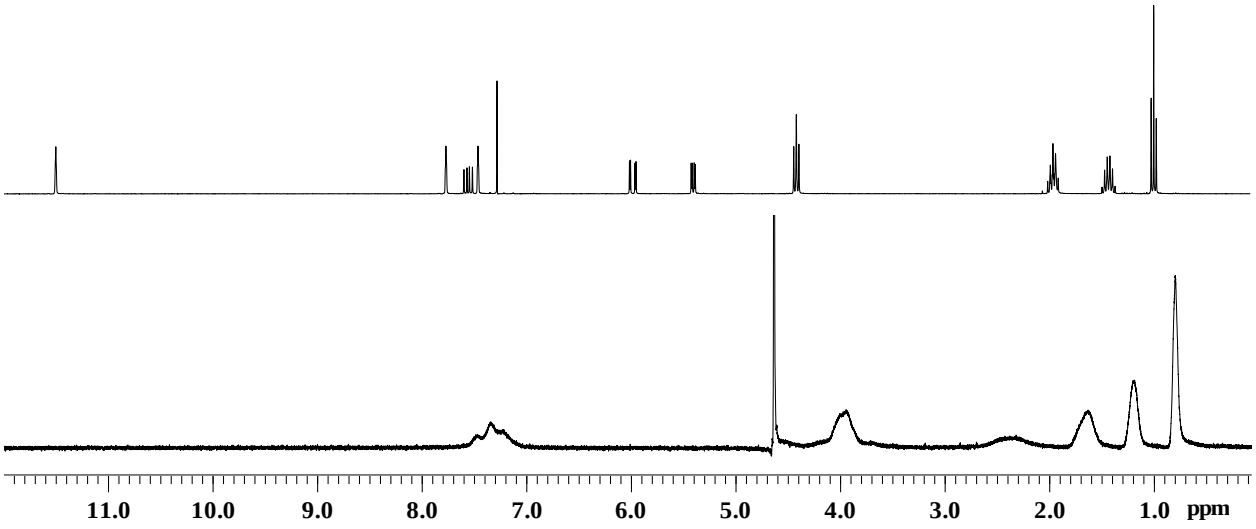

Figure 3.1 ^{1}H NMR spectra of [BVIM]Cl in $CDCl_3$ (top) and P[BVIM]Cl in D_2O (bottom) at 25 ℃, with internal reference chloroform and water peaks at 7.27 and 4.62 ppm respectively.

PIL-Supported metal (Cr, Al) catalysts. Polystyrene-supported butylimidazolium chloride, PS[BIM]Cl, was prepared according to the literature procedure.[41] Merrifield resin (1.2 g) in *N*-butylimidazole (20 mL) was stirred at 90 ℃ for 3 d. After cooling down to room temperature, the resin was filtered and washed in sequence with dichloromethane, methanol, acetone-water (1:1), water, methanol, acetone and diethyl ether. After drying under vacuum,

PS[BIM]Cl (1.1 g) was obtained as yellow solid. Next, PS[BIM]Cl (0.2 g) was premixed with $CrCl_2$ (2.6 mg) in 1 mL DMF and heated at 120 ℃ for 3 h under shaking. The resin was filtered, washed with acetone several times, and dried under vacuum for 3 h, affording the complex PS[BIM]Cl-$CrCl_2$ as light-green solid. PIL-metal complexes, P[BVIM]Cl-$CrCl_2$ and P[BVIM]Cl-Et_2AlCl, were obtained in a different procedure. P[BVIM]Cl (0.20 g) and $CrCl_2$ or Et_2AlCl (0.022 mmol, 10 mol% relative glucose used in the subsequent glucose-to-HMF conversion) in DMF solution was stirred at 120 ℃ for 3 h. The reaction mixture, after being cooled to room temperature, was precipitated into excess acetone and centrifuged. The collected solid was dried under vacuum at 50 ℃ for 3 h to give the corresponding PIL-supported catalysts. ICP-OES analysis gave 3.3 mol% of Cr and 2.5 mol% Al in their respective PIL-supported catalysts.

Conversion of biomass into HMF. In a typical experiment, glucose (40 mg, 0.22 mmol) was premixed with P[BVIM]Cl (0.20 g, 5/1 wt. PIL/glucose) in a 5 mL vial in an argon-filled glove box, followed by further loading of catalyst (0.022 mmol, 10 mol% relative to glucose) and co-solvent (1 mL) when applicable. The sealed vial was placed in a temperature-controlled orbit shaker (120 ℃, 300 RPM) and heated at this temperature for 3 h. The reaction was quenched with ice-water and then diluted with a known amount of deionized water. The recyclability experiments were carried out by premixing P[BVIM]Cl and $CrCl_2$ or Et_2AlCl with DMF as co-solvent, followed by reacting of the mixture with glucose at 120 ℃ for 3 h. After the reaction mixture being cooled to room temperature by ice water, 2 mL ethyl acetate was used for HMF extraction four times after 0.5 mL deionized water was added. Supernatants were collected

after centrifugation and diluted with deionized water for HMF quantification by HPLC. The remaining solid was dried at 50 ℃ for 3 h under vacuum, which was used for the next conversion experiment, with the same amount of glucose and DMF added as the last run (no additional catalyst was added for all subsequent recycling runs).

For the cellulose-to-HMF conversion experiments, the stepwise cellulose hydrolysis method[29,30] was utilized due to its high glucose yield (>90%). Specifically, a 20 mL vial was charged with [EMIM]Cl (0.80 g, 5.4 mmol) and cellulose (40 mg, 0.22 mmol) and heated under 120 ℃ until a homogenous solution was formed. Water (0.04 mL) was then added, along with Dowex G-26 H-Form Resin (25 mg), and then timing started. During this 3-h cellulose hydrolysis time period at 120 ℃, portions of water were added stepwise at 10 min (0.16 mL), 30 min (0.24 mL), and 60 min (0.32 mL). The reaction mixture was dried overnight at 50 ℃ under vacuum, which was used for subsequent conversion to HMF in the presence of the PIL based catalyst and DMF (if applicable) at 120 ℃ for 3 h.

HMF was quantified with calibration curves generated from the commercially available standard in water. A typical HPLC chromatogram of the reaction product is shown in Figure 3.2.

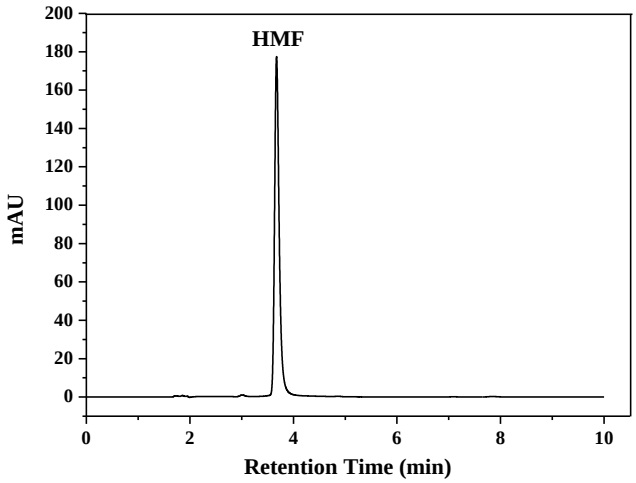

Figure 3.2 HPLC Chromatogram for the P[BVIM]Cl-$CrCl_2$ catalyzed glucose conversion to HMF in DMF at 120 ℃ for 3 h.

3.4 Results and Discussion

Effects of PIL structure on glucose-to-HMF conversion. At the outset, we examined the structure of PILs on the glucose conversion to HMF. Five different PILs varying *N*-substituents and counteranions were prepared for this study (see Experimental). Use of PILs for the glucose-to-HMF conversion requires a polar co-solvent, such as DMSO, DMF or DMA, which makes a homogenous mixture containing the PIL, catalyst, and glucose, because T_g of such PILs is typically above the reaction temperature (120 ℃) employed in this study; for instance, T_g of P[BVIM]Cl is 213 ℃. Table 3.1 summarizes the results of this investigation.

Table 3.1 HMF yield obtained from the glucose-to-HMF conversion by $CrCl_2$ in the presence of PIL or P(NHC) at 120 ℃ for 3 h.

PIL	co-solvent	HMF yield (%)
P[EVIM]Br	DMSO	15.1
P[BVIM]Br	DMSO	29.7
P[BVIM]Cl	DMSO	54.6
P[VBzBIM]Cl	DMSO	45.6

PS[BMIM]Cl	DMF	27.7

Under identical conditions (5 /1 wt. PIL/glucose, 10 mol% $CrCl_2$ relative to glucose, DMSO, 120 ℃, 3 h), the butyl-substituted PIL, P[BVIM]Br, doubled the HMF yield (29.7%), compared to that by the ethyl derivative P[EVIM]Br (15.1%). Interestingly, switching the counteranion Br^- into Cl^- nearly doubled the HMF yield further to 54.6% for P[BVIM]Cl, suggesting an important role of anion—in terms of its relative nucleophilicity and coordinating ability—in catalyzing the glucose-to-fructose isomerization, a key step proposed for the glucose-to-HMF conversion process.[3] It is interesting to note that the far better performance of Cl^- vs. Br^- is opposite of that observed for the conversion with the molecular IL system.[4] Also noteworthy is that the conversion by $CrCl_2$ alone in DMSO (i.e., no IL or PIL) gave an HMF yield of 38.2%, which was even higher than that achieved by the system with further addition of P[BVIM]Br.

Keeping the same anion (Cl^-), a change of the cation structure from [BVIM] to [VBzBIM] (i.e., insertion of the benzyl group between the polyvinyl main chain and the imidazolium side chain) noticeably lowered the HMF yield to 45.6% by P[VBzBIM], due to its poor solubility in DMSO. The HMF yield further decreased to only 27.7% when the preformed Merrifield resin (PS) supported catalyst, PS[BIM]Cl-$CrCl_2$, was used in the heterogeneous conversion in DMF.

Effects of co-solvent on glucose-to-HMF conversion. Having established P[BVIM]Cl as the most effective PIL support within the current series of PILs investigated for the glucose-to-HMF conversion, we further examined potential co-solvent effects on the HMF yield, the results of which study were depicted in Figure 3.3. It should be noted here that analysis of

sugars in the reaction products produced by representative chromium catalyst systems or the relevant aluminum catalyst systems[25] showed quantitative conversion of glucose has always been achieved at the maximum yield of HMF (the major product). Hence, in these instances the reported HMF yield is equivalent of the HMF selectivity.

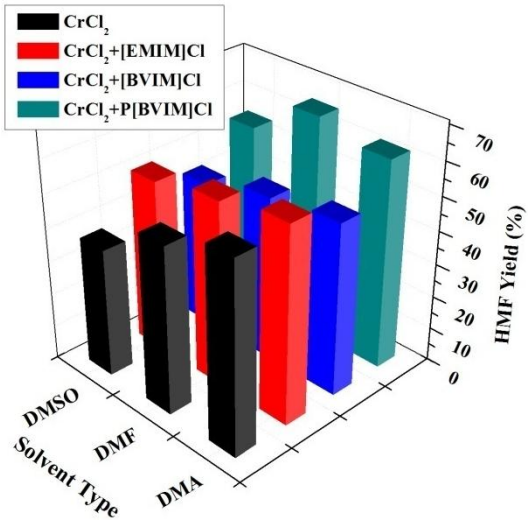

Figure 3.3 HMF yield (120 ℃, 3 h) as a function of solvent and ionic liquid type.

Control runs for the glucose conversion to HMF by $CrCl_2$ in an organic solvent (without a molecular IL or polymeric IL) showed that DMA is the most effective solvent. Thus, under the standard conditions employed in this study (120 ℃ for 3 h), the HMF yield in DMA was 56.7%, compared to 49.7% and 38.2% in DMF and DMSO, respectively (black columns, Figure 3.3). Further addition of the molecular IL [EMIM]Cl enhanced the HMF yield noticeably to give an HMF yield of 51.3%, 54.9%, and 58.4% in DMSO, DMF, and DMA, respectively (red columns, Figure 3.3). Substituting [EMIM]Cl with [BVIM]Cl (i.e., the monomer of the PIL) led to a less effective conversion system in all three solvents (blue columns, Figure 3.3). Most interestingly, replacing the monomeric IL, [BVIM]Cl, with its polymeric analog, P[BVIM]Cl, afforded a much

more effective conversion system, thus increasing the HMF yield to reach 54.6%, 65.8%, and 62.2% in DMSO, DMF, and DMA, respectively (green columns, Figure 3.3). These results clearly showed that the P[BVIM]Cl-$CrCl_2$ catalyst system in DMF is most effective, achieving the highest HMF yield of 65.8% at 120 ℃ for 3 h.

Experiments in optimizing the HMF yield showed that runs at higher or lower temperature than 120 ℃ led to a lower HMF yield; for example, the HMF yield was 60.8% at 130 ℃ for 3 h. Fixing the temperature (120 ℃), the yield vs. time profile (Figure 3.4) revealed that the highest HMF yield of 65.8% was achieved after 3 h and yields were lowered for reactions at shorter or longer times (Figure 3.4). The lowest yield of 38.2% after the extended reaction time of 24 h is primarily due to HMF degradation at elevated temperature for a long period of time.[42] Noteworthy is that the reaction after 1 h already reached an HMF yield of 64.2%, comparable to the optimized yield, indicating a rather rapid conversion process by the current PIL-$CrCl_2$ catalyst system.

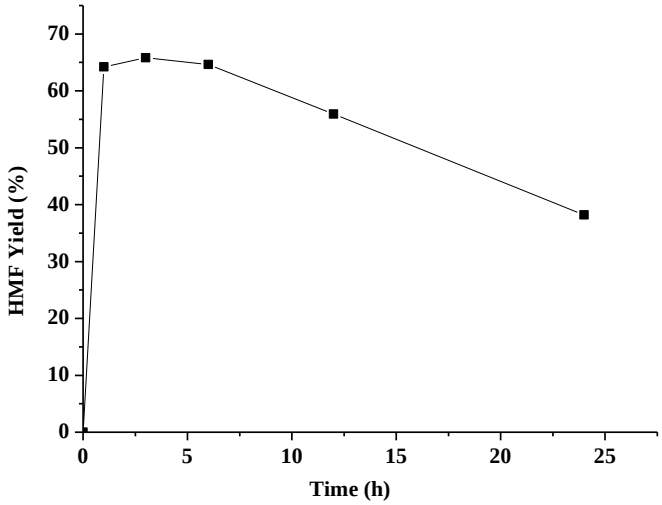

Figure 3.4 Plot of HMF yield as a function of reaction time for the glucose-to-HMF conversion by P[BVIM]Cl-$CrCl_2$ (10 mol% catalyst) in DMF at 120 ℃.

As co-solvent strongly affects the HMF yield by the PIL-based catalyst system, we further examined other organic solvents with a high dielectric constant as co-solvent for the glucose-to-HMF conversion by P[BVIM]Cl-$CrCl_2$ under identical conditions (10 mol% catalyst, 120 ℃ for 3 h). This investigation showed that the polar aprotic solvent DMF gave the highest HMF yield (Figure 3.5).

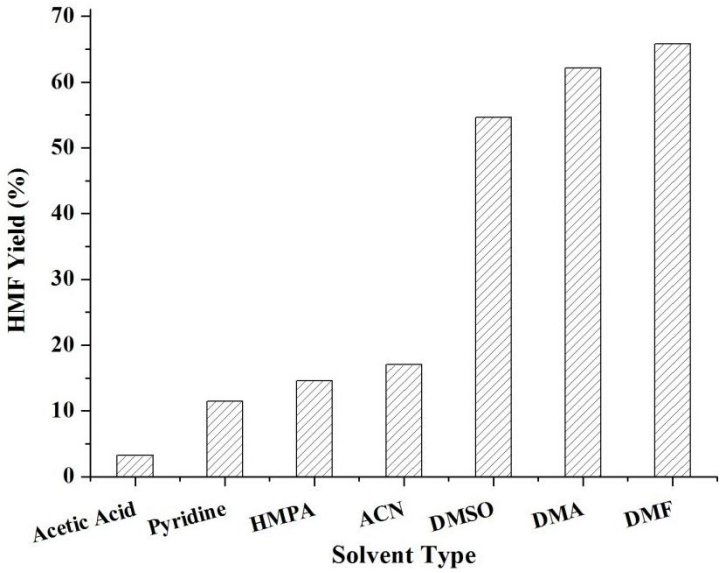

Figure 3.5 HMF yield as a function of co-solvent type for the conversion by P[BVIM]Cl-$CrCl_2$ at 120 ℃ for 3 h.

PIL-aluminum catalyst system. We previously showed that, under the same conditions employed for the glucose-to-HMF conversion in [EMIM]Cl (120 ℃, 6 h), simple trialkyl and trialkoxy aluminum species such as $AlEt_3$ and $Al(O^iPr)_3$, which are much less expensive than $CrCl_2$ (by a factor of 5 for $AlEt_3$ or 180 for $Al(O^iPr)_3$), are at least as effective as $CrCl_2$ to catalyze the same conversion process.[25] Hence, it is of interest to investigate the performance of the PIL-based aluminum catalyst, in reference to the PIL-$CrCl_2$ catalyst.

Table 3.2 summarizes the results of this study. Of the six common aluminum Lewis acid

catalysts investigated for the glucose-to-HMF conversion in P[BVIM]Cl and DMF, Et_2AlCl is most effective, giving the highest HMF yield of 49.0%, which is 12~20% higher than those achieved by other aluminum catalysts in the series. This trend is in *drastic contrast* to that observed for the conversion by the same series of aluminum catalyst in the molecular IL [EMIM]Cl without the DMF co-solvent;[25] in [EMIM]Cl, aluminum alkyls or alkoxides gave a typical HMF yield of ~50%, whereas aluminum trichloride and alkylchlorides ($AlCl_3$, $MeAlCl_2$ and Et_2AlCl) afforded much lower HMF yields of 1.6–17%. Apparently the combination of the PIL and the polar co-solvent DMF stabilizes the chlorinated aluminum catalysts, which are more sensitive to the water formed during glucose dehydration (conversion) to HMF than those alkyl or alkoxide aluminum catalysts. This reasoning was supported by the water titration experiments that showed that the HMF yield was held nearly constant upon addition of 0, 5, and 10 equiv of water to the conversion system by the PIL-chlorinated Al catalysts.

Table 3.2 HMF yield obtained from the glucose-to-HMF conversion by P[BVIM]Cl-Al catalysts (DMF, 120 ℃, 3 h).

Al catalyst	HMF yield (%)
$AlCl_3$	34.7
$MeAlCl_2$	34.1
Et_2AlCl	49.0
Et_3Al	32.4
$Al(O^iPr)_3$	29.1
$MeAl(BHT)_2$	37.3

Additional studies were carried out to optimize the best-performing PIL-Et_2AlCl catalyst. First, replacing the co-solvent DMF with DMSO and DMA led to lower (42.2%) and comparable

(48.7%) HMF yields, respectively. Second, a plot of the HMF yield vs. reaction temperature (Figure 3.6) revealed the best yield was achieved at 120 ℃ for 3 h. Third, at the fixed temperature of 120 ℃, the reaction at 3 h gave a higher yield than other (shorter or longer) times (Figure 3.7). Fourth, with the optimized temperature (120 ℃) and reaction time (3 h), the molar ratio of Et_2AlCl (relative to glucose) was varied from 0 mol% to 30 mol% (Figure 3.7). Under the current conditions, the control run with P[BVIM]Cl (no Al catalyst) produced HMF only in 0.5% yield; with a loading of the Et_2AlCl catalyst from 5 to 10 mol%, the HMF yield increased from 23.7% to 49.0%. A further increase in the catalyst loading to 20 and 30 mol% actually decreased the HMF yield to 42.5% and 31.8%, respectively, presumably due to the Lewis acid-assisted degradation of HMF. In short, the optimized conditions for the glucose-to-HMF conversion catalyzed by P[BVIM]Cl-Et_2AlCl were: 120 ℃, 3 h, 10 mol% catalyst loading. This optimized yield of 49.0% is lower than the 65.8% yield achieved by the P[BVIM]Cl-$CrCl_2$ catalyst.

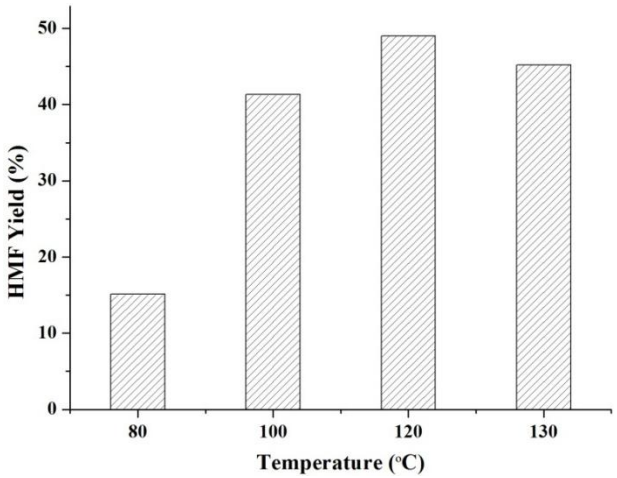

Figure 3.6 HMF yield as a function of the reaction temperature for the glucose-to-HMF conversion by P[BVIM]Cl-Et_2AlCl (10 mol% catalyst) in DMF for 3 h.

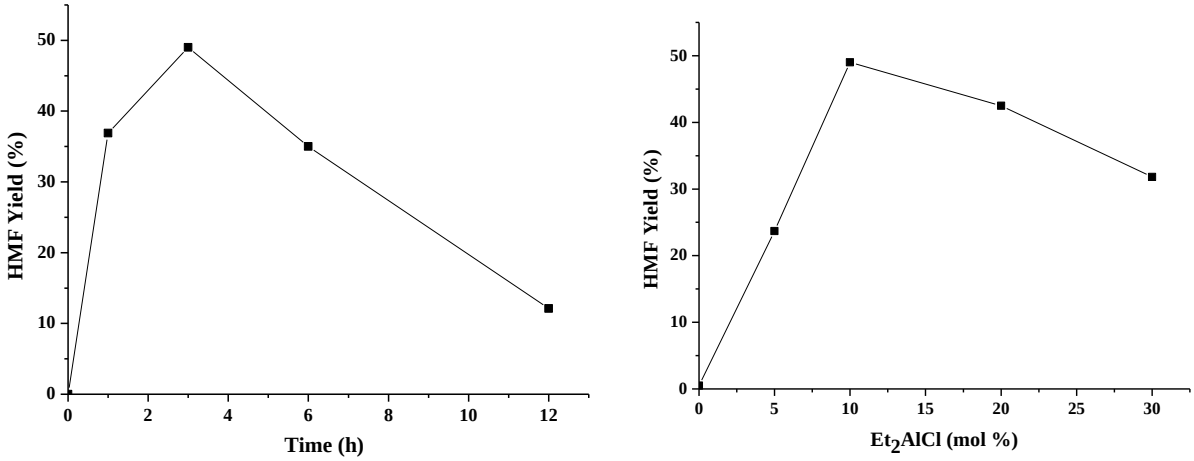

Figure 3.7 Plots of HMF yield as a function of reaction time (left column) and catalyst loading (right column, 3 h) for the glucose-to-HMF conversion by P[BVIM]Cl-Et_2AlCl (10 mol% for the time profile) in DMF at 120 ℃.

Recyclability of PIL-metal (Cr, Al) catalysts. To test the recyclability of the PIL-based catalysts, P[BVIM]Cl-$CrCl_2$ and P[BVIM]Cl-Et_2AlCl were recovered after the first run and then reused for subsequent runs. An issue of concern in this study was to identify a suitable solvent that can ideally extract all HMF produced from each run out of the reaction mixture before next run. To this end, we examined several different solvents adopted in the literature, including acetone, methyl isobutyl ketone, and ethyl acetate (EtOAc), and found the EtOAc/H_2O (20%) mixture gave the highest HMF recovery of typically greater than 90%. For example, a single conversion run by P[BVIM]Cl-$CrCl_2$ in DMF at 120 ℃ for 3 h gave an HMF yield of 65.8%, given by the analysis of the directly quenched reaction mixture with ice-water. In comparison, the HMF yield was 59.5%, obtained by the extraction procedure used in the recycling experiment, thus achieving a respectable 90.4% recovery. In the case of P[BVIM]Cl-Et_2AlCl, the recovery was even higher (96%).

Figure 3.8 summarizes the HMF yield at each recycle for both PIL-metal (Cr, Al) catalyst

systems in DMF. In the case of P[BVIM]Cl-$CrCl_2$, the HMF yield kept nearly constant at 60% during the first three recycles, after which the yield gradually decreased from 52.2% on the 4^{th} to 37.6% on the 6^{th} run, presumably due to Cr leaching from the PIL support. As a comparison, for the molecular IL based system, [EMIM]Cl-$CrCl_2$ without DMF addition, the HMF yield for the first single run was only 48.3% in otherwise identical condition (5/1 IL/glucose, 10 mol% catalyst, 120 ℃ and 3 h). Noteworthy is that even after 5 recycles, the P[BVIM]Cl-$CrCl_2$ system still achieved comparable HMF yield to that by the [EMIM]Cl-$CrCl_2$ system in a single run. Behaving differently, the P[BVIM]Cl-Et_2AlCl gave an HMF yield of 47.1% initially and then reached a stable HMF yield averaging ~42% at subsequent recycles; although it is not as effective as the P[BVIM]Cl-$CrCl_2$ system initially, it is more robust, thus sustaining a good HMF yield even after 6 cycles. These results show the good recyclability of P[BVIM]Cl-Et_2AlCl and its potential to replace both the molecular IL and the $CrCl_2$ catalyst.

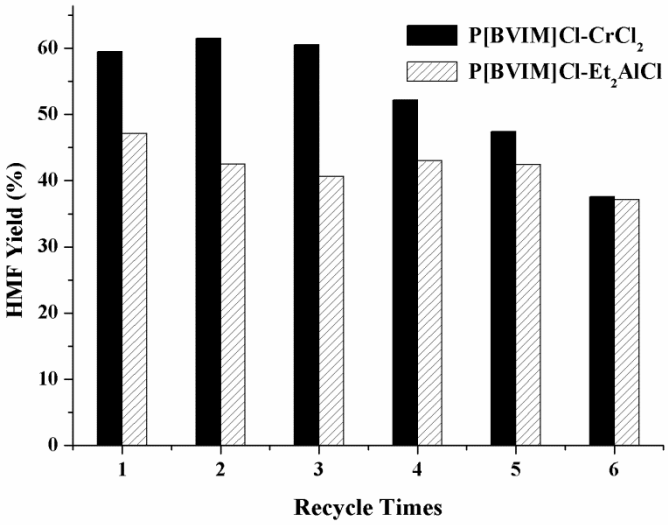

Figure 3.8 Comparison of HMF yield (av. value of 2-3 runs with typical errors within ±3%) at each of 6 recycles between P[BVIM]Cl-$CrCl_2$ and P[BVIM]Cl-Et_2AlCl (10 mol% catalyst, 120 ℃ for 3 h).

To confirm that it was the metal species attached to the PIL that catalyzed the glucose-to-HMF conversion, we carried out the following two experiments. First, a control run by P[BVIM]Cl alone for the glucose conversion in DMF at 120 ℃ for 3 h gave a marginal HMF yield of only 0.5%, which showed that P[BVIM]Cl itself, without combining with $CrCl_2$ or Et_2AlCl, was not the effective catalyst. Second, the use of the preformed, washed, and isolated metallate complex $P[BVIM]^+[CrCl_3]^-$ (see Experimental) for the same conversion reaction in DMF produced HMF in 61.5% yield, comparable to the yield achieved by the *in situ* mixing of P[BVIM]Cl with $CrCl_2$. This result implied that $CrCl_2$ anchored on the PIL and formed the PIL-metallate complex (Scheme 3.1), which serves as the catalyst for the glucose-to-HMF conversion. The hypothesized PIL-metallate complex was further supported by ICP-OES (see Experimental) and DSC (Figure 3.9) analyses of the isolated complexes. The DSC trace of P[BVIM]Cl showed a high T_g of 213 ℃, but upon its complexation with Et_2AlCl and $CrCl_2$, the T_g was lowered to 207 ℃ and 151 ℃, corresponding to the ion-pairing complexes $P[BVIM]^+[Et_2AlCl_2]^-$ and $P[BVIM]^+[CrCl_3]^-$, respectively. Larger anions give looser ion pairs and promote the higher chain mobility of polycations, thus lowering T_g of the complexes more pronouncedly.

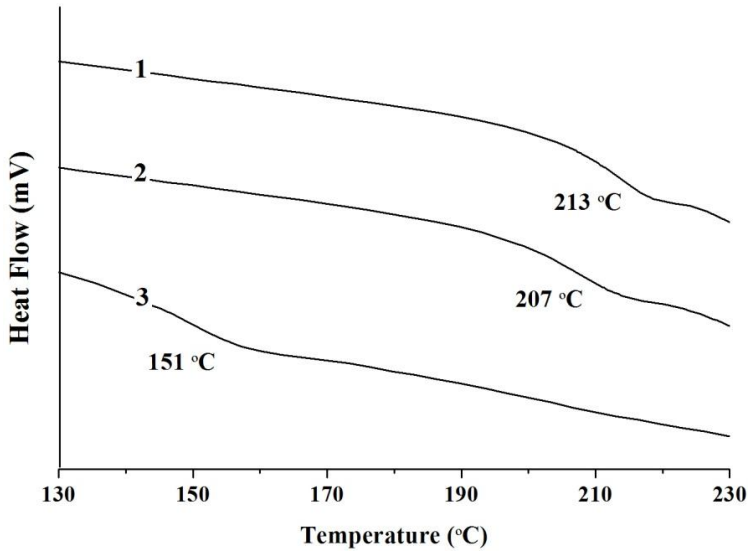

Figure 3.9 DSC overlay of (1) P[BVIM]Cl; (2) $P[BVIM]^+[Et_2AlCl_2]^-$; and (3) $P[BVIM]^+[CrCl_3]^-$.

Cellulose-to-HMF conversion by PIL-Metal (Cr, Al) catalysts. As both PIL-metal catalyst systems produced good HMF yields in the glucose-to-HMF conversion, we were interested in examining their effectiveness in the cellulose-to-HMF conversion via a two-step process consisting of controlled hydrolysis of cellulose to glucose in [EMIM]Cl, followed by addition of the PIL-based catalyst for the glucose conversion to HMF (see Experimental). Gratifyingly, P[BVIM]Cl-$CrCl_2$ (no co-solvent for the second step) remained rather effective for the two-step cellulose-to-HMF conversion, achieving an HMF yield of 49.6% starting from cellulose. In comparison, the use of $CrCl_2$ only for the second step gave a lower HMF yield of 42.0% (an average value of 2 runs) under otherwise identical conditions. Compared to $CrCl_2$, Et_2AlCl is more moisture and air sensitive, thus giving a lower HMF yield of 36.3% in the two-step cellulose-to-HMF conversion process.

3.5 Conclusions

Polymeric ionic liquid based metal (Cr, Al) catalysts effectively catalyze the conversion of glucose or cellulose to HMF and are recyclable. Their catalytic efficiency is sensitive to the structure of the PIL (e.g., *N*-substituent and counteranion), co-solvent, and metal catalyst. Hence, the best-performing PIL of the five PILs investigated in this study, P[BVIM]Cl, when combined with $CrCl_2$ in DMF, which forms the metallate complex $P[BVIM]^+[CrCl_3]^-$, converts glucose to HMF in 65.8% yield at 120 ℃ for 3 h.; this yield is considerably higher than the 49.0% yield achieved by the catalyst system based on its monomer, [BVIM]Cl-$CrCl_2$, and is also higher than the 54.9% yield afforded by the most commonly used molecular IL based catalyst, [EMIM]Cl-$CrCl_2$, under otherwise identical conditions. The P[BVIM]Cl-$CrCl_2$ catalyst system also works well for the cellulose-to-HMF conversion, achieving an HMF yield of 49.6% starting from cellulose, which is noticeably more effective than the use of $CrCl_2$ alone for the second step (42.0%).

The analogous PIL-Al catalyst system, P[BVIM]Cl-Et_2AlCl, is less effective than P[BVIM]Cl-$CrCl_2$ for both conversions of glucose and cellulose to HMF. However, recyclability tests indicate the PIL-Al system is more robust and recyclable, maintaining a sustainable HMF yield averaging ~ 42% upon 6 cycles. Hence, although it is not as effective as the PIL-supported Cr catalyst initially, P[BVIM]Cl-Et_2AlCl sustains a similar HMF yield during 6 cycles, after which it achieves a comparable HMF yield to that by P[BVIM]Cl-$CrCl_2$ which, on the other hand, shows a considerable decline in the HMF yield after 3 cycles presumably due to Cr loss. These results demonstrate the good recyclability of P[BVIM]Cl-Et_2AlCl and its potential to

replace IL-$CrCl_2$, the most effective benchmark Lewis acid catalyst to date.

3.6 References

(1) (a) Alonso, D. M.; Bond, J. Q.; Dumesic, J. A. *Green Chem.* **2010,** *12*, 1493-1513. (b) Stöcker, M. *Angew. Chem. Int. Ed.* **2008**, *47*, 9200-9211. (c) "NSF 2008. Breaking the Chemical and Engineering Barriers to Lignocellulosic Biofuels: Next Generation Hydrocarbon Biorefineries", Huber, G. W. Ed. report from the NSF Workshop. (d) Corma, A.; Iborra, S.; Velty, A. *Chem. Rev.* **2007**, *107*, 2411-2502; (e) Chheda, J. N.; Huber, G. W.; Dumesic, J. A. *Angew. Chem. Int. Ed.* **2007**, *46*, 7164-7183. (f) Huber, G.W.; Iborra, S; Corma, A. *Chem. Rev.* **2006**, *106*, 4044-4098.

(2) "Top Value Added Chemicals from Biomass", Werpy, T.; Petersen, G. Eds. U.S. Department of Energy (DOE) report: DOE/GO-102004-1992, **2004**.

(3) Zhao, H. B.; Holladay, J. E.; Brown, H.; Zhang, Z. C. *Science* **2007**, *316*, 1597-1600.

(4) Binder, J. B.; Raines, R. T. *J. Am. Chem. Soc.* **2009**, *131*, 1979-1985.

(5) Rosatella, A. A.; Simeonov, S. P.; Frade, R. F. M.; Afonso, C. A. M. *Green Chem.* **2011**, *13*, 754-793.

(6) Roman-Leshkov, Y.; Barrett, C. J.; Liu, Z. Y.; Dumesic, J. A. *Nature* **2007**, *447*, 982-985.

(7) Liu, D.; Zhang, Y.; Chen, E. Y. X. *Green Chem.* **2012**, *14*, 2738-2746.

(8) Roman-Leshkov, Y.; Chheda, J. N.; Dumesic, J. A. *Science* **2006**, *312*, 1933-1937.

(9) Chheda, J. N.; Roman-Leshkov, Y.; Dumesic, J. A. *Green Chem.* **2007**, *9*, 342-350.

(10) Qi, X. H.; Watanabe, M.; Aida, T. M.; Smith, R. L. *Green Chem.* **2008**, *10*, 799-805.

(11) Amarasekara, A. S.; Williams, L. D.; Ebede, C. C. *Carbohydr. Res.* **2008**, *343*, 3021-3024.

(12) Lai, L. K.; Zhang, Y. G. *ChemSusChem* **2010**, *3*, 1257-1259.

(13) (a) Ionic liquids in synthesis, 2nd ed., Wasserscheid, P.; Welton, T. Eds. Wiley-VCH: Weinheim, **2008**. (b) P âvulescu, V. I.; Hardacre, C. *Chem. Rev.* **2007**, *107*, 2615-2665. (c) Stark, A.; Seddon, K. Ionic liquids in Kirk-Othmer encyclopedia of chemical technology; John Wiley and Sons: New York, **2007**; Vol. *26*; pp 836-920.

(14) (a) Sun, N.; Rodriguez, H.; Rahman, M.; Rogers, R. D. *Chem. Commun.* **2011**, *47*, 1405-1421. (b) Pinkert, A.; Marsh, K. N.; Pang, S.; Staiger, M. P. *Chem. Rev.* **2009**, *109*, 6712-6728.

(15) Danford, J. J.; Arif, A. M.; Berreau, L. M. *Acta Cryst.* **2009**, *E65*, m227.

(16) Pidko, E. A.; Degirmenci, V.; van Santen, R. A.; Hensen, E. J. M. *Angew. Chem. Int. Ed.* **2010**, *49*, 2530-2534.

(17) Yong, G.; Zhang, Y.; Ying, J. Y. *Angew. Chem. Int. Ed.* **2008**, *47*, 9345-9348.

(18) Hu, S. Q.; Zhang, Z. F.; Song, J. L.; Zhou, Y. X.; Han, B. X. *Green Chem.* **2009**, *11*, 1746-1749.

(19) Zhang, Z. H.; Wang, Q. A.; Xie, H. B.; Liu, W. J.; Zhao, Z. B. *ChemSusChem* **2011**, *4*, 131-138.

(20) Qi, X.; Watanabe, M.; Aida, T. M.; Smith, R. L. *Biores. Tech.* **2012**, *109*, 224-228.

(21) Sievers, C.; Musin, I.; Marzialetti, T.; Olarte, M. B. V.; Agrawal, P. K.; Jones, C. W. *ChemSusChem* **2009**, *2*, 665-671.

(21) Lima, S; Neves, P.; Antunes, M. M.; Pillinger, M.; Ignatyev, N.; Velente, A. A. *Appl. Catal. A Gen.* **2009**, *363*, 93-99.

(22) Chidambaram, M.; Bell, A. T. *Green Chem.* **2010**, *12*, 1253-1262.

(23) Stahlberg, T.; Rodriguez-Rodriguez, S.; Fristrup, P.; Riisager, A. *Chem. Eur. J.* **2011**, *17*, 1456-1464.

(24) Liu, D.; Chen, E. Y. X. *Appl. Catal. A Gen.* **2012**, *435-436*, 78-85.

(25) Yu, S.; Brown, H. M.; Huang, X. W.; Zhou, X. D.; Amonette, J. E.; Zhang, Z. C. *Appl. Catal. A Gen.* **2009**, *361*, 117-122.

(26) Kim, B.; Jeong, J.; Lee, D.; Kim, S.; Yoon, H. J.; Lee, Y. S.; Cho, J. K. *Green Chem.* **2011**, *13*, 1503-1506.

(27) Zhang, Y. T.; Du, H. B.; Qian, X. H.; Chen, E. Y. X. *Energy & Fuels* **2010**, *24*, 2410-2417.

(28) Binder, J. B.; Raines, R. T. *Proc. Natl. Acad. Sci. U. S. A.* **2010**, *107*, 4516-4521.

(29) Qi, X. H.; Watanabe, M.; Aida, T. M.; Smith, R. L. *Cellulose* **2011**, *18*, 1327-1333.

(30) Li, C. Z.; Zhang, Z. H.; Zhao, Z. B. K. *Tetrahedron Lett.* **2009**, *50*, 5403-5405.

(31) Qi, X. H.; Watanabe, M.; Aida, T. M.; Smith, R. L. *ChemSusChem* **2010**, *3*, 1071-1077.

(32) Wang, P.; Yu, H.; Zhan, S.; Wang, S. *Biores. Tech.* **2011**, *102*, 4179-83.

(33) Tao, F.; Song, H.; Yang, J.; Chou, L. *Carbohydrate Polym.* **2011**, *85*, 363-368.

(34) De, S.; Dutta, S.; Saha, B. *Green Chem.* **2011**, *13*, 2859-2868.

(35) (a) Buchmeiser, M. R. *Chem. Rev.* **2009**, *109*, 303-321. (b) Madhavan, N.; Jones, C. W.; Weck, M. *Acc. Chem. Res.* **2008**, *41*, 1153-1165. (c) Benaglia, M.; Puglisi, A.; Cozzi, F. *Chem. Rev.* **2003**, *103*, 3401-3430.

(36) Shreve, A. P.; Mulhaupt, R.; Fultz, W.; Calabrese, J.; Robbins, W.; Ittel, S. D. *Organometallics* **1988**, *7*, 409-416.

(37) Marcilla, R.; Blazquez, J. A.; Fernandez, R.; Grande, H.; Pomposo, J. A.; Mecerreyes, D. *Macromol. Chem. Phys.* **2005**, *206*, 299-304.

(38) Marcilla, R.; Blazquez, J. A.; Rodriguez, J.; Pomposo, J. A.; Mecerreyes, D. *J. Polym. Sci. Part A: Polym. Chem.* **2004**, *42*, 208-212.

(39) Tang, H. D.; Tang, J. B.; Ding, S. J.; Radosz, M.; Shen, Y. Q. *J. Polym. Sci. Part A: Polym. Chem.* **2005**, *43*, 1432-1443.

(40) Kim, D. W.; Chi, D. Y. *Angew. Chem. Int. Ed.* **2004**, *43*, 483-485.

(41) Ståhlberg, T.; Sorensen, M. G.; Riisager, A. *Green Chem.* **2010**, *12*, 321-325.

Chapter 4

Organocatalytic Upgrading of the Key Biorefining Building Block by a Catalytic Ionic Liquid and *N*-Heterocylic Carbenes

4.1 Summary

The present study of rapid degradation of the key biorefining building block 5-hydroxymethylfurfural (HMF) in an ionic liquid (IL), 1-ethyl-3-methylimidazolium acetate ([EMIM]OAc), has led to selective and efficient upgrading of HMF to 5,5'-di(hydroxymethyl)furoin (DHMF), a promising C_{12} kerosene/jet fuel intermediate. This HMF upgrading reaction is carried out under industrially favourable conditions (i.e., ambient atmosphere and 60–80 ℃), catalyzed by *N*-heterocyclic carbenes (NHCs), and complete within 1 h; this process selectively produces DHMF with yields up to 98% (by HPLC or NMR) or 87% (unoptimized, isolated yield). Mechanistic studies have yielded four lines of evidence that support the proposed carbene catalytic cycle for this upgrading transformation catalyzed by the acetate IL and NHCs.

4.2 Introduction

Owing to their unique ability to dissolve lignocellulosic biomass [1] and related carbohydrates[2] under relatively mild conditions, plus several other concurrent advantages (e.g., as designable and recyclable solvents with low volatility and toxicity), ionic liquids (ILs) such as

1-alkyl(R)-3-methyl(M)imidazolium(IM) chloride salts, [RMIM]Cl, have attracted rapidly growing interest,[3] particularly in the pursuit of renewable energy and sustainable chemicals from plant biomass.[4] For instance, ILs enabled homogenous hydrolysis of cellulose to sugars in high to quantitative conversion, with[5] or without[6] additional catalyst, and catalyzed conversion of glucose or cellulose into the biomass platform chemical 5-hydroxymethylfurfural (HMF),[6,7] a key and versatile biorefining building block for value-added chemicals and liquid fuels.[8] Upgrading of HMF can be achieved by acid-catalyzed etherification,[9] metal-catalyzed transformations such as hydrogenation/hydrogenolysis to 2,5-dimethylfuran,[10] a liquid fuel with a 40% higher energy density than ethanol, and aldol condensation with enolizable organic compounds followed by dehydration/hydrogenation into C_9 to C_{15} liquid alkanes (fuels),[11] thus upgrading it into the kerosene/jet fuel range (C_{12} to C_{15}). Direct coupling of two HMF molecules would make a C_{12} biofuel intermediate, but HMF or furfural cannot undergo aldol self-condensation because they possess no α-H.[11]

The acetate-based room-temperature (RT) IL 1-ethyl-3-methyl imidazolium acetate, [EMIM]OAc, has been identified as a better solvent than chloride-based ILs for biomass solution *processing* (i.e., dissolution, fractionation, and re-precipitation), due to its lower melting point, viscosity and corrosive character as well as higher loading and non-toxicity.[4a,12] However, for biomass *conversion* into sugars and HMF, the chloride-based ILs such as [RMIM]Cl (R = Et, ^{n}Bu) are preferred solvents,[6,7] and we have found [EMIM]OAc is completely *ineffective* for the glucose (or cellulose)-to-HMF conversion.[7a] A recent report disclosed that [EMIM]OAc rapidly degrades HMF (>99% degradation at 100 ℃ after 8 h), but neither was the degradation

mechanism given nor was the degradation product identified.[7f] We found this IL also rapidly degrades glucose (70% degradation at 100 ℃ after 1 h, *vide infra*). To this end, we hypothesized that the observed rapid HMF degradation in [EMIM]OAc is likely rendered by *N*-heterocyclic carbene (NHC) catalysis,[13] because it is known that a small concentration of carbene exists in this IL with the basic acetate anion,[14] as demonstrated experimentally by its carbene-type reaction with elemental sulfur or selenium[15] and as catalyst for benzoin condensation of benzaldehyde.[16] While addressing the mechanism of HMF degradation in [EMIM]OAc, we discovered that this "detrimental" degradation process can be utilized for highly efficient upgrading of HMF into a high-value biorefinery product, 5,5'-di(hydroxymethyl)furoin (DHMF)—a potential C_{12} kerosene/jet fuel intermediate, through NHC-catalyzed self-condensation enabled by this organocatalytic IL. Subsequent use of a discrete NHC (5 mol%), the Enders triazolylidene carbene TPT (1,3,4-triphenyl-4,5-dihydro-1*H*-1,2,4-triazol-5-ylidene),[17] leads to rapid (1 h), highly selective and high-yield synthesis of DHMF from HMF. The *in-situ* generated NHC by treating the chloride-based IL [EMIM]Cl with an organic base also rapidly upgrades HMF to DHMF in high yield (96%).

4.3 Experimental

Materials, Reagents, and Methods. All syntheses and manipulations of air- and moisture-sensitive materials were carried out in flamed Schlenk-type glassware on a dual-manifold Schlenk line, on a high-vacuum line, or in an inert gas (Ar or N_2)-filled glovebox.

HPLC-grade organic solvents were first sparged extensively with nitrogen during filling 20 L solvent reservoirs and then dried by passage through activated alumina (for Et_2O, THF, and CH_2Cl_2) followed by passage through Q-5 supported copper catalyst (for toluene and hexanes) stainless steel columns. HPLC-grade DMF was degassed and dried over CaH_2 overnight, followed by vacuum distillation (CaH_2 was removed before distillation). DMSO-d_6 was first degassed and dried over CaH_2, followed by vacuum distillation. NMR-scale reactions were conducted in Teflon-valve-sealed J. Young-type NMR tubes with hexamethylbenzene as the internal standard. NMR spectra were recorded on a Varian Inova 300 (FT 300 MHz, ^1H; 75 MHz, ^{13}C) or a Varian Inova 400 MHz spectrometer. Chemical shifts for ^1H and ^{13}C spectra were referenced to internal NMR solvent residual resonances and are reported as parts per million relative to $SiMe_4$.

The water-soluble products were analyzed by Agilent 1260 Infinity HPLC system equipped with either an Agilent Eclipse Plus C18 Column (100×4.6 mm; 80/20 water/methanol, 0.6 ml/min, 30 ℃) with a UV detector (284 nm) for HMF and DHMF detection and quantification, or a Biorad Aminex HPX-87H Column (300×7.8 mm; water, 0.6 ml/min, 45 ℃) with an Agilent 1260 Infinity ELSD detector (65 ℃, 3.5 bar, gain 6) for glucose and other sugars detection. High-resolution mass spectrometry (HRMS) data were collected on an Agilent 6220 Accurate time-of-flight LC/MS spectrometer.

D-Glucose (Granular powder, Fisher Chemical), $CrCl_2$ (Alfa Aesar), HMF (Acros Organics), hexamethylbenzene (Alfa Aesar), 1,8-diazabicyclo [5.4.0] undec-7-ene (DBU, Acros Organics), acetic acid (Mallinckrodt Chemicals, ACS grade), silver acetate (Strem Chemical)

were used as received. *N*-Heterocyclic carbenes (NHCs), 1,3-bis(2,4,6-trimethyl-phenyl)imidazol-2-ylidene (IMes) and 1,3-di-*tert*-butylimidazol-2-ylidene (I^tBu), were purchased from Strem Chemical Co. Literature procedures were used to prepare 1,3,4-triphenyl-4,5-dihydro-1*H*-1,2,4-triazol-5-ylidene (TPT),[18] while 1-ethyl-2,3-dimethylimidazolium acetate ([EDMIM]OAc) [19] was prepared using an anion exchange route (*vide infra*). 1-Ethyl-3-methylimidazolium acetate ([EMIM]OAc, Aldrich) and 1-ethyl-2,3-dimethylimidazolium chloride ([EDMIM]Cl, Aldrich) were dried under vacuum at 100 ℃ for 24 h. 1-Ethyl-3-methylimidazolium chloride ([EMIM]Cl, Fluka) was dried under vacuum at 100 ℃ for 24 h, followed by repeated recrystallization from CH_2Cl_2 and hexanes at room temperature. The purified ionic liquids were stored in an argon-filled glovebox.

Modified synthesis of [EDMIM]OAc. [EDMIM]OAc[19] was synthesized from the commercially available [EDMIM]Cl through anion exchange with AgOAc. [EDMIM]Cl (2.0 g, 0.012 mol) was mixed with AgOAc (2.09 g, 0.012 mol) in a conical flask, followed by addition of 25 mL deionized water. The suspension was covered with aluminum foil (avoiding the photo-degradation of AgOAc) and stirred overnight at room temperature. The resulting mixture was filtered to remove AgCl, and aliquots were taken from time to time for surplus anions test using the $AgNO_3$ or HCl solution. $AgNO_3$-resulted precipitation (AgCl) showed that there was a surplus of [EDMIM]Cl (*vice versa*). Accordingly, the [EDMIM]Cl or AgOAc solution was added into the mother solution dropwise until the anion test turned negative by both $AgNO_3$ and HCl solutions. The final reaction mixture was filtered and the filtrate was dried azeotropically with toluene. The resulting white solid was collected by filtration and washed with hexanes. After

being dried at 50 ℃ under vacuum, [EDMIM]OAc was obtained as white solid (1.68 g, 80.0%). Note that [EDMIM]OAc is highly hygroscopic and should be stored in a glovebox or a similar water-free environment. ^{1}H NMR ($CDCl_3$) for [EDMIM]OAc: δ 7.85 (d, $J_{H\text{-}H}$ = 2.1 Hz, 1H, imidazolium ring H), 7.63 (d, $J_{H\text{-}H}$ = 1.8 Hz, 1H, imidazolium ring H), 4.24 (q, $J_{H\text{-}H}$ = 7.2 Hz, 2H, N-CH_2CH$_3$), 3.95 (s, 3H, N-CH_3), 2.73 (s, 3H, NCCH_3N), 1.84 (s, 3H, OAc), 1.44 (t, $J_{H\text{-}H}$ = 7.2 Hz, 3H, N-CH$_2$CH_3). ^{13}C NMR ($CDCl_3$) for [EDMIM]OAc: δ 176 (*C*=O), 124 (N*C*N), 122, 121 (N-*C*H*C*H-N), 44.0 (N-*C*H$_2$CH$_3$), 35.8 (N-*C*H$_3$), 26.0 (NC*C*H$_3$N), 15.4 (O=C-*C*H$_3$), 10.0 (N-CH$_2$*C*H$_3$).

Typical procedure for studying HMF degradation in [EMIM]OAc. HMF (0.10 g, 0.79 mmol) was mixed with [EMIM]OAc (0.14 g, equimolar to HMF) in a 5 mL vial. The vial was sealed and heated at 80 ℃ for a predetermined time in a temperature-controlled orbit shaker (300 RPM). The reaction was quenched with ice-water and diluted with a known amount of deionized water. HMF was quantified with calibration curves generated from the commercially available standard in water.[7a]

For investigation of the HMF degradation kinetics in [EMIM]OAc, HMF (40.0 mg, 0.32 mmol) and hexamethylbenzene (2.0 mg, 0.012 mmol) were fully dissolved in 0.5 mL DMSO-d_6, followed by addition of [EMIM]OAc (1 equiv relative to HMF) in 0.5 mL DMSO-d_6. The mixture was transferred into a J. Young-type NMR tube and sealed with the Teflon valve. The mixture was heated to 80 ℃ on an NMR spectrometer and the reaction was followed by taking ^{1}H NMR spectra of the reaction mixture at predetermined time intervals. The results of HMF degradation in [EMIM]OAc monitored by NMR were summarized in Figure 4.1 (profile of HMF

degradation as a function of time).

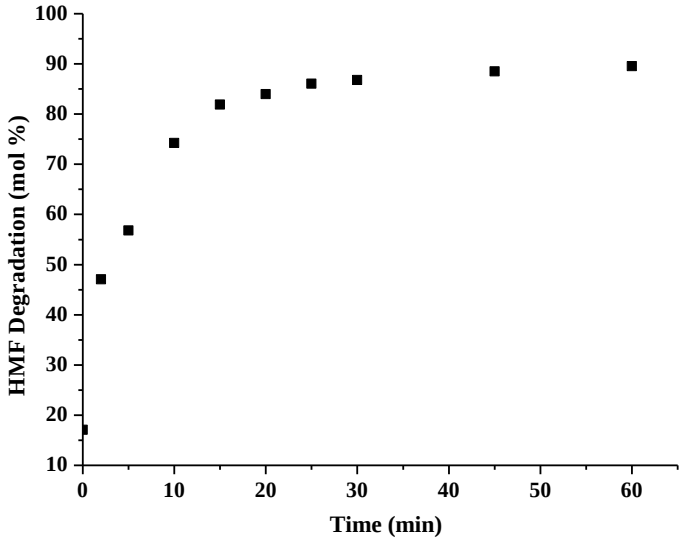

Figure 4.1 Profile (by NMR) of HMF degradation in [EMIM]OAc (1:1 molar ratio) at 80 ℃.

Isolation and characterization of DHMF produced from HMF degradation in [EMIM]OAc. As Figure 4.2 shows, the HPLC chromatogram of the reaction mixture from the incomplete HMF degradation in [EMIM]OAc exhibited a peak at 3.72 min for the unreacted HMF, plus a large peak at 5.15 min for a new compound formed during HMF degradation in [EMIM]OAc. To separate the new compound from the reaction mixture after the reaction at 80 ℃ for 30 min, 1 mL water was added to fully dissolve the mixture, after which 2 mL ethyl acetate (EtOAc) was added for extraction. The upper layer (EtOAc phase) was collected and the extraction was repeated four times. The new compound was obtained as light yellow powder (50% isolated yield based on HMF) after purification by the silica gel column chromatography (eluent: EtOAc/hexane/methanol =8/2/1) and vacuum drying.

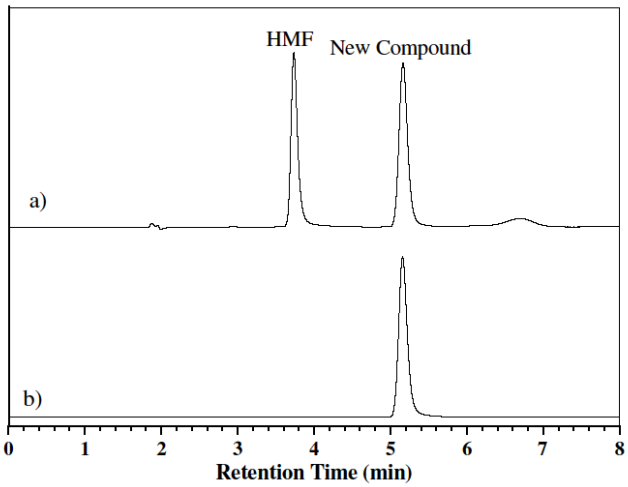

Figure 4.2 Formation of a new compound as detected by HPLC from the HMF degradation reaction mixture in [EMIM]OAc at 80 ℃: a) crude sample; b) after purification.

The degradation product (new compound) was identified as 5,5'-di(hydroxymethyl)furoin (DHMF), as clearly shown by its ^{1}H and ^{13}C NMR spectra. ^{1}H NMR (CD_3OD): δ 7.39 (d, $J_{H\text{-}H}$ = 3.6 Hz, 1H, furan ring proton), 6.52 (d, $J_{H\text{-}H}$ = 3.6 Hz, 1H, furan ring proton), 6.40 (d, $J_{H\text{-}H}$ = 3.3 Hz, 1H, furan ring proton), 6.30 (d, $J_{H\text{-}H}$ = 3.3 Hz, 1H, furan ring proton), 5.87 (s, 1H, C*H*OH), 4.60 (s, 2H, CH_2OH), 4.49 (s, 2H, CH_2OH). ^{13}C NMR (CD_3OD): δ 187 (C=O), 163, 158, 154, 152, 123, 112, 111, 110 (a total of 8 resonances for the furan ring carbons), 71.7 (*C*HOH), 58.4 (*C*H_2OH), 58.2 (*C*H_2OH). Note that the ^{1}H NMR spectrum taken in DMSO-d_6 showed three broad peaks centered at ~5.3 ppm, 5.5 ppm, and 6.1 ppm for three types of the OH groups present in DHMF. M.p. = 124 –125 ℃; HRMS calculated for $C_{12}H_{11}O_6$ $[M\text{-}H]^-$: 251.0556; found: 251.0561.

The DHMF purified by the silica gel column chromatography was recrystallized by slow diffusion of hexanes into a methanol solution of DHMF at room temperature over 7 d, affording colorless single crystals suitable for X-ray diffraction analysis. Single crystals were quickly

covered with a layer of Paratone-N oil (Exxon, dried and degassed at 120 ℃/10^{-6} Torr for 24 h) after decanting the mother liquor. A crystal was then mounted onto a thin glass fiber and transferred into the cold nitrogen stream of a Bruker SMART CCD diffractometer. The structure was solved by direct methods and refined using the Bruker SHELXTL program library.[20] The structure was refined by full-matrix least-squares on F^2 for all reflections. All non-hydrogen atoms were refined with anisotropic displacement parameters, whereas hydrogen atoms were included in the structure factor calculations at idealized positions. There are two independent molecules with minor structural differences in the unit cell (Figure 4.8). Selected crystallographic data for DHMF: $C_{24}H_{24}O_{12}$, Orthorhombic, space group $Pna2_1$, a = 23.5497(17) Å, b = 5.9975(4) Å, c = 15.8768(10) Å, α = 90 °, β = 90 °, γ = 90 °, V = 2242.4(3) $Å^3$, Z = 4, D_{calcd} = 1.494 Mg/m^3, GOF = 1.040, $R1$ = 0.0524 [$I > 2\sigma(I)$], w$R2$ = 0.1309. CCDC-887451 contains the supplementary crystallographic data for this paper. These data can be obtained free of charge from The Cambridge Crystallographic Data Centre via www.ccdc.cam.ac.uk/ data_request/cif.

The identification as well as spectroscopic and structural characterizations of the HMF degradation product (DHMF) allowed for monitoring of DHMF formation and HMF degradation simultaneously by NMR (DMSO-d_6, 80 ℃, hexamethylbenzene as the internal standard). The results were summarized in Figure 4.3, showing that a maximum yield of 72.4% was achieved at 86.1% HMF conversion (degradation) after 25 min.

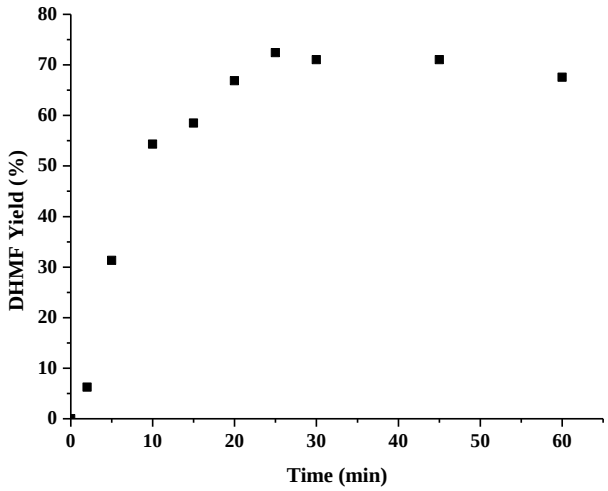

Figure 4.3 DHMF yield (by NMR) as a function of HMF degradation time in [EMIM]OAc (1:1 molar ratio) at 80 ℃.

Identification of intermediate II from the reaction of HMF with [EMIM]OAc. The 1:1 reaction of HMF with [EMIM]OAc at RT was monitored by NMR (DMSO-d_6) in a J. Young-type NMR tube using hexamethylbenzene as the internal standard. This study showed that 17% HMF was consumed immediately upon mixing HMF with [EMIM]OAc at RT, which approximately corresponds to the amount of the NHC catalyst accessible in [EMIM]OAc at this temperature for its reaction with HMF to form intermediate **II** (Scheme 4.1). This intermediate is not converted into DHMF at RT, even after 24 h, and the ^{1}H NMR remained the same from the beginning of the reaction up to 24 h at RT. To aid analysis of the spectra of the in situ reactions, the chemical shifts of the four species involved in the reaction of HMF with [EMIM]OAc were summarized as follows. All the chemical shifts were reported in DMSO-d_6, and the NMR solvent residual signal was referenced at 2.54 ppm, based on the chemical shift of the hexamethylbenzene internal standard set at 2.15 ppm.

^{1}H NMR for HMF (known compound): δ 9.56 (s, 1H, C*H*O), 7.51, 6.59 (d, 2H, furan ring

H), 4.54 (s, 2H, CH_2OH). ^{1}H NMR for [EMIM]OAc (known compound): δ 9.60 (s, 1H, NC*H*N), 7.84, 7.76 (d, 2H, imidazolium ring H), 4.24 (q, 2H, NCH_2CH$_3$), 3.89 (s, 3H, NCH_3), 1.65 (s, 3H, OAc), 1.44 (t, 3H, NCH$_2$CH_3). ^{1}H NMR for DHMF: δ 7.54, 6.54, 6.38, 6.25 (d, 4H, furan ring H), 5.78 (s, 1H, C*H*OH), 4.50 (s, 2H, CH_2OH), 4.35 (s, 2H, CH_2OH). ^{1}H NMR for Intermediate **II**: δ 7.98 (d, $J_{H\text{-}H}$ = 2.1 Hz, imidazol ring H), 7.93 (d, $J_{H\text{-}H}$ = 1.8 Hz, 1H, imidazol ring proton), 6.74 (s, 1H, C*H*-OH), 6.38 (d, $J_{H\text{-}H}$ = 3.3, 1H, furan ring H), 6.24 (d, $J_{H\text{-}H}$ = 3.0 Hz, 1H, furan ring H), 4.41 (m, 2H, NCH_2CH$_3$), 4.36 (s, 2H, CH_2OH), 3.96 (s, 3H, NCH_3), 1.64 (s, 3H, OAc), 1.31 (t, $J_{H\text{-}H}$ = 7.2 Hz, 3H, NCH$_2$CH_3). ^{13}C NMR: δ 175 (*C*=O), 158 (N*C*N), 151, 146, 109, 108 (4 resonances for the furan ring), 125, 122 (2 resonances for the imidazol ring), 60.4 (*C*H-OH), 56.3 (*C*H$_2$OH), 44.2 (N*C*H$_2$CH$_3$), 36.2 (N*C*H$_3$), 26.5 (O=C-*C*H$_3$), 16.3 (NCH$_2$*C*H$_3$).

The reaction with a 1:5 molar ratio of HMF:[EMIM]OAc was carried out in the same fashion, producing the intermediate exclusively (i.e., devoid of HMF and DHMF), plus excess [EMIM]OAc. ^{1}H NMR spectrum (Figure 4.9) of this reaction showed clean formation of intermediate **II** in the presence of excess [EMIM]OAc, which is further confirmed by its ^{13}C NMR spectrum (Figure 4.10), thus enabling more conclusive spectroscopic characterization of intermediate **II**.

Typical procedure for studying umpolung condensation of HMF into DHMF by NHCs. In a typical procedure, HMF (115 mg, 0.91 mmol) was fully dissolved in 5 mL THF, followed by addition of TPT (5 mol %) in 0.5 mL THF. The resulting solution was stirred at room temperature, and aliquots were taken from time to time and dried under vacuum for analysis by ^{1}H NMR in DMSO-d_6. To isolate DHMF from the HMF self-condensation catalyzed

by TPT, the reaction mixture was stirred at room temperature for 24 h and then concentrated, followed by addition of toluene to precipitate the product DHMF. DHMF (99 mg, 86 % yield) was obtained as white solid after filtration and vacuum drying. ^{1}H NMR in DMSO-d_6 (Figure 4.4) of the product confirmed the clean formation of DHMF. The same reaction was repeated at 60 ℃ for 1 h, affording DHMF in 87 % isolated yield.

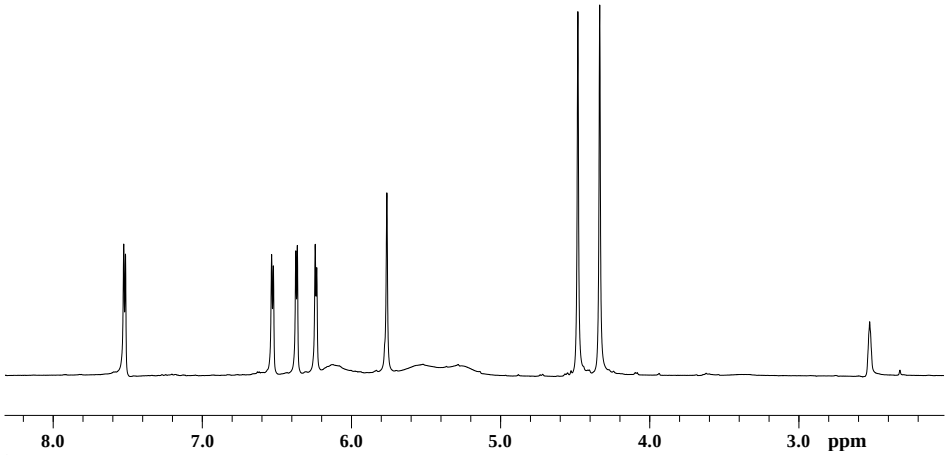

Figure 4.4 ^{1}H NMR (DMSO-d_6) of DHMF derived from umpolung condensation of HMF by TPT. Note the three broad peaks centered at ~5.3 ppm, 5.5 ppm, and 6.1 ppm, not appeared in the ^{1}H NMR taken in methanol-d_4, are for three types of the OH groups present in DHMF, and the peak at 2.54 ppm is from the NMR solvent residual signal.

Typical procedure for studying glucose degradation in [EMIM]OAc. This study followed the procedure similar to that used for the HMF degradation in [EMIM]OAc as described above. Glucose (0.04 g, 0.22 mmol) was mixed with [EMIM]OAc (0.2 g, 1:5 w/w) in a 5 mL vial. The vial was sealed and heated at 100 ℃ for 30 min in a temperature-controlled orbit shaker (300 RPM). The reaction was quenched with ice-water and transferred to a 5 mL volumetric flask. A fraction of the solution (0.5 mL) was removed of [EMIM]OAc by cation-anion exchange columns washed with distilled water. An initial 5 mL eluent was collected for sugar analysis by HPLC. Glucose was quantified with calibration curves generated from the

commercially available standard in water. The recovery of glucose (if any left after the degradation reaction) by this method was shown to be ≥96 % based on control experiments. The HPLC results showed no fructose and cellubiose formation from the degradation of glucose in [EMIM]OAc. Figure 4.7 summarized the results of glucose degradation in [EMIM]OAc, which showed that [EMIM]OAc also rapidly degrades glucose at 100 ℃; thus, glucose degraded by 58.9, 70.3, and 83.0 mol% after only 0.5, 1, and 3 hrs, respectively.

Typical procedure for two-step glucose conversion into DHMF. For the first step, glucose (100 mg, 0.56 mmol) was premixed with [EMIM]Cl (500 mg, 1:5 w/w) in a 5 mL vial in a argon-filled glove box, followed by further loading of the $CrCl_2$ catalyst (10 mol% relative to glucose). The sealed vial was placed in a temperature-controlled orbit shaker (100 ℃, 300 RPM) and heated at this temperature for 3 h. The reaction was quenched with 1 mL deionized water, and HMF was extracted with ethyl acetate (2 mL × 4). HMF was recovered by ethyl acetate extraction, and the HMF yield from glucose was 57 % as determined by HPLC. The resulting solution was purified by the silica gel column chromatography (eluent: EtOAc/Hexane=7/3), and the eluent fraction for HMF was collected and dried under vacuum. For the second step, the obtained HMF was subsequently converted into DHMF by the TPT catalyst in THF, employing the same procedure already described.

4.4 Results and Discussion

Degradation of HMF and glucose in [EMIM]OAc. HPLC monitoring of the HMF degradation in [EMIM]OAc (1:1 molar ratio) revealed rapid degradation of HMF even at

temperatures far below 120 ℃, a typical temperature employed for biomass conversion; for example, 70% and 94% of HMF has been degraded after 1 h at 50 ℃ and 80 ℃, respectively (Figure 4.5). The degradation kinetics at 80 ℃ were examined with NMR by performing the degradation in DMSO-d_6 in a J. Young-type NMR tube with a 1/1 HMF/[EMIM]OAc molar ratio and using hexamethylbenzene as the internal standard. The results of kinetics performed in this NMR solvent containing the non-interreacting internal standard were very similar to those obtained by HPLC without this solvent and standard. A first-order kinetic plot (Figure 4.6) of the initial degradation process (2–15 min) yielded a rate constant of k = 0.085 min^{-1} at 80 ℃, corresponding to a degradation half-life of 8.2 min at this temperature.

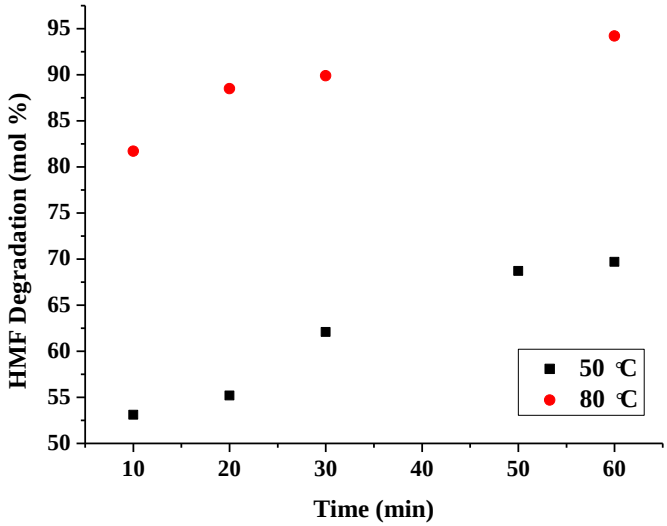

Figure 4.5 Graphical profiles of HMF degradation in [EMIM]OAc (1:1 molar ratio) vs. time at two different temperatures (50 ℃ and 80 ℃), monitored by HPLC.

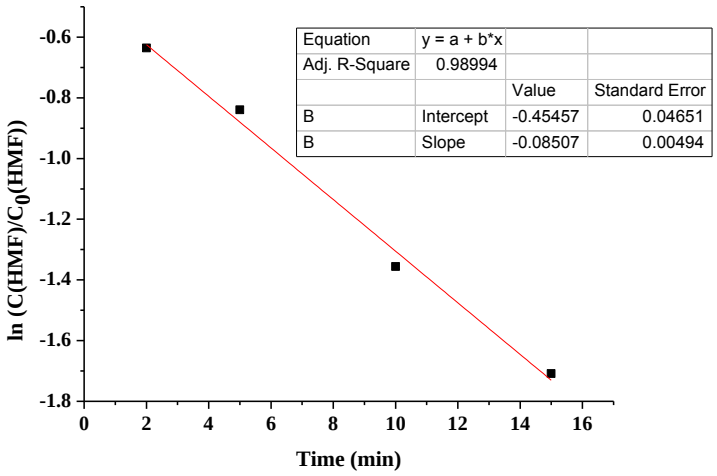

Figure 4.6 The first-order plot of HMF degradation in [EMIM]OAc (1:1 molar ratio) at 80 ℃ monitored by NMR for the initial time period (2–15 min).

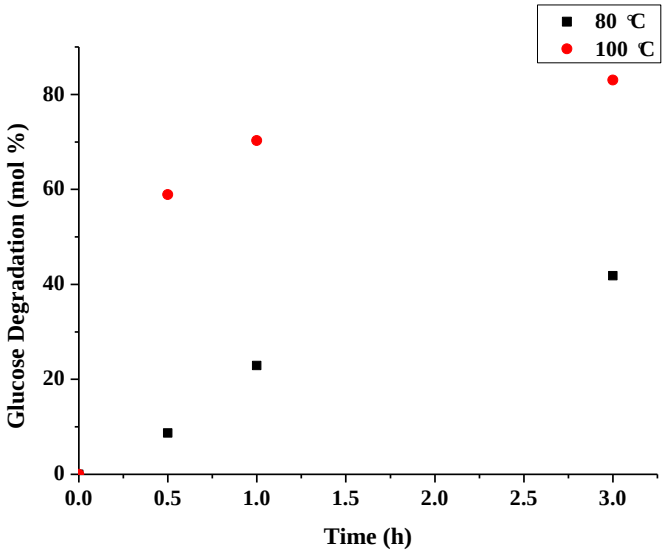

Figure 4.7 Graphical profiles of glucose degradation in [EMIM]OAc at two different temperatures (**80 ℃** and **100 ℃**), monitored by HPLC.

Glucose also undergoes rapid degradation in [EMIM]OAc; for example, at 100 ℃, glucose degraded by 70% and 83% after 1 and 3 h, respectively (Figure 4.7). Interestingly, even the chloride-based IL, [BMIM]Cl, was reported to react with HMF at higher temperatures (≥200 °C), to form 1-butyl-2-(5’methyl-2’-furoyl)imidazole, although the yield was rather low

(9.3% at 250 ℃).[21] This unusual product was determined by NMR and MS analysis, and the mechanism of its formation was proposed to proceed through an initial adduct formation between HMF and [BMIM]Cl, followed by elimination of H_2O and CH_3Cl.[21]

Parallel scale-up runs of HMF degradation in [EMIM]OAc clearly showed formation of a new compound by HPLC as the predominant product (Figure 4.2). Monitoring of the reaction by NMR showed a maximum yield of 72 % at HMF conversion of 86 % at 80 ℃ (Figure 4.3). Subsequent separation and purification afforded the pure compound (Figure 4.4) in 50% isolated yield. This compound is stable in water and air, as it was isolated from the aqueous medium and no decomposition or oxidation was observed after exposing the solid sample to air for a week. NMR and MS data (see Experimental) clearly indicate it is a C_{12} furoin, DHMF.

The molecular structure of DHMF has been confirmed by X-ray diffraction analysis (Figure 4.8). Structural data clearly show a C=O double bond for C(6) with a bond length of 1.224(7)Å and a CH–OH single bond for C(7) with a bond length of 1.420(10)Å, the latter of which is identical to the terminal CH_2–OH bond distance [e.g., C(12)–O(6)H = 1.420(6) Å]. This assignment is further confirmed by the sum of the angles around C(6) (carbonyl) and C(7) (hydroxyl) carbons of 360.1 ° and 332.3 °, for sp^2-hybridized trigonal-planar and sp^3-hybridized tetrahedral carbon centers, respectively. There are two independent molecules with minor structural differences in the unit cell, which are associated with each other by moderate hydrogen bonds, as indicated by d(D–H) (O6–H6) = 0.820 Å, d(H---A) (H6---O12) = 1.896 Å, <D–H---A = 173.77 º, and d(D---A) = 2.712 Å; d(D–H) (O7–H7) = 0.820 Å, d(H---A) (H7---O1) = 1.881 Å, <D–H---A = 179.19 º, and d(D---A) = 2.701 Å.

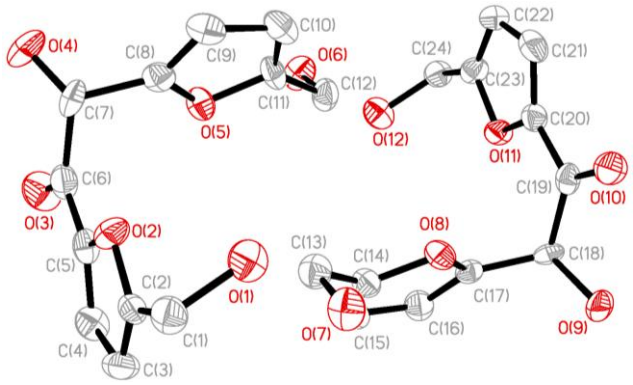

Figure 4.8 X-ray crystal structure of 5,5'-di(hydroxymethyl)furoin (DHMF). Hydrogen atoms have been omitted for clarity and ellipsoids drawn at 50% probability.

Catalytic cycle for umpolung self-condensation of HMF to DHMF. The identification and characterization of the structure of the main product formed from the HMF degradation in [EMIM]OAc prompted us to realize that DHMF is the umpolung condensation product of HMF catalyzed by [EMIM]OAc. The catalytic cycle for this unique process enabled by the organocatalytic [EMIM]OAc is proposed in Scheme 4.1. The catalyst is 1-ethyl-3-methylimidazolin-2-ylidene carbene **I**, present in the [EMIM]OAc equilibrium that favors the ion pair form.[14,15,16] The early steps of the proposed elementary reactions involved in the catalysis deviate somewhat from those put forth for the NHC-catalyzed umpolung of aldehydes[13,22] and α,β-unsaturated esters,[23] due to the important role of HOAc, which co-exists with carbene **I** in the [EMIM]OAc equilibrium. Specifically, nucleophilic addition of the carbene **I** to the carbonyl group of HMF generates a zwitterionic tetrahedral intermediate, which is protonated by HOAc to afford a 2-(5-hydroxymethyl-2-α-hydroxyfuranyl)imidazolium acetate salt, the resting intermediate **II**.[24] Under elevated temperature, intermediate **II** is deprotonated by the acetate anion to form a nucleophilic enaminol (**III**'). Like the Breslow intermediate

involved in the benzoin reaction,[25] this enaminol is the acyl anion equivalent (**III**), thus attacking the carbonyl group of a second HMF molecule to form another tetrahedral intermediate (**IV**). Collapse of this tetrahedral intermediate, via proton transfer and elimination of **I**, produces DHMF and regenerates the NHC catalyst, thus closing the catalytic cycle (Scheme 4.1). Based on the data to-date (*vide infra*), the step from **I** to **II** is fast (and reversible), relative to the slow step of going from **II** to **III**. This proposed overall mechanism explains the observed catalysis for upgrading of HMF into DHMF by [EMIM]OAc and is consistent with the four lines of evidence presented as follows.

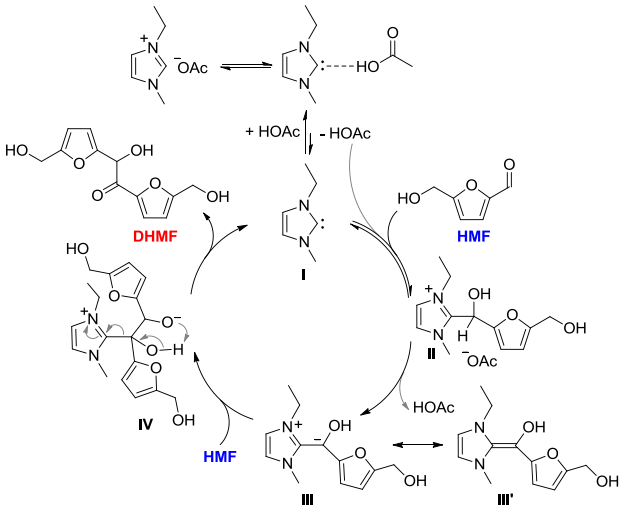

Scheme 4.1 Proposed catalytic cycle for umpolung self-condensation of HMF to DHMF by a catalytic IL, [EMIM]OAc.

Four lines of evidence that support the proposed carbene catalysis. First, previous studies have shown that a small concentration of carbene exists in [EMIM]OAc,[14,15] which is capable of executing carbene catalysis.[16] To further confirm this point, we replaced [EMIM]OAc with 1-ethyl-2,3-dimethylimidazolium acetate, ([EDMIM]OAc, in which the acidic proton at C(2) of the imidazolium ring is substituted with the methyl group. As predicted, the carbene catalysis

is completely shut down and there is no condensation of HMF into DHMF, thereby supporting the proposed catalyst being the NHC released from [EMIM]OAc.

Second, on the basis of the proposed mechanism, ILs paired with non-basic anions, which are incapable of self-releasing NHCs like [EMIM]OAc, should be ineffective for this carbene catalysis but could be activated, with a strong organic base, to deliver the NHC catalyst and thus effect the same type of carbene catalysis. Indeed, [EMIM]Cl, while itself is ineffective for this catalysis, becomes a highly effective HMF upgrading catalyst system, when treated with DBU (1,8-diazabicyclo[5.4.0] undec-7-ene) which generates the NHC catalyst *in situ*; thus, with a 5 mol% catalyst loading, which was controlled by the amount of DBU added, DHMF was obtained in 96% yield (by HPLC) at 80 °for 1 h. Potential co-solvent effects were also examined, showing a minimal effect on the DHMF yield; thus, addition of the THF co-solvent gave a DHMF yield of 96.7 %, while the yield was 93.8% when employing DMF as a co-solvent.

Third, we obtained direct evidence for the formation of the resting intermediate **II** through NMR monitoring of the HMF reaction with [EMIM]OAc (1:1 molar ratio) in DMSO-d_6 at RT and 80 ℃ with hexamethylbenzene as the internal standard. At RT, 17% HMF was consumed immediately upon mixing HMF with [EMIM]OAc, which approximately corresponds to the amount of the NHC catalyst accessible in [EMIM]OAc at this temperature for its reaction with HMF to form intermediate **II**; this intermediate is not converted into DHMF at RT, even after 24 h. With this valuable information, next we carried out the same reaction at RT but with a 1:5 molar ratio of HMF:[EMIM]OAc to form the intermediate exclusively (i.e., devoid of HMF and DHMF), plus excess [EMIM]OAc; the reaction in this ratio at RT enabled conclusive

spectroscopic characterization of intermediate **II** (Figures 9 and 10). Noteworthy is that the most characteristic peak for the α-hydroxymethyl group *CH*(OH) at 6.74 ppm (DMSO-d_6) or 6.47 ppm (D_2O) in the ^{1}H NMR and 60.4 ppm (DMSO-d_6) in the ^{13}C NMR of intermediate **II** is comparable to the chemical shifts observed for the analogous 2-(α-hydroxybenzyl)thiazolium ions derived from the reaction of thiazolium salts and benzaldehydes, employing either *t*-BuOK as a base or $Et_3N/Et_3NH^+Cl^-$ as a buffer.[24]

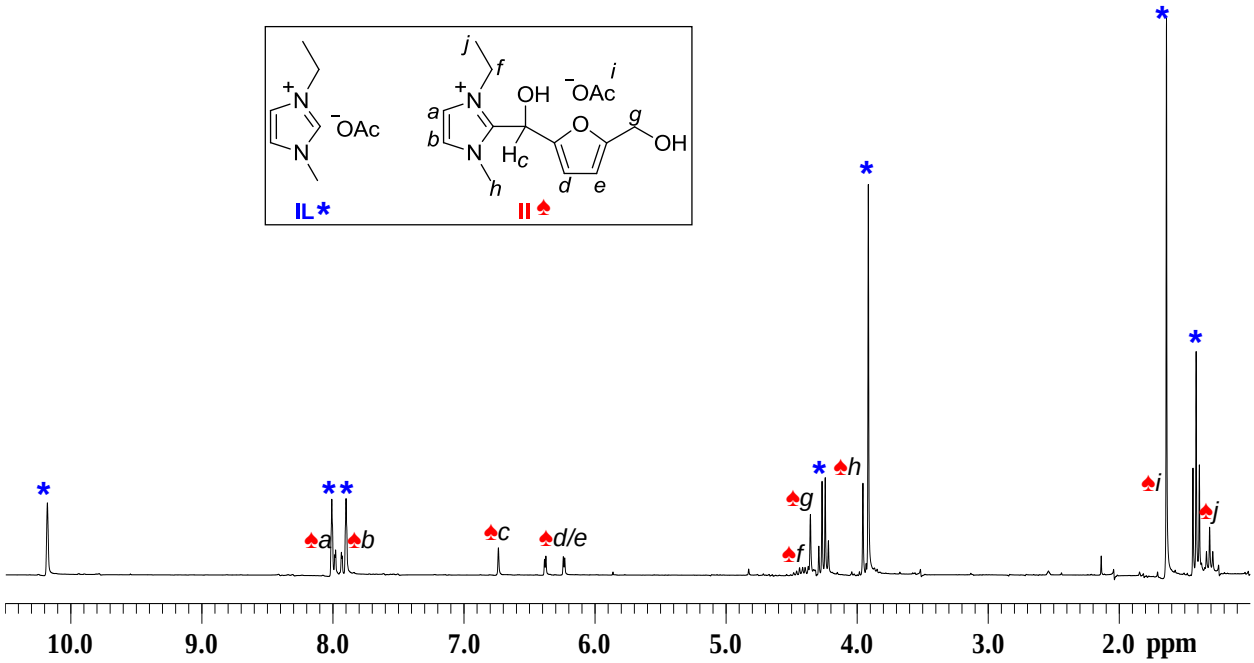

Figure 4.9 ^{1}H NMR (DMSO-d_6)) spectrum of the reaction between HMF and [EMIM]OAc (1:5 molar ratio) at RT for 1.5 h, showing clean formation of intermediate **II** in the presence of excess [EMIM]OAc (small unlabeled peaks are for a trace amount of the residual solvents brought from the IL).

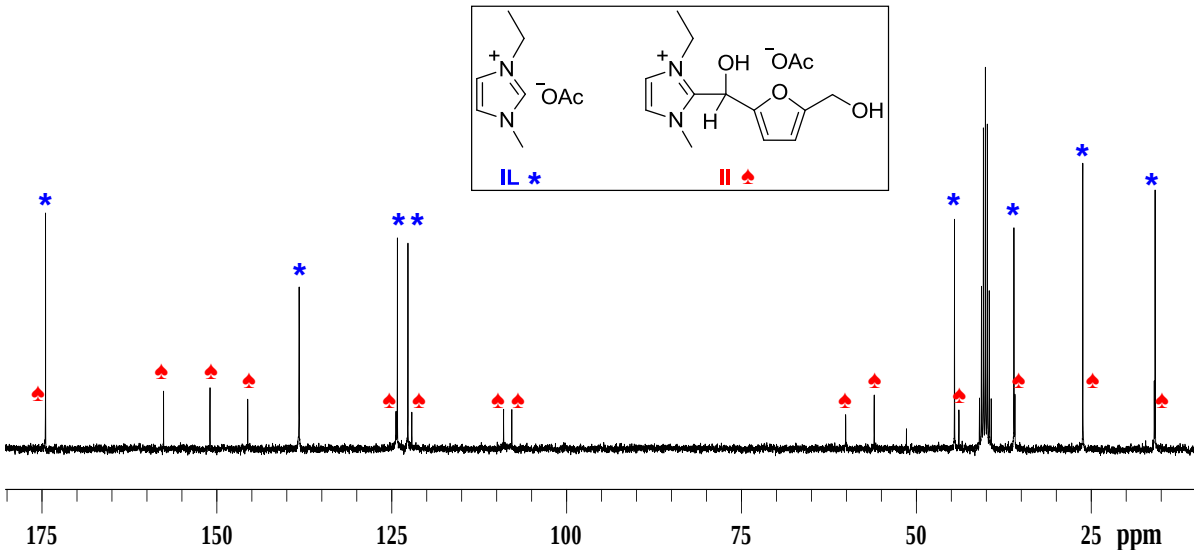

Figure 4.10 ^{13}C NMR (DMSO-d_6) spectrum of the reaction between HMF and [EMIM]OAc (in a 1:5 molar ratio) at RT for 1.5 h, showing clean formation of intermediate **II** in the presence of excess [EMIM]OAc (a peak unlabeled is for a trace amount of the residual solvent (CH_2Cl_2) brought from the IL).

At 80 ℃, on the other hand, as the reaction proceeded from 2 min to 25 min, Figure 4.11 shows a gradual consumption of HMF and intermediate **II**, formed instantaneously upon mixing HMF with [EMIM]OAc (1:1 ratio), which was accompanied by concurrent formation of DHMF. Another experiment that heating of the intermediate in the absence of HMF led to formation of DHMF suggests that the reaction of NHC **I** with HMF to form intermediate **II** is reversible (i.e., release of HMF is needed to further convert **II** to DHMF at elevated temperature). Overall, the above results indicate the formation of intermediate **II** is fast (and reversible), relative to the **II**-to-**III** step.

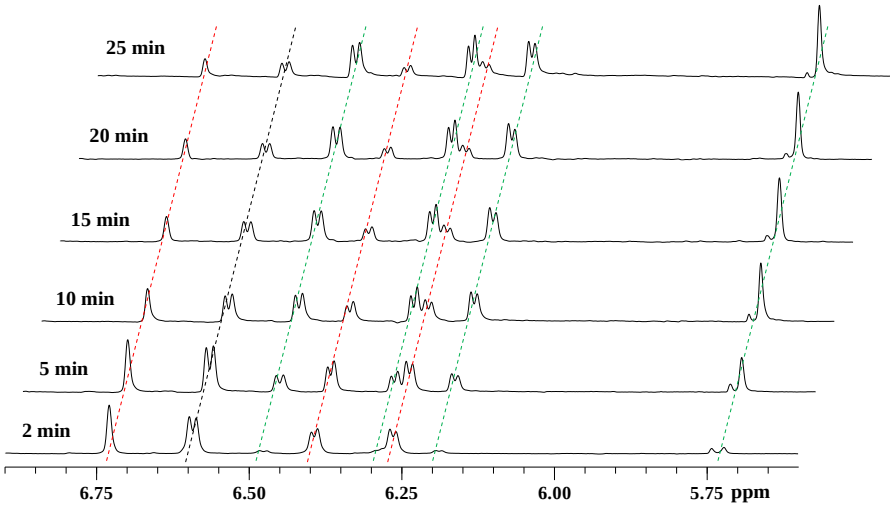

Figure 4.11 Comparison of ^{1}H NMR spectra of the reaction between HMF and [EMIM]OAc (1:1 molar ratio) in DMSO-d_6 at 80 ℃ over the initial 25 min period. This spectral overlay in the most characteristic region shows the gradual decrease in the intensities (normalized by the C_6Me_6 internal standard) of the peaks for HMF (6.59 ppm, ***black*** line) and intermediate **II** (6.73, 6.39, 6.26 ppm, ***red*** lines), with the concomitant increasing of DHMF (6.48, 6.29, 6.19, 5.72 ppm, ***green*** lines). A small shoulder peak at 5.74 with a constant intensity is the residual solvent (CH_2Cl_2) brought into the system.

Fourth, if the small concentration of NHC **I** present in [EMIM]OAc is the catalyst for self-condensation of HMF to DHMF, then the use of the preformed, discrete NHCs should lead to even more rapid and efficient upgrading of HMF to DHMF. Indeed, with the Enders TPT being the catalyst (5 mol%), near quantitative (98% by NMR) conversion of HMF to DHMF was observed in THF at RT after 24 h, resulting in a high isolated yield (86%, unoptimized, Table 4.1) of DHMF. The rate of the TPT (5 mol%)-catalyzed condensation of HMF can be greatly enhanced at elevated temperature; at 60 ℃ for 1 h, 94 % DHMF (NMR yield) was achieved within 1 h, accomplishing a 87% isolated (unoptimized) yield. The performance of the two Arduengo carbenes, 1,3-di-*tert*-butylimidazolin-2-ylidene (I^{t}Bu) and 1,3-di-mesityl-butyl-imidazolin-2-ylidene (IMes),[26] is drastically different. While IMes is also a

highly effective catalyst for umpolung condensation of HMF to DHMF (5 mol% NHC, 93% DHMF by NMR), the more nucleophilic (I^{t}Bu) is completely ineffective. When HMF is mixed with a stoichiometric amount of an NHC (TPT, IMes, or I^{t}Bu) at RT, HMF and NHC were completely consumed without producing DHMF. The remarkable activity and efficiency of TPT in this carbene catalysis is presumably related to the fact that TPT is *both a good nucleophile and leaving group*, the latter of which is essential for closing the catalytic cycle (*c.f.*, Scheme 4.1). By the same analogy, the ineffectiveness of I^{t}Bu could be attributed to its strong binding to HMF and being too poor a leaving group to close the cycle. The trend with TPT being the best catalyst and I^{t}Bu being the worst catalyst (non-activity) in this series for umpolung condensation of HMF is completely opposite of the trend observed for conjugate-addition chain-growth polymerization of α-methylene-γ-butyrolactones.[27] Overall, the above results obtained from using the authentic, discrete NHC catalysts as well as the already established reactivity and fundamental steps of such NHCs towards aldehydes (i.e., benzoin reaction)[13,22] further support the overall umpolung self-condensation of HMF to DHMF mechanism depicted in Scheme 4.1.

Table 4.1 Results on HMF self-condensation to DHMF catalyzed by NHCs

NHC	NHC loading (mol %)	temperature (℃)	time (h)	DHMF yield (NMR) (%)	DHMF yield (isolated) (%)
I^{t}Bu	5	25	24	0	0
	100	25	24	0	0
IMes	5	25	24	92.9	n.d.
	100	25	24	0	0
TPT	5	25	24	98.0	86.2
	100	25	24	trace	n.d.
	5	60	1	93.6	87.1

Solvent: THF. n.d. = not determined.

4.5 Conclusions

In summary, through organocatalysis by the catalytic acetate-based IL [EMIM]OAc, the chloride-based IL [EMIM]Cl in combination with the organic base DBU, or the discrete NHC catalysts TPT and IMes, we have developed a rapid, highly selective and high-yield upgrading of the key biorefining building block HMF into DHMF, a potential high-value biorefinery product as an intermediate to kerosene/jet fuel. The reaction time for this HMF upgrading process is within 1 h under industrially preferred conditions (i.e., ambient atmosphere, 60–80 ℃), and the DHMF selectivity is typically near quantitative and yields are up to 98% (HPLC or NMR) or 87% (unoptimized, isolated yield). This work has also yielded the carbene catalysis mechanism for this upgrading transformation by the catalytic IL, which has been supported by four lines of evidence presented in this report, including the direct identification of the resting intermediate. The technological significance of this work is that, while direct aldol self-condensation of HMF for its upgrading is not possible,[11] the direct umpolung self-condensation of HMF for its upgrading into DHMF is highly facile, which is made possible by *organocatalysis*. Additionally, as many efficient catalyst systems have been developed for conversion of plant biomass resources (glucose or cellulose) into HMF,[6,7] it should be possible to convert such nonfood biomass directly into DHMF via a two-step process. Indeed, our preliminary results in this regard showed the feasibility of transforming glucose directly into DHMF in a stepwise fashion, with the first step converting glucose into HMF by metal catalysis,[6,7a] followed by extraction of HMF and subsequent carbene catalysis. Our future studies will address integration of these two catalytic processes, transformation of DHMF into liquid fuels, and cross-condensation of HMF

with other aldehydes into jet or diesel fuel intermediates.

4.6 References

(1) (a) Remsing, R. C.; Swatloski, R. P.; Rogers R. D.; Moyna, G. *Chem. Commun.* **2006**, 1271−1273. (b) Swatloski, R. P.; Spear, S. K.; Holbrey J. D.; Rogers, R. D. *J. Am. Chem. Soc.* **2002**, *124*, 4974−4975.

(2) (a) Zakrzewska M. E.; Bogel-Łukasik E.; Bogel-Łukasik R. *Energy & Fuels* **2010**, *24*, 737–745. (b) El Seoud, O. A.; Koschella, A.; Fidale, L. C.; Dorn S.; Heinze, T. *Biomacromolecules* **2007**, *8*, 2629−2647.

(3) (a) Wasserscheid P.; Welton, T. Eds. *Ionic Liquids in Synthesis*, 2nd ed., Wiley-VCH, Weinheim, **2008**. (b) P âr vulescu V. I.; Hardacre, C. *Chem. Rev.* **2007**, *107*, 2615−2665. (c) Stark A.; Seddon, K. *Ionic Liquids in Kirk-Othmer Encyclopedia of Chemical Technology*, John Wiley and Sons: New York, **2007**, *26*, 836–920.

(4) (a) Sun N.; Rodriguez, H.; Rahman M.; Rogers, R. D. *Chem. Commun.* **2011**, *47*, 1405−1421. (b) Pinkert, A.; Marsh, K. N.; Pang S.; Staiger, M. P. *Chem. Rev.* **2009**, *109*, 6712−6728.

(5) Selected recent examples: (a) Dee S. J.; Bell, A. T. *ChemSusChem* **2011**, *4*, 1166−1173. (b) Binder J. B.; Raines, R. T. *Proc. Natl. Acad. Sci.* **2010**, *107*, 4516−4521. (c) Vanoye, L.; Fanselow, M.; Holbrey, J.; Atkins M. P.; Seddon, K. R. *Green Chem.* **2009**, *11*, 390−396. (d) Li, C.; Wang Q.; Zhao, Z. K. *Green Chem.* **2008**, *10*, 177−182. (e) Li C.; Zhao, Z. K. *Adv.*

Synth. Catal. **2007**, *349*, 1847−1850.

(6) Zhang, Y.; Du, H.; Qian X.; Chen, E. Y.-X. *Energy & Fuels* **2010**, *24*, 2410–2417.

(7) Selected recent reviews and examples: (a) Liu D.; Chen, E. Y.-X. *Appl. Catal. A: Gen.* **2012**, *435-436*, 78–85. (b) Rosatella, A. A.; Simeonov, S. P.; Frade R. F. M.; Afonso, C. A. M. *Green Chem.* **2011**, *13*, 754-793. (c) Zhang, Z.; Wang, Q.; Xie, H.; Liu W.; Zhao, Z. K. *ChemSusChem* **2011**, *4*, 131−138. (d) Kim, B.; Jeong, J.; Lee, D.; Kim, S.; Yoon, H.-J.; Lee, Y.-S.; Cho, J. K. *Green Chem.* **2011**, *13*, 1503−1506. (e) Pidko, E.; Degirmenci, V.; van Santen R. A.; Hensen, E. J. M. *Angew. Chem. Int. Ed.* **2010**, *49*, 2530−2534. (f) Stålberg, T.; Sørensen M. G.; Riisager, A. *Green Chem.* **2010**, *12*, 321−325. (g) Tao, F.; Song H.; Chou, L. *ChemSusChem* **2010**, *3*, 1298−1303. (h) Qi, X.; Watanabe, M.; Aida T. M.; Smith, R. L. Jr. *ChemSusChem* **2010**, *3*, 1071−1077. (i) Binder J. B.; Raines, R. T. *J. Am. Chem. Soc.* **2009**, *131*, 1979−1985. (j) Hu, S.; Zhang, Z.; Song, J.; Zhou Y.; Han, B. *Green Chem.* **2009**, *11*, 1746−1749. (k) Yong, G.; Zhang Y.; Ying, J. Y. *Angew. Chem. Int. Ed.* **2008**, *47*, 9345−9348. (l) Zhao, H.; Holladay, J. E.; Brown H.; Zhang, Z. C. *Science* **2007**, *316*, 1597−1600.

(8) Selected recent reviews: (a) Alonso, D. M.; Bond J. Q.; Dumesic, J. A. *Green Chem.* **2010**, *12*, 1493−1513. (b) Stöcker, M. *Angew. Chem. Int. Ed.* **2008**, *47*, 9200−9211. (c) Corma, A.; Iborra S.; Velty, A. *Chem. Rev.* **2007**, *107*, 2411−2502. (d) Chheda, J. N.; Huber G. W.; Dumesic, J. A. *Angew. Chem. Int. Ed.* **2007**, *46*, 7164−7183. (e) Huber, G. W.; Iborra S.; Corma, A. *Chem. Rev.* **2006**, *106*, 4044−4098. (f) "*Top Value Added Chemicals from Biomass*", Werpy T.; Petersen, G. Eds. U.S. Department of Energy (DOE) report:

DOE/GO-102004-1992, **2004**.

(9) Balakrishnan, M.; Sacia E. R.; Bell, A. T. *Green Chem.* **2012**, *14*, 1626−1634.

(10) (a) Thananatthanachon T.; Rauchfuss, T. B. *Angew. Chem. Int. Ed.* **2010**, *49*, 6616−6618. (b) Chidambaram M.; Bell, A. T. Green Chem. 2010, 12, 1253−1262. (c) Román-Leshkov, Y.; Barrett, C. J.; Liu Z. Y.; Dumesic, J. A. *Nature* **2007**, *447*, 982−986.

(11) Huber, G. W.; Chheda, J. N.; Barrett C. J.; Dumesic, J. A. *Science* **2005**, *308*, 1446−1450.

(12) (a) Qin, Y.; Lu, X.; Sun N.; Rogers, R. D. *Green Chem.* **2010**, *12*, 968−971. (b) Sun, N.; Rahman, M.; Qin, Y.; Maxim, M. L.; Rodríguez H.; Rogers, R. D. *Green Chem.* **2009**, *11*, 646−655.

(13) Selected recent reviews: (a) Dröge T.; Glorius, F. *Angew. Chem. Int. Ed.* **2010**, *50*, 6940−6952. (b) Chiang P.-C.; Bode, J. W. in *RSC Catalysis Series*, Royal Society of Chemistry, Cambridge, **2010**, 399–435. (c) Moore, J. L.; Rovis, T. *Top. Curr. Chem.* **2009**, *291*, 77−144. (d) Hahn F. E.; Jahnke, M. C. *Angew. Chem. Int. Ed.* **2008**, *47*, 3122−3172. (e) Nair, V.; Vellalath S.; Babu, B. P. *Chem. Soc. Rev.* **2008**, *37*, 2691−2698. (f) Marion, N.; Díez-González S.; Nolan, S. P. *Angew. Chem. Int. Ed.* **2007**, *46*, 2988−3000. (g) Enders, D.; Niemeier O.; Henseler, A. *Chem. Rev.* **2007**, *107*, 5606−5655. (h) Bourissou, D.; Guerret, O.; Gabbaï F. P.; Bertrand, G. *Chem. Rev.* **2000**, *100*, 39−91.

(14) Hollóczki, O.; Gerhard, D.; Massone, K.; Szarvas, L.; Németh, B.; Veszprémi T.; Nyulászi, L. *New J. Chem.* **2010**, *34*, 3004−3009.

(15) Rodríguez, H.; Gurau, G.; Holbrey J. D.; Rogers, R. D. *Chem. Commun.* **2011**, *47*, 3222−3224.

(16) Kelemen, Z.; Hollóczki, O.; Nagy, J.; Nyulászi, L. *Org. Biomol. Chem.* **2011**, *9*, 5362−5364.

(17) (a) Enders, D.; Breuer, K.; Kallfass U.; Balensiefer, T. *Synthesis* **2003**, 1292–1295. (b) Enders, D.; Breuer, K.; Raabe, G.; Runsink, J.; Teles, J. H.; Melder, J.-P.; Ebel K.; Brode, S. *Angew. Chem. Int. Ed.* **1995**, *34*, 1021–1023.

(18) (a) Enders, D.; Breuer, K.; Raabe, G.; Runsink, J.; Teles, J. H.; Melder, J. P.; Ebel, K.; Brode, S. *Angew. Chem., Int. Ed. Engl.* **1995**, *34*, 1021–1023. (b) Enders, D.; Breuer, K.; Kallfass, U.; Balensiefer, T. *Synthesis* **2003**, 1292–1295.

(19) Brandt, A.; Hallett, J. P.; Leak, D. J.; Murphy, R. J.; Welton, T. *Green Chem.* **2010**, *12*, 672–679.

(20) *SHELXTL*, Version 6.12; Bruker Analytical X-ray Solutions: Madison, WI, **2001**.

(21) Zhang, Z.; Liu, W.; Xie H.; Zhao, Z. K. *Molecules* **2011**, *16*, 8463–8474.

(22) Selected reviews and examples: (a) Berkessel, A.; Elfert, S.; Etzenbach-Efferts K.; Teles, J. H. Angew. *Chem. Int. Ed.* **2010**, *49*, 7120–7124. (b) Hirano, K.; Biju, A. T.; Piel I.; Glorius, F. *J. Am. Chem. Soc.* **2009**, *131*, 14190–14191. (c) Kawanaka, Y.; Phillips E. M.; Scheidt, K. A. *J. Am. Chem. Soc.* **2009**, *131*, 18028–18029. (d) Chiang, P.-C.; Rommel, M.; Bode, J. W. *J. Am. Chem. Soc.* **2009**, *131*, 8714–8718. (e) DiRocco, D. A.; Oberg, K. M.; Dalton D. M.; Rovis, T. *J. Am. Chem. Soc.* **2009**, *131*, 10872–10874. (f) Hashmi, A. S. K.; Wölfle, M.; Teles J. H.; Frey, W. *Synlett.* **2007**, 1747–1752. (g) Enders, D.; Niemeier O.; Balensiefer, T. *Angew. Chem. Int. Ed.* **2006**, *45*, 1463–1467. (h) Enders D.; Kallfass, U. *Angew. Chem. Int. Ed.* **2002**, *41*, 1743–1745. (i) Lee, C. K.; Kim, M. S.; Gong J. S.; Lee, I.-S. H. *J. Heterocyclic Chem.* **1992**, *29*, 149–153.

(23) (a) Biju, A. T.; Padmanaban, M.; Wurz N. E.; Glorius, F. *Angew. Chem. Int. Ed.* **2011**, *50*, 8412–8415. (b) Matsuoka, S.-I.; Ota, Y.; Washio, A.; Katada, A.; Ichioka, K.; Takagi K.; Suzuki, M. *Org. Lett.* **2011**, *13*, 3722–3725. (c) Fisher, C.; Smith, S. W.; Powell D. A.; Fu, G. C. *J. Am. Chem. Soc.* **2006**, *128*, 1472–1473.

(24) Analogous 2-(α-hydroxybenzyl)thiazolium ions derived from the reaction of thiazolium salts and benzaldehydes, employing either the *t*-BuOK base or the $Et_3N/Et_3NH^+Cl^-$ buffer, have been reported: (a) White M. J.; Leeper, F. J. *J. Org. Chem.* **2001**, *66*, 5124–5131. (b) Chen, Y.-T., Barletta, G. L.; Haghjoo, K.; Cheng J. T.; Jordan, F. *J. Org. Chem.* **1994**, *59*, 7714–7722. (c) Breslow R.; Kim, R. *Tetrahedron Lett.* **1994**, *35*, 699–702.

(25) Breslow, R. *J. Am. Chem. Soc.* **1958**, *80*, 3719–3726.

(26) (a) Arduengo, A. J. III; Bock, H.; Chen, H.; Denk, M.; Dixon, D. A.;Green, J. C.; Herrmann, W. A.; Jones, N. L.; Wagner M.; West, R. *J. Am. Chem. Soc.* **1994**, *116*, 6641–6649. (b) Arduengo, A. J. III; Dias, H. V. R.; Harlow R. L.; Kline, M. *J. Am. Chem. Soc.* **1992**, *114*, 5530–5534.

(27) Zhang Y.; Chen, E. Y.-X. *Angew. Chem. Int. Ed.* **2012**, *51*, 2465–2469.

Chapter 5

Diesel and Alkane Fuels From Biomass by Organocatalysis and Metal-Acid Tandem Catalysis

5.1 Summary

Reported herein is a combination of solvent-free organocatalysis and metal-acid tandem catalysis in water that leads to a highly effective new strategy for upgrading furaldehyde biorefining building blocks to oxygeneated diesel and high-quality $C_{10–12}$ linear alkane fuels. This strategy consists of organocatalytic self-condensation (umpolung) of biomass furaldehydes into $C_{10–12}$ furoin intermediates in quantitative selectivity and 100% atom-economy, followed by hydrogenation, etherification or esterification into oxygenated biodiesel, or hydrodeoxygenation by metal-acid tandem catalysis into premium alkane jet fuels.

5.2 Communication

Recognized as a key biorefining building block and a biomass platform chemical, 5-hydroxymethylfurfural (HMF)[1] has been studied extensively as part of major efforts in developing technologically and economically feasible routes for converting nonfood lignocellulosic biomass into feedstock chemicals, sustainable materials, and liquid fuels.[2] Since the important discovery of the $CrCl_2$/ionic liquid (IL) catalyst system for effective conversion of the cellulosic glucose to HMF,[3] a large number of other metal or non-metal catalyst systems

have been developed to promote effective conversion of glucose or directly cellulose into HMF.[4] In contrast, research on the upgrading of HMF or related furaldehydes into higher molecular weight and high energy-density kerosene/jet (C_8 to C_{16}, with C_{12} being the major constituent) or diesel (up to C_{22}) intermediates or fuels is scarce and thus is much needed. Considering the fact that HMF cannot undergo self-aldol condensation due to lack of α-hydrogen, Dumesic and co-workers utilized cross-aldol condensation of HMF with enolizable organic compounds such as acetone in the presence of an alkaline catalyst, followed by dehydration/ hydrogenation processes, to upgrade HMF into C_9 to C_{15} liquid alkane fuels (Scheme 5.1, route **A**).[5] Recently, Corma and co-workers developed hydroxyalkylation of 2-methylfuran to perform trimerization in the presence of an acid catalyst, the product of which is subject to high-temperature hydrodeoxygenation (HDO) to produce high-cetane number 6-alkylundecanes;[6] HMF can be used to replace one of the 2-methylfuran molecules in the trimerization step (Scheme 5.1, route **B**). Most recently, Bell and co-workers reported acid-catalyzed etherification and reductive etherification of HMF into 5-(alkoxymethyl) furfurals and 2,5-bis(alkoxymethyl)furans as potential oxygenated biodiesel candidates (Scheme 5.1, route **C**).[7] This direct HMF etherification route offers an alternative for producing usable diesel-range fuels to the etherification of the chloride derivative of HMF, 5-(chloromethyl)furfural, with alcohol.[8]

Recent research on HDO has focused on the development of bifunctional catalysts for upgrading lignin-derived pyrolysis oils (phenols, guiaiacols and syringols, etc) into hydrocarbons.[9,10] Water can be used as a suitable solvent for HDO, allowing for spontaneous separation of hydrocarbons during the reaction. Supported catalysts such as Ni/HZSM-5, Pd/C +

H_3PO_4 and Pd/C + HZSM-5 can achieve high to quantitative yield of cycloalkanes from phenols under 5 MPa H_2 at 250 ℃ within 2 h.[10] However, for furan compounds derived from cellulosic biomass, HDO products are complicated by furan-ring opening, carbon chain fragmentation, rearrangement, and cyclization, rendering a wide distribution of hydrocarbons. Using conditions similar to those employed for the HDO of the lignin-derived pyrolysis oils, the HDO of furfural gave tetrahydropyran in 36% yield besides pentane.[10a] For the HDO of 5-methylfuran trimer (5,5-bisylvyl-2-pentanone) by Pt/C and Pt/TiO_2 under 5 MPa H_2 and 400 ℃, 96 % oily products were classified as C_9 to C_{16} hydrocarbons (linear, branched, monocyclic, and bicyclic).[6] In a two-step HDO of furoin consisting of hydrogenation by Pd/Al_2O_3 to render the substrate water soluble and the subsequent HDO process with Pt/SiO_2-Al_2O_3, Dumesic et al. obtained a wide distribution of alkanes, with 34 % C_{10} selectivity.[5] The HDO of the reductive Pinacol coupling products of furfural and 5-methylfurfural (MF) by Pt/C and solid acid $TaOPO_4$ afforded high yields of alkanes.[11] Alternatively, opening the furan rings first under mild conditions (which is applicable only to certain types of furan rings[12]), followed by HDO, produces alkanes more selectively.[13]

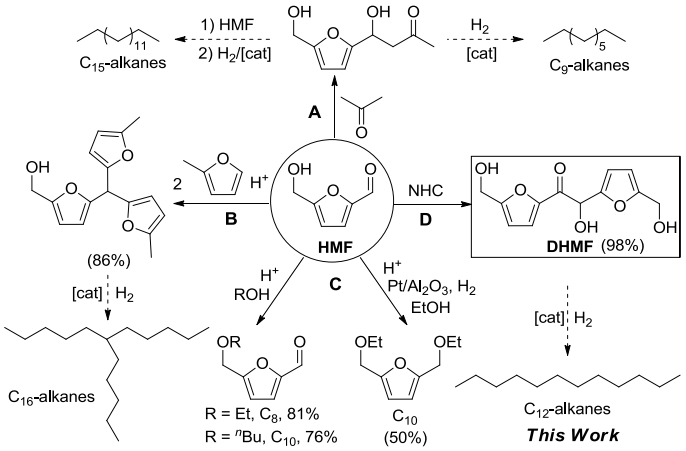

Scheme 5.1 Four different routes to upgrade HMF into kerosene or diesel intermediates or fuels.

Ideally, *direct coupling* of two HMF molecules would make a C_{12} jet/kerosene fuel intermediate, which could be catalytically transformed into liquid fuels. Herein we report the selective and quantitative coupling of HMF to 5,5'-di(hydroxymethyl)furoin (DHMF) under solvent-free conditions using 1 mol% of an organic *N*-heterocyclic carbene (NHC) catalyst and subsequent transformations of DHMF into oxygenated diesel fuels through hydrogenation, etherification or esterification, as well as high-quality kerosene/jet fuels through a highly selective HDO process that produces nearly quantitative linear hydrocarbons (96% C_{10-12} linear alkanes) in the organic phase (Scheme 5.1, route **D**).

We recently disclosed that, through the NHC-catalyzed umpolung benzoin condensation mechanism[14] in the presence of a catalytic acetate IL, 1-ethyl-3-methylimidazolium acetate, or a discrete NHC catalyst (5 mol% 1,3,4-triphenyl-4,5-dihydro-1*H*-1,2,4-triazol-5-ylidene, TPT), at 60 ℃ in THF for 1 h, HMF can be selectively self-coupled into DHMF, a promising new C_{12} kerosene/jet fuel intermediate.[15] This coupling reaction is unique to the organically catalyzed umpolung reaction, as other types of coupling reactions, such as reductive Pinacol coupling, did not work for HMF.[11] In the present study we found that this catalytic coupling reaction can be carried out *in the absence of any solvent* (except for a small amount of an organic solvent was added at the end of the reaction to remove traces of the catalyst), although both HMF and the NHC catalyst are solids (Scheme 5.2). With a TPT loading of 1 mol%, quantitative HMF conversion was observed at 60 ℃ after 1 h and DHMF was formed quantitatively (by NMR) with a high isolated yield of 95 %. Using a lower catalyst loading of 0.5 mol%, an isolated yield of 87 % can still be achieved. This coupling reaction was also carried out in toluene, where

DHMF precipitated out of the solution and the TPT catalyst remained in solution for convenient product separation/purification and catalyst recovery. Likewise, furfural and MF can also be coupled using 1 mol% TPT, even at room temperature, into 1,2-di(furan-2-yl)-2-hydroxyethanone (furoin) and 5,5'-dimethylfuroin[16] in 89 % and 94 % isolated yields, respectively. Umpolung of aldehydes catalyzed by NHCs[14] is proposed to proceed through the nucleophilic enaminol or the Breslow intermediate[17] involved in the benzoin reaction.[18] Indeed, we observed the formation of such an intermediate through the stoichiometric reaction of HMF and 1,3-bis(2,4,6-trimethylphenyl)-1,3-dihydro-2H-imidazol-2-ylidene (IMes) in DMSO-d_6 at ambient temperature (Figure 5.3). This enaminol is the acyl anion equivalent, thus attacking the carbonyl group of a second HMF molecule to form another tetrahedral intermediate. Collapse of this tetrahedral intermediate, via proton transfer and elimination of the NHC, produces DHMF and regenerates the NHC catalyst, thus closing the catalytic cycle and leading to the catalytic formation of the coupling product DHMF (Scheme 5.2).

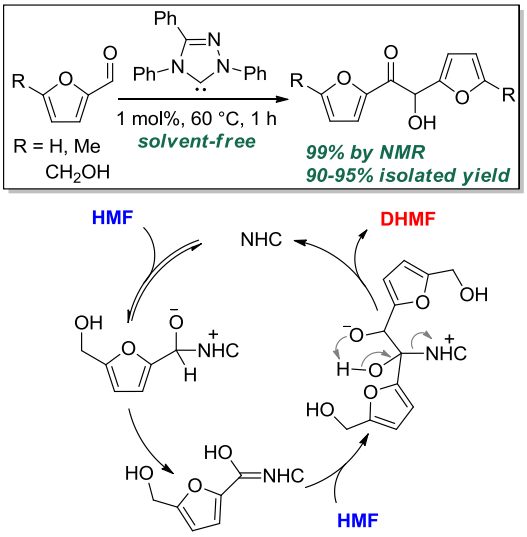

Scheme 5.2 Solvent-free self-condensation of furaldehydes to furoins catalyzed by an NHC catalyst and depicted catalytic cycle for the umpolung condensation of HMF to DHMF.

As the self-condensation products of the furaldehydes are solids, we investigated three possible routes to transform them into liquids as potential jet or diesel fuels. We first examined the hydrogenation route to convert the furoins into their saturated derivatives using the recyclable Pd/C catalyst. Under modest hydrogenation conditions (2.7 MPa H_2 and 90 ℃) in the presence of Pd/C, all three furoins were successfully converted into liquids (Scheme 5.3). The liquids were not simply fully hydrogenated products, but accompanied with some hydrogenolysis products, as suggested by the elemental results that showed C and H contents were higher than the theoretical values of the fully hydrogenated products (Table 5.1). Heating values of the hydrogenated products from furoin and 5,5'-dimethylfuroin were measured to be 32.7 and 33.3 MJ/kg, respectively, which are noticeably higher than that for ethanol (28.6 MJ/kg), approaching to the value for dimethylfuran (33.7 MJ/kg). These results indicated the potential use of furoin and 5,5'-dimethylfuroin as oxygenated liquid fuels after simple hydrogenation.

Next, following the procedures established for etherification of HMF with alcohols to form 5-(alkoxymethyl)furfurals[7] and acetylation of the hydrogenated acetal derived from furfural and glycerol,[19] we investigated etherification and esterification routes to convert DHMF into its corresponding ether with ethanol and ester with propionic anhydride. Indeed, HMF, employed as a control run, was quantitatively converted to 5-ethoxymethylfurfural by NMR in excess of ethanol at 75 ℃ for 24 h with solid acid catalyst Dowex G-26 (H-form) resin. Under similar conditions, DHMF was also quantitatively converted to the corresponding liquid ether, 5,5'-di(ethoxymethyl)furoin (DEMF), with the secondary alcohol remaining intact. On the other hand, esterification of DHMF using excess propionic anhydride esterified all three hydroxyl

groups, thus forming DHMF-tripropionic ester (Scheme 5.3). Hence, both the etherification and esterification routes can serve as alternative strategies for liquefying DHMF into diesel fuels.

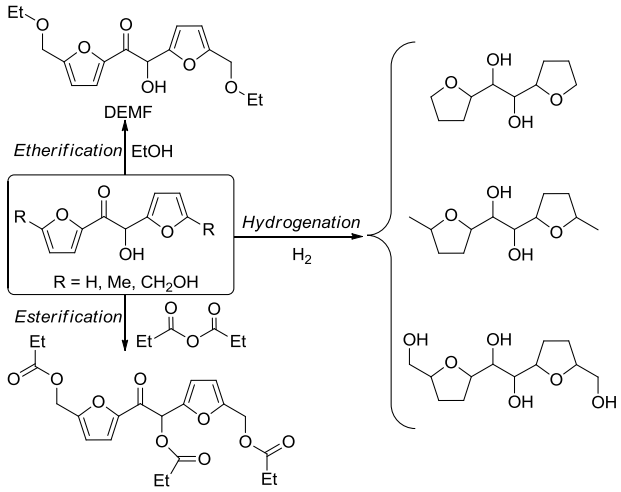

Scheme 5.3 Hydrogenation of furoins and etherification and esterification of DHMF into oxygenated liquid diesel candidates.

The third route utilized the HDO process through metal-acid tandem catalysis. The overall HDO process of DHMF to linear alkanes (Scheme 5.1) can be reasoned to proceed through metal-catalyzed hydrogenation to give the saturated polyol, acid-catalyzed ring-opening/hydrolysis of furan rings in aqueous solution to yield a straight-chain polyol, and acid-catalyzed dehydration, followed by metal-catalyzed hydrogenation to afford the final saturated linear C_{12} alkane, *n*-dodecane, ideally with minimum fragmentation, branching, or cyclization. This overall picture calls for a bifunctional catalyst with both metal and acid sites (e.g., noble metal on acidic support, $Pt/CsH_2PW_{12}O_{40}$ [20]) to promote this HDO process, comprising hydrogenation−ring-opening/hydrolysis−dehydration-hydrogenation cascade reactions. This picture is consistent with our results obtained from the above hydrogenation over Pd/C that produces the furan-containing polyol without ring-opening (*vide supra*) and the

observation by Dumesic et al. that hydrogenation, but not ring-opening, of the furan ring was the primary reaction for the furan-containing compounds when subjected to HDO conditions using metal-acid bifunctional catalysts.[5]

To generate hydrocarbon premium liquid fuels by the HDO process, we investigated HDO of DHMF under moderate conditions (250-300 ℃ and 3.5 MPa H_2 pressure) with a number of bifunctional catalyst systems. Furoin was reported to be converted to alkanes by a two-step process, with the first step being hydrogenation to make it soluble in water, followed by subsequent HDO to avoid choking problems.[5] As DHMF is water soluble, its HDO process can be carried out directly in water without prior hydrogenation. After initial catalyst screening, we identified the following three bifunctional catalyst systems that worked well for DHMF conversion to alkanes: (a) acidic solution (H_3PO_4) and Pd/C; (b) heteropoly acid ($CsH_2PW_{12}O_{40}$) supported Pt; and (c) acidic solid catalyst ($TaOPO_4$) and Pt/C. In all cases, DHMF was completely converted and no or a negligible amount of alkanes below C_{10} were observed. For the Pd/C + H_3PO_4 system (5.9 mol% Pd loading relative to DHMF, Table 5.2), the alkane selectivity in the organic phase was 38 %, consisting of 8.6 % C_{10}, 17.6 % C_{11} and 12.2 % C_{12} alkanes. A relatively higher alkane selectivity (52 %) was obtained by Pt/$CsH_2PW_{12}O_{40}$ (2.6 mol% Pt loading relative to DHMF), consisting of 11.3 % C_{11} and 40.6 % C_{12} alkanes (Figure 5.4). We also compared the performance of two different heteropoly-acids ($CsH_2PW_{12}O_{40}$ and $Cs_{2.5}H_{0.5}PW_{12}O_{40}$), revealing that Pt/$Cs_{2.5}H_{0.5}PW_{12}O_{40}$ only converted DHMF to a trace amount of alkanes. This result shows that the stronger polyacid $CsH_2PW_{12}O_{40}$ is needed to promote the furan ring opening. Varying HDO conditions, including a biphase system of hexane/water and

higher temperature at 300 ℃ (Table 5.2), actually lowered the alkane selectivity to 24.7 % and 39.7 %, respectively. The isolated liquid fuels after the HDO process contain noticeably higher carbon ratios (75-80 %) than those by hydrogenation (60-66 %). *Most excitingly*, utilizing the [Pt/C + $TaOPO_4$] catalyst system (3.2 mol% Pt loading relative to DHMF, Table 5.2), the highest alkane selectivity of **96 %** was achieved at 300 ℃ for 3 h, producing 27.0 % C_{10} (*n*-decane), 22.9 % C_{11} (*n*-undecane) and 45.6 % C_{12} (*n*-dodecane), Figure 5.1. It is remarkable to see the clean formation of three linear $C_{10–12}$ alkanes through this highly effective HDO process. Moreover, both Pt/C and $TaOPO_4$ can be readily recycled by simple filtration.

When compared with current methods for upgrading biomass furan compounds into biofuels, *the DHMF route* reported herein possesses the following four potential advantages: (1) DHMF is obtained from self-coupling of HMF, without the need for cross condensation with other petrochemicals; (2) HMF self-coupling is catalyzed by the organic NHC catalyst, which can be carried out under solvent-free conditions (in neat) at 60 ℃ and 1 h affording DHMF in near quantitative isolated yield; (3) Owing to its solubility in water, the HDO of DHMF can be carried out directly in water, allowing for spontaneous separation of hydrocarbons from the aqueous phase; and (4) DHMF hydrodeoxygenation achieves high conversion and near quantitative selectivity towards linear C_{10}–C_{12} alkanes with a narrow distribution of alkanes.

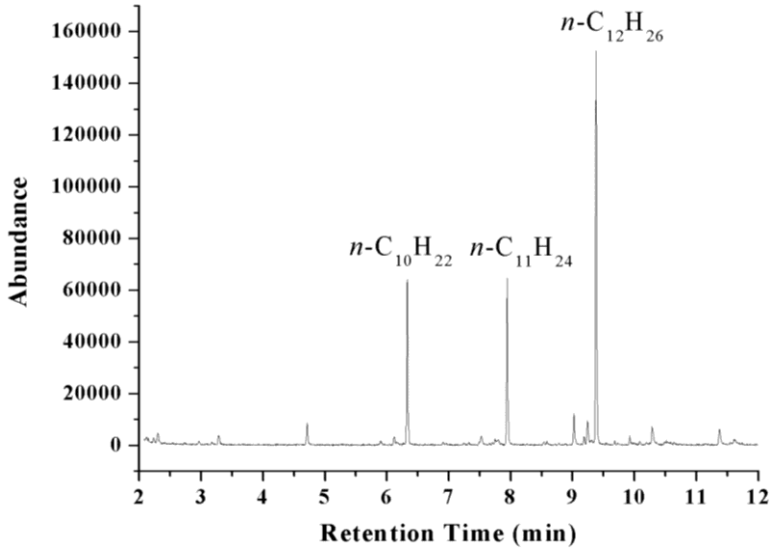

Figure 5.1 GC-MS chromatogram of the organic phase products produced by HDO of DHMF with Pt/C + $TaOPO_4$.

In summary, we have developed a highly effective new strategy for upgrading biomass furaldehydes to liquid fuels. This strategy consists of organocatalytic self-condensation (umpolung) of biomass furaldehydes into $C_{10–12}$ furoin intermediates, followed by hydrogenation, etherification or esterification into oxygenated biodiesel, or hydrodeoxygenation by metal-acid tandem catalysis into premium alkane jet fuels. The umpolung coupling step is carried out under solvent-free conditions, catalyzed by the organic NHC, and quantitatively selective and 100% atom-economical, all pointing to the hallmarks of a green process. Liquefying the $C_{10–12}$ furoin intermediates can be readily accomplished by hydrogenation, etherification or esterification, producing oxygenated liquid biodiesel with considerably higher heating values than that of bioethanol. Most significantly, premium hydrocarbon fuels can be produced through hydrodeoxygenation of the C_{12} DHMF in water under moderate conditions (300 ℃, 3 h, 3.5 MPa H_2) with the bifunctional catalyst system (Pt/C + $TaOPO_4$), which yields high quality alkane

fuels with 96% selectivity to linear $C_{10–12}$ alkanes, consisting of 27.0 % *n*-decane), 22.9 % *n*-undecane, and 45.6 % *n*-dodecane.

5.3 Experimental

Materials, Reagents, and Methods. All syntheses and manipulations of air- and moisture-sensitive materials were carried out in flamed Schlenk-type glassware on a dual-manifold Schlenk line, on a high-vacuum line, or in an inert gas (Ar or N_2)-filled glovebox. HPLC-grade organic solvents were first sparged extensively with nitrogen during filling 20 L solvent reservoirs and then dried by passage through activated alumina (for Et_2O, THF, and CH_2Cl_2) followed by passage through Q-5 supported copper catalyst (for toluene and hexanes) stainless steel columns. DMSO-d_6 was first degassed and dried over CaH_2, followed by vacuum distillation. NMR spectra were recorded on a Varian Inova 300 (FT 300 MHz, ^{1}H; 75 MHz, ^{13}C) or a Varian Inova 400 MHz spectrometer. Chemical shifts for ^{1}H and ^{13}C spectra were referenced to internal NMR solvent residual resonances and reported as parts per million relative to $SiMe_4$. High-resolution mass spectrometry (HRMS) data were collected on an Agilent 6220 Accurate time-of-flight LC/MS spectrometer. Elemental analyses were carried out by Robertson Microlit Laboratories, Madison, NJ.

All hydrogenation and hydrodeoxygenation (HDO) reactions were carried out in a Parr 4842 pressure reactor (Parr Instrument Co.). The organic products extracted by dichloromethane (DCM) were analyzed either by an Agilent 6890N GC-FID system with a Durabond DB-5ms column (30m, 0.25 mm I.D., 0.25 μm film) or by an Agilent 6890 GC-MS system equipped with

a Phenomenex Zebron ZB-5ms column (30 m, 0.25 mm I.D., 0.25 μm film). Heating values were measured by a Petrolab C2000 calorimeter. Any DHMF remained in the water phase after HDO was analyzed with an Agilent Eclipse Plus C18 Column (100×4.6 mm; 80/20 water/methanol, 0.6 ml/min, 30 ℃) and a UV detector (284 nm).

Furfural (Alfa Aesar), 5-methylfurfural (MF, Alfa Aesar), 5-hydroxymethylfurfural (HMF, Acros Organics), H_3PO_4 (85 wt% aqueous solution, Sigma Aldrich), Ta_2O_5 (Alfa Aesar), Cs_2CO_3 (Alfa Aesar), $H_3PW_{12}O_{40} \cdot x\ H_2O$ (Alfa Aesar), $PtCl_4$ (Acros Organics), Pd/C and Pt/C (5 wt%, Alfa Aesar), and 1,3-bis (2,4,6-trimethylphenyl)-1,3-dihydro- 2H-imidazol-2-ylidene (IMes) (Sigma Aldrich) were purchased and used as received. $TaOPO_4$ and $Cs_xH_{3-x}PW_{12}O_{40}$ (x = 1 and 2.5) were prepared according to literature procedures.[11,20b] The supported 4 wt% $Pt/Cs_xH_{3-x}PW_{12}O_{40}$ catalyst was prepared by incipient wetness impregnation, which was dried in an oven at 120 ℃ overnight and reduced under flowing H_2 (100 mL/min) at 250 ℃ for 3 h before use. Literature procedures were also used to prepare 1,3,4-triphenyl-4,5-dihydro-1*H*-1,2,4-triazol-5-ylidene (TPT).[21]

Solvent-Free Umpolung Procedures for Coupling of Furaldehydes: Umpolung reactions catalyzed by TPT were carried out under solvent-free (neat) conditions. Furfural (2.5 g, 26 mmol) was added in a 20 mL vial, to which TPT (71 mg, 0.26 mmol, 1.0 mol% to furfural) was added. The resulting mixture was stirred for 1 h, after which the solidified product was smashed and washed with 5 mL hexanes. Furoin (2.2 g, 89 % yield) was obtained as yellow powder after filtration and vacuum drying. Using the same procedure, 5,5'-dimethylfuroin was synthesized from MF in 94 % isolated yield. For the synthesis of 5,5'-di(hydroxymethyl)furoin

(DHMF), HMF (2.5 g, 20 mmol) was premixed with TPT (55 mg, 0.20 mmol, 1.0 mol% relative to HMF) in a 20 mL vial. The vial was sealed and heated at 60 ℃ for 1 h by a temperature-controlled orbit shaker (300 rpm). After the reaction, the solidified product was smashed and washed with 5 mL toluene to remove the residual TPT catalyst. DHMF (2.4 g, 95 % yield) was obtained as white powder after filtration and vacuum drying. Alternatively, HMF (0.10 g, 0.79 mmol) was premixed with TPT (2.2 mg, 8.0 μmol, 1.0 mol% relative to HMF) and toluene (1 mL) in a 5 mL vial. The vial was sealed and heated at 60 ℃ for 3 h by a temperature-controlled orbit shaker (300 rpm). Upon cooling the vial to room temperature, DHMF precipitated out of the solution and was isolated as white powder after filtration and vacuum drying; 86 mg, 86 % yield. ^{1}H NMR for furoin[16] ($CDCl_3$): δ 7.62, 7.38, 7.26, 6.54, 6.41, 6.36 (d, 6H, furan ring H), 5.80 (s, 1H, C*H*OH), 4.19 (s, 1H, CHO*H*). ^{1}H NMR for 5,5'-dimethylfuroin[16] ($CDCl_3$): δ 7.13, 6.26 (d, 2H, furan ring H), 6.16, 5.92 (dd, 2H, furan ring H), 5.66 (d, 1H, C*H*OH), 4.22 (d, 1H, CHO*H*), 2.39 (s, 3H, CH_3), 2.25 (s, 3H, CH_3). ^{1}H NMR for DHMF[15] (DMSO-d_6): δ 7.54, 6.54, 6.38, 6.25 (d, 4H, furan ring H), 5.78 (s, 1H, C*H*OH), 4.50 (s, 2H, CH_2OH), 4.35 (s, 2H, CH_2OH).

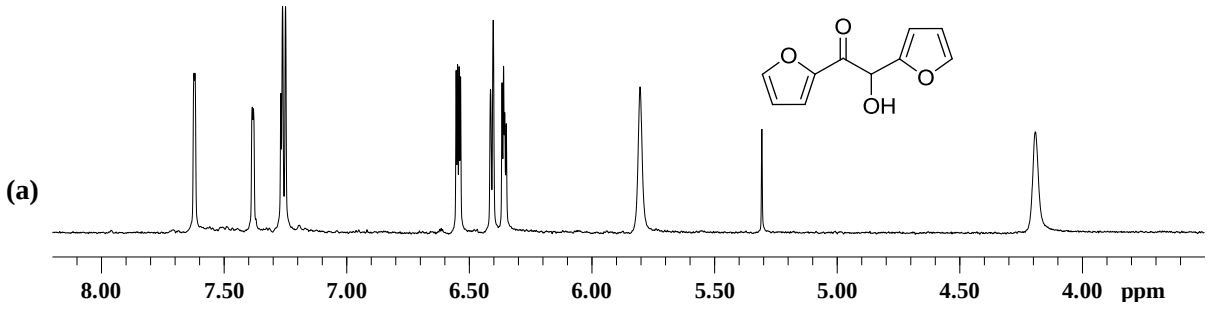

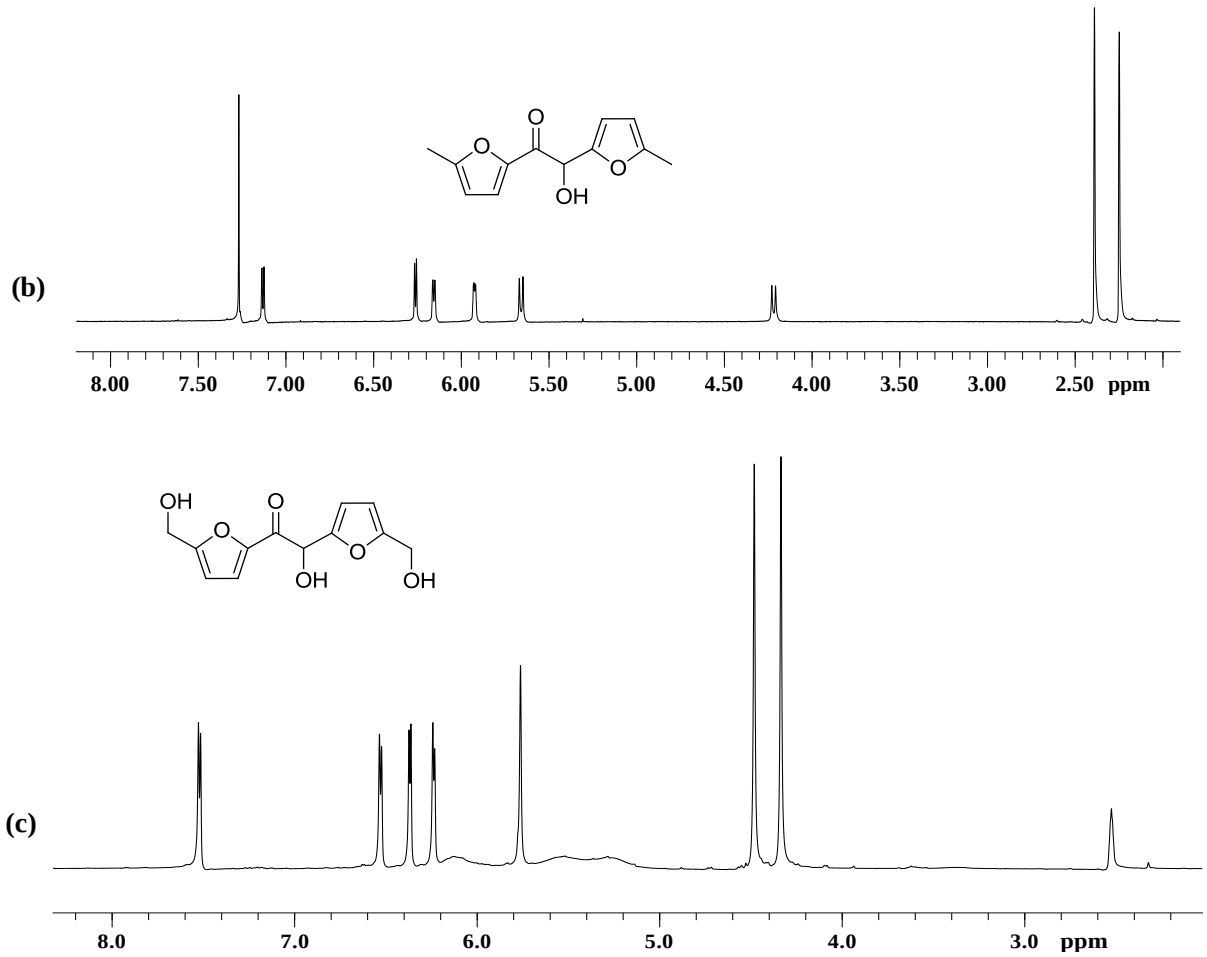

Figure 5.2 ^{1}H NMR Spectra for: (**a**) furoin in $CDCl_3$; (**b**) 5,5'-dimethylfuroin in $CDCl_3$; and (**c**) DHMF in DMSO-d_6. A peak at 5.31 in (**a**) is the residual solvent (CH_2Cl_2) brought into the system, and the three broad peaks centered at ~5.3 ppm, 5.5 ppm, and 6.1 ppm in (**c**) are for three types of the OH groups present in DHMF. Residual solvent peaks for $CDCl_3$ and DMSO-d_6 are at 7.26 and 2.50 ppm, respectively.

Stoichiometric Reaction of HMF and *N*-heterocyclic Carbene (NHC). HMF (20 mg, 0.16 mmol) was dissolved into 0.5 mL DMSO-d_6 and transferred into a J. Young-type NMR tube, to which a stoichiometric amount of IMes (48 mg, 0.16 mmol) in 0.5 mL DMSO-d_6 was added and fully mixed. After 30 min at RT, the clean formation of the resulting enaminol, the Breslow intermediate involved in the benzoin reaction,[17] was indicated by ^{1}H NMR spectrum (Figure 5.3). ^{1}H NMR (DMSO-d_6): δ 7.81 (s, 2H, imidazole ring protons), 7.14 (s, 4H, benzene ring protons),

6.11 (d, $J_{H\text{-}H}$ = 3.0 Hz, 1H, furan ring proton), 6.01 (d, $J_{H\text{-}H}$ = 3.3 Hz, 1H, furan ring proton), 4.31 (s, 2H, CH_2OH), 2.37 (s, 6H, p-CH_3), 2.08 (s, 12H, o-CH_3).

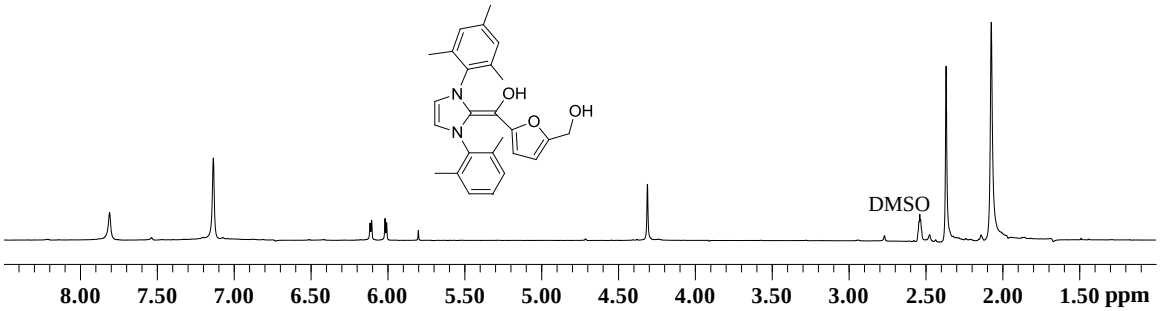

Figure 5.3 ^{1}H NMR spectrum of the resulting enaminol (the Breslow intermediate) derived from the reaction of HMF and IMes.

Etherification and Esterification of DHMF. HMF, employed as a control run, was quantitatively converted to 5-ethoxymethylfurfural by NMR in excess of ethanol at 75 ℃ for 24 h with solid acid catalyst Dowex G-26 H-form resin. ^{1}H NMR ($CDCl_3$) for 5-ethoxymethylfurfural: δ 9.64 (s, 1H, C*H*O), 7.24, 6.55 (d, 2H, furan ring H), 4.56 (s, 2H, CH_2OH), 3.62 (q, 2H, CH_2CH$_3$), 1.28 (t, 3H, CH$_2$CH_3)]. For etherification of DHMF with ethanol, DHMF (0.10 g, 0.40 mmol) was dissolved in 2.0 g ethanol in a 5 mL vial. Dowex G-26 H-form resin (24 mg) was added and the vial was heated in a temperature-controlled orbit shaker (75 ℃, 300 rpm) for 24 h. After the reaction, the supernatant liquid was decanted, dried by anhydrous $MgSO_4$ and removed by vacuum. 5,5'-Di(ethoxymethyl)furoin (DEMF) was obtained as viscous liquid. ^{1}H NMR for DEMF (DMSO-d_6): δ 7.21, 6.41, 6.31, 6.26 (d, 4H, furan ring H), 5.75 (s, 1H, C*H*OH), 4.61 (s, 2H, CH_2OH), 4.38 (s, 2H, CH_2OH), 3.69 (q, 2H, CH_2CH$_3$), 3.48 (q, 2H, CH_2CH$_3$), 1.15-1.24 (m, 6H, CH$_2$CH_3). HRMS calculated for $C_{16}H_{21}O_6$ $[M+H]^+$: 309.1338; found: 309.1333.

For esterification, DHMF (0.10 g, 0.40 mmol) was mixed with propionic anhydride (0.26 g, 2.0 mmol) in a 5 mL vial and heated at 130 ℃ for 2 h in a temperature-controlled orbit shaker. After the reaction, excess propanoic anhydride was removed by treatment with a saturated aqueous solution of $NaHCO_3$, and the DHMF-tripropionic ester was obtained as viscous liquid after extraction with ethyl acetate, drying with anhydrous $MgSO_4$ and further solvent removal and drying. ^{1}H NMR for the DHMF-tripropionic ester ($CDCl_3$): δ 7.26, 6.54, 6.50, 6.41 (d, 4H, furan ring H), 5.19 (s, 1H, C*H*OH), 5.11 (s, 2H, C*H*$_2$OH), 5.06 (s, 2H, C*H*$_2$OH), 2.39 (m, 6H, C*H*$_2$CH$_3$), 1.14-1.25 (m, 9H, CH$_2$C*H*$_3$). HRMS calculated for $C_{21}H_{28}NO_9$ $[M+NH_4]^+$: 438.1764; found: 438.1759.

Hydrogenation of Furoins. Furoin (2.20 g, 11.4 mmol) was dissolved in 100 mL THF or methanol and transferred to a Parr pressure reactor, to which Pd/C (4.84 g, 10 mol% Pd to furoin) was added. The system was purged with H_2 for 15 min and heated at 90 ℃ for 6 h under 400 psi H_2. After the reaction, Pd/C was recycled by filtration, and the filtrate was dried under vacuum. The hydrogenated furoin was obtained as liquid and subjected to elemental analysis and heating value test. 5,5'-Dimethylfuroin and DHMF were hydrogenated in a similar fashion. ^{1}H NMR spectrum shows that after hydrogenation, the furan double bonds were fully hydrogenated. HRMS calculated for DHMF after hydrogenation, $C_{12}H_{23}O_6$ $[M+H]^+$: 263.1495; found: 263.1489.

Table 5.1 Results of elemental analysis of hydrogenated coupling products

Furoins	Before Hydrogenation			After Hydrogenation					
				Value of saturated polyol			Experimental Value		
	C (%)	H (%)	O (%)	C (%)	H (%)	O (%)	C (%)	H (%)	O (%)
Furoin	62.5	4.2	33.3	59.4	8.9	31.7	65.6	11.0	23.4
5,5'-Dimethylfuroin	65.4	5.4	29.2	62.6	9.6	27.8	67.1	10.7	22.2
DHMF	57.1	4.8	38.1	55.0	8.4	36.6	60.5	10.1	29.4

Hydrodeoxygenation of DHMF. DHMF (500 mg, 1.98 mmol) was dissolved in 50 mL distilled water and transferred to a 250 mL Parr pressure reactor (note that use of the larger amount of solvent, water, than necessary here was due to the size of the pressure reactor employed for the reaction). To this reactor was added a catalyst, either Pd/C (0.25 g, 5.9 mol% Pd relative to DHMF) + H_3PO_4 (0.175 mL, 0.5 wt%) or Pt/$CsH_2PW_{12}O_{40}$ (0.25 g, 2.6 mol% Pt relative to DHMF). For the HDO by the Pt/C + $TaOPO_4$ system, the loading of DHMF, Pt/C, and $TaOPO_4$ was 0.25 g, 0.125 g (3.2 mol% Pt relative to DHMF), and 0.25 g, respectively. The reactor was purged with H_2 for 15 min and heated at 250 ℃ for 2 h under 500 psi H_2 (the Pt/C+$TaOPO_4$ system was heated at 300 ℃ for 3 h under 500 psi H_2). After the reaction, the organic phase was extracted with DCM and analyzed by GC. Alkane selectivity was reported based on the percentage of peak areas measured by GC-FID. The organic phase was further dried with anhydrous $MgSO_4$ and the solvent was removed under vacuum. The remaining oily products were subjected to elemental analysis.

Table 5.2 Analytical results of liquid fuels in the organic phase after HDO in water[a]

Catalysts	C_{10} (%)	C_{11} (%)	C_{12} (%)	Alkanes (%)	Oxygenates (%)	Isolated liquid fuels		
						C (%)	H (%)	O (%)
$Pd/C+H_3PO_4$	8.6	17.6	12.2	38.4	61.6	75.2	12.6	12.2
$Pt/CsH_2PW_{12}O_{40}$	-	11.3	40.6	51.9	48.1	79.4	13.0	7.6
$Pt/CsH_2PW_{12}O_{40}$ [b]	6.1	15.2	-	24.7	75.3	77.8	12.6	9.6
$Pt/CsH_2PW_{12}O_{40}$ [c]	4.3	16.8	18.6	39.7	60.3	76.2	12.8	11.0
$Pt/C+TaOPO_4$ [d]	27.0	22.9	45.6	95.5	4.5	81.2	14.6	4.2

[a] Reaction conditions: temperature, 250 ℃; H_2 pressure, 500 psi; reaction time, 2 h; solvent, distilled water, 50 mL, unless otherwise specified. In all cases, DHMF was completely converted and no or a negligible amount of alkanes below C_{10} were observed. [b] Biphasic system with hexanes/water = 50/50 mL. [c] Temperature was 300 ℃. [d] Temperature: 300 ℃; reaction time: 3 h.

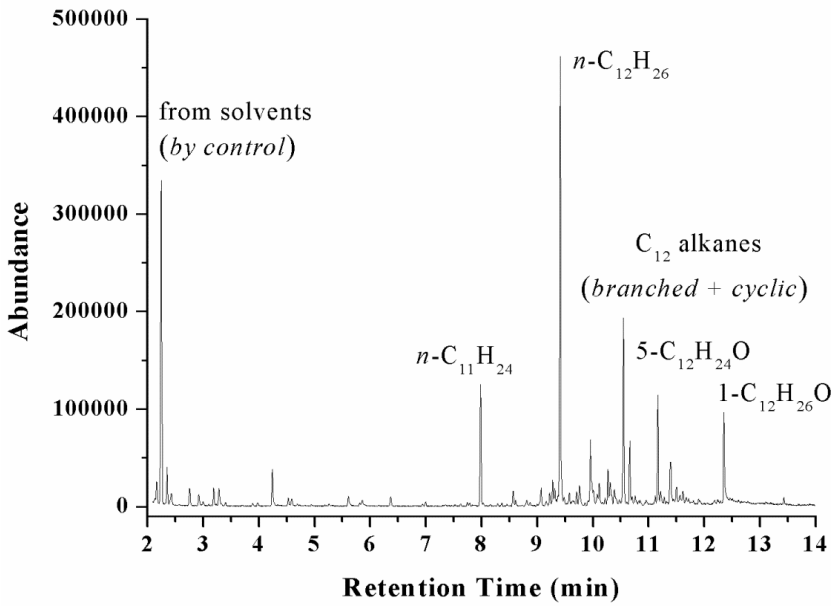

Figure 5.4 GC-MS chromatogram of the organic phase products produced by HDO of DHMF catalyzed by $Pt/CsH_2PW_{12}O_{40}$.

5.4 References

(1) For selected recent reviews on HMF, see: (a) van Putten, R.-J.; van der Waal, J. C.; de Jong, E.; Rasrendra, C. B.; Heeres H. J.; de Vries, J. G. *Chem. Rev.* **2013**, *113*, 1499–1597. (b)

Tuck, C. O.; Pérez, E.; Horváth, I. T.; Sheldon, R. A.; Poliakoff, M. *Science* **2012**, *337*, 695–699. (c) Zakrzewska, M. E.; Bogel-Łukasik, E.; Bogel-Łukasik, R. *Chem. Rev.* **2011**, *111*, 397–417. (d) Ståhlberg, T.; Fu, W.; Woodley, J. M.; Riisager, A. *ChemSusChem* **2011**, *4*, 451–458. (e) Rosatella, A. A.; Simeonov, S. P.; Frade, R. F. M.; Afonso, C. A. M. *Green Chem.* **2011**, *13*, 754–793. (f) James, O. O.; Maity, S.; Usman, L. A.; Ajanaku, K. O.; Ajani, O. O.; Siyanbola, T. O.; Sahu, S.; Chaubey, R. *Energy Environ. Sci.* **2010**, *3*, 1833–1850. (g) Bozell, J. J.; Petersen, G. R. *Green Chem.* **2010**, *12*, 539–554. (h) Werpy, T.; Petersen, G. *Top Value Added Chemicals from Biomass*; U.S. Department of Energy: Washington, DC, **2004**, Vol. 1.

(2) For selected recent examples and reviews, see: (a) Sedai, B.; Diaz-Urrutia, C.; Baker, R. T.; Wu, R.; Silks, L. A.; Hanson, S. K. *ACS Catalysis* **2011**, *1*, 794–804. (b) Climent, M. J.; Corma, A.; Iborra, S. *Green Chem.* **2011**, *13*, 520–540. (c) Yang, W.; Sen, A. *ChemSusChem.* **2011**, *4*, 349–352. (d) Alonso, D. M.; Bond, J. Q.; Dumesic, J. A. *Green Chem.* **2010**, *12*, 1493–1513. (e) Stöcker, M. *Angew. Chem. Int. Ed.* **2008**, *47*, 9200–9211. (f) Corma, A.; Iborra, S.; Velty, A. *Chem. Rev.* **2007**, *107*, 2411–2502. (g) Chheda, J. N.; Huber, G. W.; Dumesic, J. A. *Angew. Chem. Int. Ed.* **2007**, *46*, 7164–7183. (h) Huber, G. W.; Iborra, S.; Corma, A. *Chem. Rev.* **2006**, *106*, 4044–4098.

(3) Zhao, H.; Holladay, J. E.; Brown, H.; Zhang, Z. C. *Science* **2007**, *316*, 1597–1600.

(4) For selected recent examples, see: (a) Liu, D.; Chen, E. Y.-X. *Biomass & Bioenergy* **2013**, *48*, 181–190. (b) Caes, B. R.; Palte, M. J.; Raines, R. T. *Chem. Sci.* **2013**, *4*, 196–199. (c) He, J.; Zhang, Y.; Chen, E. Y.-X. *ChemSusChem* **2013**, *6*, 61–64. (d) Pagán-Torres, Y. J.; Wang,

T.; Gallo, J. M. R.; Shanks, B. H.; Dumesic, J. A. *ACS Catal.* **2012**, *2*, 930–934. (e) Simeonov, S. P.; Coelho, J. A. S.; Afonso, C. A. M. *ChemSusChem* **2012**, *5*, 1388–1391. (f) Liu, D.; Chen, E. Y.-X. *Appl. Catal. A: Gen.* **2012**, *435-436*, 78–85. (g) Ståhlberg, T.; Rodriguez-Rodriguez, S.; Fristrup, P.; Riisager, A. *Chem. Eur. J.* **2011**, *17*, 1456–1464. (h) Cao, Q.; Guo, X.; Guan, J.; Mu, X.; Zhang, D. *Appl. Catal. A.* **2011**, *403*, 98–103. (i) Zhang, Z.; Wang, Q.; Xie, H.; Liu, W.; Zhao, Z. K. *ChemSusChem* **2011**, *4*, 131–138. (j) Kim, B.; Jeong, J.; Lee, D.; Kim, S.; Yoon, H.-J.; Lee, Y.-S.; Cho, J. K. *Green Chem.* **2011**, *13*, 1593–1506. (k) Pidko, E. A.; Degirmenci, V.; van Santen, R. A.; Hensen, E. J. M. *Angew. Chem. Int. Ed.* **2010**, *49*, 2530–2534. (l) Qi, X.; Watanabe, M.; Aida, T. M.; Smith R. L. Jr. *ChemSusChem* **2010**, *3*, 1071–1077. (m) Binder, J. B.; Cefali, A. V.; Blank, J. J.; Raines, R. T. *Energy Environ. Sci.* **2010**, *3*, 765–771. (n) Binder, J. B.; Raines, R. T. *J. Am. Chem. Soc.* **2009**, *131*, 1979–1985.

(5) Huber, G. W.; Chheda, J. N.; Barrett, C. J.; Dumesic, J. A. *Science* **2005**, *308*, 1446–1450.

(6) Corma, A.; Torre, O.; Renz, M.; Villandier, N. *Angew. Chem. Int. Ed.* **2011**, *50*, 2375–2378.

(7) Balakrishnan, M.; Sacia, E. R.; Bell, A. T. *Green Chem.* **2012**, *14*, 1626–1634.

(8) (a) Mascal, M.; Nikitin, E. B. *Green Chem.* **2010**, *12*, 370–373. (b) Mascal, M.; Nikitin, E. B. *Angew. Chem. Int. Ed.* **2008**, *47*, 7924–7926.

(9) Bu, Q.; Lei, H.; Zacher, A. H.; Wang, L.; Ren, S.; Liang, J.; Wei, Y.; Liu, Y.; Tang, J.; Zhang, Q.; Ruan, R. *Bioresour. Technol.* **2012**, *124*, 470–477.

(10) (a) Zhao, C.; Lercher, J. A. *Angew. Chem. Int. Ed.* **2012**, *51*, 5935–5940. (b) Zhao, C.; Lercher, J. A. *ChemCatChem* **2012**, *4*, 64–68. (c) Zhao, C.; He, J.; Lemonidou, A. A.; Li, X.;

Lercher, J. A. *J. Catal.* **2011**, *280*, 8–16.

(11) Huang, Y.-B.; Yang, Z.; Dai, J.-J.; Guo, Q.-X.; Fu, Y. *RSC Advances*, **2012**, *2*, 11211–11214.

(12) Waidmann, C. R.; Pierpont, A. W.; Batista, E. R.; Gordon, J. C.; Martin, R. L.; Silks, L. A.; West, R. M.; Wu, R. *Catal. Sci. Technol.* **2013**, *3*, 106–115.

(13) Sutton, A. D.; Waldie, F. D.; Wu, R.; Schlaf, M.; Silks, L. A.; Gordon, J. C. *Nat. Chem.* **2013**, *5*, 428–432.

(14) Selected recent reviews: (a) Dröge, T.; Glorius, F. *Angew. Chem. Int. Ed.* **2010**, *50*, 6940–6952. (b) Chiang, P.-C.; Bode, J. W. in *RSC Catalysis Series*, Royal Society of Chemistry, Cambridge, **2010**, 399–435. (c) Moore, J. L.; Rovis, T. *Top. Curr. Chem.* **2009**, *291*, 77–144. (d) Hahn, F. E.; Jahnke, M. C. *Angew. Chem. Int. Ed.* **2008**, *47*, 3122–3172. (e) Nair, V.; Vellalath, S.; Babu, B. P. *Chem. Soc. Rev.* **2008**, *37*, 2691–2698. (f) Marion, N.; Díez-González, S.; Nolan, S. P. *Angew. Chem. Int. Ed.* **2007**, *46*, 2988–3000. (g) Enders, D.; Niemeier, O.; Henseler, A. *Chem. Rev.* **2007**, *107*, 5606–5655. (h) Bourissou, D.; Guerret, O.; Gabbaï, F. P.; Bertrand, G. *Chem. Rev.* **2000**, *100*, 39–91.

(15) Liu, D.; Zhang, Y.; Chen, E. Y.-X. *Green Chem.* **2012**, *14*, 2738–2746.

(16) (a) Hashmi, A. S. K.; Wölfle, M.; Teles, J. H.; Frey, W. *Synlett.* **2007**, 1747–1752. (b) Lee, C. K.; Kim, M. S.; Gong, J. S.; Lee, I.-S. H. *J. Heterocyclic Chem.* **1992**, *29*, 149–153.

(17) Breslow, R. *J. Am. Chem. Soc.* **1958**, *80*, 3719–3726.

(18) Berkessel, A.; Elfert, S.; Yatham, V. R.; Neudörfl, J.-M.; Schlörer, N. E.; Teles, J. H. *Angew. Chem. Int. Ed.* **2012**, *51*, 12370–12374.

(19) Wegenhart, B. L.; Liu, S.; Thom, M.; Stanley, D.; Abu-Omar, M. M. *ACS Catal.* **2012**, *2*,

2524–2530.

(20) (a) Alotaibi, M. A.; Kozhevnikova, E. F.; Kozhevnikov, I. V. *Chem. Commun.* **2012**, *48*, 7194–7196. (b) J. Tian, C. Fan, M. Cheng, X. Wang, *Chem. Eng. Technol.* **2011**, *34*, 482–486.

(21) (a) Enders, D.; Breuer, K.; Raabe, G.; Runsink, J.; Teles, J. H.; Melder, J. P.; Ebel, K.; Brode, S. *Angew. Chem., Int. Ed.* Engl. **1995**, *34*, 1021-1023. (b) Enders, D.; Breuer, K.; Kallfass, U.; Balensiefer, T. *Synthesis* **2003**, 1292-1295.

Chapter 6

An Integrated Catalytic Process for Biomass Conversion and Upgrading to C_{12} Furoin and Alkane Fuel

6.1 Summary

Report herein is an integrated catalytic process for conversion and upgrading of biomass feedstocks into 5,5'-dihydroxymethyl furoin (DHMF), through self-coupling of 5-hydroxymethyl furfural (HMF) via organocatalysis, and subsequently into *n*-$C_{12}H_{26}$ alkane fuel via metal-acid tandem catalysis. The first step of the process involves semi-continuous organocatalytic conversion of biomass (fructose, in particular) to the high-purity HMF. *N*-Heterocyclic carbenes (NHCs) are found to catalyze glucose-to-fructose isomerization, and the inexpensive thiazolium chloride [TM]Cl, a Vitamin B1 analog, catalyzes fructose dehydration to HMF of good purity (>99% by HPLC), achieving a constant HMF yield of 72% over 10 semi-continuous extraction batch runs. Crystallization of the crude HMF from toluene yields the spectroscopically and analytically pure HMF as needle crystals. The second step of the process is the NHC-catalyzed coupling of C_6 HMF produced by the semi-continuous process to C_{12} DHMF; the most effective organic NHC catalyst produces DHMF in 93% or 91% isolated yield with an NHC loading of 0.70 mol% or 0.10 mol% at 60 ℃ for 3 h under solvent-free conditions. The third step of the process converts C_{12} DHMF to linear alkanes via hydrodeoxygenation. With a bifunctional catalyst system consisting of Pd/C + acetic acid + $La(OTf)_3$ at 250 ℃ and 300 psi H_2 for 16 h,

DHMF has been transformed to liquid hydrocarbon fuel (78% alkanes), with a 64% selectivity to *n*-$C_{12}H_{26}$ and an overall C/H/O % ratio of 84/11/5.0.

6.2 Introduction

The depletion of fossil fuels has directed society's increasing interest towards the use of plant biomass as a sustainable source of building blocks for chemicals, materials, and biofuels.[1] The furan-based compounds, mostly derived from dehydration of C_5 or C_6 (poly)sugars, have emerged as the promising platform chemicals in selective transformations for: (1) benzene derivatives by the Diels-Alder reaction with dienophiles;[2] (2) levulinic acid, γ-valerolactone, and their derivatives;[3] (3) higher-energy-density fuel intermediates bearing higher carbon numbers (chain extension) derived from coupling with other chemicals.[4] In particular, 5-hydroxymethylfurfural (HMF), a selective hydrolysis product from C_6 sugars, has been identified as a versatile intermediate for top-value-added chemicals, thanks to various functional groups possibly derived from the 2,5-positioned hydroxyl and aldehyde groups in HMF.[5] Glucose, the most abundant C_6 sugar, has been extensively studied for its direct conversion to HMF in ILs[6] and bi-phase systems[7] catalyzed by Lewis and BrØnsted acids, with typically moderate to high yields of 40 – 80 %. Most recently, bifunctional catalysts consisting of superhydrophobic acid and superhydrophilic base were applied for the glucose-to-HMF conversion, achieving the HMF yield up to 95% in a THF-DMSO mixed solvent at 100 ℃ for 10 h.[8] Fructose has been proposed as the key intermediate involved in the glucose-to-HMF conversion process,[9] while the direct dehydration of fructose to HMF is facile and highly

efficient. High to quantitative yields and selectivity of HMF from fructose were achieved in organic solvents (e.g., DMSO),[10] ionic liquids (ILs),[9b,11] and even in water,[12] with or without catalysts.

In view of the facile fructose-to-HMF route, the development of an effective glucose-to-fructose isomerization process has been of great interest. In this context, heterogeneous acidic zeolite catalysts have been extensively studied for isomerization of glucose to fructose.[13,14] Specifically, Davis et al. showed that Sn or Ti modified large-pore zeolite (Beta zeolite) was an effective Lewis acid catalyst for glucose-to-fructose isomerization in water: a product containing 46% glucose, 29% fructose, and 8% mannose was obtained after reacting a 45 wt% glucose solution catalyzed by Sn-Beta for 60 min at 110 ℃.[13] Enhanced fructose yield from glucose was achieved by Riisager et al. using large-pore zeolite Y, especially H-USY (Si/Al = 6), through glucose-methyl fructoside-fructose strategy: a product containing 28% glucose, 55% fructose, and 4% methyl fructoside was obtained at 120 ℃ by a step-wise reaction.[14] This novel reaction pathway involves glucose isomerization to fructose and subsequent etherification to methyl fructoside in methanol, followed by hydrolysis to reform fructose after water addition.

In addition to the widely studied metal-based catalyst systems, the application of *organocatalysis* in biomass conversion and upgrading has also come to light recently, showing potentials of using relatively non- or less toxic, more environmentally benign, atom-economical and more sustainable catalysis for biorefining.[15] For instance, we recently demonstrated that furaldehydes (e.g., furfural, 5-methylfurfural, and HMF) undergo benzoin-condensation-type self-coupling in the presence of an *N*-heterocyclic carbene (NHC) catalyst under mild

conditions.[15b] Using a room-temperature (RT) ionic liquid, 1-ethyl-3-methylimidazolium acetate ([EMIM]OAc), where 1-ethyl-3-methylimidazol-2- ylidene ([EMIM] NHC) exists in an equilibrium with [EMIM]OAc and is stabilized by HOAc, HMF was readily dimerized to C_{12} 5,5'-dihydroxymethyl furoin (DHMF) in high conversion and good isolated yield.[15c] Understanding of the mechanism and catalytically active specie for the [EMIM]OAc-promoted HMF self-coupling led to a more effective HMF upgrading process that uses a discrete, stable NHC, 1,3,4-triphenyl-4,5-dihydro-1H-1,2,4-triazol-5-ylidene (TPT), the process of which afforded DHMF in an isolated yield up to 95% with 1 mol% of TPT in a solvent-free process at 60 ℃ for 1 h.[15b]

Compared with HMF, DHMF is a higher energy-density, and perhaps more versatile, C_{12} "platform chemical", featuring 12 carbons, 3 hydroxyl groups, 2 substituted furan rings, and 1 carbonyl group (Figure 6.1). As a C_{12} fuel intermediate, DHMF has been converted to oxygenated diesels by hydrogenation, etherification and esterification, or high-quality alkane fuels by hydrodeoxygenation (HDO) in water.[15b] As a furan derivative, DHMF could be potentially hydrolyzed under acidic conditions, rending C_{12} ketones after furan ring opening. In terms of producing polymeric materials, as a tri-ol, DHMF could be (co)polymerized into various types of polymers, such as polyethers, polyesters, polycarbonates, and polyurethanes.

Despite its great potential as a promising C_{12} "platform chemical", the current process to DHMF relies on the expensive HMF, which is commercially available (currently sold at ~$37 per g) but requires further crystallization to give the sufficiently pure HMF (with a typical 70–80% recovery yield) suitable for the subsequent organocatalytic upgrading (self-coupling) process.

Although a large number of catalytic processes were reported for biomass conversion to HMF, the dehydration of fructose and the isomerization of glucose have remained to be the two bottlenecks in the production of HMF, and the separation and purification methods of HMF to produce the high-purity HMF suitable for subsequent chemical transformations were barely studied.[16] Furthermore, although the HDO process catalyzed by Pt/C and $TaOPO_4$ converted DHMF to a mixture of C_{10} (27.0%), C_{11} (22.9%), and C_{12} (45.6%) linear alkanes,[15b] it is preferable to convert the C_{12} DHMF selectively to C_{12} alkanes from a view point of atom efficiency. Accordingly, this work was directed at accomplishing the following three goals: (a) to investigate possible glucose isomerization to fructose by organocatalysis; (b) to establish an efficient, economical, integrated catalytic process for converting inexpensive biomass feedstocks such as fructose (currently at ~$32 per 100 g) to DHMF through generation of the high-purity HMF intermediate, and (c) to identify a bifunctional HDO catalyst system that can convert C_{12} DHMF to *n*-$C_{12}H_{26}$ alkane more selectively for achieving higher atom efficiency.

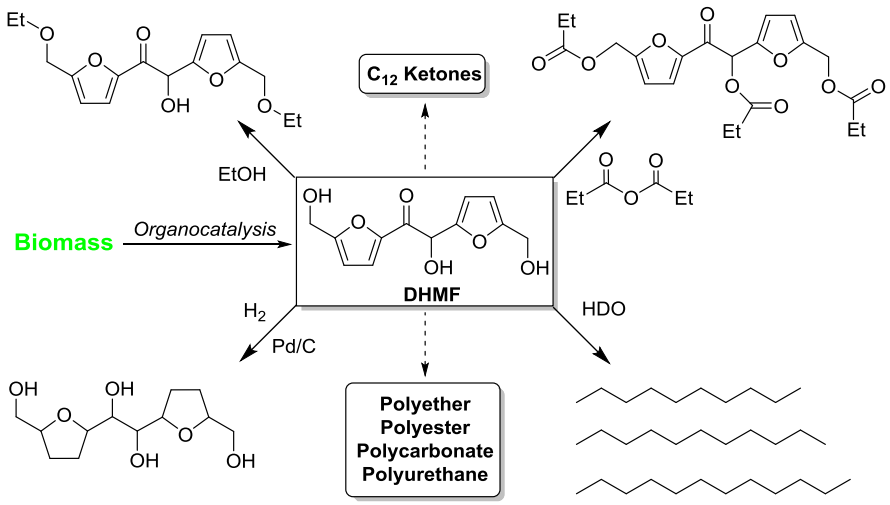

Figure 6.1 DHMF as a proposed new C_{12} "platform chemical" for renewable chemicals, materials, and biofuels.

6.3 Experimental

Materials, Reagents, and Methods. All syntheses and manipulations of air- and moisture-sensitive materials were carried out in flamed Schlenk-type glassware on a dual-manifold Schlenk line or in an inert gas (Ar or N_2) filled glovebox. HPLC-grade organic solvents were sparged extensively with nitrogen during filling of the solvent reservoir and then dried by passage through activated alumina (for Et_2O, THF, and CH_2Cl_2) followed by passage through Q-5-supported copper catalyst (for toluene and hexanes) stainless steel columns. Deuterated dimethyl sulfoxide (DMSO-d_6) was degassed, dried over CaH_2, filtered, and vacuum-distilled; the dried DMSO-d_6 was stored over activated molecular sieves.

NMR spectra were recorded on a Varian Inova 300 (FT 300 MHz) or a Varian Inova 400 MHz spectrometer. Chemical shifts for ^1H and ^{13}C NMR spectra were referenced to internal solvent resonances and were reported as parts per million relative to tetramethylsilane. HMF (5-hydroxymethylfurfural) and DHMF (5,5'-dihydroxymethylfuroin) were analyzed by Agilent 1260 Infinity HPLC system equipped with an Agilent Eclipse Plus C18 Column (100×4.6 mm; 80/20 water/methanol, 0.6 ml/min, 30 ℃) and a UV detector (284 nm). Sugar contents of the products were measured by Agilent 1260 Infinity HPLC system equipped with a Biorad Aminex HPX-87H Column (300 × 7.8 mm; water, 0.6 ml/min, 45 ℃) and a RI detector; under such conditions possible sugars (e.g., glucose and fructose) in the reaction mixture can be well separated and quantified. Hydrodeoxygenation (HDO) reactions were carried out in a Parr 4842 pressure reactor (Parr Instrument Co.). The products were analyzed either by an Agilent 6890N GC-FID system with a Durabond DB-5 column (60 m, 0.25 mm I.D., 0.25 μm film) or by an

Agilent 6890 GC-MS system equipped with a Phenomenex Zebron ZB-5ms column (30 m, 0.25 mm I.D., 0.25 μm film). Any DHMF remained in the acetic acid after HDO was analyzed by HPLC. Elemental analyses were carried out by Robertson Microlit Laboratories, Ledgewood, NJ.

Sugars (fructose, glucose, and cellulose, Sigma Aldrich), furfural (Alfa Aesar), HMF (Acros Organics), 5-methyl-2-furaldehyde (Alfa Aesar), 3-benzyl-5-(2-hydroxyethyl)-4-methylthiazolium chloride ([TM]Cl, Alfa Aesar), thiamine·HCl (Alfa Aesar), potassium bis(trimethylsilyl)amine (KHMDS, Alfa Aesar), tetraethylammonium chloride (TEAC, Alfa Aesar), KO^{t}Bu (Acros Organics), Amberlyst-15 cation exchange resin (Acros Organics), and Dowex M43 Anion Exchange Resin (Supelco) were used as received. The ionic liquid 1-ethyl-3-methylimidazolium chloride ([EMIM]Cl, Sigma Aldrich) was dried under vacuum at 100 ℃ for 24 h, followed by repeated recrystallization from CH_2Cl_2 and hexanes at room temperature. Catalysts for HDO reactions, including Pd/C (10 wt% Pd on activated carbon, wet support, Sigma Aldrich), La(OTf)$_3$ (Alfa Aesar) were used as received. NHCs (*N*-heterocyclic carbenes), 1,3-di-tert-butylimidazol-2-ylidene (I^{t}Bu, TCI America) and 1,3-bis(2,4,6-trimethylphenyl)-1,3-dihydro-2H-imidazole-2-ylidene (IMes, Sigma Aldrich) were used as received. Literature procedures were used to prepare 1,3,4-triphenyl-4,5-dihydro-1H-1,2,4-triazol-5-ylidene (TPT).[17] [TM]-NHC and thiamine-NHC were pre-formed through deprotonation of [TM]Cl and thiamine·HCl by KHMDS in THF, followed by extensively washing with hexanes to remove excess amount of KHMDS. Polymeric NHC precursor P[BVIM]-CO_2 and polymeric NHC P[^{i}PrVIM] (Figure 6.2) were synthesized

from their respective bromide salts following literature procedures.[18]

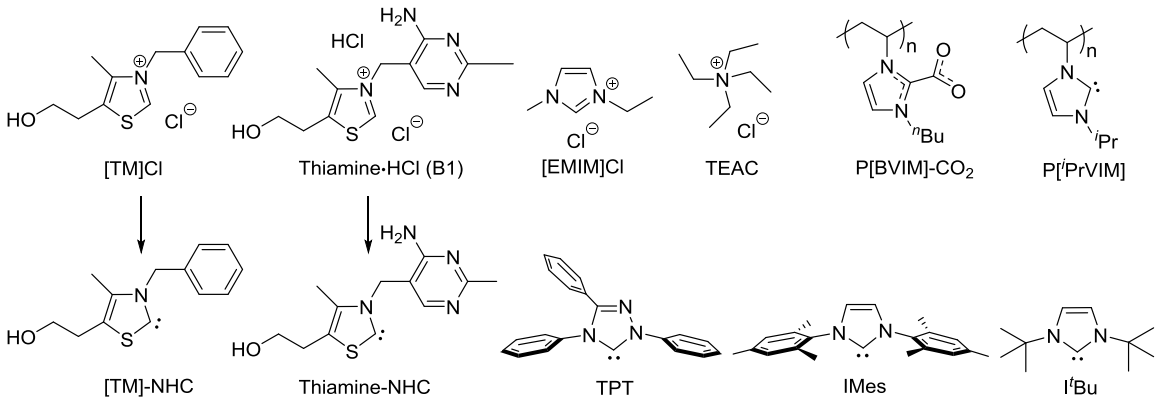

Figure 6.2 Structures of chloride salts and NHCs employed in this study.

Glucose isomerization to fructose catalyzed by NHCs. In a typical reaction, 20 mg glucose was loaded into a 5 mL vial, to which 3.3 mg IMes (10 mol% relative to glucose) in 0.5 mL dry DMSO was added. After stirring at room temperature for 3 h, the solution was quenched and diluted by 25 mL water for HPLC test. For reactions carried in ILs, glucose and fructose contents were measured by HPLC analysis (RI detector) after the diluted ILs phase passing through the cation and anion exchange columns to discharge ILs.

The integrated three-step process of fructose conversion to C_{12} alkane fuel. Experimental procedures were briefly described herein. In the first step, the commercial fructose was converted to the high-purity HMF by a semi-continuous process followed by crystallization. For the semi-continuous extraction of HMF by the THF/[TM]Cl biphasic system, 2.0 g fructose was mixed with 10 g [TM]Cl in a 75 mL pressure glass reactor, to which 20 mL THF was added. The reactor was capped and heated at 120 ℃ for 1.5 h under stirring. When the glass reactor was cooled to room temperature after the reaction, the THF phase was collected. For each of further 9

batches, 2.0 g fructose and 20 mL THF were loaded to the reactor, which was capped and heated at 120 ℃ for 1 h. The THF phases obtained were combined and de-colored by activate carbon. Analysis of the THF phases by HPLC showed HMF was formed in good purity (>99% by HPLC), perhaps sutiable for some applications without further purification, but in this work, HMF was subsequently isolated as crystals according to the following procedures. THF was removed by evaporation under vacuum, and the remaining liquid product was re-dissolved in toluene and crystallized to afford HMF needle crystals. A typical yield for the isolated high-purity, crystalline HMF was about 30 – 36%, depending on the reaction scale.

In the second step, the purified HMF was upgraded into DHMF catalyzed by TPT or *in-situ* generated [TM] NHC. The HMF umpolung catalyzed by TPT was performed similarly as previously reported.[15] HMF (3.0 g, 24 mmol) was premixed with [TM]Cl (0.60 g, 10 mol% to HMF) and KO^{t}Bu (0.40 g, 15 mol% to HMF) in a 20 mL vial. The sealed vial was placed in a temperature-controlled orbit shaker (80 ℃, 300 rpm) and heated for 3 h. The crude product was purified by silica-gel chromatography. After removing the solvent under vacuum, DHMF (1.6 g) was isolated in 53% yield. On the other hand, the same reaction catalyzed by TPT (0.7% mol) achieved a high yield of 93%.

In the third step, DHMF was converted to *n*-$C_{12}H_{26}$ alkane fuel by HDO. DHMF (0.25 g, 0.99 mmol) was dissolved in 40 mL glacial acetic acid and transferred to a Parr pressure reactor. To this reactor was added water-wetted Pd/C (0.12 g, ~12 mol% Pd relative to DHMF) and $La(OTf)_3$ (0.25 g, 43 mol% relative to DHMF). The reactor was purged with H_2 for 15 min and heated at 250 ℃ for 16 h under 300 psi H_2. After completion of the reaction, an aliquot was

analyzed by GC-MS, GC-FID and HPLC. To separate the HDO products, the acetic acid solution was concentrated and extracted by hexanes; the extracts were dried by anhydrous $MgSO_4$ and the solvent was removed under vacuum. The resulting oil product was subjected to elemental analysis.

6.4 Results and Discussion

Step 1: Semi-Continuous Organocatalytic Process for High-Purity HMF Production

Organocatalyzed glucose-to-fructose isomerization. In view of facile conversion of fructose to HMF, at the outset of this project we sought to develop organocatalyzed isomerization of glucose to fructose, thus possibly enabling conversion of glucose to HMF via organocatalysis. This possible route was prompted by our recent study, which revealed that NHCs (e.g. IMes) actually poisoned the $CrCl_2$ catalyst for the glucose-to-HMF conversion in [EMIM]Cl.[19] When a stoichiometic amount IMes (1 equiv. to $CrCl_2$) was added, HMF yield decreased from 58% to 40% (Table 6.1, entries 1 and 2); further addition of IMes led to complete catalyst poisoning towards HMF production. On the other hand, we observed up to 20% of fructose yield and 32% fructose selectivity from glucose when a superstoichiometic amount (2 or 3 equiv. to $CrCl_2$) of NHCs was added (entries 3 and 4). Control experiments (entries 1, 5, and 6) clearly showed that: (1) the glucose-to-fructose isomerization was not achieved in the IL alone (entry 6); (2) in the presence of $CrCl_2$, the isomerization was achieved in high efficiency, but with a faster rate for further fructose dehydration to HMF, the overall reaction afforded HMF in 58% yield but no fructose (entry 1); and (3) IMes catalyzed the isomerization in [EMIM]Cl while impeding fructose

dehydration to HMF, thus forming fructose in 16% yield but no HMF (entry 5). Although there was no further dehydration of fructose to HMF, the fructose selectivity was only 19%.

Table 6.1 Glucose-to-fructose isomerization catalyzed by NHCs[a]

Entry	Solvent	Catalysts	Temp. (℃)	Glucose Conversion (%)	Fructose Yield (%)	Fructose Selectivity (%)	HMF Yield (%)
1	[EMIM]Cl	$CrCl_2$	100	>99	-	-	58
2	[EMIM]Cl	$CrCl_2$ + 1IMes	100	97	-	-	40
3	[EMIM]Cl	$CrCl_2$ + 2IMes	100	46	15	33	5
4	[EMIM]Cl	$CrCl_2$ + 3IMes	100	63	20	32	3
5	[EMIM]Cl	IMes	100	83	16	19	-
6	[EMIM]Cl	none	100	20	-	-	-
7	[EMIM]Cl	IMes	80	83	13	16	-
8	DMF	IMes	80	59	24	40	-
9	DMSO	IMes	80	57	26	45	-
10	DMSO	IMes	25	26	16	62	-
11	DMSO	TPT	60	12	1	10	-
12	DMSO	I^{t}Bu	25	25	20	83	-

[a] Catalyst loading: 10 mol%, reaction time: 3 h.

Searching ways to possibly increase the fructose yield and selectivity, we varied the temperature, solvents, and NHC catalysts. It was revealed that under the same conditions (10 mol% IMes, 80 ℃, 3 h), fructose yield increased from 13% to 24% and 26% by changing the IL [EMIM]Cl to organic solvents DMF and DMSO, with an increase in fructose selectivity from 16% (entry 7) to 40% and 45%, respectively (entries 8 and 9). Interestingly, this isomerization can even be carried out at RT (entry 10), achieving a similar fructose yield (16%) but relatively high fructose selectivity (62%). For other types of NHCs, the weaker base TPT was unable to catalyze the glucose-to-fructose isomerization in high efficiency (entry 11), while the stronger base I^{t}Bu rendered a higher fructose yield (20%) and selectivity (83%) (entry 12). Accordingly, this

glucose-to-fructose isomerization catalyzed by NHCs is proposed to follow the base-catalyzed isomerization mechanism (Scheme 6.1).[13b] A fast mutarotation from α-D-glucose to β-D-glucose with a molar ratio of 1:1.8 was observed upon the initial mixing of I^{t}Bu with glucose, through the open-chain form (**A**) of glucose. Deprotonation of the C-2 proton of **A** by an NHC base affords the enolate intermediate (**B**). Through further proton transfer steps involving enolate intermediates, fructose is formed and the NHC catalyst is regenerated (Scheme 6.1). Hence, in this NHC-catalyzed glucose-to-fructose isomerization, the yield and selectivity of fructose are strongly related to the basicity of NHCs. As expected, besides TPT, other weaker bases (e.g., NaOH and DBU) achieved only less than 5% of fructose yield under similar conditions. Noteworthy is that this reaction cycle is also *reversible* under the NHC-catalyzed conditions: when starting from fructose, a 30% glucose yield and a 61% glucose selectivity were observed at 60 ℃ for 1 h catalyzed by IMes.

Recently Chi et al. reported an interesting finding that NHCs can catalyze the retro-benzoin condensation of glucose to form acyl anion intermediates through C–C bond cleavage of glucose.[20] In their case, glucose was used as the acyl anion resource for subsequent Stetter reaction with chalcone. A high yield of Stetter product (80%) from the glucose and chalcone reaction was formed, which was catalyzed by *in-situ* generated thiazolium-based NHCs in 30 min at 130 ℃ under microwave irradiation. Interesting, they revealed that the imidazolium-based NHCs were not effective for the retro-benzoin condensation of glucose under their reaction conditions, while the current results showed that the imidaozlium-based NHCs such as I^{t}Bu and IMes are effective for catalyzing the glucose-to-fructose isomerisation even at

room temperature.

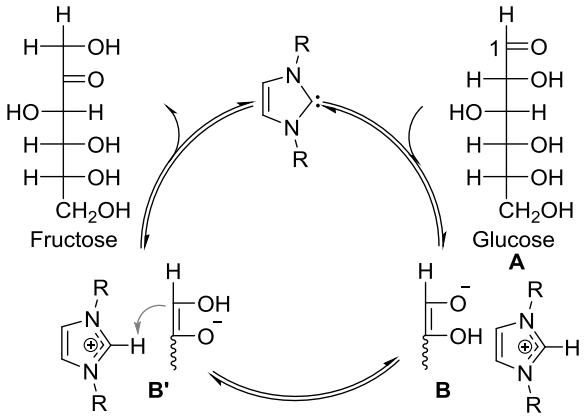

Scheme 6.1 Proposed proton transfer mechanism for isomerization of glucose to fructose catalyzed by NHCs.

HMF from biomass (fructose, glucose, and cellulose). To explore inexpensive alternatives to commonly used imidazolium-based ILs for biomass conversion to HMF, we found that [TM]Cl, an analog of thiamine (Vitamin B1), which is about 3.5 times less expensive than the typically employed IL [EMIM]Cl, can catalyze fructose conversion to HMF in high efficiency. Although the melting point of [TM]Cl (142–144 ℃) is well above 100 ℃, a homogenous solution is readily formed from the mixture of fructose and [TM]Cl upon heating to 100 ℃, affording HMF in 56% yield after heating the mixture at this temperature for 1 h (Table 6.2, entry 2). At higher temperatures of 120 and 130 ℃, the HMF yield increased to 72% (entry 3) and 68% (entry 4), respectively, which was comparable with that achieved by [EMIM]Cl (entry 1). As for the thiamine·HCl (B1) catalyzed fructose-to-HMF conversion, no homogeneous solution was formed by heating the mixture of thiamine·HCl and fructose, and no HMF was produced. However, adding water (50 wt% relative to thiamine·HCl) to increase fructose solubility in thiamine·HCl, a moderate HMF yield of 56% was obtained at 120 ℃ after 1 h

(entry 5).

Table 6.2 Biomass conversion to HMF by an organic or metal catalyst.[a]

Entry	Biomass	ILs	Catalyst	Temp. (℃)	Time (h)	HMF Yield (%)
1	fructose	[EMIM]Cl	-	100	1	74
2	fructose	[TM]Cl	-	100	1	56
3	fructose	[TM]Cl	-	120	1	72
4	fructose	[TM]Cl	-	130	0.5	68
5[b]	fructose	thiamine·HCl	-	120	1	56
6	glucose	[EMIM]Cl	$CrCl_2$	100	3	58
7	glucose	[TM]Cl	$CrCl_2$	120	1	51
8	glucose	[TM]Cl	$CrCl_3 \cdot 6H_2O$	120	1	45
9	glucose	[TM]Cl	$CrCl_3 \cdot 6H_2O$	130	0.5	47
10	cellulose	[TM]Cl	$CrCl_3 \cdot 6H_2O$	140	1	1
11[c]	cellulose	TEAC	$CrCl_3 \cdot 6H_2O$	130	0.5	27
12[d]	cellulose	TEAC	$CrCl_3 \cdot 6H_2O$	130	0.5	42

[a] Biomass/ILs 1/5 wt%, 10 mol% catalyst loading. [b] 50 wt% water relative to thiamine·HCl was added. [c] Cellulose/ILs 1/10 wt%. [d] Cellulose/ILs 1/10 wt%, 50 wt% water relative to cellulose was added.

For glucose conversion to HMF, an isomerization catalyst (e.g. $CrCl_2$, $CrCl_3 \cdot 6H_2O$) is required. In the presence of 10 mol% of $CrCl_2$, HMF was obtained in 51% yield from glucose in [TM]Cl at 120 ℃ after 1 h (entry 7), which was comparable with the glucose conversion in [EMIM]Cl at 100 ℃ after 1 h (entry 6). A lower HMF yield (45%) was achieved by $CrCl_3 \cdot 6H_2O$ (entry 8), while a slightly higher HMF yield (47%) was obtained within 0.5 h by increasing the reaction temperature to 130 ℃ (entry 9). Direct conversion of cellulose to HMF in [TM]Cl and TEAC was also investigated. While a low HMF yield was observed with [TM]Cl and $CrCl_3 \cdot 6H_2O$ even at 140 ℃ (entry 10), 27% of HMF was achieved with $CrCl_3 \cdot 6H_2O$ in TEAC at 130 ℃ after 0.5 h (entry 11). Addition of water (50 wt% relative to cellulose) enhanced HMF yield to 42% (entry 12), presumably because water facilitated the initial hydrolysis of cellulose

to reducing sugars.

High-purity HMF from fructose by semi-continuous extraction. Based on the above established one-pot conversion of fructose to HMF in [TM]Cl, semi-continuous extraction between the organic and [TM]Cl phases was adopted to separate HMF from [TM]Cl. THF was selected as the organic solvent, considering the high solubility of HMF, while low solubility of [TM]Cl, in this solvent. Moreover, THF can continuously remove water generated from fructose dehydration to HMF, thus suppressing HMF rehydration to organic acids and humins. During the initial 5 batches, HMF yield extracted by THF gradually increased to 70%, after which it remained nearly constant (Figure 6.3). It is noteworthy that this semi-continuous process for HMF production from fructose is efficient and robust: (1) 72% HMF yield and 74% of HMF selectivity were achieved over the 10 batch runs, and 90% of HMF formed was extracted by THF; (2) no apparent loss of the HMF yield was observed even after 10 batches, with a consistent HMF yield after the 5th batch; and (3) for each of subsequent batches, fructose and THF were loaded to the reactor and no more [TM]Cl was needed. After completion of the reaction, the product HMF was isolated and the collected THF can be recycled. Overall, this semi-continuous process is efficient and economical, representing a net transformation of the inexpensive feedstock fructose to the high-value platform chemical HMF, which is currently about 100 times more expensive than the starting fructose.

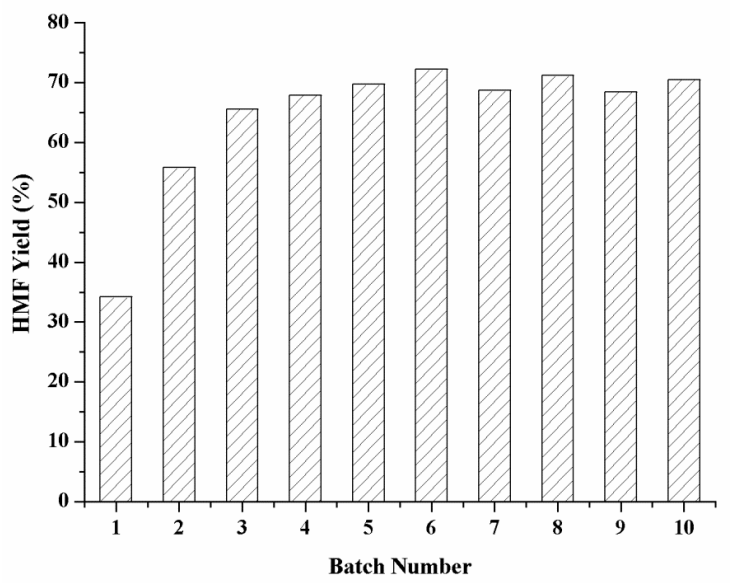

Figure 6.3 HMF yields obtained from fructose conversion in [TM]Cl at 120 ℃ for 1 h (1.5 h for the first batch) by semi-continuous extraction with THF. Data were shown as the average value of at least two runs with typical errors within ±3%.

The above semi-continuous process in [TM]Cl and extraction with THF was also applied to the glucose-to-HMF conversion in the presence of $CrCl_3$ $6H_2O$ (10 mol% relative to glucose). During the initial 4 batches, HMF yield gradually reached the maximum at 50%, after which it decreased to 44% at the 6th batch (Figure 6.4), presumably due to the Cr catalyst loss upon repeated extractions with THF. After 6 batches, HMF was obtained from glucose in 49% yield and 52% selectivity, and 92% of HMF formed was extracted by THF. When EtOAc was used as the organic solvent, HMF yield (31%) was consistently lower than that extracted by THF, although no loss of catalyst activity was observed after the 5th batch. For the cellulose-to-HMF conversion, semi-continuous extraction of HMF by THF/TEAC gave a low HMF yield. Nevertheless, extraction with water/EtOAc (1/4 v/v) after the reaction achieved 39% of HMF yield and 94% of HMF recovery.

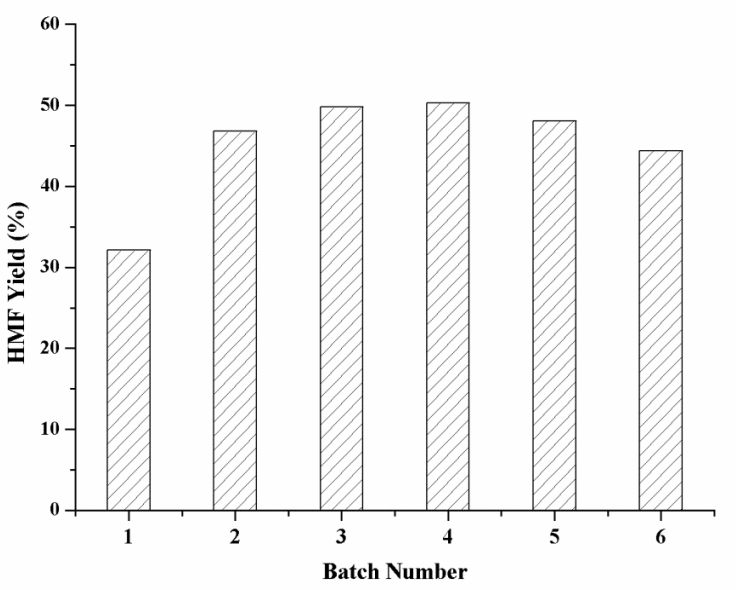

Figure 6.4 HMF yields obtained from glucose conversion in [TM]Cl/$CrCl_3$ $6H_2O$ (10 mol%) at 130 ℃ for 0.5 h (1 h for the first batch) by semi-continuous extraction with THF. Data were shown as the average of at least two runs with errors within ±3%.

The HMF product obtained from fructose dehydration by the above described semi-continuous extraction was sufficently pure (>99% by HPLC), presumbably sutiable for most applications without further purification. However, there were still a small amount of impurities (e.g., [TM]Cl, H_2O, and organic acids) present in the product according to ^{1}H NMR analysis (Figure 6.6a). To produce the spectroscopically and analytically HMF, we investigated two purification routes. This first route was extraction with diethyl ether and subsequent solvent removal under vacuum, affording the purer HMF (54% yield) as dark yellow liquid (Figure 6.5, route 1), but ^{1}H NMR analysis showed the presence of only a tiny amount of an impurity appeared as a broad signal at ~2.8 ppm (Figure 6.6b). The second route was recrystallization of the crude HMF product (Figure 6.5, route 2). Screening of solvents suitable for recrystallization led to toluene, which yielded the analytically and spectroscopically pure HMF as needle crystals

(Figure 6.6c). In this purification route, the crude HMF obtained from the above semi-continuous process was dissolved in hot toluene (50-60 ℃) and crystallized in a freezer overnight, affording the pure HMF as needle crystals (yield 30-36%). A step of decoloration with activated carbon can be added to treat the crude HMF before crystallization. The crystallized HMF was used for further umpolung to DHMF catalyzed by either TPT or other NHC catalysts.

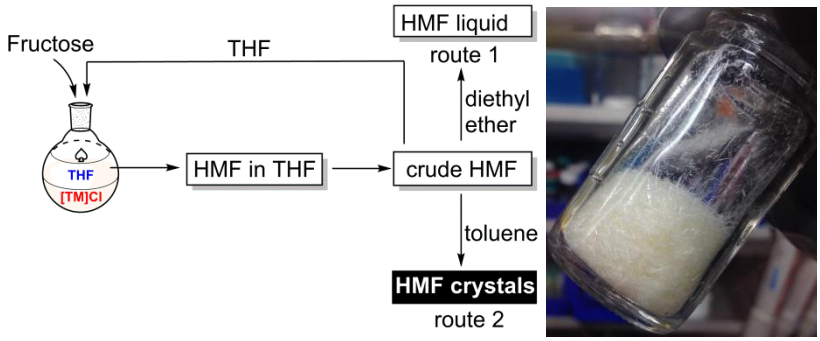

Figure 6.5 Integrated process for the production of the spectroscopically and analytically pure HMF from fructose catalyzed by [TM]Cl.

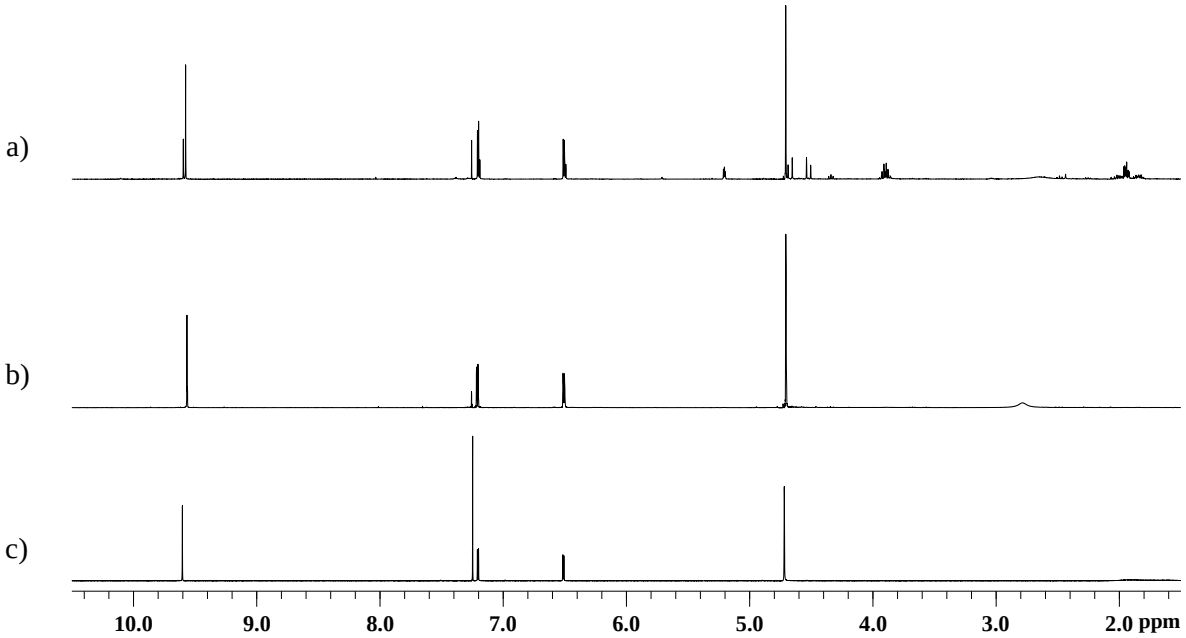

Figure 6.6 ^{1}H NMR ($CDCl_3$) of HMF (δ 9.61, 7.21, 6.52, 4.72 ppm) by two different purification routes: a) crude HMF; b) HMF after extraction with diethyl ether (*c.f.*, Figure 6.5, route 1); and c) HMF needle crystals after recrystallization from toluene (*c.f.*, Figure 6.5, route 2).

Step 2: HMF Coupling to C_{12} DHMF by Organocatalysis

We have previously shown that furaldehydes, such as furfural, 5-methylfurfural and HMF, can be efficiently self-coupled in a 100% atom-economical manner into furoin, 5,5'-dimethylfuroin (5,5'-DMF), and C_{12} furoin (DHMF), respectively, through an organocatalytic umpolung process (i.e., self-condensation) involving an enol intermediate (Scheme 6.2).[15] In this study, we explored the NHC catalysts derived from readily available, inexpensive precursors, including [TM] NHC, thiamine NHC and poly(NHC)s. The more expensive, proven efficient TPT catalyst was also used for comparison and for examining the purity and suitability of the HMF produced from fructose by the current semi-continuous process. The results of this investigation were summarized in Table 6.3.

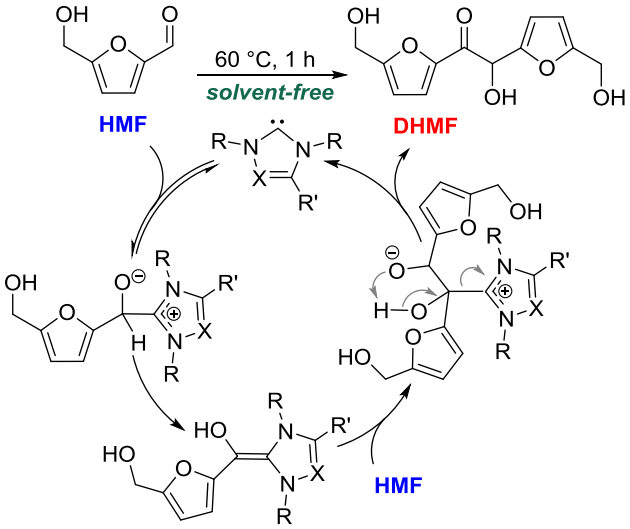

Scheme 6.2 Solvent-free NHC-catalyzed self-condensation of HMF to DHMF and depicted umpolung catalytic cycle.

Table 6.3 DHMF yields from the HMF umpolung reaction catalyzed by NHCs.

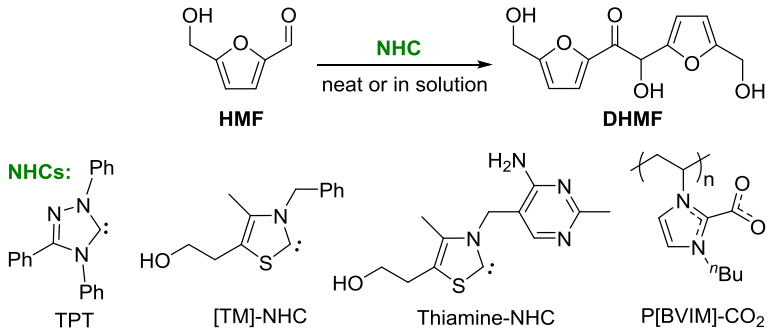

entry	solvent	NHCs	NHC loading (mol%)	temp (℃)	time (h)	DHMF (%)
1	none	TPT	0.7	60	1	93
2	none	TPT	0.1	60	3	91
3	toluene	[TM]-NHC	10	80	3	60
4	none	*in-situ* [TM]-NHC	10	80	3	53
5	toluene	thiamine-NHC	10	60	3	0
6	THF	P[BVIM]-CO_2	10	80	3	32
7	THF	P[^{i}PrVIM]	10	80	3	18

The results showed that TPT is still the most efficient catalyst. With a low catalyst loading of 0.70 mol% at 60 ℃ for 1 h, the HMF self-condensation in neat gave DHMF in 93% isolated yield (Table 6.3, entry 1). The catalyst loading can be further lowered to only 0.10 mol%, while DHMF can still be isolated in high yield (91%, entry 2). These results clearly demonstrated that the HMF produced from fructose by our semi-continuous process was in high purity and readily suitable for this critical chain-extension coupling step by organocatalysis.

In comparison, [TM]-NHC produced DHMF in only moderate isolated yield of 60%, even with a 10 mol% catalyst loading (entry 3). Using the *in-situ* generated [TM]-NHC through deprotonation of [TM]Cl by KO^{t}Bu, a comparable DHMF yield (53%, entry 4) was obtained

after purification by silica-gel chromatography. However, thiamine-NHC exhibited no catalytic activity towards DHMF formation under similar conditions (entry 5). We also employed poly(NHC)s as catalysts for HMF coupling. Specifically, the masked poly(NHC), P[BVIM]-CO_2, and the preformed poly(NHC), P[^{i}PrVIM], produced DHMF in only 32% and 18% yields (by ^{1}H NMR), respectively. These results were sharply different from those obtained by adopting poly(NHC)s to catalyze the umpolung of benzaldehyde, in which up to 92% yield of benzoin was achieved at room temperature for 24 h.[18b] This difference can be attributed to the acidic proton in the hydroxyl group of HMF which impedes the catalytic activity of poly(NHC)s. Supporting this reasoning, furfural behaved much like benzaldehyde in the umpolung reaction catalyzed by NHCs. For example, with a low loading of [TM]-NHC (1 mol%), furfural was readily coupled to furoin in 86% isolated yield, as compared to a much lower yield of 60% in the case of the HMF umpolung reaction, under otherwise identical conditions.

Step 3: HDO of DHMF to *n*-$C_{12}H_{26}$ Alkane Fuel by Metal-Acid Tandem Catalysis

Previously, we reported a method of converting DHMF to mixture of linear alkanes consisting of C_{10} (27.0%), C_{11} (22.9%), and C_{12} (45.6%) using a bifunctional catalyst system containing Pt/C and $TaOPO_4$ in water under 500 psi H_2 at 300 ℃.[15b] Recently, a highly selective HDO process utilizing acetic acid, Pd/C and $La(OTf)_3$ was developed, which converted cross-aldol condensation products (e.g., furan aldehydes and enolizable ketones) into their corresponding alkanes under relatively mild conditions (200 ℃ and 300 psi H_2).[21] In light of

this important development, we employed this metal/acid (Brønsted + Lewis acid) catalyst system, Pd/C + acetic acid + $La(OTf)_3$, for the HDO of DHMF, the results of which study were shown in Table 6.4.

Table 6.4 Analytical results of liquid fuels after HDO in acetic acid[a]

Entry	Furoins	Temperature (℃)	Pressure (psi)	*n*-$C_{11}H_{24}$ (%)	*n*-$C_{12}H_{26}$ (%)	Alkanes (%)	Oxygenated (%)	Isolated Fuels		
								C (%)	H (%)	O (%)
1	DHMF	200	300	1.5	26	31	69	76	11	13
2	DHMF	200	500	-	22	25	75	73	10	17
3	DHMF	250	300	5.7	64	78	22	84	11	5.0
4	5,5'-DMF	200	300	1.5	66	75	25	83	13	4.0

[a] Reaction conditions: reaction time, 16 h; solvent, acetic acid, 40 mL; catalysts, Pd/C + $La(OTf)_3$. In all cases, furoins were completely converted. Branched and cyclic C_{11} and C_{12} were included in the calculation of alkane selectivity. 5,5'-DMF = 5,5'-dimethylfuroin.

The initial HDO process carried out at 200 ℃ and 300 psi H_2 gave a selectivity of 26% for *n*-$C_{12}H_{26}$ and 1.5% for *n*-$C_{11}H_{24}$, and the HDO products contained 31% alkanes (including branched and cyclic C_{11} and C_{12} alkanes) and 69% oxygenated compounds (entry 1). Although a low selectivity of *n*-$C_{12}H_{26}$ was obtained from this trial run, the majority of the oxygenated compounds were found to be C_{12} esters and ketones, which could be further converted to C_{12} alkanes under modified conditions. Hence, two reaction parameters, H_2 pressure and reaction temperature, were varied. By increasing the H_2 pressure from 300 psi to 500 psi, even lower *n*-$C_{12}H_{26}$ selectivity (22%) was obtained (entry 2). On the other hand, increasing the reaction temperature from 200 ℃ to 250 ℃ while keeping the H_2 pressure the same (300 psi) resulted in a significant increase of the *n*-$C_{12}H_{26}$ selectivity from 26% to 64% (entry 3), under otherwise

identical conditions. The fuel produced at this temperature contained 78% alkanes and 22% oxygenated compounds (Figure 6.7), and the elemental analysis showed 84% C, 11% H and 5.0% O. Using 5,5'-DMF as a comparable substrate to DHMF, the HDO process at 200 ℃ and 300 psi H_2 for 16 h afforded alkane fuel with a selectivity of 66% for *n*-$C_{12}H_{26}$ (43% yield) and 1.5% for *n*-$C_{11}H_{24}$ without the formation of C_{12} esters (entry 4). Meanwhile, the isolated fuel exhibited similarly high C and H molar ratios (83% and 13%) and a correspondingly low O ratio of 4.0%.

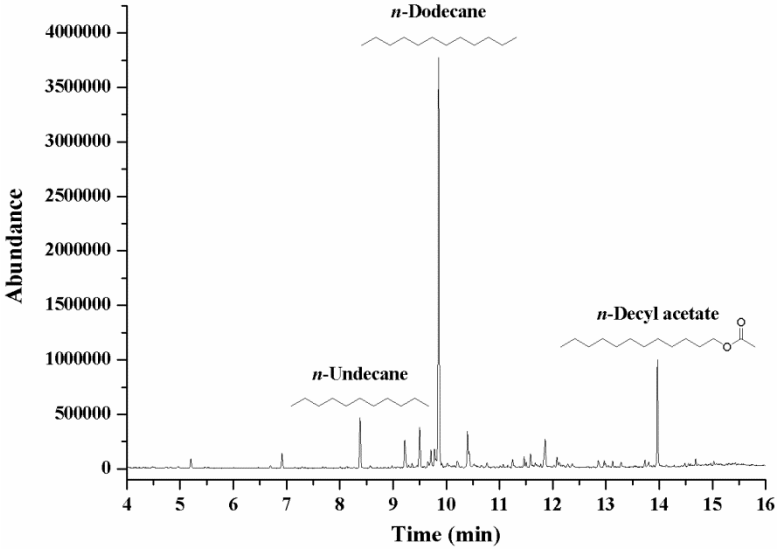

Figure 6.7 GC-MS chromatogram of the crude products produced by the HDO of DHMF in acetic acid catalyzed by Pd/C+ $La(OTf)_3$ at 250 ℃ under 300 psi H_2 for 16 h (Table 4, run 3).

6.5 Conclusions

In summary, we have developed an integrated catalytic process for biomass conversion and upgrading to C_{12} DHMF and subsequently to *n*-$C_{12}H_{26}$ alkane by organocatalysis and subsequent metal-acid tandem catalysis. The first step of the process involves semi-continuous organocatalytic conversion of biomass (fructose, in particular) to the high-purity HMF. In this step, NHCs were found to be effective in catalyzing glucose-to-fructose isomerization, even at

room temperature. Particularly, treatment of glucose with 10 mol% of I^{t}Bu in DMSO for 3 h afforded fructose in 20% yield with a 83% selectivity. For biomass conversion to HMF, the inexpensive [TM]Cl, a Vitamin B1 analog, was utilized for fructose and glucose dehydration to HMF for the first time, achieving a 72% HMF yield from fructose (no metal catalysts) and up to 51% yield from glucose (in the presence of additional chromium(II) or (III) catalyst) at 120 ℃ for 1 h. The semi-continuous extraction process developed for the HMF production from fructose is efficient and robust: a constant HMF yield of 72% was achieved over 10 batch runs. The HMF product obtained from the semi-continuous process is sufficently pure (>99% by HPLC), presumably sutiable for most applications without further purification. On the other hand, further purification by extraction with diethyl ether gave the purer HMF (54% yield) as a liquid, or by crystallization from toluene afforded the spectroscopically and analytically pure HMF as needle crystals. Overall, this semi-continuous process represents a net transformation of the inexpensive feedstock fructose to the higher-value platform chemical HMF (~100-fold price increase) as the [TM]Cl and the extraction solvent THF can be readily recycled for subsequent batch runs.

The second step of the process is the organocatalytic coupling of the C_6 HMF produced by the above semi-continuous process to C_{12} DHMF in the presence of an NHC catalyst. Among several types of NHCs investigated for this coupling reaction, TPT was proven to be most effective, achieving 93% or 91% isolated yield of DHMF in the presence of 0.70 mol% or 0.10 mol% TPT at 60 ℃ for 3 h (in a solvent-free process). The [TM]Cl derived NHC is less effective, affording DHMF in 60% isolated yield with a 10 mol% catalyst loading. The two poly(NHC)s investigated are least effective, producing DHMF in much lower yields of only 18–32%. Overall,

the TPT-catalyzed HMF self-condensation (chain-extension) process to DHMF can be regarded as a greener process, with 100% atom-economy, solvent-free operation, and near quantitative yield from an organocatalytic reaction.

The third step of the process is the hydrodeoxygenation of C_{12} DHMF to linear alkanes as a potential high-quality hydrocarbon fuel. With the metal (Pd/C)/acid ($La(OTf)_3$) catalyst system, the HDO of DHMF in acetic acid at 250 ℃ and 300 psi H_2 for 16 h afforded liquid hydrocarbon fuel (78% alkanes) with a 64% selectivity to *n*-$C_{12}H_{26}$ and an overall C/H/O % ratio of 84/11/5.0.

6.6 References

(1) Selective Reviews: (a) van Putten, R.-J.; van der Waal, J. C.; de Jong, E.; Rasrendra, C. B.; Heeres, H. J.; de Vries, J. G. *Chem. Rev.* **2013**, *113*, 1499-1597; (b) Alonso, D. M.; Wettstein, S. G.; Dumesic, J. A. *Green Chem.* **2013**, *15*, 584-595; (c) Gallezot, P. *Chem. Soc. Rev.* **2012**, *41*, 1538-1558; (d) Lange, J.-P.; Van der Heide, E.; Van Buijtenen, J.; Price, R. *ChemSusChem* **2012**, *5*, 150-166; (e) Gallezot, P. *Chem. Soc. Rev.* **2012**, *41*, 1538-1558; (f) Lange, J.-P.; Van der Heide, E.; Van Buijtenen, J.; Price, R. *ChemSusChem* **2012**, *5*, 150-166; (g) Rosatella, A. A.; Simeonov, S. P.; Frade F. M.; Afonso, A. M. *Green Chem.* **2011**, *13*, 754-793; (h) James, O. O.; Maity S.; Usman, L. A.; Ajanaku, K. O.; Ajani, O. O.; Siyanbola, T. O.; Sahu, S.; Chaubey, R. *Energy Environ. Sci.* **2010**, *3*, 1833-1850; (i) Alonso, D. M.; Bond, J. Q.; Dumesic, J. A. *Green Chem.* **2010**, *12*, 1493- 1513.

(2) (a) Cheng, Y.-T.; Wang, Z.; Gilbert, C. J.; Fan W.; Huber, G. W. *Angew. Chem. Int. Ed.* **2012**,

51, 11097-11100; (b) Shiramizu, M.; Toste, F. D. *Chem. Eur. J.* **2011**, *17*, 12452-12457.

(3) (a) Bui, L.; Luo, H.; Gunther, W. R.; Román-Leshkov, Y. *Angew. Chem. Int. Ed.* **2013**, *52*, 8022-8025; (b) Bond, J. Q.; Alonso, D. M.; Wang, D.; West R. M.; Dumesic, J. A. *Science* **2010**, *327*, 1110-1114.

(4) (a) Wegenhart, B. L.; Liu, S.; Thom M.; Stanley, D.; Abu-Omar, M. M. *ACS Catal.* **2012**, *2*, 2524-2530; (b) Balakrishnan, M.; Sacia, E. R.; Bell, A. T. *Green Chem.* **2012**, *14*, 1626-1634; (c) Corma, A.; de la Torre, O.; Renz, M. *Energy Environ. Sci.* **2012**, *5*, 6328-6344; (d) Corma, A.; de la Torre, O.; Renz, M.; Villandier, *Angew. Chem. Int. Ed.* **2011**, *50*, 2375-2378; (e) Huber, G. W.; Chheda J. N.; Barrett C. J.; Dumesic J. A. *Science* **2005**, *308*, 1446-1450.

(5) (a) Bozell, J. J.; Petersen G. R. *Green Chem.* **2010**, *12*, 539-554; (b) "*Top Value Added Chemicals from Biomass*", Werpy, T.; Petersen, G., Eds. U.S. Department of Energy (DOE) report: DOE/GO-102004-1992, **2004**.

(6) (a) Song, J.; Zhang, B.; Shi, J.; Fan, H.; Ma, J.; Yang, Y.; Han, B. *RSC Adv.* **2013**, *3*, 20085-20090; (b) He, J.; Zhang, Y.; Chen, E. Y.-X. *ChemSusChem* **2013**, *6*, 61-64; (c) Liu, D.; Chen, E. Y. -X. *Appl. Catal. A: Gen.* **2012**, *435-436*, 78-85; (d) Zhao, H.; Holladay, J. E.; Brown, H.; Zhang, Z. C. *Science* **2007**, *316*, 1597-1600.

(7) (a) Shi, N.; Liu, Q.; Zhang, Q.; Wang, T.; Ma, L. *Green Chem.* **2013**, *15*, 1967-1974; (b) Ordomsky, V. V.; van der Schaaf, J.; Schouten, J. C.; Nijhuis, T. A. *ChemSusChem* **2013**, *6*, 1697-1707; (c) Pagán-Torres, Y. J.; Wang, T.; Gallo, J. M. R.; Shanks, B. H.; Dumesic, J. A.

ACS Catal. **2012**, *2*, 930-934; (d) Chheda, J. N.; Román-Leshkov Y.; Dumesic J. A. *Green Chem.* **2007**, *9*, 342-350.

(8) Wang, L.; Wang, H.; Liu, F.; Zheng, A.; Zhang, J.; Sun, Q.; Lewis, J. P.; Zhu, L.; Meng, X.; Xiao, F.-S. *ChemSusChem* **2014**, *7*, 402-406.

(9) Pidko, E. A.; Degirmenci, V.; van Santen, R. A.; Hensen, E. J. M. *Angew. Chem. Int. Ed.* **2010**, *49*, 2530-2534.

(10) (a) Amarasekara, A. S.; Williams, L. D.; Ebebe, C. C. *Carbohydr. Res.* **2008**, *343*, 3021-3024; (b) R. M.; Munavu, R. M. *Biomass*, **1987**, *13*, 67-74.

(11) (a) Li, Y.-N.; Wang, J.-Q.; He, L.-N.; Yang, Z.-Z.; Liu, A.-H.; Yu, B.; Luan, C.-R. *Green Chem.* **2012**, *14*, 2752-2758; (b) Xie, H.; Zhao Z. K.; Wang Q. *ChemSusChem* **2012**, *5*, 901-905; (c) Cao Q.; Guo X.; Guan J.; Mu X.; Zhang D. *Appl. Catal. A: Gen.* **2011**, *403*, 98-103; (d) Binder, J. B.; Raines, R. T. *J. Am. Chem. Soc.* **2009**, *131*, 1979-1985; (e) Hu, S.; Zhang, Z.; Zhou, Y.; Han, B.; Fan, H.; Li, W.; Song J.; Xie, Y. *Green Chem.* **2008**, *10*, 1280-1283; (f) Moreau, C.; Finiels, A.; Vanoye, L. *J. Mol. Catal. A: Chem.* **2006**, *253*, 165-169.

(12) Ranoux, A; Djanashvili K.; Arends, I. W. C. E.; Hanefeld, U. *ACS Catal.* **2013**, *3*, 760-763.

(13) (a) Román-Leshkov, Y.; Davis, M. E. *ACS Catal.* **2011**, *1*, 1566-1580; (b) Román-Leshkov, Y.; Moliner, M.; Labinger, J. A.; Davis, M. E. *Angew. Chem. Int. Ed.* **2010**, *49*, 8954-8957; (c) Moliner M.; Román-Leshkov, Y.; Davis, M. E. *Proc. Natl. Acad. Sci. U.S.A.* **2010**, *107*, 6164-6168.

(14) Saravanamurugan, S.; Paniagua, M.; Melero, J. A.; Riisager, A. *J. Am. Chem. Soc.* **2013**, *135*, 5246-5249.

(15) (a) Liu, D.; Chen, E. Y.-X. *Green Chem.* **2014**, *16*, 964–981; (b) Liu, D.; Chen, E. Y.-X. *ChemSusChem* **2013**, *6*, 2236-2239; (c) Caes, B. R.; Palte, M. J.; Raines, R. T. *Chem. Sci.* **2013**, *4*, 196-199; (d) Liu, D.; Zhang, Y.; Chen, E. Y.-X. *Green Chem.* **2012**, *14*, 2738-2746; (e) Stålberg, T.; Rodriguez-Rodriguez, S.; Fristrup, P.; Riisager, A. *Chem. Eur. J.* **2011**, *17*, 1456-1464.

(16) (a) Simeonov, S. P.; Coelho, J. A. S.; Afonso, C. A. M. *ChemSusChem* **2013**, *6*, 997-1000; (b) Simeonov, S. P.; Coelho, J. A. S.; Afonso, C. A. M. *ChemSusChem* **2012**, *5*, 1388-1391.

(17) (a) Enders, D.; Breuer, K.; Kallfass, U.; Balensiefer, T. *Synthesis* **2003**, 1292-1295; (b) Enders, D.; Breuer, K.; Raabe, G.; Runsink, J.; Teles, J. H.; Melder, J. P.; Ebel, K.; Brode, S. *Angew. Chem., Int. Ed. Engl.* **1995**, *34*, 1021-1023.

(18) (a) Liu, D.; Chen, E. Y.-X. *Biomass Bioenergy* **2013**, *48*, 181-190; (b) Pinaud, J.; Vignolle, J.; Gnanou, Y.; Taton, D. *Macromolecules* **2011**, *44*, 1900-1908.

(19) Dunn, E. F.; Liu, D.; Chen E. Y.-X. *Appl. Catal. A: Gen.* **2013**, *460-461*, 1-7.

(20) Zhang, J.; Xing, C.; Tiwari, B.; Chi, Y. R. *J. Am. Chem. Soc.* **2013**, *135*, 8113-8116.

(21) (a) Sutton, A. D.; Waldie, F. D.; Wu, R.; Schlaf, M.; 'Pete' Silks III, L. A.; Gordon, J. C. *Nature Chem.* **2013**, *5*, 428-432; (b) Waidmann C. R.; Pierpont, A. W.; Batista, E. R.; Gordon, J. C.; Martin R. L.; "Pete" Silks, L. A. ; West R. M.; Wu R. *Catal. Sci. Technol.* **2013**, *3*, 106-115.

Chapter 7

Organocatalysis in Biorefining for Biomass Conversion and Upgrading

7.1 Summary

Organocatalysis using small-molecule organic compounds as catalysts has risen to prominence in organic synthesis and polymer synthesis. However, its application in biorefining for catalytic biomass conversion and upgrading into sustainable chemicals, materials, and biofuels has come to light only recently. The emergence of organocatalysis for biorefining has not only broadened the scope of organocatalysis and offered metal-free "greener" alternatives for biomass conversion and upgrading, it has also shown some unique activity and selectivity in birefining transformations compared to metal-mediated processes. This review captures highlights of this emerging area by focusing on the utilization of organocatalytic means of conversion of cellulose, glucose and fructose, upgrading of furaldehydes, and organocatalytic polymerization of biomass feedstocks.

7.2 Introduction

Organocatalysis and green chemistry. The use of relatively non-toxic, environmentally benign and inherently sustainable small-molecular organic compounds as efficient catalysts to promote catalytic chemical transformations has flourished over the last decade and continued to attract ever increasing attention. The field of organocatalysis[1-3] has enjoyed dramatic expansion,

thanks to its versatile synthetic utilities developed for the efficient "greener" synthesis of pharmaceuticals and fine chemicals[4-10] as well as polymeric materials.[11-15] Organocatalysis is especially advantageous when metal-free products or processes are of primary concern. Like any other types of catalysis, organocatalysis addresses a key principle of green chemistry:[16,17] *catalysis*. However, what separates organocatalysis from other types of catalysis is that carbon-based organic catalysts are relatively non- or less toxic, more environmentally benign, and more renewable as compared to metal-based catalysts. Hence, in addition to catalysis, organocatalysis embodies three more key principles of green chemistry:[16,17] *less hazardous chemical syntheses, designing safer chemicals, and use of renewable feedstocks*.

Scope of review. This review covers catalytic conversions of C_6 (poly)sugars, including cellulose, glucose and fructose, as well as upgrading of furaldehydes, including furfural (FF), 5-methylfurfural (MF) and 5-hydroxymethylfurfural (HMF), via organocatalytic means. Organocatalytic polymerization of plant biomass feedstocks to sustainable polymeric materials is also highlighted. On the other hand, biomass conversion by non-organocatalytic transformations are not covered, as many reviews[18-36] have already covered general topics of biomass conversion by processes other than organocatalytic transformations. However, examples of non-organocatalytic biomass conversion systems, when they are part of the integrated process involving organocatalysis, are commented. Biomass conversion using large biological organic substances (enzymes or proteins) is not covered. Except for few examples included, patents and meeting proceedings are not reviewed.

7.3 Mono- and Polysaccharide Conversion

Lignocellulosic biomass is generated from CO_2 and H_2O via photosynthesis utilizing solar energy. The primary components of lignocellulose are cellulose (40–50%, a polymer of glucose containing linear polymeric d-glucose chains through β-1,4-glycosidic linkages), and the remaining components are hemicelluloses (25–35%, a polymer of glucose and xylose) and lignin (15–20%, a cross-linked polymer built of phenols to support plants).[37,38]

A strong desire to reduce societal dependence on fossil fuels has directed researchers' interests towards the use of biomass as a sustainable alternative source of transportation fuels and chemical building blocks. For the production of transportation fuels, the treatment of biomass using the petrochemical refinery strategy (e.g., catalytic cracking and hydrotreating) is extensively reviewed by Corma et al.[33,34] Although the process of converting biomass into alkane fuels can be simply demonstrated by Equation 7.1 where the oxygen is removed in the form of H_2O from the highly oxygenated biomass sources, the key problems are that catalysts must be sufficiently tolerant to oxygen and water under high temperature and high H_2 pressure.

$$(CH_2O)_n + (n+1)\,H_2 \xrightarrow{\text{catalyst}} C_nH_{2n+2} + n\,H_2O$$

Equation 7.1 Demonstration of biomass conversion to alkane fuels.

On the other hand, being oxygen-rich biomass feedstocks present an advantage over petroleum counterparts: biomass can be selectively converted into oxygenated chemical building blocks and materials. For example, HMF, a selective dehydration product from C_6 (poly)sugars (e.g., cellulose, glucose and fructose), has been identified as a versatile intermediate for top-value-added chemicals (Figure 7.1).[28,35,39] Specifically, the 2,5-positioned hydroxyl and

aldehyde groups can be readily converted to other functionalities, such as methyl, ethoxyl, hydroxyl, aldehyde, and carboxyl groups; such biomass-derived compounds offer renewable alternatives to similar petroleum-derived chemicals. In addition, HMF can be rehydrated to levulinic acid, which is the precursor of α-methylene-γ-butyrolactone monomers for polymerization in replacement of the currently petroleum-based methyl methacrylate (MMA). The highlighted work on the organocatalytic polymerization of biomass-derived monomers to sustainable polymeric materials is reviewed in Section 7.5.

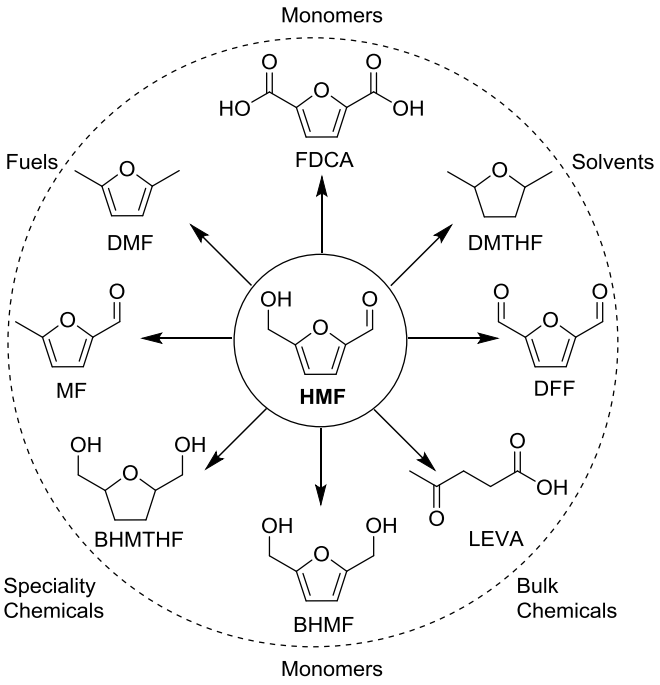

Figure 7.1 HMF can be converted into many types of biomass-based compounds now obtained from petroleum sources. Selected examples include: 2,5-furandicarboxylic acid (FDCA); 2,5-dimethyltetrahydrofuran (DMTHF); 2,5-diformylfuran (DFF); levulinic acid (LEVA); 2,5-bis(hydroxymethyl)furan (BHMF); 2,5-bis(hydroxymethyl)tetrahydro- furan (BHMTHF); 5-methylfurfural (MF); 2,5-dimethylfuran (DMF).

Table 7.1 Selected results of biomass conversion to HMF by organocatalysis.[a]

Sugars	Solvent	Catalysts	Temp. (℃)	Time (min)	Yield (%)	Selectivity (%)	Ref.
Fructose	DMSO	-	150	120	92.0	ND	46
	DMSO	CNT-PSSA	120	30	89.0	89.0	48
	H_2O	-	190	40	70.0	61.0	56
	[HMIM]Cl	-	90	15	92	ND	49
	[EMIM]Cl	-	120	180	70	70.0	43
	[BMIM]Br	-	100	60	92	92.9	50
	[BMIM]Cl	LS	100	10	94.3	95.0	51
	TEAC	-	120	70	81.3	81.3	52
	TEAB	-	110	30	79	ND	54
	ChoCl	-	120	70	70	ND	52
	ChoCl	Malonic acid	80	60	41.0	45.0	55
	ChoCl	Oxalic acid	80	60	62.0	62.0	55
	ChoCl	Citric acid	80	60	76.3	83.8	55
Glucose	[EMIM]Cl	Boric acid	120	180	41	43	59
	DMSO	CNT-PSSA	140	60	57	57	48
Cellulose	[EMIM]Cl	Boric acid	120	480	32	ND	59

[a] [HMIM]Cl = 1-H-3-methylimidazolium chloride; [BMIM]Cl = 1-butyl-3-methylimidazolium chloride; [BMIM]Br = 1-butyl-3-methylimidazolium bromide; TEAC = tetraethylammonium chloride; TEAB = tetraethylammonium bromide; ChoCl = choline chloride; LS = lignosulfonic acid; CNT-PSSA = poly(*p*-styrenesulfonic acid)-grafted carbon nanotubes; ND = not determined.

In a typical hydrothermal method of cellulose conversion to HMF by aqueous acid hydrolysis, only ~30% HMF yield was obtained under high temperature (250-400 ℃) and pressure (10 MPa) conditions.[40] Significant improvement on biomass conversion has been made possible by performing the conversion in ionic liquids (ILs)—a class of organic salts that have a melting point lower than 100 ℃—thanks to Rogers's finding that cellulose can be dissolved up to 25 wt% in ILs.[41,42] In the presence of a metal halide salt that catalyzes isomerization of glucose to fructose,[43] cellulose upon dissolution in ILs can be converted to HMF in good yields under mild conditions.[44,45] Another advantage using ILs for biomass conversion to HMF is that

HMF can be simply extracted from the IL phase with a low boiling organic solvent (e.g. tetrahydrofuran, ethyl acetate, diethyl ether, butanol, and methyl isobutyl ketone), thus rendering the recycling of ILs. Besides metal halides, organic catalysts have also been applied to biomass conversion to HMF, and some selected examples are summarized in Table 7.1. Accordingly, reviewed in this section are organocatalysts, typically ILs, serving as both solvent and catalyst for the conversion of C_6 (poly)sugars (e.g., fructose, glucose and cellulose) to HMF, with organocatalysis playing a major role in such conversion systems.

7.3.1 Monosaccharide conversion

Fructose conversion to HMF. Fructose dehydration is the most facile method of producing HMF. Although this reaction typically employs acids to facilitate removal of 3 equiv. of water molecules, some organic solvents or salts not only serve as the solvent, but also function as the catalyst. For example, in 1987 Musau and Munavu revealed that DMSO functions as both the solvent and the catalyst for fructose dehydration to HMF. The conversion conditions were optimized at 150 ℃ for 2 h and with a fructose to DMSO molar ratio of 8, under which conditions HMF yield up to 92 % was achieved.[46] A mechanism for this DMSO-induced fructose dehydration was recently proposed to proceed through intermediate **1** (Scheme 7.1), (4*R*, 5*R*)-4-hydroxy-5-hydroxymethyl-4,5-dihydrofuran-2-carbaldehyde, which was detected by ^{1}H and ^{13}C NMR.[47] By adding a heterogeneous catalyst (e.g., CNT-PSSA) into the fructose-DMSO solution, HMF was obtained in high yield (89.0%) and selectivity (89.0%) under relatively mild conditions (120 ℃, 30 min).[48]

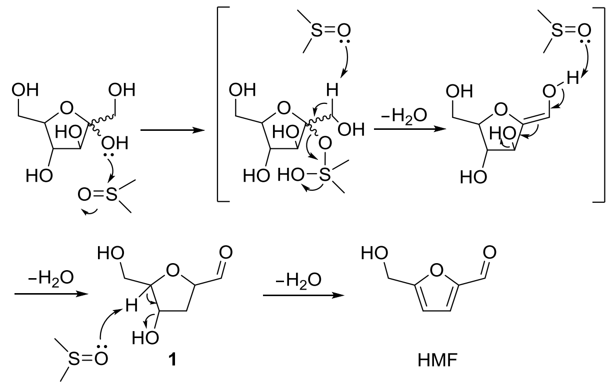

Scheme 7.1 Proposed mechanism for fructose dehydration to HMF in DMSO at 150 ℃.[47]

Interestingly, being organic salts, ILs can also catalyze fructose dehydration to HMF in a high to quantitative yield at 80 –120 ℃ without adding acid catalysts.[43,49,50] Moreau et al. found that 1-H-3-methylimidazolium chloride [HMIM]Cl, being an acidic IL, catalyzes fructose-to-HMF conversion affording HMF in up to 92% yield within 15–45 min at 90 ℃.[49] Non-acidic ILs such as [EMIM]Cl were also reported to convert fructose to HMF in 70% yield at 120 ℃ for 3 h.[43] With the aid of LS (a waste byproduct from the paper industry), a high yield (94.3%) of HMF was achieved in [BMIM]Cl at 100 ℃ for only 10 min.[51] By changing the counterion from Cl^- to Br^-, a higher HMF yield of 92 % was obtained when the same conversion was carried out in [BMIM]Br at 100 ℃ for 1 h. In terms of the IL-catalyzed fructose dehydration mechanism, it was suggested that the bromide anion interacts with hydroxyl groups of fructose and reaction intermediates through H-bonding (e.g., **2**), thus promoting fructose dehydration (Scheme 7.2).[50]

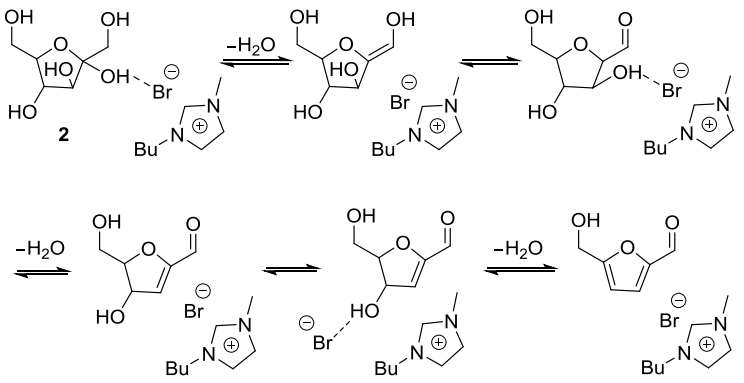

Scheme 7.2 Proposed mechanism of fructose dehydration to HMF in [BMIM]Br.[50]

Organic quaternary ammonium salts, such as tetraethylammonium chloride (TEAC),[52,53] tetraethylammonium bromide (TEAB),[54] and choline chloride (ChoCl),[52,55] can also be used as both the solvent and catalyst, effectively converting fructose to HMF in good yields ranging from 60% to 80%. For the fructose conversion in TEAC without added catalysts, the reaction temperature was a key factor influencing the HMF yield.[52] When the fructose loading was 50%, the HMF yield was only 33% at 100 ℃ after 70 min, with 58% fructose conversion. When the reaction temperature was elevated to 110 ℃ and 120 ℃, the HMF yield was increased to 72% and 81%, respectively, achieving quantitative fructose conversion in both cases. A further increase in temperature to 140 ℃ decreased the HMF yield to 75%. In the case of TEAB, a mixture of TEAB and water (10 wt%) converted fructose to HMF of high purity in up to 79% isolated yield. This conversion procedure involved a two-step heating process: initial heating at 80 ℃ for 10 – 15 min, followed by second-step heating at 100 – 120 ℃ for 15 – 90 min. While in the case of ChoCl, a blank (50 wt% fructose in ChoCl) run without added acid catalyst showed that the HMF yield can reach up to 70% at 120 ℃ for 70 min.[52] Further addition of an organic acid, such as malonic acid, oxalic acid, and citric acid, converted fructose to HMF at a much

lower temperature (80 ℃, 1 h) in 41%, 62%, 76.3% yield, respectively. It is noteworthy that a mixture of fructose and ChoCl can readily form a homogeneous solution upon heating, although the reaction temperature is much lower than the melting point of ChoCl (302 ℃, dec.); this is presumably because such organic salts are highly soluble in water, generated from the dehydration of fructose.

Hanefeld et al. recently revealed that HMF in good yields can be obtained directly from fructose in a neutral, salt-free aqueous medium.[56] With a high fructose loading of 30 wt %, up to 70% fructose conversion was observed with a HMF selectivity of 61% at 190 ℃ for 40 min. This reaction was suggested to be *autocatalytic*: formic acid, a side product formed from the dehydration of HMF is the real catalyst that catalyzes the dehydration of fructose to HMF (Scheme 7.3). The final pH of the solution after the reaction was found to be about 3, even no acid was added before the reaction. This unexpected acidity can be explained by the formation of levulinic acid (LEVA, **3**) and formic acid (FA) as the dehydration co-products of HMF. Titration experiments using LEVA and FA to catalyze the fructose-to-HMF conversion revealed three interesting observations of the two organic acids: (a) FA has a much higher catalytic effect than LEVA, presumably due to its stronger acidity (pK_a = 3.74 for FA vs. 4.59 for LEVA); (b) the highest yield and selectivity of HMF in the absence of added acids was obtained by an ideal amount of FA ranging from 2~4 mol%; and (c) such a small amount of FA can enhance HMF production and depress the formation of humins. In comparison, when the solution was maintained neutral by buffers during the reaction, as expected, extremely low yield (4%) of HMF was obtained, with a rather higher amount of LEVA and humins formed than those reactions

carried in solutions without buffers.

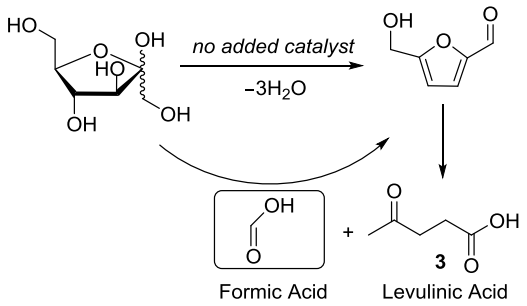

Scheme 7.3 Autocatalytic fructose conversion to HMF in a neutral, salt-free aqueous medium.[56]

Glucose conversion to-HMF. Glucose conversion to HMF is a well-recognized two-step process: glucose is first isomerized to fructose, followed by facile dehydration of fructose to HMF, with the isomerization being the rate-limiting step. Since the important discovery of the $CrCl_2$/IL catalyst system for effective conversion of glucose to HMF, a large number of other metal or non-metal catalyst systems have been developed.[43,57-62]

In an effort to replace metal catalysts with organic acids for the glucose-to-HMF conversion, boric acid was employed to convert glucose in [EMIM]Cl to HMF, achieving 41% HMF yield and 43% of selectivity,[59] but the loading of boric acid was relatively high (78 mol% to glucose). On the basis of density functional theory (DFT) calculations, a mechanism for the boric acid catalyzed glucose-to-fructose isomerization was proposed, as outlined in Scheme 7.4. In this mechanism, the interaction between the hydroxyl groups (C3 and C4 positions of glucose) and the boron center of boric acid, as depicted as **4a** in Scheme 7.4, renders the chain opening product **4b**. Through keto-enol tautomerization to **4c** and further proton transfers, fructose is generated by the elimination of boric acid. Subsequent dehydration of fructose in [EMIM]Cl leads to the formation of HMF. This method was also applied for cellulose conversion to HMF,

obtaining 32 % of HMF yield in the presence of boric acid (0.5 equiv) in [EMIM]Cl at 120 ℃ for 8 h.[59] Heterogeneous catalysts based on carbon nanotube were also developed for glucose-to-HMF conversion, affording quantitative glucose conversion and moderate HMF yield (46-57%).[48]

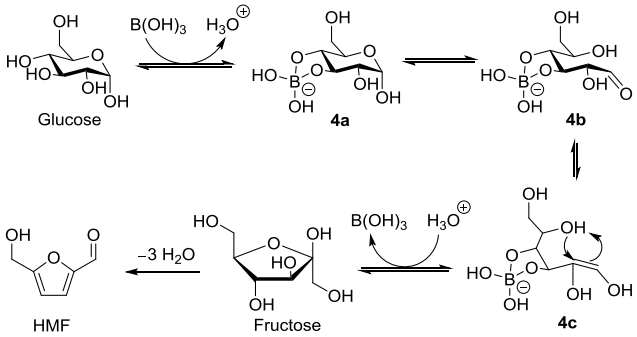

Scheme 7.4 Proposed mechanism of glucose conversion to HMF by boric acid in [EMIM]Cl.[59]

In a procedure involving a biphasic system (e.g., water/ methylisobutylketone (MIBK)) to produce HMF from C6 (poly)sugars,[63-65] ChoCl was found to be capable of enhancing the selectivity of HMF from isomerization/dehydration of glucose, which was catalyzed by metal chlorides such as $AlCl_3$, $FeCl_3$ and $CuCl_2$, achieving an optimized HMF yield of 70% and selectivity of 78%.[66] The ChoCl ratio was optimized at 50 wt%, which was a trade-off between the catalyst activity/selectivity and the extraction of HMF from the aqueous phase. This ChoCl-enhanced biphasic system also promoted cellulose conversion to HMF, affording HMF in up to 49% yield.

Glucose to "HCHO" via retro-benzoin reaction. As is well recognized, glucose is in equilibrium between its cyclic form (acetal) and acyclic form (aldehyde) in solution. Chi et al. recently realized that C–C bonds of glucose can be cleaved in the presence of an *N*-heterocyclic

carbene (NHC) catalyst under microwave or oil-bath heating conditions, which can be utilized for generating acyl anion **5e**, for Stetter reaction with chalcone **5f** to form enone **5g** (Scheme 7.5).[67] NHC **5b** was produced from the in-situ deprotonation of thiazolium **5a** by the mild base K_2CO_3 in CH_3CN under microwave heating. In a subsequent step, **5b** attacks the aldehyde group of glucose and forms the NHC-glucose complex **5c**. Through subsequent proton transfers, the cleavage of the C1–C2 bond is achieved, and thus the C_5 sugar (in its aldehyde form) is formed. Through iterative catalytic cycles that cleave C2–C3 and C3–C4 bonds, the C_3-sugar is formed and confirmed by GC-MS. Further C_2-sugar formation was not detected in this reaction. The acyl anion **5e**, a strong nucleophile, further attacks the double bond of chalcone **5f**, generating the final enone **5g** through Stetter reaction. The whole process using microwave heating was proved to be highly efficient. The optimized yield of **5g** (80%) was achieved from the glucose and chalcone reaction (1:1 molar ratio) in the presence of K_2CO_3 (20 mol%) and **5a** (20 mol%) in CH_3CN at 130 ℃ for 30 min under microwave irradiation. Using only 0.2 equiv of glucose, 53% yield of **5g** was still achieved, because 1 equiv of glucose can generate multiple equiv of the one-carbon acyl anion intermediate **5e**. Other sugars (C_6 and C_5 monosaccharides as well as di- and polysaccharides) have also been examined, and the results showed that C_5 sugars led to the quantitative conversion of the chalcone substrate, achieving 70% – 83% yield of **5g** under similar conditions, even with a shorter reaction time (10 min). However, the di- and polysaccharides (i.e., cellobiose, sucrose and cellulose) produced only trace amount of **5g**.

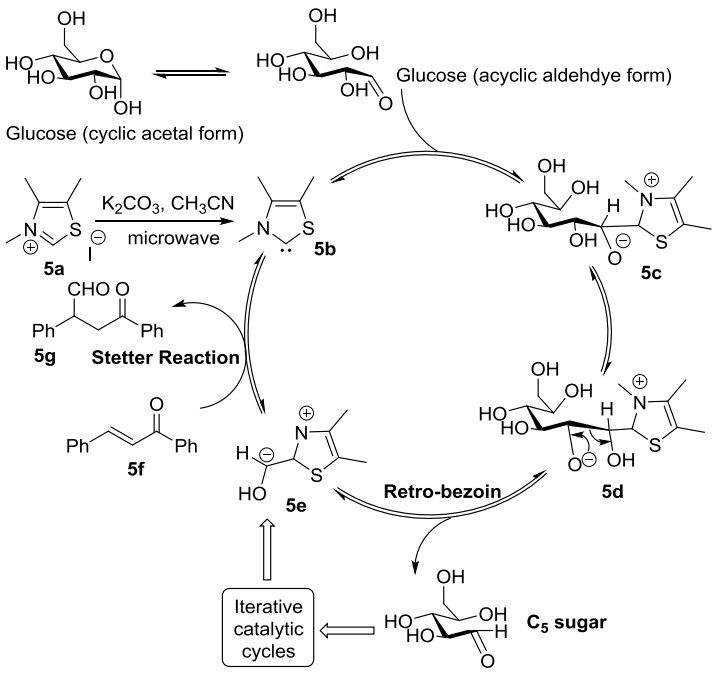

Scheme 7.5 NHC-catalyzed acyl anion formation from glucose for Stetter reaction with chalcone.[67]

Conversion of other sugars to HMF. Besides glucose, mannose and galactose (Figure 7.2), two most abundant C_6 sugars in hemicellulose after glucose, have been systematically studied for their conversion to HMF.[68-71] Mannose, a C2 epimer of glucose, performed similarly to glucose in the aspect of HMF yield, which reached up to 69% in the presence of $CrCl_2$ in either DMA-LiBr or [EMIM]Cl system.[70] The mechanism was suggested to be similar to glucose *via* fructose formation through 1,2-hydride shift and subsequent fructose dehydration to HMF. Although there are few studies on application of organocatalysis on mannose dehydration to HMF, it is anticipated that similar high yields of HMF could be obtained. While for galactose conversion to HMF, only low yields (< 40%) were obtained under similar conditions to mannose.[70] Using κ-carrageenan (sulfated polysaccharides composed of repeating galactose and 3,6-anhydrogalactose) as the source of galactose, up to 43% of HMF yield was generated, which

was catalyzed by $Mg(HSO_4)_2$ in aqueous solution at 105 ℃ for 1 h.[71] The difficulty of galactose conversion to HMF is presumably due to the stereochemical difference between galactose and mannose. The isomerization of galactose results in tagatose, a C4 epimer of fructose. Unlike the high-efficient fructose dehydration to HMF, tagatose conversion to HMF typically rendered low yields, thus preventing high HMF yield from galactose.[70] In addition, as another abundantly available disaccharide, sucrose was efficiently converted to HMF in the presence of [EMIM]Br and an amino acid (e.g. tyrosine), achieving an HMF yield of 76.0% under mild conditions (160 ℃, 4 h).[72]

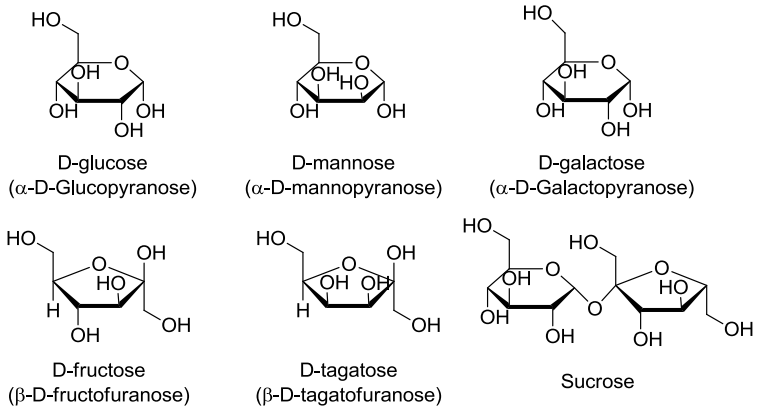

Figure 7.2 Mono/di-saccharide precursors of HMF.

7.3.2 Polysaccharide hydrolysis to reducing sugars

Cellulose, poly(*β*-1,4-d-glucose), is the most abundance organic substance on earth. However, the usage of cellulose is limited by its essential insolubility in common solvents due to the presence of extensive intra- and intermolecular hydrogen bonds. Solvation of cellulose is the key issue for facilitating subsequent conversion, to mono/oligosaccharides through hydrolysis, or directly to HMF, levulinic acid and/or formic acid.

Cellulose hydrolysis carried under catalysis of mineral acids (HCl, H_2SO_4) and solid

acids (metal oxides, polymer based acids, sulfonated carbonaceous based acid, heteropoly acids, H-form zeolites, magnetic solid acids, and supported metal catalysts) was recently reviewed by Huang and Fu.[73] The good solubility of cellulose in ILs suggests the potential of hydrolyzing cellulose in a homogenous solution into water-soluble reducing sugars (RDS with the glucosidic unit = 1–16). More importantly, addition of acid catalysts may not be necessary for such cellulose hydrolysis, since the IL-water mixture exhibits intrinsic acidity [H^+] (Figure 7.3) to effect the catalysis.[44] The equilibrium solutions of commercially available ILs [RMIM]Cl (≥95%) in H_2O (1:1 wt ratio) gave pH values of 6.51–6.93 at RT. However, upon removal of impurities (mostly water and ~0.2 – 0.5 mol % of the basic methyl imidazole, the starting material of the IL), the pH value of the 1:1 mixture of the purified IL and H_2O dropped considerably to only 5.12 (R = Et) and 4.37 (R = ^{n}Bu), which is attributed to the significantly increased K_w of the water by ILs in the IL-water mixture. In a typical hydrolysis procedure, 5.5 equiv of [EMIM]Cl and 1 equiv of H_2O to cellulose was premixed and heated at desired temperature. The total reducing sugar (TRS) yield reached up to 95% at 120 ℃ after 24 h, including 19% yield of glucose and 18 % of cellubiose (Figure 7.4).

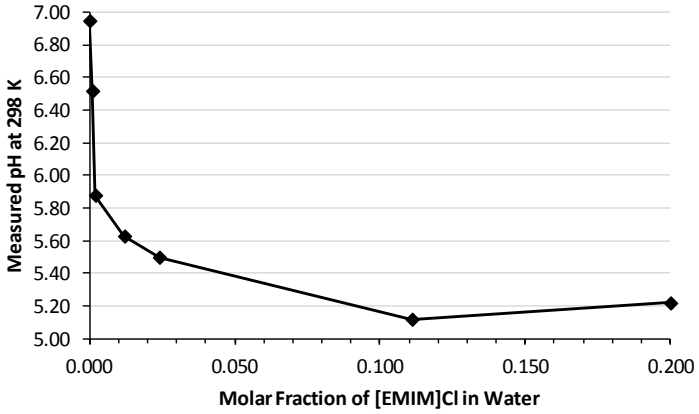

Figure 7.3 Plot of measured pH values of the [EMIM]Cl–H_2O mixture vs the molar fraction of [EMIM]Cl in the mixture at 298 K.[44]

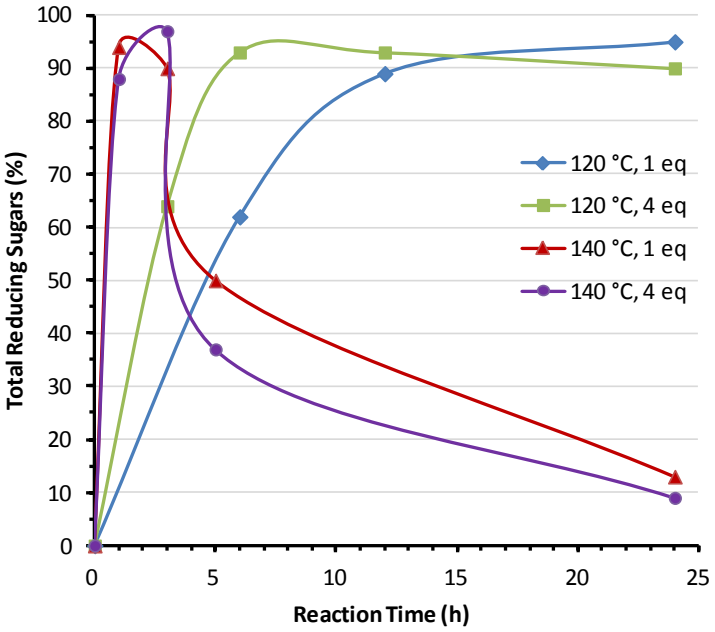

Figure 7.4 Plots of water-soluble TRS yield vs reaction time at different temperatures (120 or 140 ℃) and added water equivalents (1 or 4 equiv) for cellulose hydrolysis by the [EMIM]Cl–H_2O mixture.[44]

7.4 Upgrading of Furaldehydes

Upgrading of furaldehydes (e.g., FF, MF, and HMF) can be readily achieved through molecule modifications, such as acetylation, etherification, esterification, hydrogenation/ hydrogenolysis, and oxidation or reduction, which do not involve new C–C bond formation (Figure 7.1). These approaches have already been covered in many review articles.[18-36] The current review will concentrate on the other type of upgrading that involves new C–C bond formation for higher molecular weight and higher energy-density molecules through organocatalysis. These upgrading routes utilize benzoin condensation, aldol condensation, and hydroxylation/alkylation process, etc., to produce the upgraded intermediates or products with more carbon numbers (e.g., C_{12} intermediate **6** from the C_6 HMF, Scheme 7.6). As an integrated process of further furaldehyde upgrading, hydrodeoxygenation (HDO) processes of these

intermediates to generate kerosene/jet fuels (C_8 to C_{18}) or diesel fuels (up to C_{22}) are also highlighted.

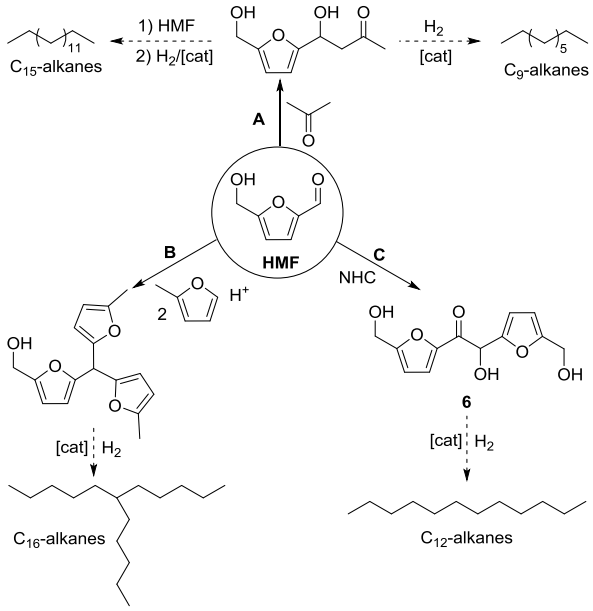

Scheme 7.6 Three different routes to upgrade HMF into kerosene/jet hydrocarbon fuels.[74]

7.4.1 Benzoin Condensation

Benzoin condensation is a direct coupling (either homo- or cross-coupling) reaction between two aldehydes catalyzed by a nucleophile such as the cyanide anion (CN^-) or the NHC.[75] In 1958, Breslow proposed a mechanism for the benzoin condensation catalyzed by the NHC (Scheme 7.7).[76-78] In this mechanism, thiazolium salt **7a** is deprotonated by a strong base (e.g. Et_3N, 1,8-diazabicyclo[5.4.0]undec-7-ene or DBU) to form thiazolin-2-ylidene **7b**, which is a nucleophile that attacks an aldehyde (e.g. benzaldehyde), generating the carbene-aldehyde adduct **7c**. Subsequent protonation/deprotonation or proton transfer affords the Breslow intermediate, **7d**. This amino enol intermediate functions as an acyl anion equivalent and attacks a second aldehyde, forming adduct **7e**.[77] After the proton transfer and the elimination of the

benzoin product, the carbene catalyst **7b** is regenerated. This process is also termed aldehyde umpolung (polarity inversion) that converts the electrophilic carbonyl carbon to a nucleophilic center as an acyl anion equivalent. As for biomass-derived furaldehydes, benzoin condensation of furfural is catalyzed by NHCs in a similar fashion, affording furoin in high to quantitative yield.[79-83]

Structural characterizations of some analogues of the Breslow (amino enol) intermediate by X-ray diffraction analysis were not accomplished until recently by Rovis using an NHC-aza analogue **8a**[84] and Teles using NHC-2,4-bis(trifluoromethyl)benzaldehyde **8b** (Scheme 7.8).[85] In the latter case, evidence obtained from ^{1}H and ^{13}C NMR spectra showed direct formation of Breslow intermediate **8c** upon mixing the NHC and the aldehyde in a 1:1 molar ratio, but the exact crystal structure was not obtained. Similarly, the direct formation of Breslow intermediates between NHCs and furaldehydes, furfural[85] and HMF,[74] were also observed by NMR.

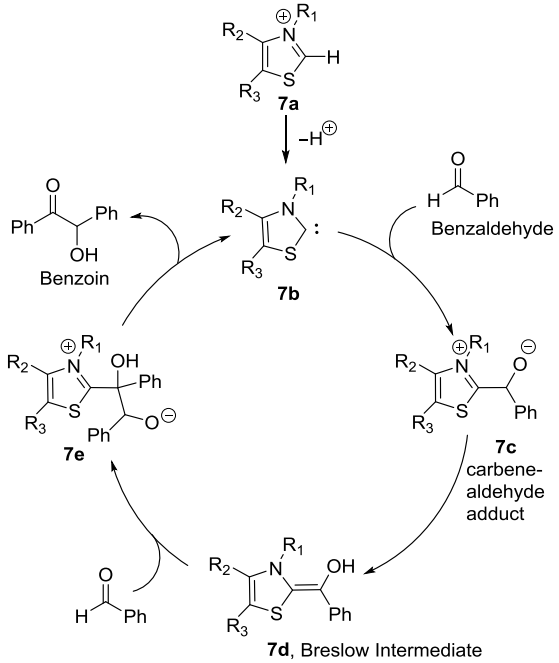

Scheme 7.7 Catalytic cycle of the benzoin condensation through the Breslow intemediate.[76,77]

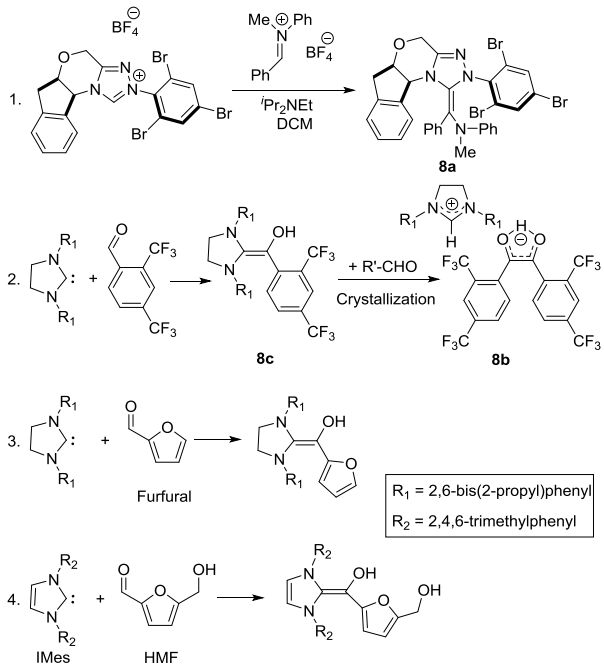

Scheme 7.8 Breslow intermediate characterizations.[74,84,85]

Unlike FF, HMF carries the acidic $–CH_2OH$ group at the 5-position, which may have eluded attempts to apply benzoin condensation for self-coupling of HMF until recently.[86] It was disclosed earlier that 1-ethyl-3-methylimidazolium acetate, [EMIM]OAc, rapidly degrades HMF (>99% degradation at 100 ℃ after 8 h),[87] and that no HMF was obtained from the glucose (or cellulose)-to-HMF conversion when carried out in [EMIM]OAc, regardless of the catalyst used.[88] In light of these observations, it was hypothesized that the rapid degradation of HMF in [EMIM]OAc is likely rendered by NHC catalysis, because it is known that a low concentration of carbene exists in the IL with the basic acetate anion,[89] as demonstrated by its carbene-type reaction with elemental sulfur or selenium[90] and as a catalyst for benzoin condensation of benzaldehyde.[91] Indeed, this "detrimental" degradation can be utilized for highly efficient upgrading of HMF into a high-value biorefining product, 5,5'-di (hydroxymethyl)furoin

(DHMF), as a potential C_{12} kerosene/jet fuel intermediate, through NHC-catalyzed HMF self-condensation enabled by this organocatalytic [EMIM]OAc.[86]

The catalytic cycle for the HMF umpolung into DHMF enabled by the organocatalytic [EMIM]OAc is proposed in Scheme 7.9.[86] The catalyst in this carbene catalysis is 1-ethyl-3-methylimidazolin-2-ylidene carbene **9a**, present in the [EMIM]OAc equilibrium that favors the ion pair form.[89-91] The early steps of the cycle deviate somewhat form those put forth for the NHC-catalyzed umpolung of aldehydes[79-83] and α,β-unsaturated esters,[92-94] due to the important role of HOAc, which co-exists with carbene **9a** in the [EMIM]OAc equilibrium. Subsequently, nucleophilic addition of **9a** to the aldehyde group of HMF generates a zwitterionic tetrahedral intermediate, which is protonated to afford a 2-(5-hydroxymethyl-2-α-hydroxyfuranyl)imidazolium acetate salt, the resting intermediate **9b**.[95-97] Under elevated temperature (e.g. 80 ℃), intermediate **9b** is deprotonated by the acetate anion to form a nucleophilic enaminol (**9c**). Like the Breslow intermediate involved in the benzoin reaction, this enaminol is the acyl anion equivalent (**9d**), thus attacking the aldehyde group of a second HMF molecule to form another tetrahedral intermediate (**9e**).[77] Collapse of this tetrahedral intermediate, via proton transfer and elimination of **9a**, produces DHMF and regenerates the NHC catalyst **9a**, thus closing the catalytic cycle.

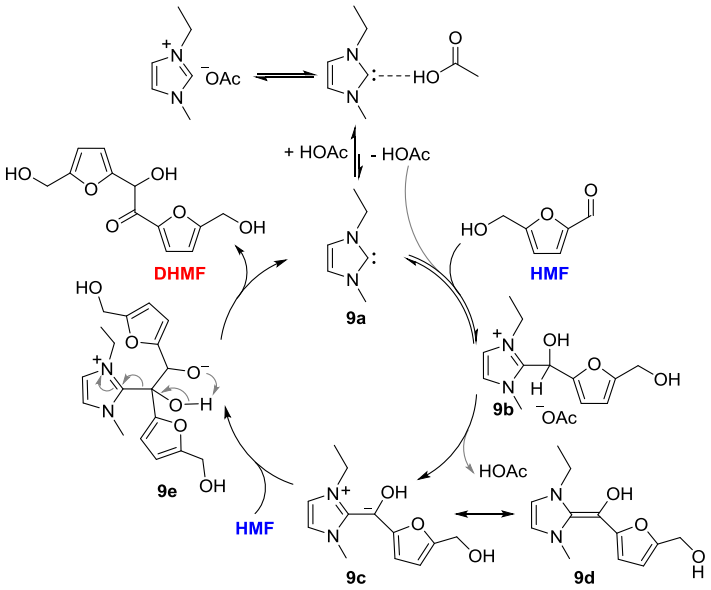

Scheme 7.9 Proposed catalytic cycle for umpolung self-condensation of HMF to DHMF by an organocatalytic IL, [EMIM]OAc.[86]

Subsequent use of a discrete NHC (1 mol%), namely the Enders triazolylidene carbene TPT (1,3,4-triphenyl-4,5-dihydro-1H-1,2,4-trizaol-5-ylidene),[98,99] led to high-yield (98%) and solvent-free synthesis of DHMF from HMF.[74] As a C_{12} diesel or kerosene/jet fuel intermediate, DHMF can be readily modified through reactions such as etherification (**10a**), esterification (**10b**), and hydrogenation (**10a**), to provide oxygenated biodiesel fuels, or by HDO with metal-acid tandem catalysis to provide premium hydrocarbon fuels (Scheme 7.10). Thus, the HDO of DHMF in water by the bifunctional acidic solid catalyst ($TaOPO_4$) and Pt/C at 300 ℃ and 500 psi H_2 for 3 h produced premium alkane fuels with 96% selectivity to linear $C_{10–12}$ alkanes, consisting of 27.0% *n*-decane, 22.9% *n*-undecane, and 45.6% *n*-dodecane (Scheme 7.10).[74]

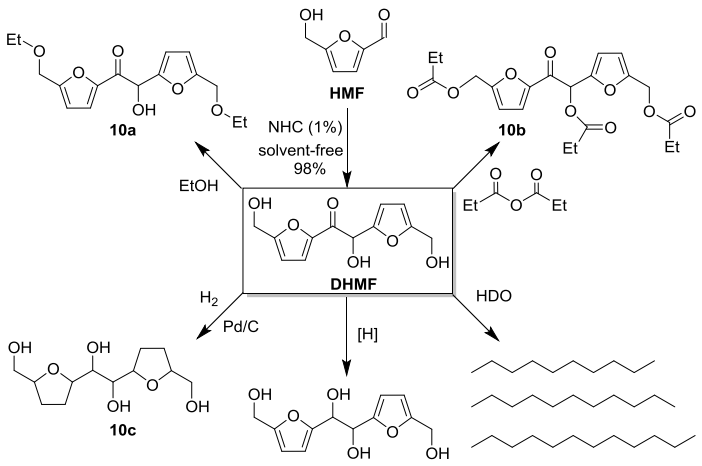

Scheme 7.10 Upgrading of HMF to chemicals and oxygenated diesel or alkane jet/kerosene fuels.[74]

When compared to other methods of upgrading biomass derived furan compounds into biofuels, the DHMF route possesses four potential advantages:[74] (1) DHMF is obtained from self-coupling of HMF, without losing any atoms (i.e., 100% atom economy) and the need for cross-condensation with other petrochemicals; (2) HMF self-coupling is catalyzed by organic catalysts, which can be carried out under solvent-free conditions at 60 ℃ in 1 h, affording DHMF in near quantitative isolated yield; (3) owing to its solubility in water, the HDO of DHMF can be carried out directly in water, allowing for spontaneous separation of hydrocarbons from water phase; and (4) DHMF hydrodeoxygenation achieves high conversion and near quantitative selectivity towards linear C_{10}–C_{12} alkanes with a narrow distribution of alkanes.

7.4.2 Aldol Condensation

Another effective method of extending the carbon chain length is aldol condensation catalyzed by a base or an acid, which requires a substrate to carry both an enolizable α-H atom

and a carbonyl functional group. Since furaldehydes, including FF, MF, and HMF, lack enolizable α-H atoms, they cannot undergo self-aldol condensation, unless the furan ring becomes saturated through selective hydrogenation.[100] Alternatively, furaldehydes can be coupled with other organic compounds carrying enolizable α-H, such as acetone, hydroxyacetone (HA), dihydroxyacetone (DHA), homoethyllevulinate, and decane-2-one, for C–C bond formation through *cross-aldol* condensation (Scheme 7.11).[100-104] Through further hydrogenation and HDO, high-quality fuels with longer-chain alkanes can be obtained.[100,102,104]

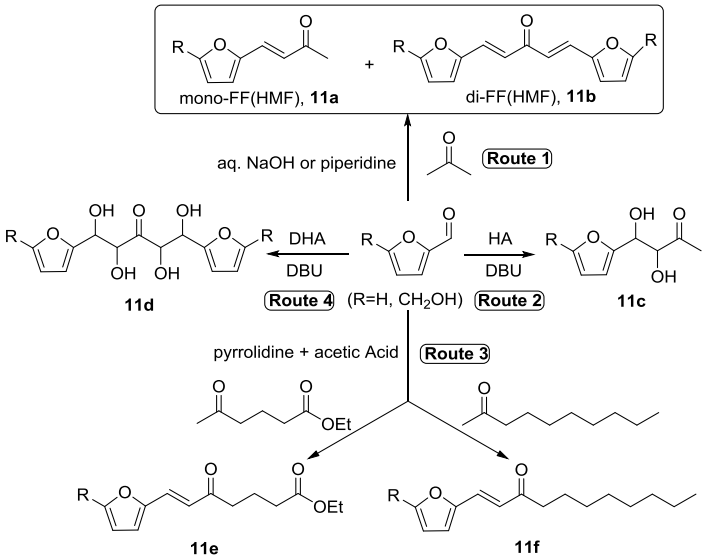

Scheme 7.11 Cross-aldol condensation of furaldehydes with enolizable ketones.[100-104]

Specifically on the catalysts for cross-aldol condensation, it is well recognized that alkaline conditions can promote this reaction. Dumesic[100] used Mg-Zr-oxide heterogeneous catalysts for aldol condensation in aqueous phase, which promotes the carbon chain extension with acetone, but in a non-selective manner, as a result of self- and cross-aldol condensation. In addition, this method was shown to be unsuccessful with ketones other than acetone, including HA, DHA and glyceraldehde. Complementary work by Huber[101] revealed that using NaOH as a

catalyst for the cross-coupling of FF and acetone in a 2:1 molar ratio, 97 % yield of mono-FF and di-FF mixture was obtained (Scheme 7.11, Route 1). However, FF + HA or FF + DHA coupling cannot be achieved due to the formation of alkoxide anion. On the other hand, using DBU as the neutral organic base to catalyze the reaction afforded a high yield of cross-aldol condensation products from FF + HA (**11c**, 88 %, Route 2) and FF + DHA (**11d**, 79 %, Route 4) coupling reactions. The mechanism is illustrated in Scheme 7.12. In this scheme, DBU first deprotonates the methylene hydrogen of HA (which is more acidic than the methyl proton), producing enolate **12**, which is stabilized by the intra-molecule hydrogen bonding. The hydrogen bonding between the protonated DBU and aldehyde activates FF and facilitates the nucleophilic attack of **12** to aldehyde. Owing to the steric hindrance and inductive effects, pathway a shown in Scheme 7.12 is more favorable than pathway b, thus forming the linear coupling product **11c**.

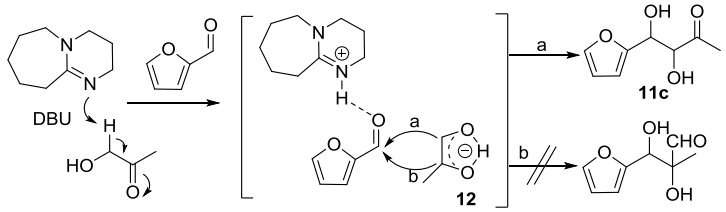

Scheme 7.12 Proposed mechanism for cross-aldol condensation of FF with HA.[101]

Other types of effective organocatalysts have been revealed for cross-aldol condensation between furaldehydes and enolizable ketones.[102-104,] When 5 mol% of piperidine was used for HMF cross coupling with acetone in 1:1 molar ratio, a mixture of mono-HMF adduct **11a** (23 %) and di-HMF adduct **11b** (68 %) was obtained at room temperature after 20 h (Scheme 7.11, Route 1). The yield of di-HMF adduct was about 73 % when 0.5 equiv. of acetone were used.[103] Furthermore, the adduct of pyrrolidine and acetic acid can catalyze cross-aldol condensation in

high efficiency and selectivity (Scheme 7.11, Route 3). For example, 93% isolated yield of the cross-aldol condensation product **11e** was obtained between HMF with homoethyllevulinate at room temperature after 12 h, while for coupling with decane-2-one, 70% isolated yield of the product **11f** was obtained.[104]

There are other possible reactions using cross-aldol condensation for carbon chain extension. For example, the coupling of furaldehydes (FF, MF, HMF) and 2,5-hexanedione (HD) can form possible products of C_{11}, C_{12}, C_{16} and C_{18} intermediates (**13b** and **13c**, Scheme 7.13), which could be catalyzed by organocatalysts. A possible side reaction is to form 3-methyl-2-cyclopentenone (**13a**), a result of self-aldol condensation of HD. Noteworthy is that HD is also a biomass-derived chemical, because it can be prepared from the chain-opening of 2,5-dimethylfuran, which is originally derived from HMF.[105]

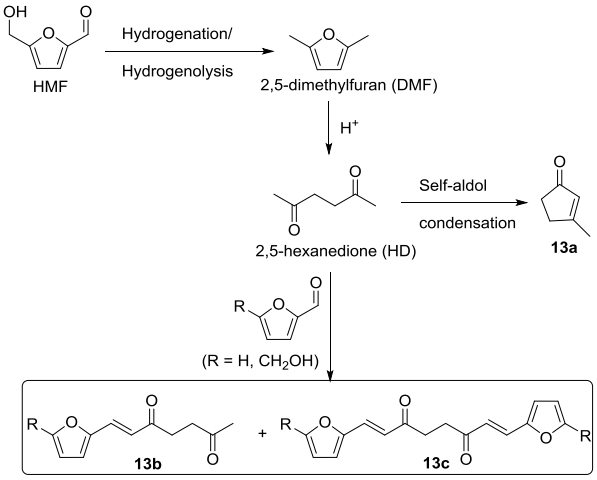

Scheme 7.13 Possible aldol condensation of 2,5-hexanedione (HD) for carbon chain extension.[105]

For subsequent upgrading of cross-aldol condensation products to alkanes, several HDO methods have been developed. Dumesic et al. developed a method of a four-phase reactor system,

consisting of (1) an aqueous inlet stream, containing the water-soluble organic reactant; (2) a hexadecane (C_{16} alkane) inlet stream; (3) an H_2 inlet gas stream; and (4) a solid catalyst (Pt/SiO_2-Al_2O_3).[100] The HDO was carried out at 250–265 ℃, 52–50 bars, and H_2 gas hourly space velocities of 1000 to 3000 h^{-1}. Before the HDO, cross-aldol products of HMF and acetone were hydrogenated to make them water-soluble, also to avoid choking problems in the HDO process. The results showed that high to quantitative recovery of carbon (>70%) was achieved in the organic phase (C_{16} alkane phase), and only a small amount of carbon remained in the gas phase (<10%) and the aqueous phase (<3%). However, due to the non-selective and non-quantitative conversion of cross-aldol reaction catalyzed by the Mg-Zr-oxide catalyst, alkanes with a wide distribution of carbon numbers (ranging from C_1 to C_{15}) were obtained. Complimentarily, Gordon et al. reported a selective way of producing alkanes from cross-aldol condensation products.[102] Starting from mono-HMF product **11a** from the cross-aldol condensation of HMF and acetone (1:1 molar ratio), they established a selective "hydrogenation-furan ring opening-HDO" route to generate alkanes in acetic acid/H_2O solution. The first step involves the selective hydrogenation of the side-chain C=C double bond by Pd/C under H_2, followed by the ring-opening of furan at 100 ℃ for 3 h. After the ring-opening products were formed/isolated, subsequent HDO (Pd/C, $La(OTf)_3$, 2.07 MPa H_2, 200 ℃, 16 h) produced high yield of C_9 alkane (87 % isolated yield). Following the similar procedure, di-HMF **11b** from cross-aldol condensation of 2:1 HMF and acetone, C_{15} alkane was isolated in 65% yield. Applying the same HDO procedures to cross-aldol condensation product **11e**, C_{12} alkane was obtained in 76% isolated yield.

7.4.3 Hydroxyalkylation/alkylation

Corma et al. reported a differnt approach of upgrading biomass-derived furaldehydes by hydroxyalkylation/alkylation with 2-methylfuran (2-MF) under acidic conditions (Scheme 7.14).[106,107] 2-MF is obtained from FF in the production of furfuryl alchol[108] and its selectivity can be increased up to 93 % when the reaction temperature is raised from 135 ℃ (for furfuryl alcohol production) to 250 ℃.[108,109] Starting with butanal reaction with 2-MF, organic acid *para*-toluenesulfonic acid (*p*-TsOH) was shown to be more efficient than the mineral acid H_2SO_4 and solid acid Amberlyst-15 resin. With a 2.5 wt% loading of *p*-TsOH and a 2:1 molar ratio of 2-MF and butanal, 85 % conversion with 91 % selectivity for 2,2'-butylidenebis(5-methylfuran), **14a** (C_{14} intermediate), was obtained at 50 ℃ after 6 h. By increasing the 2-MF to butanal ratio to 3.5:1, 93 % conversion and 95 % selectivity was achieved. The resulting product **14a** can be easily separated from the aqueous phase and purified by distillation. Subsequent HDO was carried out through a tubular reactor at 350 ℃, 50 bar H_2 flow (450 mL/min), and a flow rate of 0.15 mL/min, catalyzed by Pt/C and Pt/Al_2O_3 catalysts. The obtained liquid organic phase consists of 94.6% of alkanes (linear, branched or cyclic, 16.6 % C_9, 1.6% C_{12} and 76.4% C_{14}), 0.6% of oxygenated, and 4.7% unidentified species.

Furaldehydes MF and HMF were also used for the hydroxyalkylation/alkylation with 2-MF (Scheme 7.14). Under similar conditions to those for butanal (50 ℃, 6 h) but a higher 2-MF to MF ratio (5:1), 93 % yield of the final product **14c** (C_{16} intermediate) was obtained. With HMF, 86% yield of **14b** was obtained. Ketones can also react with 2-MF, but they are less reactive.[107] Starting from 2-MF and 2-pentanone in the presence of *p*-TsOH, only 63 %

conversion and 76 % selectivity to **14e** were obtained at 60 ℃ for 22.5 h, with many side products being produced as well. For example, formation of **14d** is due to the self-trimerization of 2-MF under acidic conditions. For the reaction of 2-MF with *α,β*-unsaturated ketones (e.g., 4-methylpent-4-en-2-one), this reaction generated mainly the mono-coupling product **14f** across the C=C double bond rather than the carbonyl bond.

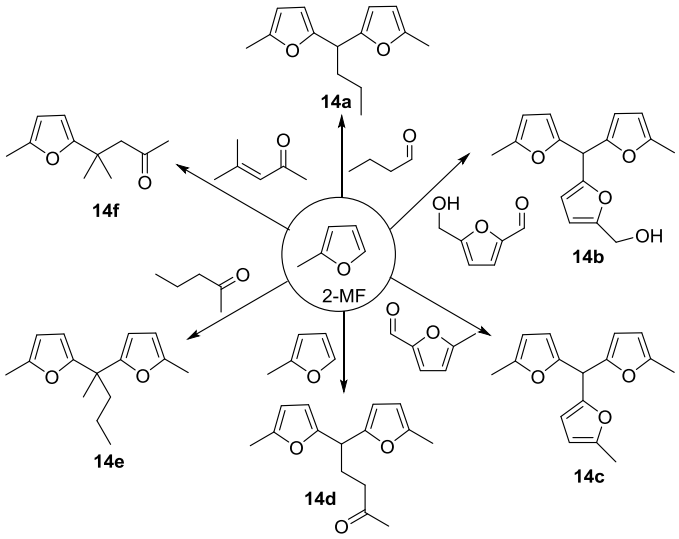

Scheme 7.14 Reaction of 2-MF with aldehydes, ketones, and *α,β*-unsaturated ketones through hydroalkylation/alkylation.[106,107]

7.4.4 Other Strategies of C-C bond formation

Utilizing the Morita-Baylis-Hillman reaction, Huber et al. showed an atom-economical C–C bond formation by the reaction between a furaldehyde and acrolein (Scheme 7.15).[101] This process involves the reaction between an activated alkene (**15a**, Baylis-Hillman donor, BHD) and an activated carbonyl compound such as FF and HMF, in the presence of tertiary amine-based catalysts such as NMe_3, 1,4-diazabicyclo[2.2.2]octane (DABCO). Methyl acrylate (R = OMe) was selected as the model BHD compound, and FF and HMF as the Baylis-Hillman acceptor compounds. Catalyzed by DABCO, the yield of product **15b** was 82% and 63% from

FF and HMF, respectively, while better yields were achieved by using NMe_3 as the base catalyst, with 89% and 76% yield, respectively. As the authors pointed out, product **15b** can be further upgraded into C_{13} and C_{18} compounds by subsequent reaction with furan in the presence of sulfuric acid. Another potential usage of **15b** lies on its potential of polymerization into functional materials, considering the presence of the conjugated C=C and C=O double bonds.

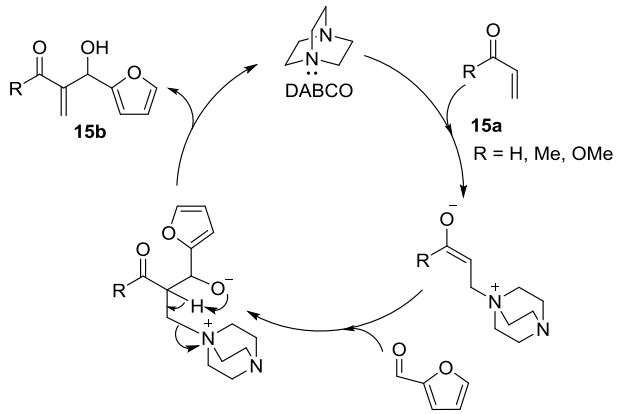

Scheme 7.15 Catalytic cycle proposed for DABCO-catalyzed coupling between an activated alkene and a furaldehyde via the Morita-Baylis-Hillman reaction.[101]

7.5 Organocatalytic Polymerization of Biomass Feedstocks

Sustainable polymers derived from naturally occurring or biomass-derived renewable feedstocks are a huge topic of current concern and have been reviewed extensively.[11-15, 110-113] Accordingly, this section is focused on only three representative families of the biomass-derived monomers: isosorbide, lactide, and methylene butyrolactones, and their polymerization to respective renewable polymeric materials via organocatalysis.

7.5.1 Isosorbide platform

Isosorbide is derived from dehydration of sorbitol, the hydrogenation product of glucose. Isosorbide consists of two *cis*-fused tetrahydrofuran rings with a 120° angle between the

rings.[114,115] The hydroxyl groups are situated at carbons 2 and 5 and positioned on either inside (*endo*) or outside (*exdo*) the molecule. As a diol from products of biomass feedstocks, its potential replacement of petroleum-based diols for the synthesis of polyesters and polyethers through condensation polymerization has been extensively studied and reviewed.[115,116] These types of polymerization include condensation with removal of small molecules (H_2O, HCl), which can be simply catalyzed under alkaline aqueous solution and is not reviewed in this section. Another major application of diols is through their condensation polymerization with diisocyanates, such as 4,4′-diphenylmethanediisocyanate (MDI) and toluene diisocyanate (TDI), into polyurethanes. Although termed "condensation", this type of polymerization does not include removal of small molecules. More importantly (and pertinent to this article), the reaction is usually catalyzed by organic catalysts such as tertiary amines (e.g., DABCO) or NHCs, e.g., 1,3-di-*tert*-butyl-imidazol-2-ylidene (I*t*Bu)) as well as organometallic compounds (e.g., dibutyltin dilaurate (**16**), Scheme 7.16.

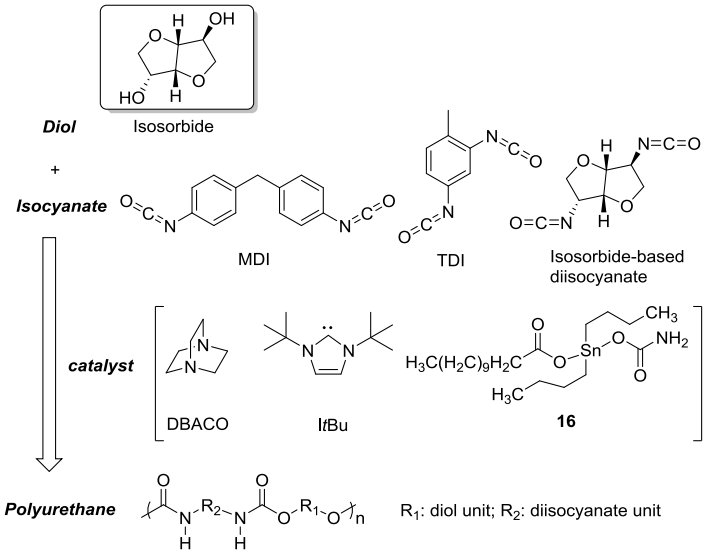

Scheme 7.16 Production of polyurethanes from condensation polymerization of isoborbide and diisocyanates catalyzed by organo- and organometallic catalysts.

The polymerization of isosorbide and the three types of diisocyanates listed in Scheme 7.16 catalyzed by tri-*n*-butylamine in DMSO was reported to produce linear polyurethanes with molecular weight in the range of 10,000 to 15,000 g/mol.[117] A kinetic study of the polymerization of isosorbide with monoisocyanate *p*-tolyl isocyanate and MDI revealed the equi-reactivity of the hydroxyl groups in the isosorbide and isocyanate groups in the MDI under experimental conditions (in THF or in bulk, 50 ℃, catalyzed by **16**).[118] The resulting polymer had M_n = 13,000 – 15,000 g/mol, with molecular weight distribution (MWD) ranging from 2.4 to 2.7. The glass-transition temperature (T_g) is relatively high, ranging from 154 – 187 ℃.

Considering the fact that the diisocyanates such as MDI and TDI are still petroleum-based, a method of preparing biorenewable isocyanates based on isosorbide was recently reported by Kessler et al.[119] The synthesis of diisocyanate **17c** is outlined in Scheme 7.17. Isosorbide was first reacted with succinic anhydride to form diacid **17a** in a quantitative yield. Subsequent conversion to diacid chloride (step b) followed by a two-step Curtius rearrangement afforded 60 % overall yield of diisocyanate **17c** (steps c and d). Polymerization of isosorbide-derived diisocyanate **17c** with isosorbide, catalyzed by catalyst **16**, produced polyurethane in 90 % yield with a molecular weight similar to that of the MDI-isosorbide polyurethane (M_n = 14,300 g/ mol, MWD = 1.50).

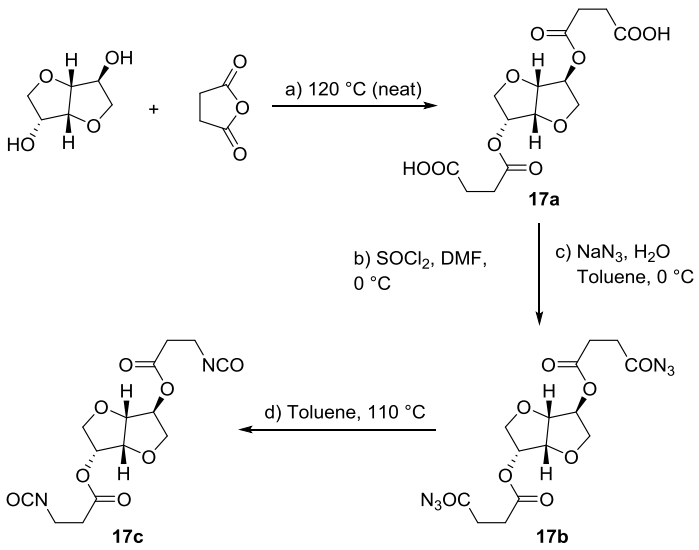

Scheme 7.17 Synthesis of an isosorbide-based diisocyanate.[119]

Taton et al. employed NHCs for the synthesis of polyurethanes.[120] Specifically, they showed that condensation polymerization of primary diols and aliphatic diisocyanates can be catalyzed with I*t*Bu (1 mol%). In the proposed catalytic cycle outlined in Scheme 7.18, the alcohol is activated by the NHC through deprotonation to generate imidazolium alkoxide **18a**. Subsequent nucleophilic attack of the activated alcohol onto the isocyante leads to the formation of a urethane bond in **18b**, followed by release of the NHC catalyst and the polymer. However, the molecular weight obtained by this method was rather low, ranging from 2000 – 3000 g/mol. Nonetheless, it would be interesting to see whether this NHC-catalyzed condensation method could be applied to the polyurethane synthesis from isosorbide and more reactive aromatic diisocyanates (i.e., MDI or TDI).

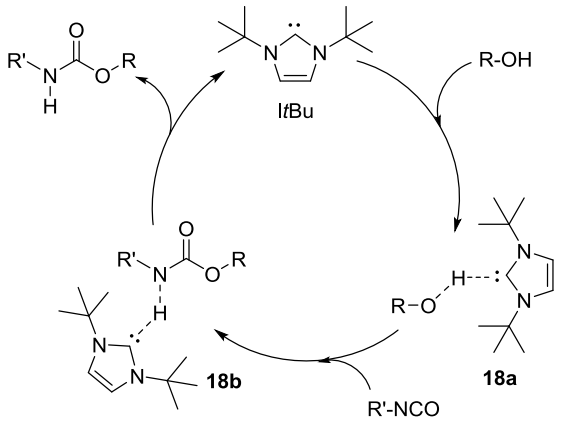

Scheme 7.18 Proposed mechanism of condensation polymerization catalyzed by I*t*Bu for polyurethane formation.[120]

7.5.2 Lactide platform

Lactide is obtained from dimerization of lactic acid, which is one of the most extensively studied carboxylic acids from natural resources. Ring opening polymerization (ROP) of lactide into poly(lactic acid) (PLA) catalyzed by organic catalysts offers not only the high polymerization rates, but also the excellent polymerization control and versatile design of functional materials.[15, 121] This type of polymerization can be generally described as a nucleophile-catalyzed, alcohol initiated reaction, generating the linear PLA with one chain end of an alkoxide ester and the other end of a hydroxyl group (Scheme 7.19). On the other hand, the polymerization of lactide mediated by NHCs without addition of the alcohol initiator leads to formation of the cyclic PLA, through zwitterionic ring-opening polymerization. Besides this general nucleophilic monomer activation mechanism, other mechanisms such as alcohol (initiator) activation and monomer-initiator dual (bifunctional) activation can also be operative.[14]

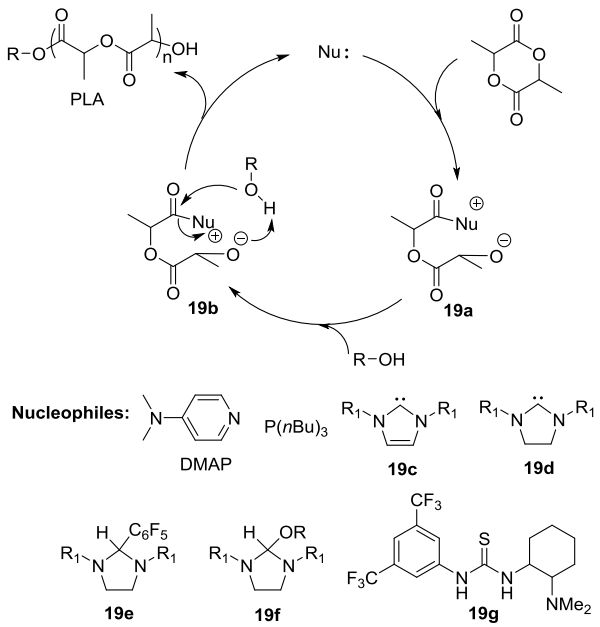

Scheme 7.19 A generalized mechanism of the nucleophile catalysed, alcohol initiated ROP of lactide.[122-126]

The first living ROP of lactide was developed in 2001 using 4-dimethylaminopyridine (DMAP).[122] The PLA produced using DMAP as the catalysts and ethanol or benzyl alcohol as the initiator has a low polydispersity index (PDI) of <1.2 and a degree of polymerization up to 120. The polymerization was proposed to proceed through an activated-monomer mechanism (Scheme 7.19). In this mechanism, the initiation step involves the reaction between a nucleophile (e.g., an alcohol) and a lactide-DMAP complex (**19a**). The α-chain end of the PLA bears an ester functionality derived from the alcohol, and the polymerization proceeds through **19b** in that the terminal ω-hydroxyl group attacks another molecule of lactide to facilitate the chain growth. Phosphines can be also used as a Lewis base for lactide polymerization;[123] being weaker nucleophiles than DMAP, phosphines showed a much lower reactivity towards lactide polymerization. Higher temperature (>130 ℃) and lower monomer/initiator ratio (< 60) were

necessary to achieve high lactide conversion.

Waymouth and Hedrick have further explored a series of NHCs (which are stronger nucleophiles than DMAP and phosphines) in lactic polymerization, including in-situ generated NHCs (**19c, 19d**), NHC-pentafluorobenzene adduct **19e**, and NHC-alcohol adduct **19f**.[124-126] For the in-situ generated carbenes, thiazole carbene **7b** and imidazole-2-ylidene carbene **19c** were compared for their performance in lactide polymerization.[124] The results showed that the imidazole-2-ylidene carbene is significantly more active for the ROP of lactide than the thiazole carbene. Using benzyl alcohol as the initiator and a catalyst/initiator ratio of 1.5, PLA materials with M_n > 25,000 g/mol and a narrow PDI of <1.2 can be readily produced in high yields (>90%) in THF within 15 min at room temperature. It is noteworthy that imidazolin-2-ylidene carbene **19d** (4,5-saturated imidazole-2-ylidene carbene) is even more active, generating PLA in 99% yield but with somewhat broader MWD (1.2 – 1.5) under similar polymerization conditions.

To render NHCs stable as solids at room temperature, self-releasing NHC complexes were designed as NHC adducts with pentafluorobenzene (**19e**)[125] and primary/secondary alcohol (**19f**).[126] The key difference between these two types of the adducts is that the alcohol-NHC complex can readily release NHCs and alcohol in solution at room temperature. Moreover, the alcohol is released as the initiator for the polymerization of lactide, rendering the reaction with a 1:1 molar ratio of the NHC catalyst and the alcohol initiator. Hence, the ROP of lactide by the NHC-alcohol adduct achieved a quantitative monomer conversion within 10 min at room temperature in THF, without further addition of alcohol as an initiator, leading to the PLA with a controlled molecular weight by variation of the monomer/catalyst ratio and a narrow MWD. In

addition, through the synthesis of diol or triol-NHC complexes, branched PLA can be obtained.

The bifunctional thiourea-amine catalyst **19g** was shown to be effective towards lactide polymerization producing PLA with a controlled molecular weight and a very narrow MWD (< 1.1).[126] At a monomer-to-initiator ratio of 100, lactide was converted to PLA in 97% conversion after 48 h at room temperature. The PLA generated exhibited M_n = 23,000 g/mol with a very narrow MWD (M_w/M_n = 1.05). Slightly different from the mechanism of lactide polymerization by nucleophiles such as DMAP, phosphines, and NHCs, the thiourea-amine catalyzed polymerization was promoted by the hydrogen bonding interaction as depicted in the transition state **20** (Scheme 7.20). On one hand, the carbonyl is activated via the hydrogen bonding to the thiourea group of the catalyst, while on the other hand, the alcohol is activated by the Lewis basic site (tertiary amino group) of the catalyst, thereby with the catalyst providing dual activation of both monomer and initiator. Nucleophilic ring-opening of the lactide leads to propagation, where the ring-opened lactide acts as a nucleophile for the chain propagation.

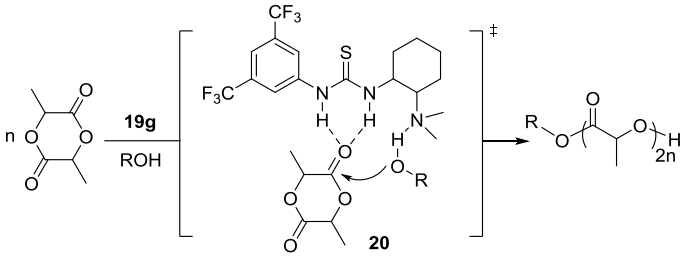

Scheme 7.20 Proposed mechanism for thiourea-amine catalyzed polymerization of lactide.

Cinchona alkaloids are one of the earliest known classes of organocatalysts.[127,128,129] Recently, cinchonidine (CD) and *β*-isocupreidine (*β*-ICD), consisting of both a chiral nucleophilic (Nu) amine catalyst site and an electrophilic (El) hydroxyl site, has been

investigated as bifunctional, stereoselective organocatalysts for ROP of l-LA and *rac*-LA (Scheme 7.21).[130] While CD, when used alone or combined with an alcohol or phenol initiator, is ineffective for the ROP of l-LA, the ROP by *β*-ICD proceeds smoothly without noticeable epimerization, thus affording PLA with a quantitative isotacticity. Alcohols such as benzyl alcohol can be added as an external protic initiator to render the efficient ROP that proceeds to high monomer conversions without transesterification, thus producing isotactic PLA with controlled MW and narrow MWD. More significantly, the ROP of *rac*-LA by the *β*-ICD (**21**, Scheme 7.21)/alcohol catalyst/initiator system affords crystalline isotactic-rich, stereogradient PLA that exhibits multiple melting-transition temperatures, as a result of a partial kinetic resolution polymerization that preferentially polymerizes l-LA and kinetically resolves d-LA (Scheme 7.21). However, the best selectivity factor (3.8) and ee's of partially resolved d-LA (71%ee) achieved by the current organic catalyst system are only modest, thus achieving only partial kinetic resolution polymerization. The ability of an organocatalyst to optically resolve d-LA from *rac*-LA will be significant as d-LA is unnatural and far more expensive than l-LA.

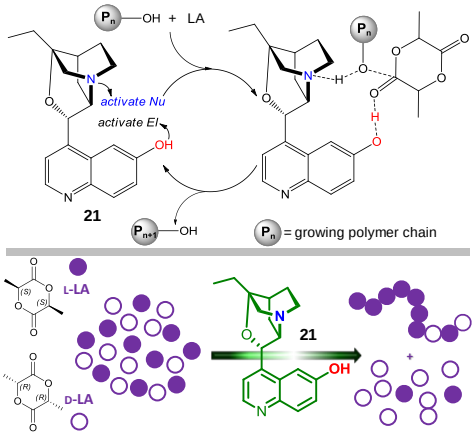

Scheme 7.21. Proposed catalytic cycle in the ROP of LA (top) and schematic representation of the kinetic resolution polymerization (bottom) catalyzed by bifunctional, chiral organocatalyst *β*-ICD.

Following the similar ROP strategy of LA, a glucose-based carbonate monomer **22** was polymerized with 4-methylbenzyl alcohol as the initiator, which was catalyzed by 1,5,7-triazabicyclo[4.4.0]dec-5-ene (TBD) at room temperature (Scheme 7.22).[131] The polymerization proceeded efficiently with a tunable degree of polymerization, narrow MWD (1.11–1.16) and well-defined end groups. The polycarbonate has a glass transition temperature (T_g) above 106 ℃ and an initial onset thermal degradation temperature of 250 ℃ (until complete mass loss at 320 ℃).

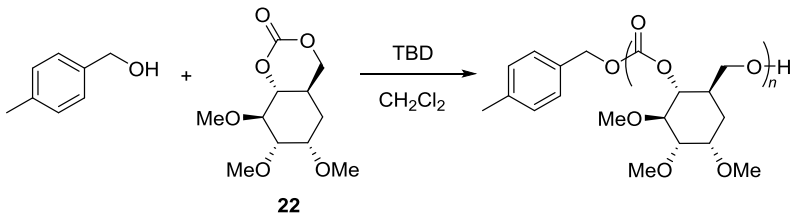

22

Scheme 7.22 ROP of glucose-based monomer **22** via organocatalysis by TBD.[131]

7.5.3 Methylene butyrolactone platform

Renewable methylene butyrolactones based on the tulipaline family, tulipaline A or α-methylene-γ-butyrolactone (MBL), found in tulips,[132,133] and γ-methyl-α-methylene-γ-butyrolactone ($_\gamma$MMBL), have been explored for the prospects of substituting the currently petroleum-based acrylic monomers such as MMA for acrylic polymers and specialty chemicals production.[12,134] Chemically, MBL can be synthesized from sugar-based itaconic anhydride,[135] while $_\gamma$MMBL can be readily prepared via a two-step process from biomass-derived levulinic acid.[136,137] Poly(α-methylene-γ-butyrolactone) (PMBL) has good durability, optical properties, a high refractive index of 1.540, and a high T_g of 195 ℃ (for atactic polymer).[12] The T_g of poly(γ-methyl-α-methylene-γ-butyrolactone) (P$_\gamma$MMBL) is even higher, up

to 227 ℃ (for atactic polymer), [138], [139] while the T_g of poly(β-methyl-α-methylene-γ-butyrolactone (P$_\beta$MMBL) is the highest, reaching up to 290 ℃ (for isotactic polymer).[140,141] Various types of polymerization processes have been employed to polymerize (MMBL, including radical, anionic, group-transfer, zwitterionic, and metal-mediated coordination polymerization methods.[12] Most recently, stereoselective polymerization of the β-methyl derivative, $_\beta$MMBL, has also been developed for the synthesis of stereo-defect-free polymers using single-site chiral metallocene catalysts. [142] This section focuses on polymerization of such methylene butyrolactone monomers through organocatalytic polymerization mediated by silylium catalysts, derived from activation of silyl ketene acetals (SKAs, **23**, Scheme 7.23), and NHCs.

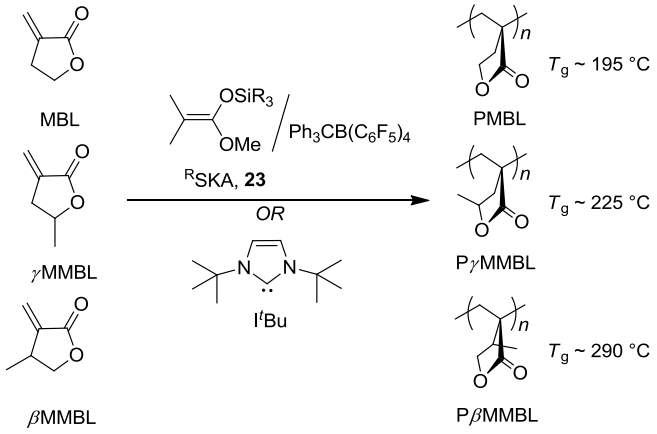

Scheme 7.23 Naturally occurring or biomass-derived renewable α-methylene-γ-butyrolactone monomers, their corresponding polymers, and selected organocatalytic polymerization methods.

Silylium-catalyzed living polymerization of MBL and $_\gamma$MMBL. The recently established silylium-catalyzed living anionic-addition polymerization of acrylic monomers [143,144] uses the precursory trialkylsilyl methyl dimethylketene acetal (^{R}SKA, $Me_2C{=}C(OMe)OSiR_3$) initiators, which are commonly employed in the conventional group-transfer polymerization

(GTP),[145,146] but both chain initiation and propagation of the silylium-catalyzed polymerization are fundamentally different from those steps of GTP. Specifically, the initiation involves vinylogous hydride abstraction of ^{R}SKA by Ph_3C^+ $[Ph_3CB(C_6F_5)_4]$ leading to the R_3Si^+-activated MMA; subsequent Michael addition of ^{R}SKA to the silylated MMA, generates the bifunctional active propagating species **24a** (Scheme 7.24). The chain propagation consists of a fast step of recapturing the silylium catalyst from the ester group of the growing chain by the incoming MMA, followed by a rate-determining step (*r.d.s.*) of C–C bond coupling via intermolecular Michael addition of the polymeric SKA (**24b**) to the silylated MMA. Furthermore, this silylium-catalyzed polymerization offers advantages over the conventional GTP in terms of its ability to readily produce high MW poly(methacrylate)s and effects living polymerization of acrylates under ambient temperature and low catalyst loading conditions.[143,144]

This R_3Si^+-catalyzed, highly active and living/controlled (meth)acrylate polymerization system has been recently applied to the MBL and $_{\gamma}$MMBL polymerization.[147] The studies revealed large effects of SKA (thus the resulting R_3Si^+ catalyst) and activator (thus the resulting counteranion) structures on polymerization characteristics and found that the $Me_2C{=}C(OMe)OSi\textit{i}Bu_3/Ph_3CB(C_6F_5)_4$ combination is the most active and controlled system for MBL and $_{\gamma}$MMBL polymerizations. The resulting large $\textit{i}Bu_3Si^+$ cation (relative to the smaller Me_3Si^+ cation), when paired with the weakly coordinating anion $[B(C_6F_5)_4]^-$, exhibits exceptional activity and control. Thus, the polymerization of $_{\gamma}$MMBL by this catalyst system in a low catalyst loading of 0.05 mol% (relative to monomer) is complete in 10 min at RT, proceeding in a living fashion to produce polymers with controlled low to high (M_n = 5.43 × 10^5

g/mol) MW and narrow MWD's (1.01–1.06). Copolymerization studies with the best catalytic system $^{i\text{Bu}}$SKA/$Ph_3CB(C_6F_5)_4$ produced the well-defined block copolymer P_γMMBL-*b*-PMBL (PDI = 1.02) displaying two T_g's of 197 and 212 °C and statistical P_γMMBL-*co*-PMBL (PDI = 1.01) with one T_g at 213 °C.[147] The study of kinetics of the polymerization of $_\gamma$MMBL by $^{i\text{Bu}}$SKA/$Ph_3CB(C_6F_5)_4$ revealed that the polymerization follows zero-order dependence on monomer concentration, thus proceeding through the same mechanism that has been established previously for the polymerization of MMA (*c.f.* Scheme 7.24).

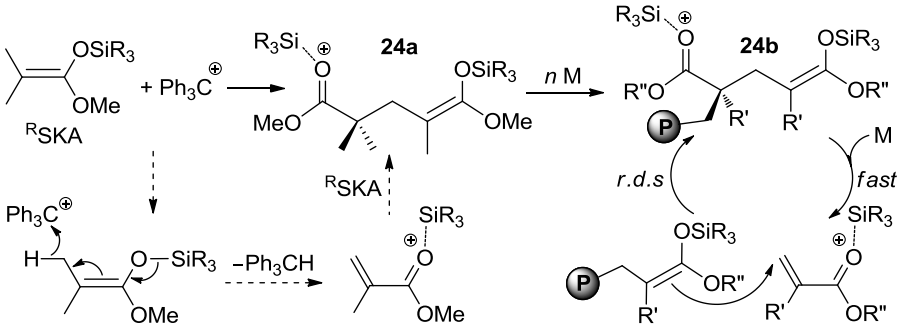

Scheme 7.24 Initiation and propagation involved in living/controlled (meth)acrylate polymerization catalyzed by R_3Si^+.[143,144]

This bimolecular, activated monomer propagation mechanism imposes certain limitations on polymerizations under highly dilute initiator or catalyst conditions and on the stereochemical control of polymerization. A new strategy to overcome those limitations has been developed by covalently linking electrophilic R_3Si^+ and nucleophilic SKA active sites into a single, dinuclear catalyst/initiator molecule.[148] This strategy was based on a hypothesis that such active species can convert the bimolecular-activated monomer propagation into a unimolecular process involving an intermediate formed by an intramolecular delivery of the SKA nucleophile to the monomer activated by the silylium ion electrophile being placed in proximity within the same

molecule. The results achieved from this new binuclear catalyst system indeed showed large rate enhancements due to this site cooperativity manifested by multinuclear catalysts in catalysis.[148]

Rapid zwitterionic polymerization of M(M)BL. The strong NHC nucleophile I^{t}Bu directly and rapidly polymerizes a large excess (e.g., 800 equiv or higher, up to 3000 equiv) of MBL and $_\gamma$MMBL in DMF at RT to medium or high molecular weight polymers in less than 1 min.[149] The M_n of the resulting P$_\gamma$MMBL increased from 38.5 kg/mol to 69.0 kg/mol to 84.7 kg/mol with respect to [$_\gamma$MMBL]/[NHC] ratio from 200 to 400 to 800, exhibiting the ability of the system to control M_n by monitoring the [$_\gamma$MMBL]/[NHC] ratio in this range. The use of IMes resulted in a considerable initial polymerization rate reduction by more than 30-fold, and the polymer M_n was also lowered by more than 2-fold, whereas the least nucleophilic TPT exhibited no polymerization activity up to 24 h. The β-methyl derivative, $_\beta$MMBL, can also be rapidly polymerized by I^{t}Bu in DMF at RT. The proposed propagation "catalysis" cycle through zwitterionic propagating intermediate **25** is depicted in Scheme 7.25.

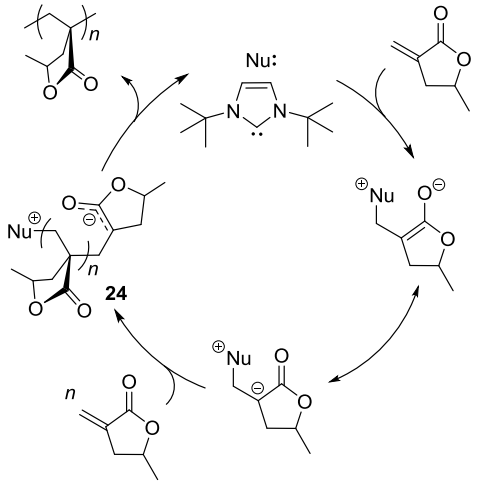

Scheme 7.25 Proposed catalytic cycle in the polymerization of $_\gamma$MMBL by I*t*Bu in DMF at room temperature.[149]

7.6 Conclusions

Organocatalysis, although widely adopted in organic synthesis and polymer synthesis, only recently has it emerged as a highly active, selective, and efficient catalytic process in biorefining for selected biomass conversion and upgrading under mild conditions into sustainable chemicals, materials, and biofuels. This emergence has not only broadened the utility of organocatalysis and offered metal-free "greener" alternatives for biomass conversion and upgrading, it has also showed some unique activity and selectivity in such transformations as compared to metal-mediated processes. In a balanced view, applying organocatalysis for biorefining also faces some important challenges, such as the availability of raw materials, recyclability of catalyst, process integration, scale up and discharge of effluent; such issues need to be addressed in future studies.

For biomass conversion, the discovery of dissolution of lignocellulosic materials in ILs renders the development of homogenous biomass conversion into value-added and platform chemicals such as mono- or oligo-saccharides and HMF. Moreover, ILs with halide anions, typically Cl^- and Br^-, act not only as the solvent but also as the catalyst for fructose-to-HMF conversion in >70% yield. Organic boric acid is found to catalyze the conversion of glucose to HMF, achieving 41% yield and 43% of selectivity. This catalyst can also promote cellulose conversion to HMF, obtaining 32 % of HMF yield in [EMIM]Cl at 120 ℃ for 8 h. On the basis of DFT calculations, the glucose-to-MHF conversion proceeds through initial isomerization of glucose to fructose, followed by fructose dehydration to HMF. Sugars can also be a source of the acyl anion (in retro-benzoin condensation, catalyzed by NHCs) for Stetter reaction with

chalcone.

As for upgrading or chain-extension of furaldehydes (FF, MF, and HMF) through new C–C bond formation, several effective strategies have been developed; they include benzoin condensation (via direct coupling of two furaldehydes catalyzed by cyanide or NHCs), cross-aldol condensation (via coupling of furaldehydes with enolizable ketones by organic bases such as DBU), and hydroxylation/alkylation (via reaction of furaldehydes with 5-methylfuran catalyzed by *p*-TsOH). Other reactions, such as Morita-Baylis-Hillman reaction, have also been utilized for C–C bond formation. Among the available furaldehyde upgrading routes, the DHMF route through direct self-coupling of two HMF molecules is particularly attractive because: (a) self-coupling of HMF by NHC is 100% atom economical (no atom loss); (b) HMF self-coupling is a "greener" process catalyzed by non-toxic organic catalysts and carried out under solvent-free conditions; (c) the coupling reaction affords DHMF in quantitative isolated yield; (d) the HDO of DHMF can be carried out directly in water, allowing for spontaneous separation of hydrocarbons from water phase; and (e) the DHMF hydrodeoxygenation achieves high conversion and near quantitative selectivity towards linear C_{10}-C_{12} alkanes with a narrow distribution of alkanes as candidates for premium transportation fuels.

Concerning the organocatalytic polymerization of biomass feedstocks to sustainable polymeric materials, three important biomass feedstock platforms are highlighted herein: isosorbide, lactide, and methylene butyrolactone monomers. First, as a diol from products of biomass feedstocks, isosorbide has been explored as a sustainable alternative to petroleum-based diols for the synthesis of polyesters, polyethers, and polyurethanes. In particular,

organocatalyzed condensation polymerization of isosorbide with diisocyanates offers an attractive route for the synthesis of biomass-based polyurethanes. Second, organocatalytic ROP of lactide through nucleophilic monomer activation, monomer/initiator dual activation, or enantioselection leads to formation of the biodegradable PLA materials with defined chain structures or topologies, or kinetically resolved unnatural D-LA. Biobased lignin-PLA renewable composite materials have recently been synthesized through graft polymerization of lactide onto lignin in a solvent-free process catalyzed by an organic catalyst (tri-azabicyclodecene).[150] Lastly, the naturally occurring or biomass-derived α-methylene-γ-butyrolactone platform includes MBL, $_{\gamma}$MMBL, and $_{\beta}$MMBL. The recently developed organocatalytic polymerization of such renewable monomers offers the rapid or precision synthesis of high-performance engineering bioplastics with enhanced thermal stability and solvent resistance. Such polymers not only offer a sustainable alternative to petroleum-based acrylic polymers, they also exhibit superior physical and mechanical properties as compared to their petroleum-based analogs.

7.7 References

(1) *Organocatalysis*, Jacobsen E. N.; MacMillan, D. W. C. Eds. *PNAS* **2010**, *107*, Special Features issue (#8).

(2) *The Advernt and Development of Organocatalysis*, MacMillan, D. W. C. *Nature* **2008**, *455*, 304−308.

(3) *Asymmetric Organocatalysis*, Houk, K. N.; List, B. Eds. *Acc. Chem. Res.* **2004**, *37*, 487−631 (Special Edition issue).

(4) Bugaut, X.; Glorius, F. *Chem. Soc. Rev.* **2012**, *41*, 3511−3522.

(5) Wende R. C.; Schreiner, P. *Green Chem.* **2012**, *14*, 1821−1849.

(6) Grondal, C.; Jeanty M.; Enders, D. *Nat. Chem.* **2010**, *2*, 167−178.

(7) Dröge, T.; Glorius, F. *Angew. Chem. Int. Ed.* **2010**, *50*, 6940−6952.

(8) Marcelli, T.; Hiemstra, H. *Synthesis* **2010**, 1229−1279.

(9) Marion, N.; Díez-González, S.; Nolan, S. P. *Angew. Chem. Int. Ed.* **2007**, *46*, 2988−3000.

(10) Enders, D.; Niemeier, O.; Henseler, A. *Chem. Rev.* **2007**, *107*, 5606−5655.

(11) Brown, H. A.; Waymouth, R. M. *Acc. Chem. Res.* 2013, **46**, doi: 10.1021/ar400072z.

(12) Gowda, R. R.; Chen, E. Y.-X. *Encyclo. Polym. Sci. Tech.* **2013**, doi: 10.1002/0471440264.pst606.

(13) Fèvre, M.; Pinaud, J.; Gnanou, Y.; Vignolle, J.; Taton, D. *Chem. Soc. Rev.* **2013**, *42*, 2142−2172.

(14) Kiesewetter, M. K.; Shin, E. J.; Hedrick, J. L.; Waymouth, R. M. *Macromolecules*, **2010**, *43*, 2093−2107.

(15) Kamber, N. E.; Jeong, W.; Waymouth, R. M.; Pratt, R. C.; Lohmeijer, B. G. G.; Hedrick, J. L. *Chem. Rev.* **2007**, *107*, 5813−5840.

(16) Lancaster, M. *Green Chemistry: An Introductory Text*; RSC Publishing, 2nd Ed. **2010**.

(17) Anastas, P. T.; Warner, J. C. *Green Chemistry: Theory and Practice*; Oxford University Press, **1998**.

(18) Lewkowski, J. *Arkivoc*, **2001**, *i*, 17-54.

(19) van Putten, R.-J.; van der Waal, J. C.; de Jong, E.; Rasrendra, C. B.; Heeres, H. J.; de Vries, J. G. *Chem. Rev.* **2013**, *113*, 1499–1597.

(20) Tuck, C. O.; Pérez, E.; Horváth, I. T.; Sheldon, R. A.; Poliakoff, M. *Science* **2012**, *337*, 695–699.

(21) Lange, J.-P.; Van der Heide, E.; Van Buijtenen, J.; Price, R. *ChemSusChem* **2012**, *5*, 150–166.

(22) Zakrzewska, M. E.; Bogel-Łukasik, E.; Bogel-Łukasik, R. *Chem. Rev.* **2011**, *111*, 397–417.

(23) Serrano-Ruiz, J. C.; Dumesic, J. A. *Energy Environ. Sci.* **2011**, *4*, 83–99.

(24) Ståhlberg, T.; Fu, W.; Woodley, J. M.; Riisager, A. *ChemSusChem* **2011**, *4*, 451–458.

(25) Climent, M. J.; Corma, A.; Iborra, S. *Green Chem.* **2011**, *13*, 520-540.

(26) Rosatella, A. A.; Simeonov, S. P.; Frade, R. F. M.; Afonso, C. A. M. *Green Chem.* **2011**, *13*, 754-793.

(27) James, O.; Maity, S.; Usman, L. A.; Ajanaku, K. O.; Ajani, O. O.; Siyanbola, T. O.; Sahu, S.; Chaubey, R. *Energy Environ. Sci.* **2010**, *3*, 1833–1850.

(28) Bozell J. J.; Petersen, G. R. *Green Chem.* **2010**, *12*, 539–554.

(29) Alonso, D. M.; Bond, J. Q.; Dumesic, J. A. *Green Chem.* **2010**, *12*, 1493−1513.

(30) Stöcker, M. *Angew. Chem. Int. Ed.* **2008**, *47*, 9200−9211.

(31) Corma, A.; Iborra, S.; Velty, A. *Chem. Rev.* **2007**, *107*, 2411−2502.

(32) Chheda, J. N.; Huber, G. W.; Dumesic, J. A. *Angew. Chem. Int. Ed.* **2007**, *46*, 7164−7183.

(33) Huber, G. W.; Corma, A. *Angew. Chem. Int. Ed.* **2007**, *46*, 7184−7201.

(34) Huber, G. W.; Iborra, S.; Corma, A. *Chem. Rev.* **2006**, *106*, 4044−4098.

(35) "*Top Value Added Chemicals from Biomass*", Werpy, T.; Petersen, G. Eds. U.S. Department of Energy (DOE) report: DOE/GO-102004-1992, **2004**.

(36) Gallezot, P. *Chem. Soc. Rev.* **2012**, *41*, 1538-1558.

(37) Wyman, C. E.; Dale, B. E.; Elander, R. T.; Holtzapple, M.; Ladisch, M. R.; Lee, Y. Y. *Bioresour. Technol.* **2005**, *96*, 1959-1966.

(38) Maki-Arvela, P.; Holmbom, B.; Salmi, T.; Murzin, D. *Catal. Rev. Sci. Eng.* **2007**, *49*, 197-340.

(39) Jacoby, M. *C&EN*, **2009**, *July 6*, 26-28.

(40) Kono, T.; Matsuhisa, H.; Maehara, H.; Horie, H.; Matsuda, K. Jpn. Pat. Appl. 2005232116, **2005**.

(41) Swatloski, R. P.; Spear, S. K.; Holbrey, J. D.; Rogers, R. D. *J. Am. Chem. Soc.* **2002**, *124*, 4974-4975.

(42) Smiglak, M.; Metlen, A.; Rogers, R. D. *Acc. Chem. Res.* **2007**, *40*, 1182-1192.

(43) Zhao, H.; Holladay, J. E.; Brown, H.; Zhang, Z. C. *Science* **2007**, *316*, 1597-1600.

(44) Su, Y.; Brown, H. M.; Huang, X.; Zhou, X.-D.; Amonette, J. E.; Zhang, Z. C. *Appl. Catal. A.* **2009**, *361*, 117−122.

(45) Zhang, Y.; Du, H.; Qian, X.; Chen, E. Y.-X. *Energy & Fuels* **2010**, *24*, 2410-2417.

(46) Musau, R. M.; Munavu, R. M. *Biomass* **1987**, *13*, 67-74.

(47) Smarasekara, A. S.; Williams, L. D.; Ebede, C. C. *Carbohydr. Res.* **2008**, *343*, 3021-3024.

(48) Liu, R.; Chen, J.; Huang, X.; Chen, L.; Ma, L.; Li, X. *Green Chem.* **2013**, *15*, 2895-2903.

(49) Moreau, C.; Finiels, A.; Vanoye, L. *J. Mol. Catal. A: Chem.* **2006**, *253*, 165-169.

(50) Li, Y.-N.; Wang, J.-Q.; He, L.-N.; Yang, Z.-Z.; Liu, A.-H.; Yu, B.; Luan, C.-R. *Green Chem.* **2012**, *14*, 2752-2758.

(51) Xie, H.; Zhao, Z. K.; Wang, Q. *ChemSusChem* **2012**, *5*, 901-905.

(52) Cao, Q.; Guo, X.; Guan, J.; Mu, X.; Zhang, D. *Appl. Catal. A: Gen.* **2011**, *403*, 98-103.

(53) Hu, L.; Sun, Y.; Lin, L. *Ind. Eng. Chem. Res.* **2012**, *51*, 1099-1104.

(54) Simeonov, S. P.; Coelho, J. A. S.; Afonso, C. A. M. *ChemSusChem* **2012**, *5*, 1388-1391.

(55) Hu, S.; Zhang, Z.; Zhou, Y.; Han, B.; Fan, H.; Li, W.; Song, J.; Xie, Y. *Green Chem.* **2008**, *10*, 1280-1283.

(56) Ranoux, A.; Djanashvili, K.; Arends, I. W. C. E.; Hanefeld, U. *ACS Catal.* **2013**, *3*, 760-763.

(57) Caes, B. R.; Palte, M. J.; Raines, R. T. *Chem. Sci.* **2013**, *4*, 196-199.

(58) He, J.; Zhang, Y.; Chen, E. Y.-X. *ChemSusChem* **2013**, *6*, 61-64.

(59) Ståhlberg, T.; Rodriguez-Rodriguez, S.; Fristrup, P.; Riisager, A. *Chem. Eur. J.* **2011**, *17*, 1456-1464.

(60) Zhang, Z.; Wang, Q.; Xie, H.; Liu, W.; Zhao, Z. K. *ChemSusChem* **2011**, *4*, 131-138.

(61) Kim, B.; Jeong, J.; Lee, D.; Kim, S.; Yoon, H. –J.; Lee, Y.-S.; Cho, J. K. *Green Chem.* **2011**, *13*, 1593-1506.

(62) Qi, X.; Watanabe, M.; Aida, T. M.; Smith, R. L. Jr. *ChemSusChem* **2010**, *3*, 1071-1077.

(63) Román-Leshkov, Y.; Chheda, J. N.; Dumesic, J. A. *Science* **2006**, *321*, 1933-1937.

(64) Román-Leshkov, Y.; Barrett, C. J.; Liu, Z. Y.; Dumesic, J. A. *Nature* **2007**, *447*, 982-985.

(65) Pagán-Torres, Y. J.; Wang, T.; Gallo, J. M. R.; Shanks, B. H.; Dumesic, J. A. *ACS Catal.* **2012**, *2*, 930-934.

(66) Liu, F.; Audemar, M.; Vigier, K. D. O.; Cartigny, D.; Clacens, J.-M.; Gomes, M. F. C.; Pádua, A. A. H.; Campo, F. D.; Jérôme, F. *Green Chem.* **2013**, *15*, 3205-3213.

(67) Zhang, J.; Xing, C.; Tiwari, B.; Chi, Y. R. *J. Am. Chem. Soc.* **2013**, *135*, 8113-8116.

(68) Seri, K.-i.; Inoue, Y.; Ishida, H. *Chem. Lett.* **2000**, 22-23.

(69) Seri, K-i.; Inoue, Y.; Ishida, H. *Bull. Chem. Soc. Jpn.* **2001**, *74*, 1145-1150.

(70) Binder, J. B.; Cefali, A. V.; Blank, J. J.; Raines, R. T. *Energy Environ. Sci.* **2010**, *3*, 765-771.

(71) Mondal, D.; Sharma, M.; Maiti, P.; Prasad, K.; Meena, R.; Siddhanta, A. K.; Bhatt, P.; Ijardar, S.; Mohandas, V. P.; Ghosh, A.; Eswaran, K.; Shah, B. G.; Ghosh, P. K. *RSC Advances* **2013**, *3*, 17989-17997.

(72) Su, K.; Liu, X.; Ding, M.; Yuan, Q.; Li, Z.; Cheng, B. *J. Mol. Catal. A.* **2013**, *379*, 350-354.

(73) Huang, Y.-B.; Fu, Y. *Green Chem.* **2013**, *15*, 1095-1111.

(74) Liu, D.; Chen, E. Y.-X. *ChemSusChem* **2013**, *6*, 2236-2239.

(75) Moore, J. L.; Rovis, T. *Top. Curr. Chem.* **2009**, *291*, 77−144.

(76) Breslow, R. *J. Am. Chem. Soc.* **1957**, *79*, 1762-1763.

(77) Breslow, R. *J. Am, Chem. Soc.* **1958**, *80*, 3719-3726.

(78) Kluger, R.; Tittmann, K. *Chem. Rev.* **2008**, *108*, 1797-1833.

(79) Stetter, H.; Raemsch, R. Y.; Kuhlmann, H. *Synthesis* **1976**, 733-735.

(80) Lee, C. K.; Kim, M. S.; Gong, J. S.; Lee, I.-S. H. *J. Heterocycl. Chem.* **1992**, *29*, 149-153.

(81) Enders, D.; Kallfass, U. *Angew. Chem. Int. Ed.* **2002**, *41*, 1743-1745.

(82) Hashmi, A. S. K.; Wölfle, M.; Teles, J. H.; Frey, W. *Synlett.* **2007**, 1747-1752.

(83) Kabro, A.; Escudero-Adán, E. C.; Grushin, V. V.; van Leeuwen, P. W. N. M. *Org. Lett.* **2012**, *14*, 4014-4017.

(84) DiRocco, D. A.; Oberg, K. M.; Rovis, T. *J. Am. Chem. Soc.* **2012**, *134*, 6143-6145.

(85) Berkessel, A.; Elfert, S.; Yatham, V. R.; Neudörfl, J.-M.; Schlörer, N. E.; Teles, J. H. *Angew. Chem. Int. Ed.* **2012**, *51*, 12370-12374.

(86) Liu, D.; Zhang, Y.; Chen, E. Y.-X. *Green Chem.* **2012**, *14*, 2738-2746.

(87) Ståhlberg, T.; Sørensen, M. G.; Riisager, A. *Green Chem.* **2010**, *12*, 321-325.

(88) Liu, D.; Chen, E. Y.-X. *Appl. Catal. A: Gen.* **2012**, *435-436*, 78-85.

(89) Hollóczki, O.; Gerhard, D.; Massone, K.; Szarvas, L.; Németh, B.; Veszprémi, T.; Nyulászi, L. *New J. Chem.* **2010**, *34*, 3004-3009.

(90) Rodríguez, H.; Gurau, G.; Holbrey J. D.; Rogers, R. D. *Chem. Commun.* **2011**, *47*, 3222-3224.

(91) Kelemen, Z.; Hollóczki, O.; Nagy, J.; Nyulaszi, L. *Org. Biomol. Chem.* **2011**, *9*, 5362-5364.

(92) Biju, A. T.; Padmanaban, M.; Wurz, N. E.; Glorius, F. *Angew. Chem. Int. Ed.* **2011**, *50*, 8412-8415.

(93) Matsuoka, S.-I.; Ota, Y.; Washio, A.; Katada, A.; Ichioka, K.; Takagi, K.; Suzuki, M. *Org. Lett.* **2011**, *13*, 3722-3725.

(94) Fisher, C.; Smith, S. W.; Powell, D. A.; Fu, G. C. *J. Am, Chem. Soc.* **2006**, *128*, 1472-1473.

(95) Analogous 2-(α-hydroxybenzyl)thiazolium ions derived from the reaction of thiazolium salts and benzaldehydes. White, M. J.; Leeper, F. J. *J. Org. Chem.* **2011**, *66*, 5124-5131.

(96) Chen, Y.-T.; Barletta, G. L.; Haghjoo, K.; Cheng, J. T.; Jordan, F. *J. Org. Chem.* **1994**, *59*, 7714-7722.

(97) Breslow, R.; Kim, R. *Tetrahedron Lett.* **1994**, *35*, 699-702.

(98) Enders, D.; Breuer, K.; Raabe, G.; Runsink, J.; Teles, J. H.; Melder, J.-P.; Ebel, K.; Brode, S. *Angew. Chem. Int. Ed.* **1995**, *34*, 1021-1023.

(99) Enders, D.; Breuer, K.; Kallfass, U.; Balensiefer, T. *Synthesis* **2003**, 1292-1295.

(100) Huber, G. W.; Chheda, J. N.; Barrett, C. J.; Dumesic, J. A. *Science* **2005**, *308*, 1446-1450.

(101) Subrahmanyam, A. V.; Thayumanavan, S.; Huber, G. W. *ChemSusChem* **2010**, *3*, 1158-1161.

(102) Sutton, A. D.; Waldie, F. D.; Wu, R.; Schlaf, M.; Silks, L. A. III; Gordon, J. C. *Nature Chem.* **2013**, *5*, 428-432.

(103) Silks, L. A.; Gordon, J. C.; Wu, R.; Hanson, S. K. US Pat. 8507700 (B2), **2013**.

(104) Gordon, J. C.; Silks, L. A.; Sutton, A. D.; Wu, R.; Schlaf, M.; Waldie, F.; West, R.; Collias, D. I. PCT Int. Appl. WO 2013/040311, **2013**.

(105) "*Aldol Condensation of 2,5-hexanedione as a Tunable Platform Molecule for Gasoline and Diesel Fuel Products*", Sacia, E.; Bell, A. T. 23rd North American Catalysis Society Meeting Abstract: O-Tu-BRA-16, **2013**.

(106) Corma, A.; de la Torre, O.; Renz, M.; Villandier, N. *Angew. Chem. Int. Ed.* **2011**, *50*, 2375-2378.

(107) Corma, A.; de la Torre, O.; Renz, M. *Energy Environ. Sci.* **2012**, *5*, 6328-6344.

(108) "Methylfuran": Zeitsch, K. J. in *The Chemistry and Technology of Furfural and its Many By-Products*, Sugar Series Vol. 13, Elsevier Science, Dordrecht, **2000**, pp. 229-230.

(109) Zheng, H.-Y.; Zhu, Y.-L.; Teng, B.-T.; Bai, Z.-Q.; Zhang, C.-H.; Xiang, H.-W.; Li, Y.-W. *J. Mol. Catal.* **2006**, *246*, 18-23.

(110) Coates, G. W.; Hillmyer, M. A. A virtual issue on "Polymers from Renewable Resources", *Macromolecules* **2009**, *42*, 7987–7989.

(111) Gandini, A. Polymers from Renewable Resources: a Challenge for the Future of Macromolecular Materials, *Macromolecules* **2008**, *41*, 9491–9504.

(112) Wiliams, C. K.; Hillmyer, M. A. Polymers from Renewable Resources: A Perspective for a Special Issue of Polymer Reviews. *Polym. Rev.* **2008**, *48*, 1–10.

(113) Meier, M. A. R.; Metzger, J. O.; Schubert, U. S. Plant Oil Renewable Resources as Green alternatives in Polymer Science. *Chem. Soc. Rev.* **2007**, *36*, 1788–1802.

(114) Stoss, P.; Hemmer, R. *Adv. Carbohydr. Chem. Biochem.* **1991**, *49*, 93-173.

(115) Fenouillot, F.; Rousseau, A.; Colomines, G.; Saint-Loup, R.; Pascault, J.-P. *Prog. Polym. Sci.* **2010**, *35*, 578-622.

(116) Raquez, J.-M.; Del église, M.; Lacrampe, M.-F.; Krawczak, P. *Prog. Polym. Sci.* **2010**, *35*, 487-505.

(117) Braun, D.; Bergmann, M. *J. Prakt. Chem.* **1992**, *334*, 298-310.

(118) Cognet-Georjon, E.; Mechin, F.; Pascault, J. P. *Marcromol. Chem. Phys.* **1996**, *197*, 3593-3612.

(119) Zenner, M. D.; Xia, Y.; Chen, J. S.; Kessler, M. R. *ChemSusChem* **2013**, *6*, 1182-1185.

(120) Coutelier, O.; Ezzi, M. E.; Destarac, M.; Bonnette, F.; Kato, T.; Baceiredo, A.; Sivasankarapillai, G.; Gnanou, Y.; Taton, D. *Polym. Chem.* **2012**, *3*, 605-608.

(121) Yao, K.; Tang, C. *Macromolecules* **2013**, *46*, 1689-1712.

(122) Nederberg, F.; Connor, E. F.; Müller, M.; Glauser, T.; Hedrick, J. L. *Angew. Chem. Int. Ed.* **2001**, *40*, 2712-2715.

(123) Myers, M.; Connor, E. F.; Glauser, T.; Möck, A.; Nyce, G.; Hedrick, J. L. *J. Polym. Sci. Part A: Polym. Chem.* **2002**, *40*, 844-851.

(124) Nyce, G. W.; Glauser, T.; Connor, E. F.; Möck, A.; Waymouth, R. M.; Hedrick, J. L. *J. Am. Chem. Soc.* **2003**, *125*, 3046-3056.

(125) Nyce, G. W.; Csihony, S.; Waymouth, R. M.; Hedrick, J. L. *Chem. Eur. J.* **2004**, *10*, 4073-4079.

(126) Csihony, S.; Culkin, D. A.; Sentman, A. C.; Dove, A. P.; Waymouth, R. M.; Hedrick, J. L. *J. Am. Chem. Soc.* **2005**, *127*, 9079-9084.

(127) Marcelli, T.; van Maarseveen, J. H.; Hiemstra, H. *Angew. Chem. Int. Ed.* **2006**, *45*, 7496–7504.

(128) Tian, S.; Chen, Y.; Hang, J.; Tang, L.; McDaid, P.; Deng, L. *Acc. Chem. Res.* **2004**, *37*, 621–631.

(129) Marcelli, T.; Hiemstra, H. *Synthesis* **2010**, 1229–1279.

(130) Miyake, G. M.; Chen, E. Y.-X. *Macromolecules* **2011**, *44*, 4116–4124**.**

(131) Mikami, K.; Lonnecker, A. T.; Gustafson, T. P.; Zinnel, N. F.; Pai, P.-J.; Russell, D. H.; Wooley, K. L. *J. Am. Chem. Soc.* **2013**, *135*, 6826-6829.

(132) Kitson, R. R. A.; Millemaggi, A.; Taylor, R. J. K. *Angew. Chem., Int. Ed. Engl.* **2009**, *48*, 9426–9451.

(133) Hoffman, H. M. R.; Rabe, J. *Angew. Chem., Int. Ed. Engl.* **1985**, *24*, 94–110.

(134) Agarwal, S.; Jin, Q.; Maji, S. *ACS Symp. Ser.* **2012**, *1105*, 197–212.

(135) Yokota, K.; Hirabayashi, T. J. P. Pat. 04049288 A, **1992**.

(136) Manzer, L. E. *ACS Symp. Ser.* **2006**, *921*, 40–51

(137) Manzer, L. E. *Appl. Catal. A: Gen.* **2004**, *272*, 249–256.

(138) Hu, Y.; Xu, X.; Zhang, Y.; Chen, Y.; Chen, E. Y.-X. *Macromolecules* **2010**, *43*, 9328–9336.

(139) Miyake, G. M.; Newton, S. E.; Mariott, W. R.; Chen, E. Y.-X. *Dalton Trans.* **2010**, *39*, 6710–6718.

(140) Hu, Y.; Miyake, G. M.; Wang, B.; Cui, D.; Chen, E. Y.-X. *Chem. Eur. J.* **2012**, *18*, 3345–3354.

(141) Hu, Y.; Wang, X.; Chen, Y.; Caporaso, L.; Cavallo, L.; Chen, E. Y.-X. *Organometallics* **2013**, *32*, 1459–1465.

(142) Chen, X.; Caporaso, L.; Cavallo, L.; Chen, E. Y.-X. *J. Am. Chem. Soc.* **2012**, *134*, 7278−7281.

(143) Zhang, Y.; Chen, E. Y.-X. *Macromolecules* **2008**, *41*, 36-42.

(144) Zhang, Y.; Chen, E. Y.-X. *Macromolecules* **2008**, *41*, 6353-6360.

(145) Sogah, D. Y.; Hertler, W. R.; Webster, O. W.; Cohen, G. M. *Macromolecules* **1987**, *20*, 1473–1488.

(146) Webster, O. W.; Hertler, W. R.; Sogah, D. Y.; Farnham, W. B.; RajanBabu, T. V. *J. Am. Chem. Soc.* **1983**, *105*, 5706–5708.

(147) Miyake, G. M.; Zhang, Y.; Chen, E. Y.-X. *Macromolecules* **2010**, *43*, 4902-4908.

(148) Zhang, Y.; Gustafson, L. O.; Chen, E. Y.-X. *J. Am. Chem. Soc.* **2011**, *133*, 13674−13684.

(149) Zhang, Y.; Chen, E. Y.-X. *Angew. Chem., Int. Ed.* **2012**, *51*, 2465–2469.

(150) Chung, Y.-L.; Olsson, J. V.; Li, R. J.; Frank, C. W.; Waymouth, R. M.; Billington S. L.; Sattely, E. S. *ACS Sustainable Chem. Eng.* **2013**, *1*, 1231-1238.

Chapter 8

Summary

This work develops novel, efficient catalytic processes for plant biomass conversion and upgrading into versatile platform chemicals as well as oxygenated biodiesel and premium hydrocarbon kerosene/jet fuels (Figure 8.1). As petroleum resources continue to deplete, scientists have encountered great challenges to use biomass as a sustainable alternative source of transportation fuels and chemical building blocks. For the production of transportation fuels, the petro-chemical refinery strategy (e.g., catalytic cracking and hydro-treating) has been typically applied, while catalysts that are more tolerant to oxygen and water under high temperature and high H_2 pressure need to be developed. On the other hand, oxygen-rich biomass feedstocks present an advantage over petroleum counterparts: biomass can be selectively converted into oxygenated chemical building blocks, such as HMF and its self-coupling product DHMF.

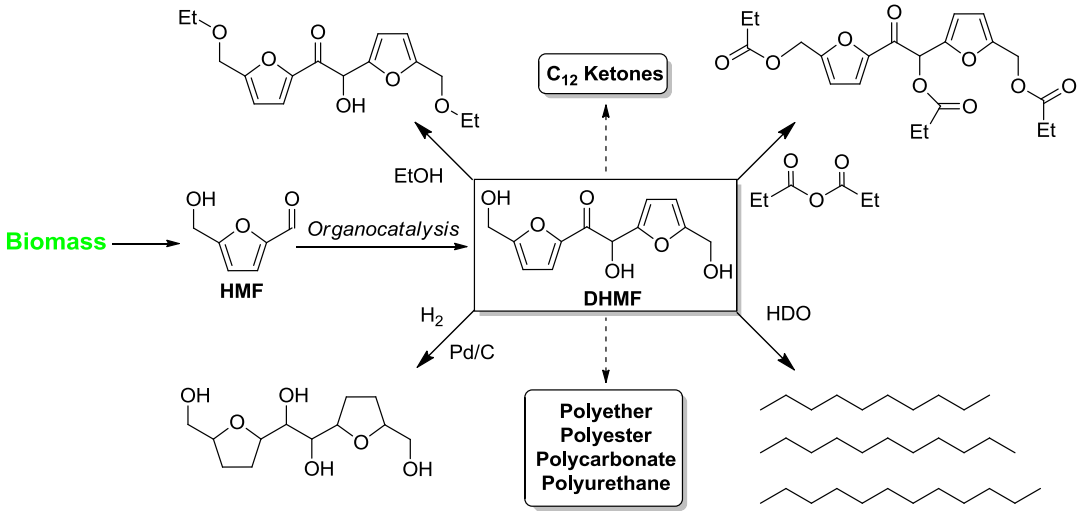

Figure 8.1 Biomass conversion and upgrading into versatile platform chemicals as well as oxygenated biodiesel and premium hydrocarbon kerosene/jet fuels.

Ubiquitous aluminum alkyls and alkoxides, such as $AlEt_3$ and $Al(O^iPr)_3$, have been successfully employed in the glucose-to-HMF conversion in ILs (Figure 8.2). The aluminum catalysts are not only much cheaper than the benchmark catalyst $CrCl_2$ for the glucose-to-HMF conversion (by a factor of 5 for $AlEt_3$ or 180 for $Al(O^iPr)_3$), but also as effective as $CrCl_2$ to catalyze this conversion process. The molecular structure $[EMIM]^+[ClAlMe(BHT)_2]^-$, formed mixing upon $MeAl(BHT)_2$ and the IL [EMIM]Cl, was characterized by single-crystal X-ray diffraction and proposed as the active intermediate responsible for the effective glucose-to-HMF conversion.

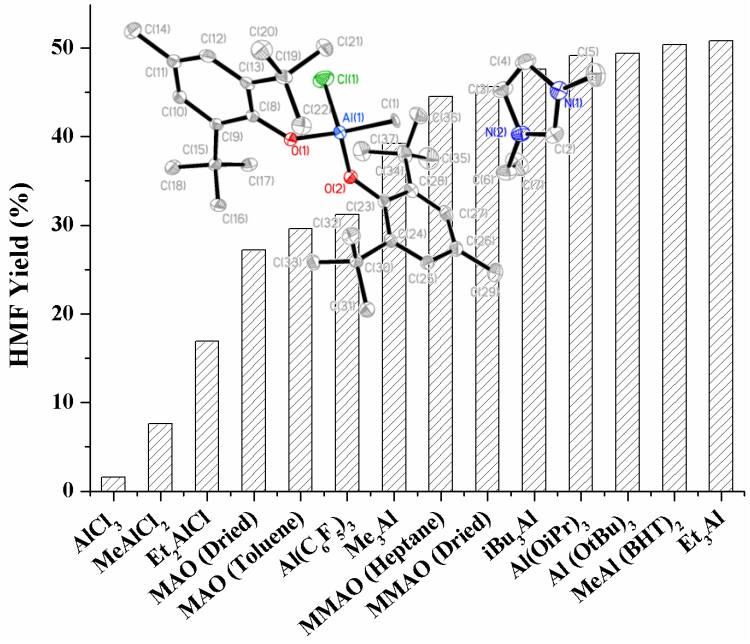

Figure 8.2 Plot of the HMF yield vs. aluminum species and proposed catalyst structure.

Recyclable PIL-supported metal (Cr, Al) catalysts have been applied for effective biomass (glucose and cellulose) conversion into HMF. Of the five different PILs investigated, poly(3-butyl-1-vinylimidazolium chloride), P[BVIM]Cl, has been found to be most effective. When anchored by $CrCl_2$, the P[BVIM]Cl-$CrCl_2$ catalyst converts glucose to HMF in 65.8%

yield at 120 ℃ for 3 h, but experiences Cr loss upon recycling. The analogous PIL-Al catalyst, P[BVIM]Cl-Et_2AlCl, is less effective but more recyclable than the PIL-$CrCl_2$ system, thus achieving a nearly constant HMF yield upon 6 cycles (Figure 8.3).

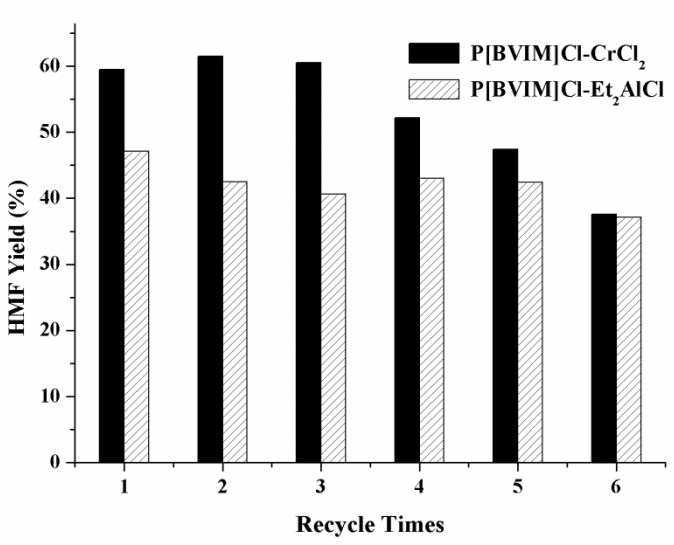

Figure 8.3 Comparison of HMF yield (av. value of 2-3 runs with typical errors within ±3%) at each of 6 recycles between P[BVIM]Cl-$CrCl_2$ and P[BVIM]Cl-Et_2AlCl (10 mol% catalyst, 120 ℃ for 3 h).

As a C_6 biorefining intermediate, HMF upgrading to a higher carbon intermediate is essential to produce high quality fuels. We developed a rapid, highly selective and efficient upgrading of HMF to DHMF, a promising C_{12} kerosene/jet fuel intermediate (Figure 8.4). This HMF upgrading reaction is carried out under industrially favorable conditions (i.e., ambient atomosphere and 60-80 ℃), catalyzed by NHCs, and complete within 1 h; this process selectively produces DHMF.

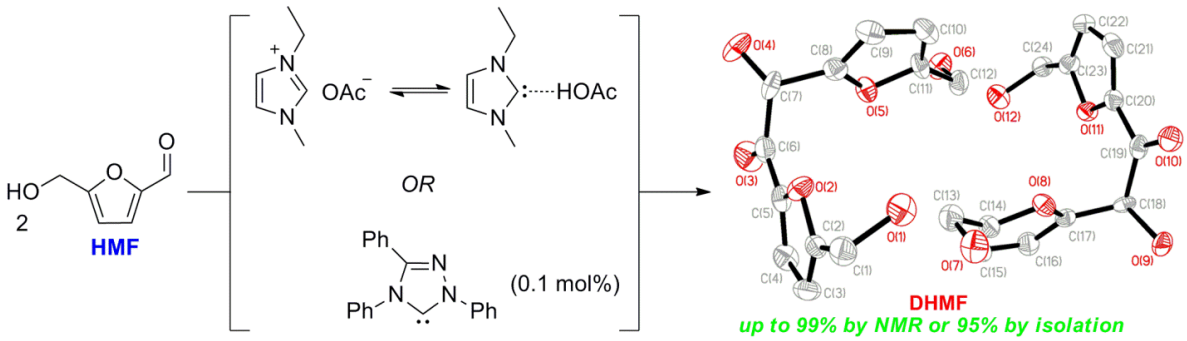

Figure 8.4 HMF upgrading to C_{12} DHMF catalyzed by NHCs.

Based on the NHC-catalyzed HMF upgrading to DHMF, we developed a highly effective new strategy for upgrading biomass-derived furaldehydes to liquid fuels. This strategy consists of NHC-catalyzed self-condensation (Umpolung) of biomass-derived furaldehyde into $C_{10\text{-}12}$ furoin intermediates, followed by hydrogenation, etherification or esterification into oxygenated biodiesel, or hydrodeoxygenation by metal-acid tandem catalysis into premium alkane jet fuels (Figure 8.5). The oxygenated liquid biodiesel has higher heating values than that of bioethanol, while HDO of DHMF in water under moderate conditions (300 ℃, 3 h, 500 psi H_2) with the bifunctional catalyst system ($Pt/C+TaOPO_4$) yields high quality alkane fuels with 96% selectivity to linear $C_{10\text{-}12}$ alkanes, consisting of 27 % *n*-$C_{10}H_{22}$, 23 % *n*-$C_{11}H_{24}$, and 46 % *n*-$C_{12}H_{26}$.

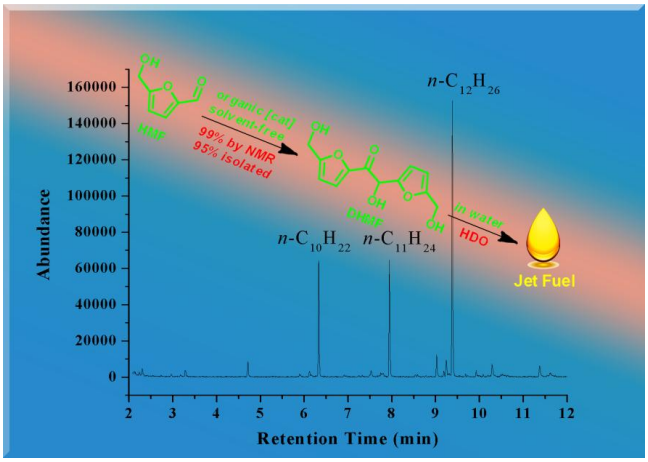

Figure 8.5 HMF upgrading to $C_{10\text{-}12}$ alkane fuels by organocatalysis and metal-acid tandem catalysis.

We further accomplished an integrated catalytic process for conversion and upgrading of biomass feedstocks into C_{12} alkane fuels, through semi-continuous organocatalytic conversion of biomass (fructose, in particular) to the high-purity HMF, self-coupling of HMF *via* organocatalysis, and subsequently into C_{12} alkane fuels *via* metal-acid tandem catalysis (Figure 8.6). NHCs are found to catalyze glucose-to-fructose isomerization, and the inexpensive thiazolium chloride [TM]Cl, a Vitamin B1 analog, catalyzes fructose dehydration to HMF of high purity (>99% by HPLC), achieving a constant HMF yield of 72% over 10 semi-continuous extraction batch runs. Crystallization of the crude HMF from toluene yields the spectroscopically and analytically pure HMF as needle crystals. The second step of the process is the NHC-catalyzed coupling of C_6 HMF to C_{12} DHMF. The third step of the process converts C_{12} DHMF to *n*-$C_{12}H_{26}$ in a high selectivity *via* hydrodeoxygenation with a bifunctional catalyst system consisting of Pd/C + acetic acid + $La(OTf)_3$ under moderate conditions (250 ℃, 16 h, 300 psi H_2).

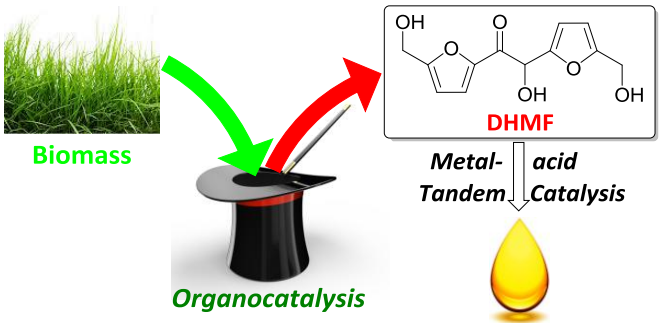

Figure 8.6 An integrated catalytic process for biomass conversion and upgrading to C_{12} DHMF and subsequently to *n*-$C_{12}H_{26}$ alkane fuel by organocatalysis and metal-acid tandem catalysis.

Organocatalysis, although widely employed in organic synthesis and polymer synthesis, only recently has it emerged as a highly active, selective, and efficient catalytic process in

biorefining for selected biomass conversion and upgrading under mild conditions into sustainable chemicals, materials, and bio-fuels (Figure 8.7). This emergence has not only offered metal-free "greener" alternatives for biomass conversion and upgrading, it has also showed some unique activity and selectivity in such transformations as compared to metal-mediated processes. For biomass conversion, the discovery of dissolution of lignocellulosic materials in ILs renders the development of homogeneous biomass conversion into value-added and platform chemicals such as mono- or oligo-saccharides and HMF. For upgrading or chain-extension of furaldehydes through new C-C bond formation, several effective strategies have been developed, including benzoin condensation (*via* direct coupling of two furaldehydes catalyzed by cyanide or NHCs), cross-aldol condensation (*via* coupling of furaldehydes with enolizable ketones by organic bases such as DBU), and hydroxylation/alkylation (*via* reaction of furaldehydes with 5-methylfuran catalyzed by *p*-TsOH). Other reactions, such as Morita-Baylis-Hillman reaction, have also been utilized for C-C bond formation. For organocatalytic polymerization of biomass feedstocks to sustainable polymeric materials, three important biomass feedstock platforms are highlighted in this review article: isosorbide, lactide, and methylene butyrolactone monomers, thus generating biomass-based polyurethanes, poly(lactic acid) and poly(methylene butyrolactone)s respectively.

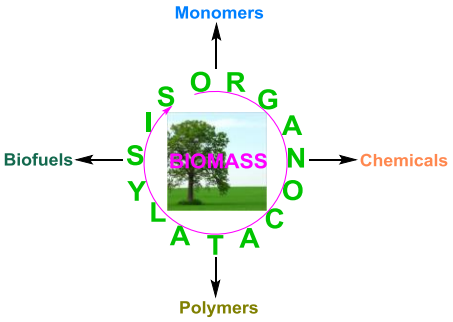

Figure 8.7 Organocatalysis in biorefining for catalytic biomass conversion and upgrading into sustainable chemicals, materials, and biofuels.

Appendix I

List of Publications by Dajiang Liu

1) Liu, D.; Chen, E. Y.-X. "An Integrated Catalytic Process for Biomass Conversion and Upgrading to C12 Furoin and Alkane Fuel", *ACS Catal. in press*.

2) Liu, D.; Chen, E. Y.-X. "Organocatalysis in Biorefining for Biomass Conversion and Upgrading", *Green Chem.* **2014**, *16*, 964-981 (*Invited Critical Review*).

3) Liu, D.; Chen, E. Y.-X. "Diesel and Alkane Fuels from Biomass by Organocatalysis and Metal-Acid Tandem Catalysis", *ChemSusChem* **2013**, *6*, 2236-2239.

4) Nakarit, C.; Kelland, M. A.; Liu, D.; Chen, E. Y.-X. "Cationic Kinetic Hydride Inhibitor Polymers and the Effects on Performance of Incorporating Cationic Monomers into N-Vinyl Lactam Copolymers", *Chem. Eng. Sci.* **2013**, *103*, 424-431.

5) Dunn, E. F.; Liu, D.; Chen, E. Y.-X. "Role of *N*-Heterocyclic Carbenes in Glucose Conversion into HMF by Cr Catalysts in Ionic Liquids", *Appl. Catal. A: Gen.* **2013**, *460-461*, 1-7.

6) Liu, D.; Chen, E. Y.-X. "Polymeric Ionic Liquid (PIL)-Supported Recyclable Catalysts for Biomass Conversion into HMF", *Biomass & Bioenergy* **2013**, *48*, 181-190.

7) Liu, D.; Zhang, Y.; Chen, E. Y.-X. "Organocatalytic Upgrading of the Key Biorefining Building Block by a Catalytic Ionic Liquid and *N*-Heterocyclic Carbenes", *Green Chem.* **2012**, *14*, 2738-2746 (*Cover Article*).

8) Liu, D.; Chen, E. Y.-X. "Ubiquitous Aluminum Alkyls and Alkoxides as Effective Catalysts for Glucose to HMF Conversion in Ionic Liquids", *Appl. Catal. A: Gen.* **2012**, *435-436*, 78-85.

Appendix II

List of Patents by Dajiang Liu

1) Chen, E. Y.-X.; Liu, D. "Biorefining Compounds and Organocatalytic Upgrading Methods", US Patent Application No.: 13/934,074: July **2013**.

2) Chen, E. Y.-X.; Liu, D. "Integrated Process for HMF Production from Biomass", US Provisional Patent Application No.: 61/933,559, **2014**.